Author:
Summers, Kim

Title:
Cardiac Survival Signalling, Oxidative Stress & Reperfusion Injury during Postnatal Development

Cardiac Survival Signalling, Oxidative Stress & Reperfusion Injury during Postnatal Development

By

Kim Zoe Summers *BSc MSc*

Supervisors: Prof. Saadeh Suleiman & Prof. Massimo Caputo

A Dissertation Submitted to the University of Bristol in accordance with the requirements for award of the degree of Doctor of Philosophy

In the Faculty of Health Sciences

The Bristol Medical School (THS)

April 2019

Word Count: 53,847

Abstract

Cardiac vulnerability to injury following ischemia/reperfusion (I/R) during postnatal development displays a biphasic pattern in rats, with 14-day olds being least vulnerable. The underlying cause for this change is not currently known. We hypothesise that developmental differences in survival signalling pathways (e.g. Reperfusion Injury Salvage Kinase (RISK) & Survivor Activating Factor Enhancement (SAFE)) contribute to these biphasic changes. The work presented therefore looked to identify any changes in the expression of relevant proteins over the course of postnatal development, as well as to examine the effects of targeted inhibition of these proteins on cardiac injury, and to assess the morphology and abundance of cardiac ultrastructures related to survival signalling and the response to I/R.

Hearts from 7-day old, 14-day old, 28-day old and adult male Wistar rats were extracted and processed for measurements of protein expression, cardiomyocyte viability, cardiac injury, and cardiac structural/ultrastructural differences. This was done using a range of techniques, including proteomics, Langendorff perfusion, cardiomyocyte isolation, western blotting, histology and electron microscopy.

Several key survival signalling proteins, including AKT, PKCε, and AMPK, showed a biphasic profile of expression that parallels the biphasic profile of cardiac vulnerability to I/R. Inhibition of these proteins reduced cardiomyocyte viability and increased cardiac infarct size in 14-day olds, but not in adults. Mitochondria, which are important endpoints for survival signalling, displayed changes in morphology indicative of less injury and disruption in 14-day old than adult hearts following I/R. Ultrastructures associated with cardioprotection (e.g. caveolae and exosome containing MVBs) were also more abundant in 14-day old hearts in comparison with adults. In conclusion, these data show that the least vulnerable age group (14-day olds) has an abundance of pro-survival proteins and that their inhibition rendered them more vulnerable to I/R, which was supported by ultrastructural changes.

Dedication

This thesis is dedicated to my mother and father, who have been supportive and caring throughout everything, who have kept me going knowing there was always someone to turn to on the difficult days, and who have often sacrificed their own comfort for the sake of my future. I would not have come this far without my parents, and am so grateful to have them in my life.

Acknowledgements

I would like to thank my supervisor Professor Saadeh Suleiman for all of the guidance and support he has provided, as well as his dedication and patience throughout the carrying out of this work and writing of this thesis. He has given a great deal of advice and many opportunities to present this work at conferences, all of which I believe will be very helpful in the next stages of my career, and for which I am incredibly grateful. Thank you also to my co-supervisor Professor Massimo Caputo for his clinically-related contributions.

I would also like to thank Hua Lin for all of the time she took to teach me experimental techniques in the lab. She has always been helpful and reliable when something goes wrong, and has taught me how to troubleshoot and overcome issues that arise. Thank you also to Martin Lewis for his help in the lab and for sharing his proteomic output, to Igor Khaliulin for sharing his expertise of the Langendorff setup, to Gini Tilly and Judith Mantell for their help with electron microscopy work, and to Kate Heesom and Marieangela Wilson for all of their help with proteomics.

Finally, I would like to give a special thank you to my family and friends for always being there to support me. To my parents, who made a huge difference knowing they would be there at home at the end of the day, and that I could always depend on for words of encouragement. To Haneen, who I am so thankful started this journey on the very same day as me, and who has been a constant friend both in and out of the lab throughout this PhD. I will miss the coffee and the laughter. And to my family and friends scattered around the country and the rest of the world, who I do not get to see very often, but are always there with a message to cheer me up.

Thank you to everyone that has helped throughout this project.

Author's Declaration

I declare that the work in this dissertation was carried out in accordance with the requirements of the University's Regulations and Code of Practice for Research Degree Programmes and that it has not been submitted for any other academic award. Except where indicated by specific reference in the text, the work is the candidate's own work. Work done in collaboration with, or with the assistance of, others, is indicated as such. Any views expressed in the dissertation are those of the author.

SIGNED: ..... DATE:.....

List of Publications & Presentations

Abstract Publications

- Summers K, Lin H, Caputo M*,* Suleiman MS. 'P13 Changes in mitochondrial morphology & distribution during postnatal development.' *Heart* 2018;**104:**A6-A7.
- Summers K, Lewis M, Lin H, Heesom K, Caputo M, Suleiman MS. 'Biphasic changes in survival signalling protein expression during postnatal development; the association with vulnerability to ischemia-reperfusion injury.' *JIOMICS* 2017;**7:**23-46
- Summers K, Lewis M, Lin H, George Sarah, Suleiman MS. 'Changes in survival signalling-related cardiac phosphoproteome during postnatal development: implications for vulnerability to ischemia/reperfusion.' *Curr Res Cardiol* 2016;**3:**89-116
- Summers K, Lewis M, Lin H, George S, Suleiman MS. 'Changes in cardiac survival signalling during postnatal development: implications for cardioprotection.' *J Mol Cell Cardiol* 2016;**97 S:**1-2

Oral Presentations

- 'Biphasic changes in survival signalling protein expression during postnatal development; the association with vulnerability to ischemia-reperfusion injury.' *5th International Congress on Analytical Proteomics conference,* **June 2017.** Lisbon, Portugal

Poster Presentations

- **'**Changes in mitochondrial morphology & distribution during postnatal development.' *BSCR Autumn Meeting 2017 – Cardiac Metabolic Disorders and Mitochondrial Dysfunction,* **September 2017.** Oxford, UK
- 'Biphasic changes in survival signalling protein expression during postnatal development; the association with vulnerability to ischemia-reperfusion injury.' *5th International Congress on Analytical Proteomics conference,* **June 2017.** Lisbon, Portugal
- 'Changes in survival signalling-related cardiac phosphoproteome during postnatal development: implications for vulnerability to ischemia/reperfusion.' *3rd European Section Meeting of the International Academy of Cardiovascular Sciences,* **October 2016.** Marseille, France

- ‘Changes in cardiac survival signalling during postnatal development: implications for cardioprotection.’ *“Ischemic conditioning and targeting reperfusion injury: a 30 year voyage of discovery” conference,* **May 2016.** Barcelona, Spain

Awards/Prizes

- Excellent Poster Presentation Award. *5th International Congress on Analytical Proteomics conference,* **June 2017.** Lisbon, Portugal
- Keld Kjelsen Biomedical Science Poster Prize. *International Academy of Cardiovascular Sciences (IACS) 3RD European Section Meeting,* **October 2016.** Marseille, France

Table of Contents

List of Figures

List of Tables

Abbreviations

Aak1 – AP2-associated protein kinase 1

ADP – Adenosine diphosphate

AIF – Apoptosis inducing factor

Aifm1 – Apoptosis inducing factor 1, mitochondrial

Akt – Protein kinase B

Akap12 – A-kinase anchor protein 12

AMP – Adenosine monophosphate

AMPK – Adenosine monophosphate-activated protein kinase

ANOVA – Analysis of variance

AR – Aspect ratio

Araf – Serine/Threonine protein kinase A-Raf

Arhgef2 – Rho guanine nucleotide exchange factor 2

ATP – Adenosine triphosphate

ATPase – ATP synthase

AUC – Area under curve

BAD – B-cell lymphoma 2-associated agonist of cell death

BAX – B-cell lymphoma 2-associated X protein

Bcl-2 – B-cell lymphoma 2

Bclaf1 – B-cell lymphoma 2-associated transcription factor 1

Birc6 – Baculoviral IAP repeat-containing protein 6

BIS – BCL2-interacting death suppressor

Bnip2 – BCL2/adenovirus E1B 19 kDa protein-interacting protein 2

bpm – Beats per minute

BSA – Albumin from bovine serum

Ca – Calcium

Ca^{2+} – Calcium ion

$CaCl_2$ – Calcium chloride

cAMP – Cyclic adenosine monophosphate

Canx - Calnexin

Carhsp1 – Calcium-regulated heat-stable protein 1

CAT – Catalase

Cav-1/-2/-3 – Caveolin-1/-2/-3

CD63 – CD63 antigen

Cd99 – CD99 antigen

Cdc42 – Cell division control protein 42

CICR – Calcium Induced Calcium Release

CID – Collision-induced dissociation

CK – Creatine kinase

CK2 – Casein kinase 2

Cl – Chloride

Cl^- – Chloride ion

COX – Cytochrome oxidase

Cox6a1 – Cytochrome c oxidase subunit 6A1, mitochondrial

Cox6a2 – Cytochrome c oxidase subunit 6A2, mitochondrial

Cox6b1 – Cytochrome c oxidase subunit 6B1, mitochondrial

Cox7a2 – Cytochrome c oxidase subunit 7A2, mitochondrial

Ctnna1 – α-Catenin

Ctnnb1 – β-Catenin

Cyt c – Cytochrome c

Dcaf8 – DDB1- and CUL4-associated factor 8

DMSO – Dimethyl sulphoxide

DNA – Deoxyribonucleic acid

Drp1 – Dynamin-1-like protein

E-C Coupling – Excitation-Contraction Coupling

ECL – Enhanced chemiluminescence

EGTA – Ethylene glycol-bis(2-aminoethylether)-N,N,N’,N’-tetraacetic acid

EGR1 – Early growth response protein 1

eNOS – endothelial Nitric Oxide Synthase

ERK1/2 – Extracellular signal-regulated protein kinases 1 and 2

ETC – Electron transport chain

FD – fold difference

Fis1 – Mitochondrial fission 1 protein

GAPDH – Glyceraldehyde 3-phosphate dehydrogenase

GLUT4 – Glucose transporter type 4

GPx – Glutathione peroxidase

GSK3β – Glycogen Synthase Kinase 3 beta

H^+ – Hydrogen ion/proton

H_2O – Water

H_2O_2 – Hydrogen peroxide

HEPES – 4-(2-Hydroxyethyl)piperazin-1-ylethanesulphonic acid

HIF – Hypoxia-inducible Factor

Hist1h3c – Histone H3

Hnrnpk – Heterogeneous nuclear ribonucleoprotein K

Hras – GTPase HRas

HSP – Heat shock protein

Hsp90aa1 – Heat shock protein 90-alpha 1/HSP90

Hsp90ab1 – Heat shock protein 90-beta 1/HSP90

Hspa12b – Heat shock 70 kDa protein 12b/HSP70

Hspa5 – Heat shock protein 70 family protein 5/Endoplasmic reticulum chaperone BiP/GRP78

Hspa9 – Heat shock 70 kDa protein 9/75 kDa glucose-related protein/GRP75

Hspb1 – Heat shock protein beta-1/HSP27

Hspb6 – Heat shock protein-beta 6

IF – Interfibrillar mitochondria

IHC – Immunohistochemistry

IKKα – Inhibitor of nuclear factor kappa-B kinase subunit alpha

IMM – Inner mitochondrial membrane

IPreC – Ischemic pre-conditioning

IPostC – Ischemic post-conditioning

I/R – Ischemia/Reperfusion

I/RI – Ischemia/Reperfusion Injury

IVS – Interventricular septum

JAK – Janus Kinase

JNK – Mitogen-activated protein kinase

K – Potassium

K^+ – Potassium ion

KCl – Potassium chloride

KH_2PO_4 – Potassium dihydrogen phosphate

Kras – GTPase KRas

LATS – Serine/threonine protein kinase LATS

LC MS/MS – liquid chromatography mass spectrometry/mass spectrometry

Ldlrap1 – Low density lipoprotein receptor adapter protein 1

LV – Left ventricle

Map2k5 – Dual specificity mitogen-activated protein kinase kinase 5

Map4k4 – Mitogen-activated protein kinase kinase kinase kinase 4

MEK – Dual specificity mitogen-activated protein kinase kinase 1

Mfn-1 – Mitofusin 1

Mfn-2 – Mitofusin 2

Mg – Magnesium

$MgCl_2$ – Magnesium chloride

$MgSO_4 \cdot 7H_2O$ – Magnesium sulphate

MitoK_{ATP} – Mitochondrial ATP-dependent K^+ channel

mPTP – Mitochondrial permeability transition pore

mRNA – Messenger ribonucleic acid

Mt-co2 – Cytochrome c oxidase subunit 2

mTOR – Mammalian target of rapamycin

mTORC1 – mTOR complex 1

MVB – Multivesicular body

Na – Sodium

Na^+ – Sodium ion

Na_2HPO_4 – Di-sodium hydrogen phosphate

NaCl – Sodium chloride

NADPH – Nicotinamide adenine dinucleotide phosphate, reduced

$NaH_2PO_4 \cdot 2H_2O$ – Sodium dihydrogen phosphate

$NaHCO_3$ – Sodium hydrogen carbonate

NaOH – Sodium hydroxide

NCX – Na^+-Ca^{2+} exchanger

NH_2 – Amine group

NO^- – Nitric oxide ion

NOS – Nitric oxide synthase

O_2 – Oxygen

$O_2^-\bullet$ – Superoxide

Opa1 – Optic atrophy 1

Ox. Phos. – Oxidative Phosphorylation

P14 – Postnatal day 14/14-days old

P28 – Postnatal day 28/28-days old

P4hb – Protein disulphide isomerase

P7 – Postnatal day 7/7-days old

PBS – Phosphate buffered saline

Pdap1 – 28 kDa heat- and acid-stable phosphoprotein

PDK1 – 3-phosphoinositide-dependent protein kinase 1

PI3K – Phosphoinositide-3-kinase

PI3K-C2α – Phosphatidylinositol-4,5-bisphosphate 3-kinase catalytic subunit type 2 alpha

PI3K-R1 – Phosphatidylinositol 3-kinase regulatory subunit alpha

PKA – Protein kinase A

PKC – Protein Kinase C

PKG – cGMP-dependent protein kinase 1

PN – Perinuclear mitochondria

Ppp1cc – Serine/threonine-protein phosphatase PP1-gamma catalytic subunit

Ppp2r1a – Serine/threonine-protein phosphatase 2A 65 kDa regulatory subunit A alpha isoform

PRAS40 – Proline-rich AKT1 substrate 1

Prkar1a – cAMP-dependent protein kinase type I-alpha regulatory subunit

Prkar2b – cAMP-dependent protein kinase type II-beta regulatory subunit

Prkcdbp – Caveolae associated protein 3/Cavin-3/Protein Kinase C delta-binding protein

Prx – Peroxiredoxin

PTEN – Phosphatidylinositol 3,4,5-trisphosphate 3-phosphatase and dual-specificity protein phosphatase

PVDF – Polyvinylidene difluoride

Raf – RAF proto-oncogene serine/threonine-protein kinase

Raptor – Regulatory-associated protein of mTOR

Ras – GTPase Ras

RhoA – Ras homolog gene family, member A

RIPA – Radio-immunoprecipitation assay

RIPC – Remote ischemic preconditioning

RISK – Reperfusion Injury Salvage Kinase

ROCK – Rho-associated protein kinase

ROS – Reactive oxygen species

rpm – Revolutions per minute

RV – Right ventricle

SA – Sino atrial

SAFE – Survivor Activating Factor Enhancement

SDS – Sodium dodecyl sulphate

SE – Standard error

Ser – Serine

SERCA – Sarco/endoplasmic reticulum Ca^{2+}-ATPase

Sim. I/R – Simulated Ischemia/Reperfusion

SOD – Superoxide dismutase

SOD-1 – Superoxide dismutase 1

Speg – Striated muscle preferentially expressed protein kinase

SR – Sarcoplasmic reticulum

SSL – Subsarcolemmal mitochondria

STAT – Signal transducer and activator of transcription

TAK1 – Nuclear receptor subfamily 2 group C member 2

Thr – Threonine

TiO_2 – Titanium dioxide

TLR4 – Toll-like Receptor 4

TMT – Tandem mass tag

TNF – Tumor necrosis factor

Tns1 – Tensin-1

Tp53i11 – Tumor protein p53-inducible protein 11

TRIM72 – Tripartite motif-containing protein 72

TSC2 – Tuberin

Tsg101 – Tumor susceptibility gene 101 protein

TTC – 2, 3, 5-triphenyl-tetrazolium chloride

T-tubule – Transverse tubule

Ube2e3 – Ubiquitin-conjugating enzyme E2 E3

Uqcrh – Cytochrome b-c1 complex subunit 6, mitochondrial

VDAC – Voltage-dependent anion channel

v/v – volume/volume

w/v – weight/volume

w/w – weight/weight

Yap1 – Yes-associated protein 1

Ywhae – 14-3-3 protein epsilon

Ywhah – 14-3-3 protein eta

Ywhag – 14-3-3 protein gamma

Ywhaz – 14-3-3 protein zeta/delta

Chapter 1: Introduction

1.1 Cardiac changes during postnatal development

The cardiac pump changes during postnatal development to cope with a growing organism (Ostadal, Ostadalova et al. 1999, Janowski, Cleemann et al. 2006). These changes include those at the molecular, cellular, structural, and functional levels, which provide the basis upon which a transition from foetal and neonatal physiology to that seen in the mature heart can be achieved. In the foetal environment, hearts exist in a state of constant physiological hypoxia, with an oxygen saturation of 18% and oxygen tensions of 47 mm Hg in comparison to the usual 97% and 160 mm Hg levels seen postnatally (Ostadal, Ostadalova et al. 2009). Foetal hearts are well adapted to this hypoxic environment, with foetal haemoglobin displaying a correlating oxygen dissociation curve with a leftward shift, and are consequently less susceptible to hypoxic injury (Ostadal, Ostadalova et al. 2014). Transition from this hypoxic environment at birth therefore requires postnatal adaptation to atmospheric oxygen levels, such as the need for pulmonary circulation and a rapid increase in metabolic rate (Ostadal, Ostadalova et al. 2009). Due to this recent transition from a hypoxic state, early neonates still remain less vulnerable to ischemia and oxygen deprivation, as they are able to revert temporarily to their foetal metabolism (Ostadal, Ostadalova et al. 2009). Over the course of postnatal development, further changes in processes such as metabolism occur in order for the heart to adapt to its new oxygen-rich environment, for example, with a switch from anaerobic in foetal and neonatal hearts to aerobic respiration in adults (Ostadal, Ostadalova et al. 2014). Several of these changes are also implicated in the injury seen following ischemia and reperfusion (I/R) (Ostadal, Ostadalova et al. 2014), and their implications in the changing vulnerability to I/R injury (I/RI) during postnatal development (Ostadal, Ostadalova et al. 2009). Key cardiac developmental changes and their potential

involvement in reperfusion injury and in the design of cardioprotective strategies will subsequently be discussed.

1.1.1 Metabolic changes & the role of mitochondria

The switch from the hypoxic foetal environment to an oxygen-rich one, and subsequent postnatal developmental changes, are accompanied by significant changes in metabolism, transitioning from predominantly anaerobic respiration to aerobic respiration (Ostadal, Ostadalova et al. 2009). Changes in metabolic activity are critical over the course of postnatal development in providing the needed energy for a growing heart and for increasing cardiac pump function. As neonates begin to consume milk, the altered availability of substrates allow for a switch from a largely glycolysis-based to fatty acid β-oxidation-based metabolism, with glycolysis contributing < 10% of total ATP production by postnatal day 7 from the < 50% contribution seen immediately after birth (Lopaschuk and Jaswal 2010). This greater dependence on fatty acid β-oxidation supports the increased demands and transition of hearts from low to higher energy utilisation, as it is able to produce a significantly greater number of ATP molecules per unit substrate (Neary, Ng et al. 2014). Whilst glycolysis is able to generate two ATP molecules per molecule of glucose (Liu 2006), a single C_{18} fatty acid molecule is able to yield 90 molecules of ATP via the citric acid (TCA) cycle and electron transport chain (ETC), with a further 30 molecules of ATP due to the capture of electrons by the β-oxidation cycle (Goetzman 2011). Fatty acid β-oxidation is known to be a key source for the oxidative metabolism of mitochondria (Lopaschuk and Jaswal 2010), and as such, these increases in fatty acid β-oxidation as the heart develops postnatally are accompanied by increases in mitochondrial number, size and functionality (Neary, Ng et al. 2014).

The mitochondria are known as the powerhouse of the cardiomyocyte, and have been found to transition from a single population with relatively high membrane potential in neonates, to two separate mitochondrial populations – the second arising during the weaning period with a lower membrane potential – in parallel with the gradual ordering of initially chaotically organised mitochondria and muscle fibres (Skarka et al. 2003, Milerova, Charvatova et al. 2010). There are also increasing cytochrome c oxidase (COX) levels and activity alongside increasing adenine nucleotide flux across the inner mitochondrial membrane during postnatal development (Johnson et al. 2006). Moreover, the number and volume of mitochondria themselves have been shown to rise during postnatal development (Olivetti, Anversa et al. 1980), with a doubling within the first 5 postnatal days of mitochondrial density, size, volume and number in rat hearts. These changes are critical to cope with increasing energy demands in rat hearts.

Unlike fragmented foetal mitochondria, postnatal mitochondria possess a more elongated morphology associated with exit from the hypoxic prenatal environment and subsequent driving of mitochondrial fusion, and correlating with the postnatal switch from glycolysis to fatty-acid β-oxidation (Neary, Ng et al. 2014). Such changes have been suggested to result from decreases in Hypoxia Inducible Factor (HIF) signalling upon entering the oxygen-rich postnatal environment, resulting in alterations to the expression of lipid metabolism related genes (Neary, Ng et al. 2014). Indeed, previous work (Narravula and Colgan 2001, Zhang, Bosch-Marce et al. 2008) demonstrated that the overexpression of HIF resulted in a reduced respiratory capacity, in addition to decreased biogenesis of mitochondria. In keeping with relatively lower levels of aerobic metabolism in the neonatal heart in comparison with adults, the underdeveloped mitochondria have large separation between cristae, but

greater intake of Ca^{2+} into the mitochondria via the Ca^{2+}-uniporter in neonates that shows a gradual decrease after 14 postnatal days in rats (Bassani, Fagian et al. 1998).

1.1.2 Changes in Ca^{2+} cycling during E-C coupling

Key processes that require a great deal of energy consumption in the heart are Ca^{2+} cycling and excitation-contraction (E-C) coupling, which change during postnatal development with the growing heart and increasing cardiac pump function, and are supported by the previously discussed changes in metabolic activity with age (**Section 1.1.1**). In the adult heart, E-C coupling involves the opening of voltage-gated Ca^{2+} channels (dihydropyridine receptors, DHPR) during an action potential (AP), allowing an influx of Ca^{2+} into the cell (Bers 2002). This in turn triggers the release of Ca^{2+} from the sarcoplasmic reticulum (SR) via the ryanodine receptors (RyR) in a process known as calcium-induced calcium release (CICR), this local release from the SR creating Ca^{2+} sparks which are eventually summed, alongside the entry of extracellular Ca^{2+}, to a sufficient cytosolic Ca^{2+} concentration for binding to troponin C present within the myofilaments and subsequent contraction (Bers 2002). During relaxation, cytoplasmic Ca^{2+} concentrations are lowered via closing of the RyRs, via the action of SR Ca^{2+}-ATPases (SERCA) which transport Ca^{2+} from the cytosol back into the SR, and via the Na^{+}-Ca^{2+} exchanger (NCX) which exports Ca^{2+} from the cardiomyocyte in exchange for Na^{+} to restore resting cytosolic Ca^{2+} concentrations (Eisner et al. 2017). In adult hearts, triggering of this signal from an AP is propagated throughout the cell via transverse tubules (t-tubules), which are invaginations of the plasma membrane extending from the cell surface and to the interior of the cardiomyocyte, allowing the rapid transmission of the signal throughout the entire cell and to the SR via the DHPR (Calderon et al. 2014).

Whilst both Ca^{2+}-influx across the sarcolemma and Ca^{2+} release from the SR play important roles in the contraction of the adult myocardium, neonatal hearts are more reliant upon the influx of extracellular Ca^{2+}, due to the underdevelopment of t-tubules and the SR (Ostadal, Ostadalova et al. 1999). As the SR develops postnatally, sufficient Ca^{2+} is accumulated within them which is subsequently available for release during E-C coupling, resulting in a switch from more extracellular to more SR-based Ca^{2+} transients (Ostadal, Ostadalova et al. 1999). This is coupled to the formation of t-tubules over the course of postnatal development. As seen in **Figure 1**, neonatal cardiomyocytes do not display the characteristic striations indicative of t-tubules that are seen in the adult cardiomyocyte, meaning there is a lack of DHPR and RyR co-localisation at this stage of development, with Ca^{2+} sparks detectable predominantly around the subsarcolemmal region (Seki, Nagashima et al. 2003). As the heart develops postnatally, there is a gradual appearance of these striations (t-tubules) with age and as the cardiomyocytes increase in size, indicating that the usual coupling seen between the DHPR and SR via RyR at the dyadic junction – not present in neonates – begins to arise at 14-days of age, and fully into adulthood (Schroder, Wei et al. 2006).

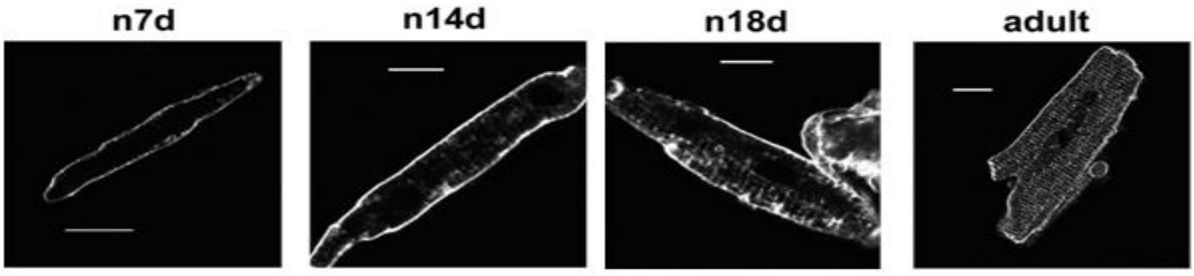

Figure 1. Figure showing the development of t-tubules during postnatal development in rat hearts. Striations within the cells do not appear until 14-days postnatally, with some striations appearing by day 18. Scale bars: P7, 10 µm; P14, 5 µm; P18, 10 µm; adult, 20 µm. (Seki, Nagashima et al. 2003)

As previously mentioned, this underdevelopment of t-tubules and lack of coupling with RyR and the SR in neonates means that cardiomyocytes at this stage of development have a much greater reliance on the entry of extracellular Ca^{2+} for contraction. It has been demonstrated that, in early postnatal cardiomyocytes, the NCX is instead key in controlling Ca^{2+} cycling, allowing entry of Ca^{2+} to the cell for direct binding and activation of myofilament components (Qu, Ghatpande et al. 2000). Correlating with this dependence on the action of the NCX for Ca^{2+} influx, higher levels of both NCX protein expression and NCX mRNA have been found in neonates in comparison with adults, followed by a gradual decrease over the course of postnatal development (Boerth, Zimmer et al. 1994).

Due to the underdevelopment of the SR and t-tubules, and reliance on the NCX, E-C coupling in immature rat hearts is slower in terms of Ca^{2+}-cycling (Balaguru, Haddock et al. 1997, Seki, Nagashima et al. 2003), with a CICR threshold 10 times lower in 2 day old hearts compared with 30 day old hearts (Fabiato and Fabiato 1978).

1.2 Cardiac structural changes during postnatal development

Another important change during postnatal development is the transition from hyperplasic to hypertrophic growth. Increases in heart mass is supported by hyperplasia of the cardiomyocytes up until 4 days postnatally in rats (Olivetti, Anversa et al. 1980), following which growth continues as a result of hypertrophy of existing cardiomyocytes (Bicknell, Coxon et al. 2004, Chen, Yu et al. 2004), resulting in an increase in heart weight over the first 11 postnatal days of 5-fold in rats (Johnson and Brown-Borg 2006). An increasing left ventricular radius accompanies this (Wu and Wu 2009). This initial period of hyperplasia correlates with a greater packing density of cardiomyocytes at this stage of postnatal development in comparison with 7-day old hearts, and with larger extracellular spaces in 7-

day old hearts that may be present in order to allow for hypertrophic growth of existing cells to occur (Wu and Wu 2009). Similarly, myocardial fibre width was shown to be greater in 7-day old hearts than 2-4 day olds, increasing further until day 21, after which point no significant changes are seen due to the cessation of hypertrophy, reflecting structural maturity at this stage of development (Wu and Wu 2009). Cardiac growth during development requires an associated and compensatory increase in blood flow to the heart to support the metabolic needs of the heart, and whilst capillaries within the heart have been shown to display corresponding growth, the same is not necessarily seen in the larger blood vessels, resulting in the increase in coronary vascular resistance over the course of postnatal development (Hudlicka and Brown 1996). Additionally, differences in Ca^{2+}-handling during postnatal development mean that myofibrils in neonates are initially disorganised and localised within the cell so as to optimise extracellular Ca^{2+} entry and binding to the contractile units (Vornanen 1996).

1.3 Cardiac functional changes during postnatal development

Due to the increasing haemodynamic load that occurs during postnatal development, developing hearts display a gradual increase in stroke volume and cardiac output, in addition to ejection fractions that have been shown in rat hearts to increase until 4 postnatal days, before decreasing at day 7, and then gradually increasing once more until day 21 (Wu and Wu 2009). At this stage, the ejection fraction stabilises, corresponding with the reaching of functional maturity. A similar change in ejection fraction with development was also described in human infants from 2 to 14 postnatal months (Oberhansli, Brandon et al. 1981). Furthermore, developing rat hearts display a change in contractile performance – as determined by measurements of developed force – that includes a decrease from day 1 to

day 4, before increasing over the course of postnatal development, mitochondrial mass, and myofibrillar ATPase activity that follows postnatal development (Oštádalová, Kolář et al. 1993, Wu and Wu 2009).

These functional changes are accompanied by developmental changes in heart rate, increasing from approximately 300 beats/min at birth to a maximum of 500 beats/min in adult rats (Wekstein 1965, Adolph 1967). It is suggested that the altered Ca^{2+}-handling seen during postnatal development (discussed in **Section 1.1.1**), with a switch from heavier dependence on extracellular Ca^{2+} influx for the activation of muscle contraction in the immature heart, to intracellular and SR-based Ca^{2+} in adult hearts, correlate with and may account for such changes in heart rate (Vornanen 1992).

1.4 Cardiac Development and ischemia/reperfusion injury

1.4.1 Ischemia/reperfusion injury: an overview

Cessation or reduced blood flow to the heart, known as ischemia, predisposes the myocardium to reperfusion injury following reintroduction of blood flow (Hausenloy and Yellon 2013). The underlying cause of I/RI is multi-factorial, the key mechanisms being oxidative stress, Ca^{2+}-overload, and opening of the mPTP. Lactate production and decreased intracellular pH resulting from the switch to anaerobic respiration during ischemia leads to activation of Na^{+}-H^{+} exchanger, and subsequent Na^{+}-overload (Hausenloy and Yellon 2013). This in turn causes an efflux of Na+ in exchange for Ca^{2+} via activation of the Na^{+}-Ca^{2+} exchanger, resulting in Ca^{2+}-overload, as shown in **Figure 2**.

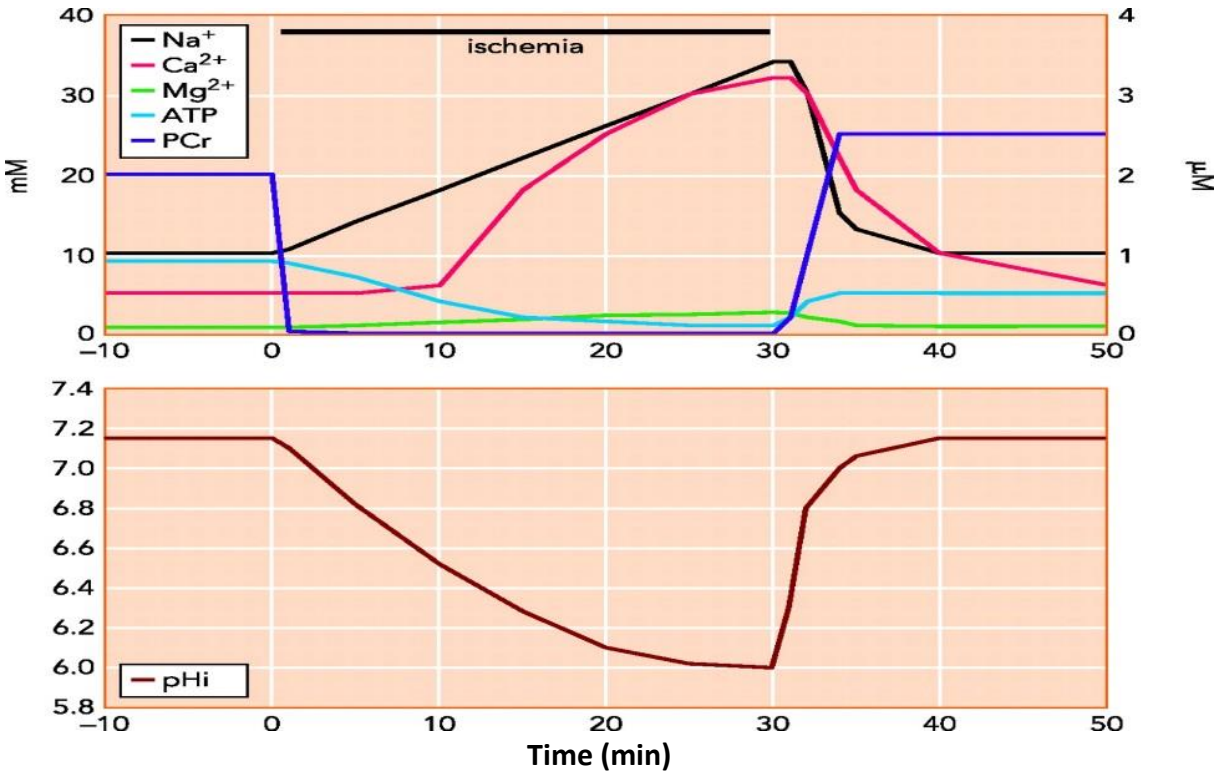

Figure 2. The cellular, metabolic and ionic changes that occur during a relatively short period of ischemia (30min) followed by reperfusion in the rat heart. (Murphy and Steenbergen 2008)

While mPTP opening does not occur during ischemia due to the high acidity, reperfusion results in restoration of pH and opening of the mPTP. Reperfusion also leads to the hyperactivity of the Electron Transport Chain (ETC), causing excessive ROS production, which in turn acts to sensitise the mPTP to Ca^{2+}, as a neutrophil chemoattractant, and as a contributing factor to SR dysfunction. This oxidative stress not only further exacerbates Ca^{2+}-overload through dysfunction of the SR, but also through damage of the plasma membrane itself (Halestrap, Clarke et al. 2007, Hausenloy and Yellon 2013). mPTP opening is an important trigger for cell death that occurs with I/RI, as it results in either necrosis via ATP-depletion, due to the permeation of the IMM resulting in collapse of the mitochondrial membrane potential needed to drive oxidative phosphorylation (Hausenloy, Ong et al.

2009), or activation of the apoptotic pathway via the release of factors such as Cytochrome c and Apoptosis Inducing Factor (AIF) (Shintani-Ishida, Inui et al. 2012).

1.4.2 Ischemia/reperfusion injury during postnatal development

The vulnerability of hearts to I/RI changes over the course of postnatal development, with a bell-shaped profile that can be seen in **Figure 3**. Ostadalova et al. (1998) demonstrated that recovery of the developed force falls from day 1 to day 7, before increasing once again from day 7 to day 10 in rats, an improvement in recovery that was shown by Riva & Hearse (1991) to further increase until a peak at 17 postnatal days that subsequently falls when going into adulthood (Riva and Hearse 1991, Ostadalova, Ostadal et al. 1998). This pattern of change in vulnerability correlates with the previously described switch from proliferative, hyperplasiac growth 4 days postnatally in rat (Bicknell, Coxon et al. 2004, Chen, Yu et al. 2004), with the highest percentage recovery levels seen at 17 and 25 postnatal days potentially reflecting the reported achievement of functional and structural maturity at 21 days of age (Wu and Wu 2009). Similarly to this, findings from Modi & Suleiman (2004) highlight a peak in functional recovery following I/RI at 14-days of age in rats, a pattern that was shown to be mimicked in rabbit hearts (Suleiman et al, unpublished data) as shown in **Figure 3A**. Notably, this apparent “triphasic” pattern of change in tolerance was found to exist only in male rats (Ostadal, Ostadalova et al. 2014), whereas female rats deviated from males in terms of cardiac vulnerability following the end of the weaning period at 28-days postnatally (Ostadal, Netuka et al. 2009, Ostadal and Ostadal 2014). Cardiac vulnerability to injury therefore shows a more “biphasic” pattern of change during postnatal development, as the decrease in tolerance seen in male rats from day 30 to day 60 is not seen in females, indicating a greater resistance in the adult female rat heart to I/RI related damage (Ostadal,

Ostadalova et al. 2014). These changes in vulnerability to cardiac injury have also been linked to changes in caloric intake and body mass during development, which has been shown to be lower both during the first days post-partum and at the start of the weaning period at around day 16, suggesting a link between tolerance to hypoxia and decreases in body mass (Ostadalova and Babicky 2012, Ostadal, Ostadalova et al. 2014).

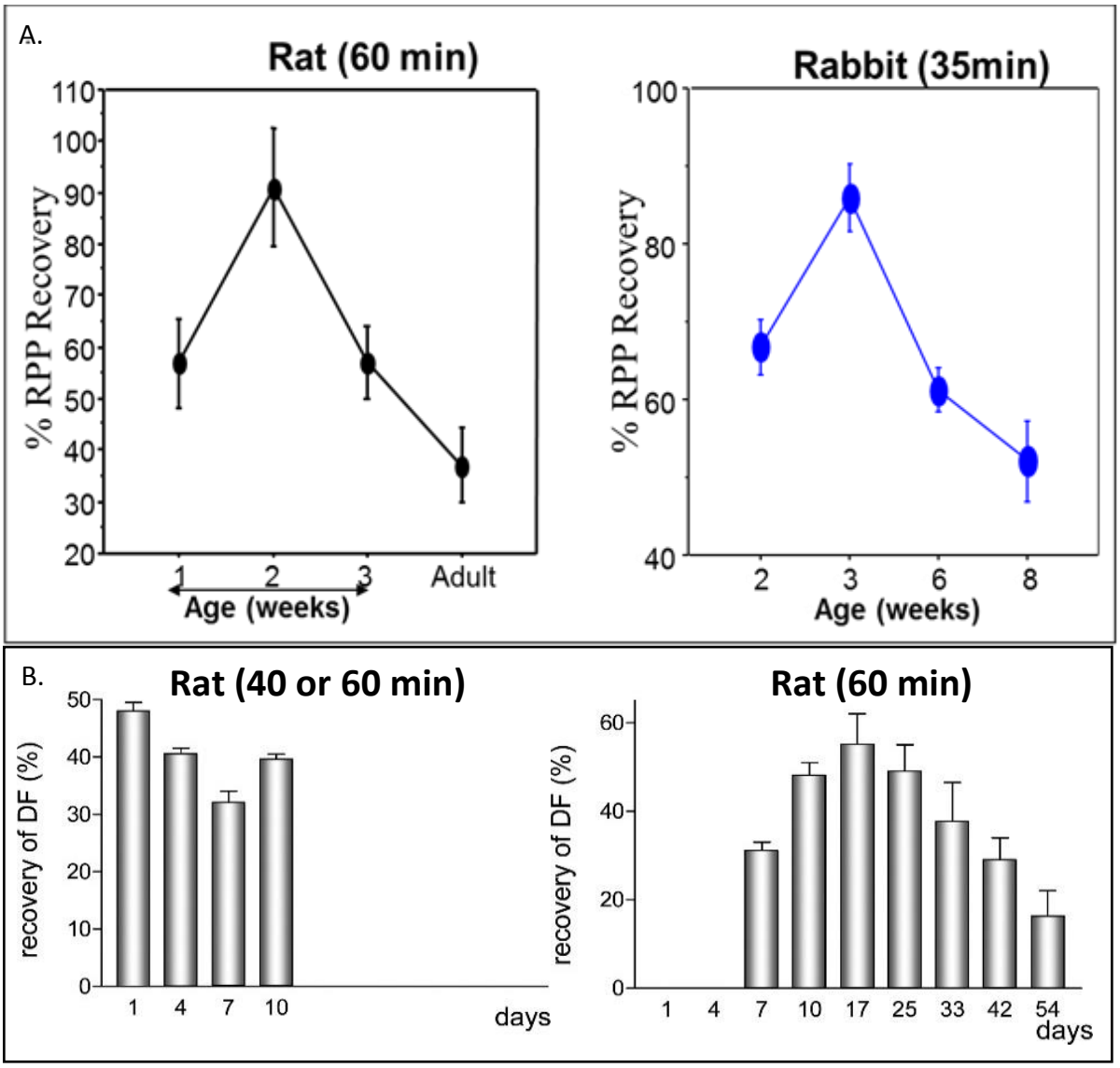

Figure 3. The cardiac vulnerability profile of developing hearts in rats (left) and rabbits (right) following 60 minutes and 35 minutes of ischemia, respectively **(A)**. The profile for earlier postnatal development in rat hearts following 40 or 60 minutes of ischemia **(B)**. RRP = Rate Pressure Product. DF = Developed Force. (Modi and Suleiman 2004, Ostadal, Ostadalova et al. 2014)

The exact underlying mechanism behind this difference in vulnerability between age groups is currently uncertain. Possible causes include some of the previously discussed changes that occur during the course of postnatal development, including the switch from glycolytic metabolism to fatty acid β-oxidation, changes in Ca^{2+}-cycling and EC-coupling, and structural and functional changes in mitochondria, as summarised in **Table 1.**

Mechanism/Factor	Change with postnatal development
Energy demand	↑
Anaerobic capacity	↓
Free radical production	↑
Glycogen reserves	↓
Free fatty acid uptake	↑
Mitochondrial:	*Altered*
mPTP sensitivity	↑
Mitochondrial oxidative phosphorylation	↑
Cytochrome c oxidase expression & activity	↑
Adenine nucleotide flux across IMM	↑
Mitochondrial population	Single, high membrane potential → Dual, second with lower membrane potential
Ca^{2+}-handling:	*Altered*
Myofibrillar sensitivity to Ca^{2+}	↑
Dependence on extracellular Ca^{2+}	↓
Magnitude of inotropic response to Ca^{2+}	Biphasic - ↓ day 1-4, ↑ up to day 7
Sensitivity to acidosis	↑
ATP catabolic pathways:	*Altered*
ATP depletion	↑
Recycling of ATP catabolites	↓
AMP accumulation during ischemia	↓

Table 1. The key changes proposed to be involved in the differences in vulnerability to Ischemia/Reperfusion Injury during postnatal development in rat hearts. Adapted from (Ostadalova, Kolar et al. 1993, Ostadal, Ostadalova et al. 1999, Ostadal, Ostadalova et al. 2014)

1.4.3 Changes in antioxidant status

As mentioned in **Section 1.4.1**, the production of ROS during I/RI is an important step leading to cardiomyocyte damage, apoptosis and necrosis (**Figure 4**). Antioxidants are important components that scavenge ROS in order to maintain normal levels in the cell, preventing such damage (Zhou, Prather et al. 2018). As a result of this, potential differences in antioxidant protein expression and activity at different stages of postnatal development has been investigated as a possible contributor to the cardiac vulnerability profile (**Figure 3**).

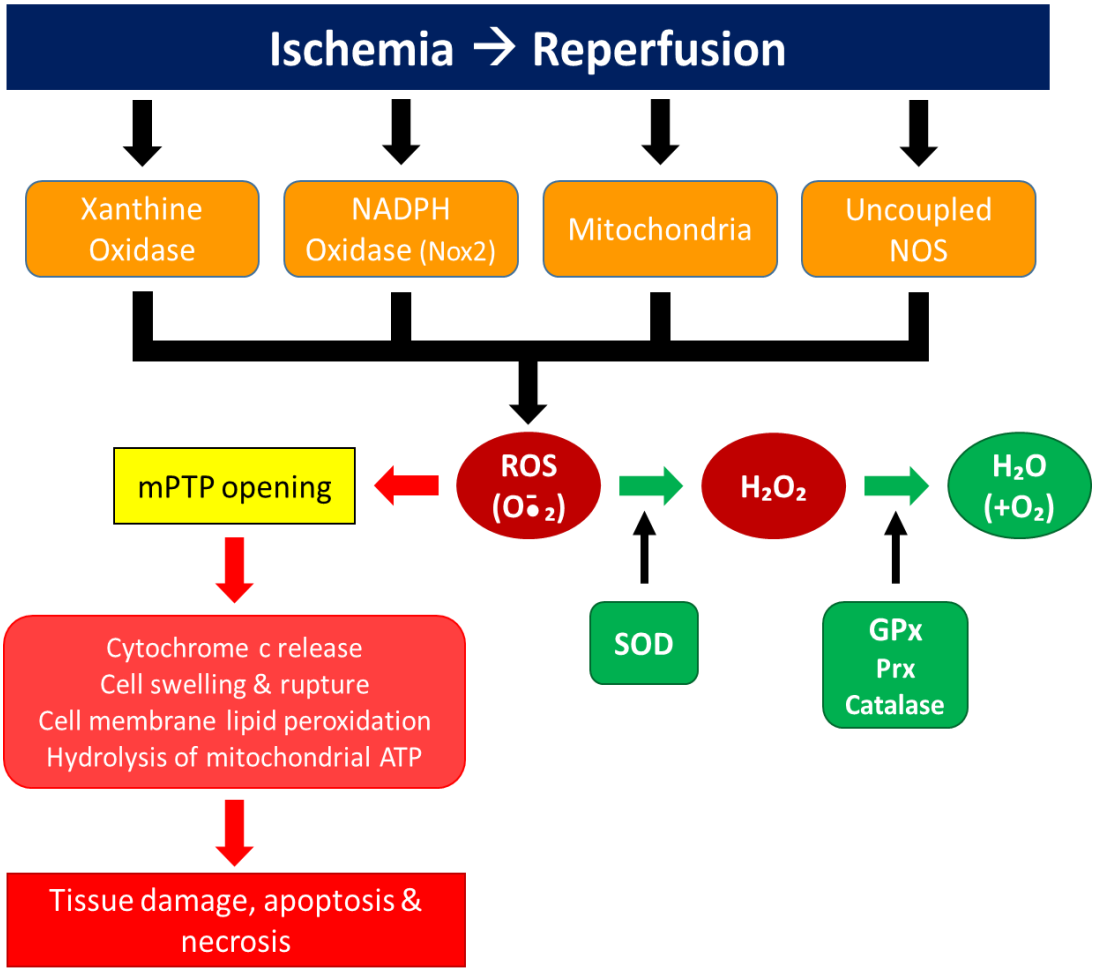

Figure 4. Summary of the production of ROS following I/RI, and the action of antioxidants in scavenging excess ROS. NADPH = nicotinamide adenine dinucleotide phosphate (reduced), NOS = nitric oxide synthase, ROS = reactive oxygen species, mPTP = mitochondrial permeability transition pore, SOD = superoxide dismutase, GPx = glutathione peroxidase, Prx = peroxiredoxin. **(Modified from** (Murphy and Steenbergen 2008) (Granger and Kvietys 2015) (Zhou, Prather et al. 2018)**)**

Whilst current knowledge of the postnatal changes in cardiac antioxidant status is limited in mammals, studies have demonstrated that postnatal differences in antioxidant expression can be found in rat hearts, with lower xanthine oxidase – a producer of reactive oxygen species (ROS) – activity with an associated reduced release of ATP-catabolites following reperfusion in neonatal hearts in comparison with adults (Achterberg, Nieukoop et al. 1988). More recent work undertaken by Sarah Martin (unpublished PhD thesis, 2010) examining the changes in antioxidant expression over the course of postnatal development found that while the activity of total superoxide dismutase (SOD) remained unchanged, SOD1 showed a gradual increase in protein expression from 4 days of age to a maximal level in adult hearts. However, this change did not follow the characteristic biphasic profile of cardiac vulnerability seen across these age groups, and therefore likely represent general developmental changes as opposed to a causal mechanism underlying these developmental differences in the response to I/RI. Furthermore, analysis of SOD1 gene expression did not mimic these age-dependent changes in protein expression.

In addition to work on SOD, Sarah Martin found that glutathione peroxidase (GPx) activity, protein expression and gene expression showed gradual changes during postnatal development that did not follow the biphasic changes seen in cardiac vulnerability. GPx activity and protein expression both displayed decreasing levels with increasing age, a trend mimicked by gene expression albeit without statistical significance, again suggesting it is involved in general developmental changes as opposed to linking directly with the differential responses to I/RI seen across these age groups.

In contrast to SOD and GPx, catalase was found to mimic the biphasic changes seen in cardiac vulnerability both in terms of activity, protein expression and gene expression. In all three,

levels peaked at 14-days of age – although protein expression did show the greatest levels at 21 days of age before dropping again at 28-days of age – in a manner similar to the peak in cardiac resistance to I/RI seen at 14-days of age. As a result, the antioxidant activity of catalase remains a potential component of the underlying mechanism below postnatal developmental changes in cardiac vulnerability.

1.4.4 Mitochondrial permeability transition in postnatal heart

Sensitivity of the mitochondrial permeability transition pore (mPTP) has also been shown to be lower in neonates than adults, with relative reductions in both rate and degree of Ca^{2+}-induced swelling associated with greater resistance to high Ca^{2+} concentrations, which is suggested to at least in part be linked to aforementioned differences in Ca^{2+}-cycling, as well as mitochondrial structure, in neonates in comparison with adults (Milerova, Charvatova et al. 2010). While this does appear to correlate with the greater vulnerability of adult hearts to I/RI, this study looked at rats that were 7-days of age, which in fact showed poorer resistance to I/RI injury than those of 14-days of age. Due to these uncertainties as to the exact mechanism by which neonatal I/RI tolerance is conferred, an alternative potential explanation for the vulnerability profile seen during postnatal development could involve the survival signalling pathways.

1.5 Role of survival signalling in ischemia/reperfusion injury

Survival signalling pathways have been shown to provide cardioprotection against I/R. Two of the key pathways that have thus far been identified are the Reperfusion Injury Salvage Kinase (RISK) and Survivor Activating Factor Enhancement (SAFE) pathways (Tamareille, Mateus et al. 2011), the summaries of which are shown in **Figure 5**. Cardioprotective strategies termed ischemic pre- (IPreC) or post-conditioning (IPostC) have been shown to

increase the expression and activity of survival signalling proteins through the application of brief episodes of coronary occlusion and reperfusion either before or after the ischemic event (Heusch 2015). This increase in survival signalling has been found to correlate with a reduction in infarct size (Tsang, Hausenloy et al. 2004), and these cardioprotective strategies have subsequently been employed during cardiac surgery or following myocardial infarction in an attempt to reduce the degree of cardiac injury that follows (Hausenloy, Lecour et al. 2011, Jones, Pepe et al. 2013).

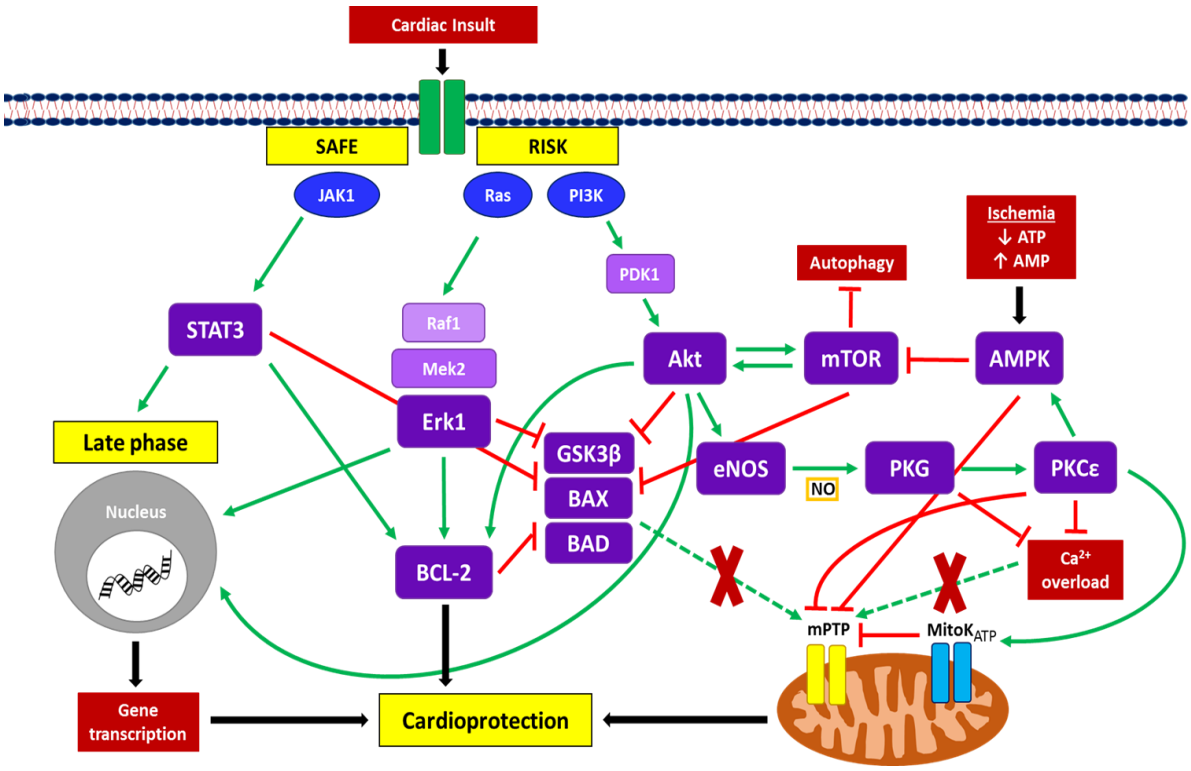

Figure 5. An overview of the RISK-SAFE survival signalling pathways, which involve activation of key survival kinases and subsequent activation of pro-survival proteins and inhibition of apoptotic proteins and pathways.

1.5.1 The RISK Pathway

The RISK pathway consists of a network of pro-survival signalling kinases, the key effectors of which are phosphatidylinositol-3 kinase (PI3K), protein kinase B (Akt), and extracellular

regulated kinase 1/2 (ERK1/2), which act to trigger a cascade of cellular signalling events that promote cell growth and survival, as well as to counteract or inhibit pro-apoptotic signalling (Hausenloy and Yellon 2007, Lecour 2009). Activation of the pathway through administration of factors such as insulin, urocortin, atorvastatin, bradykinin, opioid receptor agonists, and Glucagon-Like-Peptide 1 (GLP1) upon reperfusion of the myocardium has been demonstrated to reduce infarct size following I/R (Hausenloy, Whittington et al. 2013, Heusch 2015). Further members of the signalling pathway include kinases such as protein kinase C (PKC), protein kinase G (PKG) and p70 ribosomal S6 kinase (p70S6K), and downstream targets of phosphorylation including, but not limited to, pro-survival proteins B-cell lymphoma 2 (BCL-2), BCL-XL and heat shock proteins (HSPs), as well as pro-apoptotic proteins such as Glycogen Synthase Kinase 3 beta (GSK3β), B-cell lymphoma 2-associated agonist of cell death (BAD), B-cell lymphoma 2-associated X protein (BAX), BCL-2-like protein 11 (Bim) and members of the caspase family (Boengler, Schulz et al. 2009, Calvert, Jha et al. 2009, Lacerda, Somers et al. 2009, Lecour 2009). The overall effect of these activating or inactivating phosphorylation events is to confer cardioprotection to the heart through inhibition of the apoptotic process.

Whilst many of the other downstream effectors of the RISK pathway currently remain unidentified, ERK1/2 signalling has been shown to result in signalling via Signal Transducer and Activator of Transcription 3 (STAT3). STAT3 is a key component of the second survival signalling pathway, SAFE (Boengler, Schulz et al. 2009, Calvert, Jha et al. 2009), that has been shown, among other actions, to lead to decreases of the pro-apoptotic Bax gene and increase of the anti-apoptotic BCL-2 gene (Lecour 2009). The key proposed action of the RISK pathway in cardioprotection is via inhibition of mPTP opening (Lacerda, Somers et al. 2009, Lecour 2009). Whilst the underlying mechanism behind this effect on mPTP opening remains

uncertain, several potential pathways have been proposed, including GSK3β signalling (Juhaszova, Zorov et al. 2004), activation of eNOS, inhibition of Bax translocation to the mitochondria, and activation of mitochondrial hexokinase II (Murphy and Steenbergen 2008).

1.5.2 The SAFE Pathway

Although a degree of overlap has been proposed between the two survival signalling pathways (Lecour 2009), the key mediators of the SAFE pathway are Janus Kinase (JAK) and STAT3. Activation of this pathway has been demonstrated to occur via the actions of opioids, insulin, sphingosine-1 (Heusch 2015), in addition to Tumor Necrosis Factor α (TNFα) through binding and activation of TNF Receptor 2 and subsequent phosphorylation of JAK (Lacerda, Somers et al. 2009). Following activation of JAK, they are able to in turn phosphorylate STATs, which hetero- or homo-dimerise and translocate to the nucleus in order to promote the transcription of pro-survival proteins (Cohen and Downey 2015). Similarly to the RISK pathway, activation of STAT3 is able to reduce mPTP opening and the associated apoptotic cell death through inactivation of pro-apoptotic Bad and promotion of anti-apoptotic BCL-2 and BCL-XL (Lecour 2009).

1.5.3 The role of AMPK & GSK3β during ischemia/reperfusion

GSK3β is known to be a key target of the RISK-SAFE survival signalling pathways, with inhibition of reportedly pro-apoptotic GSK3β by pro-survival Akt resulting in cardioprotection, as previously discussed. However, studies have also shown that GSK3β activation, as well as that of energy-sensing protein AMP-activated Protein Kinase (AMPK), during ischemia specifically is actually protective to the heart. AMPK works to monitor

cellular energy levels, and is able to detect low energy environments that arise, for example, during ischemia in order to switch to energy-conserving, ATP-synthesising processes (Moussa and Li 2012). Both GSK3β and AMPK have been shown to provide cardioprotection when active during ischemia through several processes, as outlined in **Figure 6**, one of the key being the inhibition of the mTORC1 complex, which in its active state works to promote protein synthesis and inhibit autophagy in response to growth factor and stress signalling (Sciarretta, Volpe et al. 2014). The triggering of autophagy following ischemic insult is important in reducing cardiac injury, as it results in the degradation of cellular organelles and macromolecules for recycling to support ATP-synthesis, as well as the removal of damaged organelles and proteins which may otherwise remain as cytotoxic and injurious components within cells (Moussa and Li 2012). Thus, GSK3β and AMPK-mediated inhibition of mTORC1 and promotion of autophagy during ischemia serves as a cardioprotective mechanism.

As mentioned previously, GSK3β activity during reperfusion is known to be harmful as it promotes opening of the mPTP, and it is subsequently inhibited by Akt and other members of the RISK-SAFE signalling pathway. While autophagy is protective during ischemia via maintenance of energy stores and production, autophagy is also known to be harmful during reperfusion, potentially through excessive degradation of organelles and proteins resulting in autophagic cardiomyocyte death, or through suggested cross-talk between autophagic and apoptotic mechanisms (Ma, Wang et al. 2015). During reperfusion, Akt activation opposes AMPK action through the alleviation of mTORC1 inhibition, thus allowing for the attenuation of autophagy and subsequent reduction in cell injury (Chaube and Bhat 2016). While AMPK and Akt appear to have conflicting roles in terms of the activation of mTORC1

and autophagy during reperfusion, both AMPK and the RISK-SAFE pathways have been shown to be activated by the same signalling molecules and cardioprotective agents (Moussa and Li 2012)(Hausenloy and Yellon 2007), with AMPK also demonstrating the ability to inhibit mPTP opening and reduce myocardial infarct size (Paiva, Rutter-Locher et al. 2011). Other studies have indicated that autophagy during the reperfusion period is independent of AMPK, instead being mainly mediated by beclin-1, suggesting it is possible that increased AMPK activity as a response to depleted energy supplies and subsequent increased autophagy during ischemia is cardioprotective, whereas beclin-1 activity during reperfusion, which occurs regardless of the replenishment of energy supply, results in excessive autophagy, and is in fact harmful to the cell (Matsui, Takagi et al. 2007).

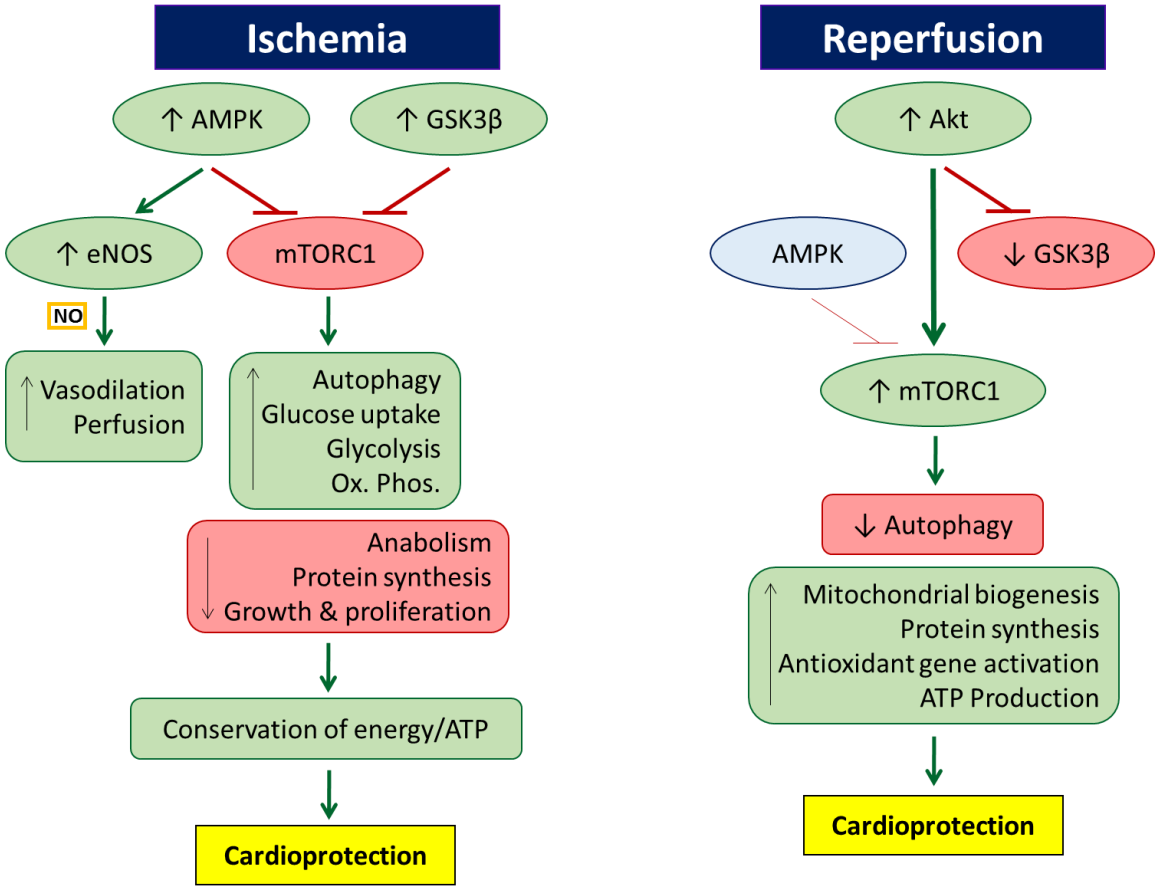

Figure 6. An overview of the roles of GSK3β, AMPK, and autophagy during ischemia and reperfusion respectively (based on figures from (Sciarretta, Volpe et al. 2014) & (Chaube and Bhat 2016)).

1.5.4 Conditioning signalling in the neonatal heart

Researchers investigating the cardioprotective efficacy of pre- and post-conditioning in neonates have shown that both were ineffective at reducing infarct size or improving functional recovery following I/RI (Jones, Pepe et al. 2013, Schmidt, Stottrup et al. 2014, Doul, Charvatova et al. 2015). It is possible that this is due to a higher baseline level of the proteins involved in survival signalling in neonatal hearts, meaning cardioprotective therapies aiming to increase activation of these pathways may have little to no effect. Indeed, work by Naqvi et al. (2014) discovered a sudden spike in IGF-1/IGF-1R/AKT pathway activation at postnatal day 15 in mice, accompanied by a spike in the proliferative capacity of cardiomyocytes at this point. Whilst this spike in activity does correlate with the improved resistance to I/RI in 14-day old rats, it does not account for the lack of cardioprotective efficacy of pre- and post-conditioning in rat hearts in the first 10 days of postnatal life (Doul, Charvatova et al. 2015). The potential role of survival signalling in the vulnerability profile to I/RI has also been supported by previous findings from Liaw et al. (2013), in which the authors found that, in neonates, a greater expression of unphosphorylated AKT, acting as a "reserve" for activation upon injury, in addition to other pro-survival proteins such as HIF1-α, Caveolin-3, BCL-2 and Bax. Moreover, Glycogen Synthase Kinase 3β (GSK3β) was found to be highly phospho-inhibited in neonatal hearts in comparison with adults (Liaw, Hoe et al. 2013, Ostadal, Ostadalova et al. 2014).

1.6 Cardiac mitochondrial morphology & subpopulations

As discussed above (see **Figure 2**) the predominant end effect of the RISK-SAFE pathways is prevention of mPTP opening. This highlights an important role of mitochondria in the response to I/RI and survival signalling pathways, which has been supported by previous

reports of significant morphological changes in mitochondria following I/R. However, recent work has uncovered a strong link between the location and the function of the mitochondria in heart cells, which may have implications for injury following cardiac insults. Three distinct mitochondrial subpopulations exist (**Figure 7**); Interfibrillar (IF) mitochondria situated between the myofibrils & predominantly responsible for providing energy for contraction, perinuclear (PN) mitochondria that cluster around the poles of the nucleus and provide energy for gene transcription, and subsarcolemmal (SSL) mitochondria that sit just below the cell membrane and generate energy for sarcolemmal activities ion channel function (Hwang and Kim 2013). These subpopulations have been shown to exhibit distinct functional characteristics, such as differences in oxidative phosphorylation and utilisation of substrates, resistance to Ca^{2+}-overload, and sensitivity to opening of the mPTP (Hollander, Thapa et al. 2014). Moreover, IF mitochondria display a greater capacity for Ca^{2+}-accumulation and slower mPTP opening times than SSL, indicating potential differences in the apoptotic response to I/RI between these subpopulations (Hollander, Thapa et al. 2014).

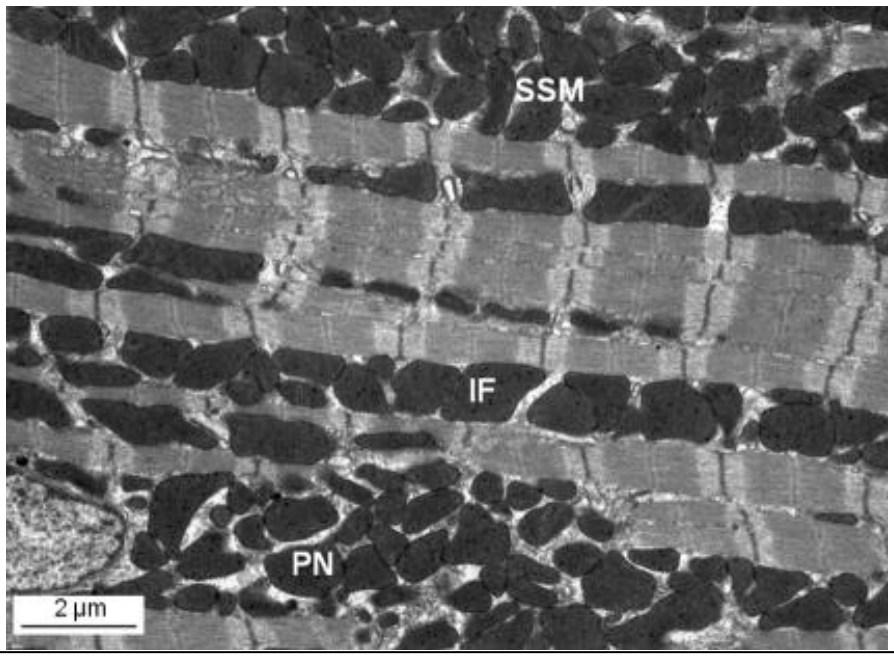

Figure 7. Mitochondrial subpopulations. Electron micrograph showing the three mitochondrial subpopulations present in cardiomyocytes. (image from (Ong and Hausenloy 2010))

The morphology of mitochondria is known to be altered by I/R. Recently, work by Kalkhoran et al. (2017) looked to identify differences in the morphology of these distinct mitochondrial subpopulations from control hearts, following ischemia, and with ischemic preconditioning (IPreC). Cardiac sections were analysed from electron microscopy images, and it was found that IF showed the most elongated morphology, with PN having the smallest areas and greatest measures of sphericity similar to SSL. Following ischemia, all three subpopulations had increased sphericity, with reduced elongation in IF and increased area in PN. However, the morphology of mitochondria was not shown to display any differences following IPreC (Kalkhoran et al. 2017). It is clear from this that ischemia does have a significant effect on mitochondrial morphology in adult heart, however, little has been reported about this effect over the course of postnatal development, and how differences in post-ischemic morphology may be linked to cardiomyocyte survival and vulnerability to I/RI.

1.7 Summary & Conclusions

It is clear that, during postnatal development, there are important changes in the vulnerability of the heart to I/RI, the causes of which are currently not fully understood. With the exception of the antioxidant catalase (**Section 1.1.3**), identified postnatal differences such as those outlined in **Table 1** above demonstrate only gradual, unidirectional changes which occur during development as opposed to the biphasic profile of cardiac vulnerability, indicating they are not contributory to these differences in the response to I/RI seen at different stages of postnatal development. Survival signalling pathways have been shown to play critical roles in the response and subsequent recovery of the heart following I/RI, with some initial reports indicating potential differences in the expressions of the proteins involved with development (**Section 1.5.4**). It is therefore crucial to further explore and

elucidate the underlying mechanisms of these differences, as this will provide potential targets for future therapies, and a foundation upon which the progression of cardioprotective strategies can occur.

1.8 Hypothesis & Aims

Current knowledge as to the contribution of survival signalling proteins to the cardiac vulnerability profile seen during postnatal development is limited. Although previous work has been undertaken to examine any changes in the expression of these proteins, this previous study excluded a critical age group required for full elucidation of the biphasic profile – 7-day olds – and instead looked only at 0-day, 14-day, 28-day and adult hearts (Liaw et al. 2013). Furthermore, this previous study did not further examine whether targeted inhibition or activation of these identified proteins had an effect on cardiac injury following I/RI. Our work therefore looked to further build upon this knowledge, examining the full biphasic profile of survival signalling protein expression and investigating potential age-dependent differences in the vulnerability of hearts to inhibition of identified proteins.

The proposed work in this thesis aims to address the following hypothesis: “Changes in cardiac vulnerability during postnatal development are due to developmental alterations in survival signalling, and that identification and targeting of significant proteins within these pathways could provide an avenue through which novel therapies could be devised to combat cardiac injury following I/R.”

As a result, the overall aims of this work are:

1. To identify any changes that occur in survival signalling through changes in the expression of pro-survival and apoptosis-related proteins during development.

2. To see if specific inhibition of the identified proteins affects the vulnerability to I/RI during postnatal development in isolated cardiomyocytes.
3. To see if specific inhibition of the identified proteins affects the vulnerability to I/RI during postnatal development in whole hearts.
4. To identify any changes that may subsequently occur in terms of survival signalling protein expression or activity following I/RI.
5. To identify differences in cardiomyocyte structure and ultrastructure that may influence the response to I/RI at different stages of development, including:
    i. blood vessel dimensions, cardiomyocyte hypertrophy and sarcomere lengths
    ii. caveolae, multivesicular body (MVB) and exosome abundance
    iii. mitochondrial subpopulation morphology and distribution
6. To observe any changes that may occur in the cardiomyocyte structure and ultrastructure following ischemic insult and reperfusion.

Chapter 2: Materials & Methods

2.1 Materials

2.1.1 Reagents

Experimental reagents used and their companies of origin are listed below:

Agar Scientific (Essex, UK)

Glutaraldehyde solution (25 %)

Bio-Rad (Hertfordshire, UK)

Laemmli sample buffer

Precision Plus Protein™ All Blue Standards

Quick Start™ Bradford 1 x Dye Reagent

BOC Healthcare (Surrey, UK)

95 % oxygen/5 % carbon dioxide medical gas mixture

Medical oxygen (99.5 % minimum)

BOC Industrial Gases (Surrey, UK)

Liquid nitrogen

Fisher Scientific UK Ltd (Leicestershire, UK)

D-glucose anhydrous

Magnesium sulphate ($MgSO_4 \cdot 7H_2O$)

Sodium chloride (NaCl)

Sodium dodecyl sulphate (SDS)

GE Healthcare Life Sciences (Buckinghamshire, UK)

Amersham hyperfilm

Enhanced chemiluminescence (ECL) western blotting detection reagents

Marvel (Lincolnshire, UK)

Original dried skimmed milk

Merck (New Jersey, USA)

Magnesium chloride ($MgCl_2$)

Randox (County Antrim, UK)

CK-NAC assay (CK113)

CK-NAC assay (CK522)

Roche (Sussex, UK)

cOmplete, EDTA-free protease inhibitor cocktail tablets

PhosSTOP phosphatase inhibitor cocktail tablets

Sigma-Aldrich™ (Dorset, UK)

2, 3, 5-triphenyl-tetrazolium chloride (TTC)

2-mercaptoethanol

Albumin from bovine serum (BSA)

Calcium chloride solution (1 M) ($CaCl_2$)

Chelerythrine Chloride

Dimethyl sulphoxide (DMSO)

Ethylene glycol-bis(2-aminoethylether)-N,N,N’,N’-tetraacetic acid (EGTA)

Folin and Ciocalteu’s phenol reagent

Formaldehyde solution (36.5-38 %)

Glycine

Methanol

Lowry reagent

Nonidet™ P 40 substitute solution

Phosphate buffered saline (PBS) tablets

Ponceau S solution

Protease from *Streptomyces griseus*, Type XIV

Sodium deoxycholate

Sodium hydroxide (NaOH)

Trizma® base

Trypan blue solution (0.4 %)

TWEEN® 20

Thermo Scientific (Leicestershire, UK)

Polyvinylidene difluoride (PVDF) transfer membrane (0.45µm)

Tocris Bioscience (Bristol, UK)

TWS 119

Dorsomorphin Dihydrochloride

VWR International Ltd (Leicestershire, UK)

4-(2-Hydroxyethyl)piperazin-1-ylethanesulphonic acid (HEPES)

Di-sodium hydrogen phosphate (Na_2HPO_4)

Hydrochloric acid fuming (37 %) (HCl)

Potassium chloride (KCl)

Potassium dihydrogen phosphate (KH_2PO_4)

Sodium hydrogen carbonate ($NaHCO_3$)

Worthington Biochemical Corportation (New Jersey, USA)

Collagenase, Type 2

2.1.2 Antibodies

Antibody	Source	Dilution	Company & code
HSP90	Rabbit, monoclonal	1:1000	Cell Signaling Technology, #4877
Caveolin-1	Rabbit, polyclonal	1:1000	Cell Signaling Technology, #3238
Caveolin-3	Rabbit, polyclonal	1:1000	abcam, ab2912
14-3-3η	Rabbit, polyclonal	1:1000	Cell Signaling Technology, #9640
AKT	Rabbit, polyclonal	1:1000	Cell Signaling Technology, #9272S
pAKT (S473)	Rabbit, polyclonal	1:1000	Cell Signaling Technology, #9271S

pAKT (S129)	Rabbit, monoclonal	1:1000	abcam, ab133458
β-Catenin	Rabbit, monoclonal	1:1000	BD Transduction Laboratories™, 610153
pβ-Catenin (S552)	Rabbit, polyclonal	1:1000	Cell Signaling Technology, #9566
PKCε	Rabbit, monoclonal	1:1000	abcam, ab124806
pPKCε (S729)	Rabbit, polyclonal	1:1000	abcam, ab63387
GSK3β	Rabbit, monoclonal	1:1000	Cell Signaling Technology, #12456
pGSK3β (S9)	Rabbit, monoclonal	1:1000	Cell Signaling Technology, #9327
AMPKα	Rabbit, polyclonal	1:1000	Cell Signaling Technology, #2532
pAMPKα (T172)	Rabbit, monoclonal	1:1000	Cell Signaling Technology, #2535
mTOR	Rabbit, polyclonal	1:1000	Cell Signaling Technology, #2972
pmTOR (S2481)	Rabbit, polyclonal	1:1000	Cell Signaling Technology, #2974
BAX	Rabbit, polyclonal	1:1000	Cell Signaling Technology, #2772
BCL-2	Rabbit, polyclonal	1:1000	abcam, ab59348
Mfn1	Rabbit, polyclonal	1:1000	abcam, ab104585
β-actin	Rabbit, polyclonal	1:1000	Abcam, ab8227
GAPDH	Rabbit, monoclonal	1:1000	Cell Signaling Technology, #5174
ECL anti-rabbit IgG-horseradish peroxidase-linked (Secondary Antibody)	Donkey	1:10000	GE Healthcare Life Sciences, NA934

Table 2. List of antibodies used in western blot experiments.

2.2 Animals

Adult Wistar Han rats were purchased by weight (**Table 3**) from Charles River (Margate, UK). Upon delivery the animals were housed at the University of Bristol animal unit, allowed to recover from transit and then used when required. Early postnatal rats, i.e. 7-day olds, 14-day olds and 28-day olds, were ordered directly from ASU Service (University of Bristol), and delivered to the DHB animal housing facility on the day of intended use. Treatment of animals and all procedures were in accordance with Home Office guidance, Animal (Scientific Procedures) Act of 1986. Prior to culling, each rat was weighed, and data for the average weights of each age group are shown in **Table 3**. Rats were then culled using Schedule 1 methods, before excision of the heart.

		Weight (g)						
Age	N	Mean	Std. Error of Mean	Range	Minimum	Maximum	Median	Std. Deviation
P14	30	31.4	.7	16.4	26.0	42.4	30.5	3.7
P28	7	144.6	18.2	109.0	91.0	200.0	175.0	48.1
Adult	31	336.8	8.8	175.0	250.0	425.0	350.0	48.9

Table 3. Descriptive data for the average weights of rats in each age group. Mean adult weight corresponds to approximately 63-70 days.

2.3 Cardiomyocyte Isolation

The cardiomyocyte isolation protocol used was based on previous work undertaken within the research group of Professor Suleiman (Williams et al. 2001), as described below.

2.3.1 Animals, weights and perfusion flow rates

Rats from 3 age groups were used for cardiomyocyte isolation; 14-day (n = 6), 28-day (n = 4), and adult (n = 3). 7-day olds were excluded due to the changes to the protocol required

in order to keep cells alive following isolation, making direct comparison between the age groups difficult. Following Schedule 1 culling, hearts were extracted from rats and placed directly into cold Solution B. Weights for each rat were taken and are shown in **Table 4.** The flow rates required for hearts from different age groups varied due to physiological and developmental differences in cardiac size and function. The flow rates used were based on previous work undertaken by Sarah Martin, who determined optimal flow rates for each age group through trial and error, the outcome of which is included in **Table 4**.

		Weight (g)							
Age	N	Mean	Std. Error of Mean	Range	Minimum	Maximum	Median	Std. Deviation	Flow rate required (ml/min)
P14	6	30.9	1.7	11.4	26.0	37.4	30.0	4.2	2.7
P28	4	182.5	6.0	25.0	175.0	200.0	177.5	11.9	5.6
Adult	3	258.3	8.3	25.0	250.0	275.0	250.0	14.4	8.5

Table 4. Average weights of animals used and the perfusion flow rates required, as outlined by previous work from Sarah Martin. Mean adult weight corresponds to approximately 49-56 days.

2.3.2 Solutions

All solutions used for heart perfusion and isolation of myocytes were made from a primary solution with no added $CaCl_2$, Solution A, containing 137 mM NaCl, 5 mM KCl, 1.2 mM $MgSO_4$, 1.2 mM NaH_2PO_4, 20 mM Hepes, 16 mM Glucose, 5 mM $C_3H_3NaO_3$, 1.8 mM $MgCl_2$, made up to 2 L with distilled water and adjusted with NaOH to pH 7.25. A series of solutions were then made up containing different levels of $CaCl_2$ from Solution A. Solution B was made with the addition of $CaCl_2$ to Solution A for a Ca^{2+} concentration of 750 µM. Solution C was made up by adding 90 µM of Ca^{2+} chelator EGTA to Solution A. Solutions E, F & G were made from Solution A with final concentrations of 150 µM Ca^{2+}, 0.5 mM Ca^{2+}, and 1 mM Ca^{2+},

respectively. Enzyme containing solution (Solution D), was made freshly on the day of isolation with 50 mg of collagenase and 5 mg protease to 50 ml of Solution A.

2.3.3 Isolation of cardiomyocytes

Extracted hearts were trimmed in a tray of cold Solution B (750 µM Ca^{2+}) to remove excess tissue, before cannulation via the aorta onto the isolation apparatus shown in **Figure 8.** Once cannulated, additional trimmings were made to allow the removal of blood clots and to ensure the heart was beating well. The heart was perfused at a constant flow rate dependent on the age of the rat (see **Section 2.3.1**) for 2 minutes with warm, oxygenated Solution B in order to wash out any remaining blood. Hearts were then perfused for 4 minutes with EGTA containing Solution C, a chelator of Ca^{2+}, thus removing resisdual calcium from buffers and from the myocardium in order to loosen connection between myocytes. Enzymatic digestion was then undertaken by perfusing hearts with enzyme-containing Solution D until soft to the touch, indicating sufficient digestion has occurred. The times required to fully digest the hearts varied with age, and are outlined in **Table 5**. However, it should be noted that these times were significantly longer than those previously reported for all ages of rat. This may in part have been due to the EGTA used at the start as, upon switching to a new source of EGTA, the time required for digestion of an adult rat heart was reduced from approximately 50 minutes to approximately 30 minutes.

Age	Average digestion time (min)	Average starting viability (%)
14-days	26	71
28-days	34	70
Adult	44	64

Table 5. Average times required for complete digestion and average starting cardiomyocyte viability, by age of the rat.

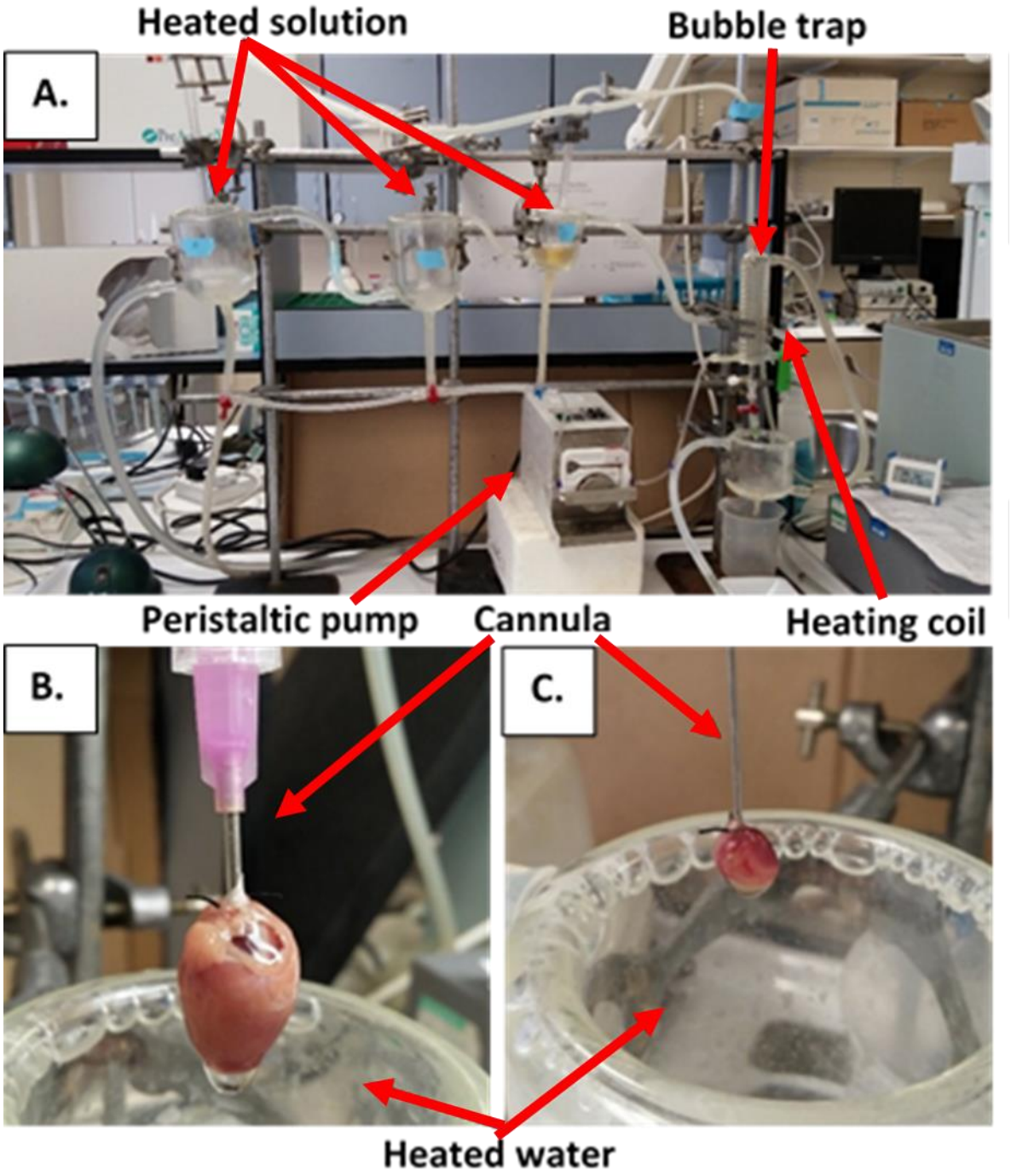

Figure 8. Cardiomyocyte isolation equipment. **A.** Experimental setup for cardiomyocyte isolation. **B.** Example of a cannulated adult rat heart. **C.** Example of a cannulated 14-day old heart.

Finally, hearts were perfused with Solution E, in order to both wash out the remaining enzyme to prevent further digestion and killing of the cells, as well as to begin the gradual reintroduction of Ca^{2+}. Following perfusion with Solution E, the heart was cut down from the apparatus and placed into a fresh tray of warmed and perfused Solution E, at which point the heart tissue was gently pulled apart to release the cardiomyocytes, and transferred to a beaker for shaking at 37°C for 4 minutes. The heart was shaken a subsequent 2 times in fresh Solution E each time to release a sufficient number of cells from the tissue for use in the next step of the experimental procedure, before each sample was combined and poured through a cheesecloth to filter the cell solution from the tissue. This solution was left to sediment for 8 minutes, before removal of the top layer of solution – containing debris and dead cells which are lighter – and addition of warmed and perfused Solution F. This process was repeated after a further 5 minutes of sedimentation, but with the addition of Solution G. These solutions containing progressively larger concentrations of Ca^{2+}, therefore allowing for the gradual reintroduction of Ca^{2+} to the cells without killing them with a sudden increase in calcium concentration. Due to the lower yield of cells from 14-day old hearts, $CaCl_2$ was added directly to the isolated cells at 0.5 mM followed by 1mM, to avoid dilution of the cell solution or loss of cells when pipetting away the top layer. A sample of cell solution was collected in a pre-weighed Eppendorf, centrifuged for 1 minute, and frozen in liquid nitrogen to obtain a pellet for future protein extraction.

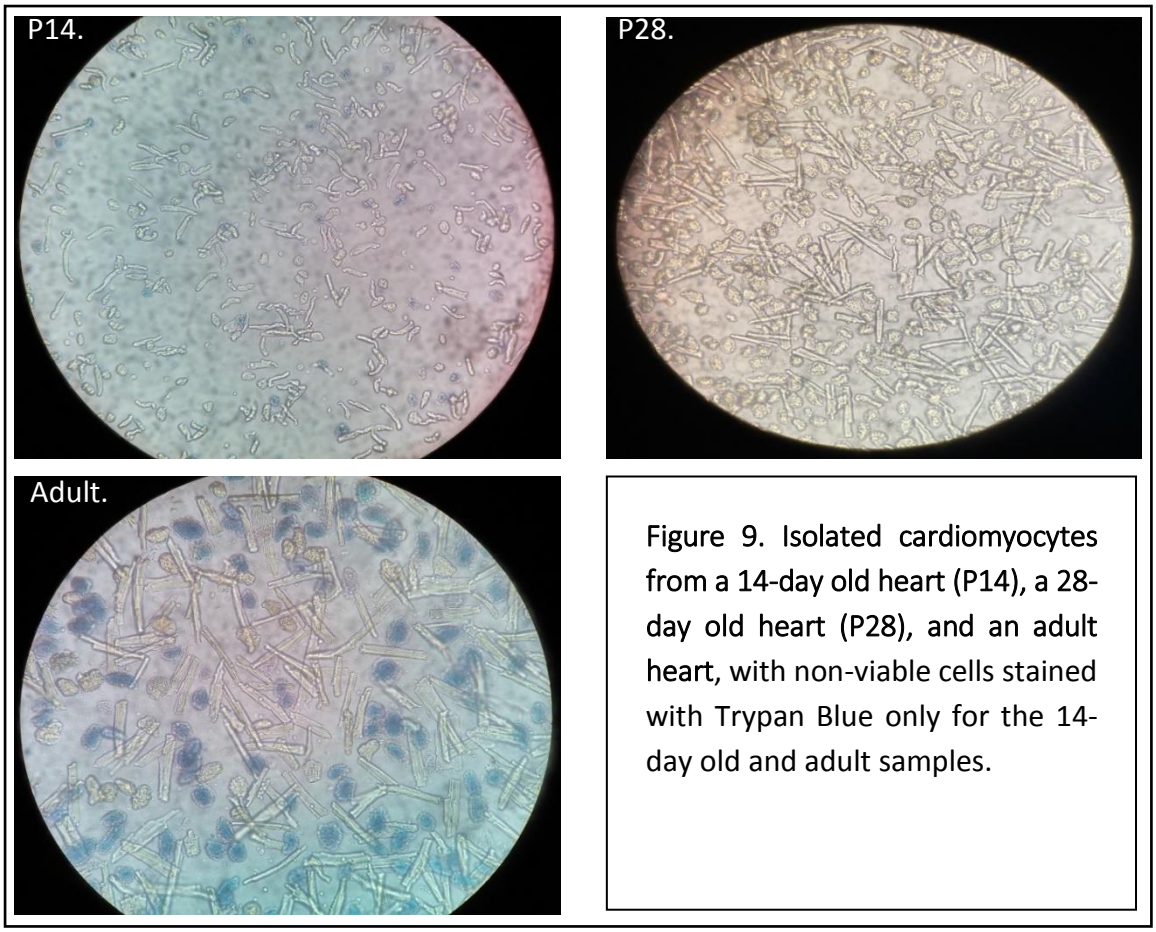

Figure 9. Isolated cardiomyocytes from a 14-day old heart (P14), a 28-day old heart (P28), and an adult heart, with non-viable cells stained with Trypan Blue only for the 14-day old and adult samples.

2.3.4 Simulation of ischemia/reperfusion injury and cell viability

Cells were kept incubated in a water bath at 37°C with gentle shaking throughout the experiment, and were only removed in order to obtain samples for examination under the microscope by pipette. Cell solutions were gently mixed by pipette prior to each separation of groups or removal of samples for cell counts, in order to ensure cells that had settled between time points were well mixed into the rest of the solution. Two groups of cells (5ml of the final cell solution each) were taken, one as a control and the other as an experimental sample. Nothing further was added to the control group, whereas I/RI was simulated within the experimental group with the addition of 3 mM $CaCl_2$ (for a final Ca^{2+} concentration of 4 mM), 20 mM KCl, and 0.5 mM H_2O_2. Cell viability was measured from the total cell solution

as a start viability, at 5 minutes post-addition of the I/RI simulation solutions, and then at 1 hour and 2 hours following the start of the experiment.

Cell viability was measured using Trypan Blue solution (0.4% in 0.81% NaCl and 0.06% KH_2PO_4), which identifies cells that are no longer viable with a blue stain, but leaves those that are unstained, as live cells maintain an intact cell membrane that does not allow entry of Trypan Blue into the cell. Cell viability was defined as the percentage of cells without Trypan Blue staining, including those that were rounded but unstained, and was taken as an average of 3 field per cell group at each time point. Examples of these stained cells at each time point are given in **Figure 10** below.

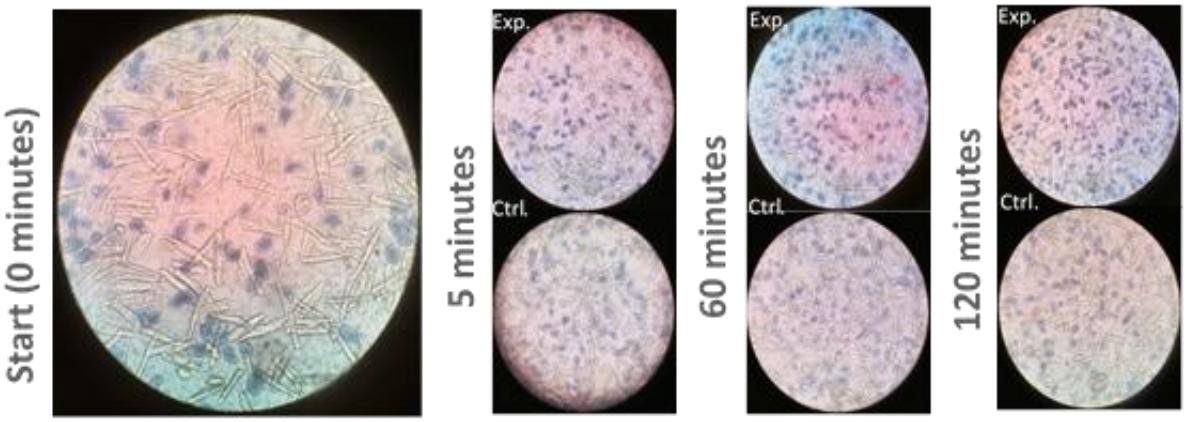

Figure 10. Examples fields of cells at each time point for the two experimental groups, taken from an adult heart. (Exp. = Experimental group, Ctrl. = Control group).

2.3.5 Cell morphometry measurements

The size of cardiomyocytes isolated from different age groups was measured using a light microscope with a grid-lined slide. Each cell length and width was measured by the number of squares spanned on the grid, and converted from this number into an actual size in micrometres using the scale 1 square = 0.01 mm.

2.4 Proteomics Studies

2.4.1 Tissue collection & protein extraction

2.4.1.1 Whole tissue samples

Samples for proteomics were collected by Dr Martin Lewis. Male Wistar rats of three age groups in the first run, 14-day old (n = 3), 28-day old (n = 3) and adult (n = 4), and four age groups in the second run, 7-day old (n = 4), 14-day old (n = 8), 28-day old (n = 8), and adult (n = 7), were used in all experiments. All animals were kept at the Animal Services Unit, University of Bristol until used. Animals were culled using Schedule 1 methods. All animals were weighed prior to killing. Treatment of animals and all procedures were in accordance with Home Office guidance under the Animals (Scientific Procedures) Act of 1986. Hearts were excised and dissected into atria, ventricles, and apex, and frozen in liquid nitrogen.

The cardiac tissue was weighed and RIPA buffer (1x PBS tablet, 1% (v/v) Nonidet P-40, 0.5% (w/v) sodium deoxycholate, 0.1% (w/v) SDS), adjusted to pH 7.4 and with the addition of one tablet of protease (Complete, mini, EDTA-free protease inhibitor cocktail tablets, Roche, UK) and phosphatase (PhosSTOP, phosphatase inhibitor cocktail tablets, Roche, UK) inhibitor, was added at 10 µl/mg of tissue. 1.4mm Zirconium oxide beads were added to 2ml tubes with the cardiac samples and RIPA buffer, before homogenisation at maximum speed twice for 10 seconds each time using the minilys tissue homogenizer (Bertin Technologies, France). Samples were then left on ice for 30 minutes, before centrifugation at 10,000 x g for 10 minutes at 4°C. The resulting supernatant was then stored at -80°C.

2.4.1.2 Protein extraction from isolated cardiomyocyte pellets

Cell pellets from cardiomyocyte isolation were weighed, subtracting the initial weight of the Eppendorf tube alone, and RIPA buffer (see **Section 2.4.1.1**) added at 1 µl/mg. These tubes were then vortexed until the pellet had fully mixed into solution, before centrifugation at 10,000 x g for 10 minutes at 4°C. The resulting supernatant was stored at -80°C.

2.4.2 Protein quantification

2.4.2.1 Lowry method

A protein standard was made using a BSA stock solution (5 mg/ml) diluted to 400 µg/ml, and was then used to create a standard curve at 10, 20, 40, 60, 80 and 100 µg/ml BSA. 400 µl of Lowry reagent (40 ml of distilled water, one bottle of *Sigma Protein Assay Kit* Lowry reagent powder) was added to each tube, and left to incubate for 30 minutes at room temperature. 200 µl of Folin-Ciocalteu reagent was then added to the standards, vortexed, and then left to incubate for a further 30 minutes. At this time, distilled water was used to blank the spectrophotometer at 750 nm, before measurement of absorbance at each concentration of BSA, producing a standard curve of concentration versus absorbance.

Samples were diluted at a 1:2 ratio (5µl protein sample to 10 µl of distilled water) to ensure the measured absorbance would remain within the range of the standard curve. The protocol above was then repeated with 4µl of each protein sample, and duplicated for each sample. Protein concentrations of each sample were calculated using the straight-line graph equation from the standard curve, and adjusted for the dilution factors used.

2.4.2.2 Bradford assay

Concerns over variations in the expression of supposed housekeeping protein, GAPDH, and thus the accuracy of protein quantification performed on samples prepared for western blotting originally done using the Lowry method were encountered, as discussed in **Section 9.3.1**. As a result, this was repeated using the Bradford method in order to rule out errors in sample protein quantification. From 5 mg/ml BSA stock solution, 1 µl, 2 µl, 3 µl, 4 µl and 5 µl was added to LP4 tubes in duplicate. 3 ml of Bradford reagent was then added, vortexed, and left to incubate for 15 minutes. Using 3 ml of Bradford reagent as a blank, absorbance for each concentration was measured at 595 nm, and a standard curve plotted from these measurements.

Protein samples were diluted at a 1:2 ratio (5 µl protein sample to 10 µl of distilled water) to ensure the measured absorbance would remain within the range of the standard curve. 3 ml of Bradford reagent was added to 5 µl of each sample, in addition to 5 µl of RIPA buffer as a blank, and left for 15 minutes before measurement of absorbance. Protein concentrations of each sample were calculated using the straight-line graph equation from the standard curve, and adjusted for the dilution factors used.

2.4.3 Proteomic analysis – Tandem Mass Tagging

2.4.3.1 Total proteins

Extracted protein samples were diluted with double distilled water to adjust the protein concentration of each sample to 2 mg/ml, according to previous protein quantification (**Section 2.2.2.2**). Samples were then sent for Tandem Mass Tag (TMT) analysis (ThermoFisher Scientific, UK) by the University of Bristol Proteomics Facility. Protein samples

were processed and digested, and the resulting peptides in each sample were labelled with a unique reporter group (126, 127, 128, 129, 130), in addition to a total pooled sample of peptides from each individual sample (131) (Littlejohns, Heesom et al. 2014), as shown in **Figure 11a**. Each TMT label consists of a NH_2 reactive group, which allows amine-specific binding to peptides, a Mass Normaliser, which ensures the overall mass of each tag is constant in spite of the differing reporter groups, in addition to a Mass Reporter group, which is specific to each sample in a single run (Abdul-Ghani, Heesom et al. 2014) (**Figure 11b**). This group is released during fragmentation by Collision Induced Dissociation (CID) following cleavage of the linker region during LC-MS/MS, allowing detection of the different reporter ions ranging 126-131 Da, which cluster at the low mass end of each MS/MS spectra to indicate the relative abundance of each peptide by sample, as outlined in **Figure 11a** (Hung and Tholey 2012).

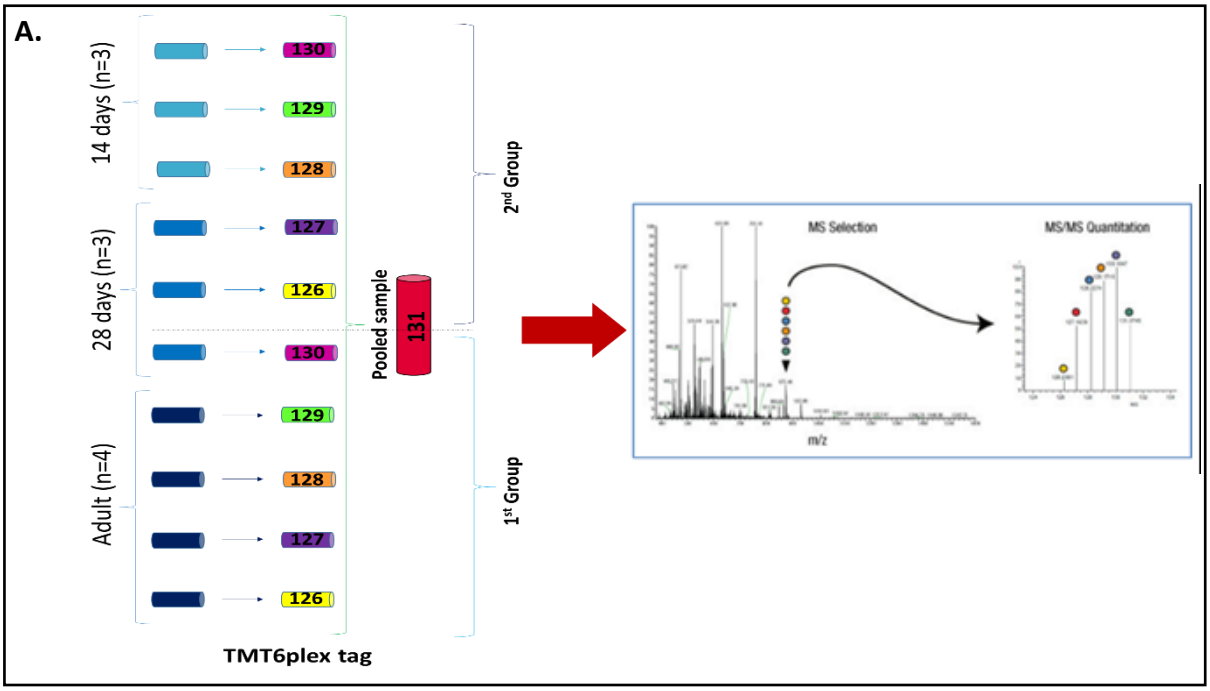

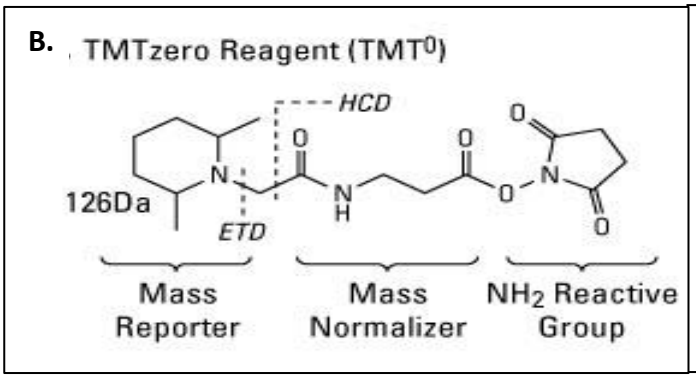

Figure 11. Summary of the protocol for proteomics. **A.** The process of proteomic analysis. **B.** General structure and function of each region of a TMT reagent molecule. (Figures modified from ThermoFisher Scientific.)

2.4.3.2 Phosphorylated proteins

Phosphorylated proteins follow a similar process of proteomic analysis as non-phosphorylated protein, with the addition of a phosphopeptide enrichment step. Following labelling with TMT reagents, the pooled samples were passed through a titanium dioxide (TiO_2) column, during which phosphorylated and non-phosphorylated peptides were separated as phosphopeptides bind to the column, whereas non-phosphopeptides pass straight through and elute first (Abdul-Ghani, Heesom et al. 2014). The phosphopeptides were subsequently eluted and underwent LC-MS/MS analysis.

2.4.4 Analysis of proteomic output

Proteomic output was presented as a *Proteome Discoverer* file. The relative levels of protein in each sample were displayed as a ratio of protein expression in the individual sample to the level of protein expressed within the total pooled sample. Proteins previously found to be involved in the apoptotic or survival signalling process were identified from the literature, relevant cell signalling pathways using the *Kegg Pathway* database, as well as the *PANTHER* protein database. Those that were present within the proteomic output were then selected,

extracted, and analysed using One-way ANOVA in *SPSS* for statistically significant differences in the mean protein levels between the age groups (**Section 2.8**).

This process was replicated for the phospho-proteomic output, before further analysis of their individual phosphosites was performed. Phosphosites with a 'low' confidence rating – as indicated within the *Proteome Discoverer* file – were excluded, in addition to those not present within each of the age groups. The remaining phosphosites were analysed using One-way ANOVA (**Section 2.8**), in order to compare the pattern of change of each individual phosphosite over age with that of the total phosphoprotein.

2.5 Western Blotting

2.5.1 Sample preparation

For western blotting, samples containing 0.15 mg were needed, therefore the amount of sample needed for 0.15 mg in a final volume of 100 µl was calculated based on protein quantification previously undertaken (see **Section 2.4.2**), and the remaining volume made up with distilled water. Loading buffer was made using 1425 µl of 2x Laemmli buffer and 75 µl β-mercaptoethanol (βME), and added to the samples at a 1:1 ratio. After vortexing, samples were then heated at 95°C for 5 minutes, releasing the pressure by opening the Eppendorf caps at the start, and then transferred to an ice box.

2.5.2 Gel electrophoresis

Running buffer was made from 10x stock solution (30.3 g TRIS base, 114 g glycine, and 10 g SDS in 1 L, pH 8.1-8.6), using 50 ml of stock solution with 450 ml of distilled water. The gel electrophoresis tank was assembled with two Mini-PROTEAN® TGX™ precast gels (4-20%

acrylamide, 15-well comb), and tested for leaks by pouring transfer buffer into the centre and checking for a decrease in the level of solution.

Following centrifugation of the samples, 10 µl of loading buffer was pipetted into the first well, with 6 µl of a known molecular weight marker to the second well and 3 µl of the marker to the end well, before 12 µl of each sample was added to the remaining wells. Samples were loaded by alternating age groups to avoid the possibility of uneven development of one end of the membrane at a later stage accounting for any differences between the age groups. The gels were then run at 100 V for approximately 10 minutes in order to allow the samples to run to the edge of the stacking gel, before increasing the voltage to 150 V until bands reached the end of the gel.

2.5.3 Membrane Transfer

Transfer buffer was made from 100 ml stock solution (250 mM Trizma base, 192 mM glycine, 10% (v/v) methanol), 100 ml methanol, and 800 ml distilled water, before placing into the fridge to cool. Two PVDF membranes were cut to size and the orientation marked with a cut to one corner, before wetting with 100% methanol, 3 washes with distilled water, and finally being left to soak in transfer buffer for approximately 15 minutes.

Following electrophoresis, the gels were removed from their plastic casing, removing the top section of the gel with the well remnants, and placed down onto 4 pieces of wet blotting paper, with one PVDF membrane placed on top of the gel. These layers were then placed into a transfer buffer filled tub containing a transfer cassette and one mesh layer. 4 additional pieces of wet blotting paper were placed onto the PVDF membrane, with a final layer of mesh, before rolling to remove any air bubbles and closing the cassette. This process was repeated for the second gel, and both cassettes were placed into a tank for transfer,

with the black side facing the black wall of the tank. An ice block and stirrer were added to the tank to ensure an even temperature was maintained throughout the tank during the transfer process, before filling the tank with transfer buffer and running at 300mA for 90 minutes in the cold room.

2.5.4 Ponceau S Staining

Following transfer, membranes were washed with TBST (100 ml stock solution – 250mM Trizma base, 136 mM NaCl, 2.7 mM KCl, and 2 % (v/v) Tween 20 – with 900ml distilled water), before incubation with Ponceau S solution (Sigma-Aldrich) for 5 minutes. Membranes were then rinsed with double distilled water to remove background staining and images were taken for analysis. Staining was removed by washing membranes in 0.1M NaOH for 1 minute, before rinsing with running double distilled water for 3 minutes. Membranes were then ready for blocking.

2.5.5 Incubating the membrane

First, the membrane was blocked using 10% milk in TBST, incubating the membranes with this solution for 1.5 hours. This was to prevent non-specific binding of the primary or secondary antibody to the membrane, which would otherwise create a high level of background binding and thus result in unclear bands for the protein of interest.

The marker band ladder was then marked with biro on each membrane, and the membranes were washed in TBST twice for 5 minutes each time. Following this, each membrane was cut in two to separate the region of the membrane with the expected molecular weight for each protein of interest from that of the housekeeping protein, GAPDH (37 kDa). Each section of

the membranes was placed into a separate container, and the relevant primary antibody was added. These were then left to rock in the cold room overnight.

The following morning, 3% milk was made using 0.9 g of milk powder in 30 ml TBST. Primary antibodies were poured back into their original containers for re-use, and the membranes were washed in TBST 3 times for 5 minutes each time. 10 ml of milk was added to the large containers containing the membranes for the proteins of interest (5 ml for the smaller GAPDH membranes), and secondary antibody corresponding to the source species of the primary antibody was added (1.25 µl in 10 ml of milk, 0.65 µl in 5 ml milk). The membranes were rocked in secondary antibody at room temperature for 1 hour.

2.5.6 Development and analysis of bands

Following this period, membranes were washed in TBST 4 times for 5 minutes each wash, before a final rinse of each membrane with water. Membranes were covered with Enhanced ChemiLuminescence (ECL) solution for 4 minutes (target protein membranes) or 2 minutes (GAPDH membranes), before being placed into cassettes for development in the dark room. High performance chemiluminescence hyperfilm was placed into and left within the cassettes for varying times depending on the strength of the bands produced, adjusted to produce bands with optimum density and definition, and developed via exposure to x-ray using the OptiMax® (UK) machine. Bands were then analysed using ImageJ, producing values of density for each band, and calculating the level of the target protein in each sample as a ratio of the target protein band density to the band density of GAPDH for that sample. Statistical analysis for the significance of any differences in protein levels between age groups was performed using SPSS.

2.5.7 Membrane stripping

In instances where a membrane needed to be re-probed, for example, to measure the level of the phosphorylated and non-phosphorylated forms of the same protein on a blot, a mild stripping method was used to remove previously bound antibodies. Stripping buffer was made using 15 g of glycine, 1 g of SDS, 10 ml of Tween-20, HCl as required to adjust the pH to 2.2, and made up to 1 L with distilled water. The membrane was covered with this stripping buffer and set to rock for 5-10 minutes, before discarding the buffer and repeating this step with fresh buffer. The membrane was then rocked in PBS twice for 10 minutes each time, followed by TBST twice for 5 minutes each, at which point the membrane was ready to be re-used beginning from the blocking stage of the western blotting protocol (as outlined in Section **2.5.5**).

2.6 Ischemia/reperfusion experiments in perfused heart

2.6.1 Ischemia protocol

Adult (n = 3) and 14-day old (n = 3) rats were culled using Schedule 1, as described in **Section 2.2**. Hearts were removed, cannulated onto Langendorff apparatus (**Section 2.3**) and perfused with Krebs-Henseleit solution (120 mM of NaCl, 25 mM of $NaHCO_3$, 11 mM of Glucose, 1.2 mM of KH_2PO_4, 1.2 mM of $MgSO_4$, 4.8 mM of KCl, 2 mM of $CaCl_2$ – made up to 2 L with double distilled H_2O). After 20 minutes of stabilisation, hearts were exposed to 30 minutes of global ischemia, before removal from the cannula. Small cardiac cubes were taken from the left ventricular wall and placed into fixative solution and left overnight, before being transferred into phosphate buffer and sent for processing. The remaining sections of heart were collected and immediately frozen in liquid nitrogen and stored in -80°C for later protein extraction.

2.6.2 Ischemia & reperfusion protocol

Hearts were extracted from 14-day old (n = 6) and adult (n = 6) rats and cannulated onto Langendorff apparatus for perfusion, as described in **Section 2.6.1**. However, in this case, following the ischemic period, flow was restarted and hearts were reperfused for 60 minutes. The effluent was collected before ischemia and at 1, 5, 10, 20, 30 and 60 minutes of reperfusion for use in creatine kinase measurements. Additionally, at the end of reperfusion, hearts were collected and tissue taken from the left ventricular wall for electron microscopy. The remaining tissue was frozen in liquid nitrogen and stored at -80°C for future protein extraction.

2.6.3 Creatine kinase measurements

The release of creatine kinase from cells is used as a marker of the degree of tissue damage resulting from I/R (Zuurbier et al. 2004). As a result, effluent samples collected during reperfusion (**Section 2.6.4**) were analysed for creatine kinase concentration using a 'Randox CK-NAC' kit. 40 µl of effluent was added to 1 ml of the kit buffer, which contained the substrates necessary for a series of reactions culminating in the production of NADPH. As these substrates were provided in excess within the buffer, the rate of NADPH production was dependent on the concentration of creatine kinase within each effluent sample. This rate of NADPH production was measured at 37°C via absorbance readings taken at 340 nm using a 'Jenway Multi-cell Changer Spectrophotometer', over a period of 4 minutes. The subsequent readings were multiplied by 4047.5 for conversion to international units of creatine kinase per litre (U/L) (Randox Laboratories Ltd. information sheet, Ben Littlejohns PhD thesis, 2013).

2.6.4 TTC staining for infarction

To measure the size of infarction, hearts were perfused with Triphenyl Tetrazolium Chloride (TTC) solution, comprised of 0.3g of TTC powder in 30ml of PBS solution, for 10 minutes at a flow rate of 2ml/min for adult hearts and 1ml/min for 14-day old hearts. Hearts were then incubated in PBS for 5 minutes at 37°C, weighed to obtain the wet weight of the heart, and then frozen for 20 minutes. Hearts were then cut into slices and stored in 4% (v/v) formalin in PBS for storage overnight at 4°C, before transfer into PBS for storage until scanning. Both sides of each heart were imaged using an Epson scanner, and slices were then left to dry in order to obtain the dry weight of each slice. Images were analysed using Image J in order to determine the percentage of each slice that was made up of infarcted tissue, identified as any regions not stained brick red (viable tissue) and are instead pale areas of tissue. Alongside the dry weights of each slice, these areas were used to calculate the volume of infarcted tissue as a percentage of the total volume of the heart.

2.7 Histology

2.7.1 Light Microscopy

2.7.1.1 Tissue Fixation

Hearts were extracted from 14-day old (n = 4), 28-day old (n = 5), and adult (n = 5) rats, flushed with Krebs-Henseleit buffer (120mM NaCl, 25mM $NaHCO_3$, 11mM D-glucose anhydrous, 1.2mM KH_2PO_4, 1.2mM $MgSO_4.7H_2O$, 4.8mM KCl and 1.2mM $CaCl_2$), and cut to remove the apex and any excess tissue. The remaining heart sections were placed into 5ml tubes containing fixative solution (10% paraformaldehyde in 0.01M phosphate buffer) and left to fix for 24 hours. Following this fixation period, the fixative solution was pipetted out

of the tube, replacing it with phosphate buffer to wash, and again with fresh buffer to be left in the fridge until processing.

2.7.1.2 Tissue processing and embedding

Each heart section was placed into a white cassette, which were then stored in 0.01 M phosphate buffer ready for tissue processing. This was performed using the ThermoFisher Scientific Excelsior™ AS Tissue Processor, which automatically undertakes the process of dehydrating the tissue with a graded ethanol series, gradually displacing water from the tissue to allow the infiltration of paraffin wax. Processed tissue was embedded in paraffin wax using the Thermo Scientific™ HistoStar™ Embedding Workstation, by first pouring a layer of molten wax into the metal moulds, before placing the tissue in the desired orientation, covering this with a final layer of wax, and then placing the mould onto an ice block to allow the wax to solidify. The back section of the cassette was then placed on top and additional wax poured in order to fix the sample block to the labelled cassette.

2.7.1.3 Production of slides – Microtome and staining

Tissue was sectioned using the Thermo Scientific™ Shandon™ Finesse™ 325 Manual Microtome to a thickness of 5µm, and each section was placed into a water bath to flatten the sections, before being lifted from the water with a microscope slide. These slides were then left overnight to dry out in a 37°C oven. Slides were then ready for staining, and this was carried out using the Thermo Scientific™ Varistain™ 24-4 Automatic Slide Stainer in order to stain for blood vessels with Elastic Van Gieson. Stained slides were mounted using Thermo Scientific™ DPX Mounting Media, before placing a coverslip over the tissue, and left to dry.

2.7.1.4 Measurement of cardiac blood vessels

Images were taken with the Olympus BX40 Microscope and QImaging QICAM Fast 1394 digital camera, and analysed using the Image-Pro 6.2 software. The largest vein and artery present as a complete cross-section were selected in each region of the heart (left ventricle, right ventricle and interventricular septum), for comparison of the size of the largest vessels by age group and localisation. Vessel cross-sections were measured using the "Count/Size" option, in order to obtain the area in micrometers^2 of the selected area in addition to the width and height measurements for each vessel.

2.7.2 Electron Microscopy

Rats were culled using Schedule 1 and hearts were removed from 14-day old (n = 3) and adult (n = 3) animals **(Table 4)**, before being placed directly into ice cold cardioplegic solution (147 mM NaCl, 20 mM KCl, 16 mM $MgCl_2$, 2 mM $CaCl_2$, adjusted to pH 7.4), used to halt contractility of the heart. Hearts were cannulated via the aorta, and perfused with cardioplegia at a rate of 1 ml/min, in order to wash out any remaining blood. This was then repeated with EM fixative solution (0.1 M phosphate buffer, 0.5 mM $CaCl_2$, 1.7 mM D-glucose anhydrous, 1% (w/v) glutaraldehyde, 1% (w/v) paraformaldehyde) at a rate of 1 ml/min for 4-6 minutes. Following perfusion, hearts were cut into small cubes taken from the left ventricular wall, and left in the fridge overnight in fixative, before being transferred into phosphate buffer and sent for processing and mounting by the Wolfson Bioimaging Facility, University of Bristol. The resulting grids were then imaged, with electron micrographs taken using the FEI Tecnai^{TM} 12 Transmission Electron Microscope (TEM) and analysed using Image J.

2.8 Statistical analysis of data

Statistical analysis was predominantly performed using IBM SPSS Statistics 24, and data presented as mean values ± SE. Outliers were detected using Boxplots and Q-Q Plots. On a few occasions, results were presented with or without outliers with emphasis on those deemed to result from experimental errors removed. Data was checked for normal distribution using a Shapiro-Wilks test and for homogeneity of variance using a Levene's test. Those that did not violate these assumptions underwent either independent t-test (for experiments with two experimental groups) or one-way ANOVA (for experimental groups of 3 or more) with Bonferroni post-hoc testing. Those that violated these assumptions underwent non-parametric Kruskal-Wallis testing. For data that included two independent variables, for example in experiments that factor in data collected across a succession of time points, Mauchly's test for sphericity was performed in addition to Shapiro-Wilks testing for normal distribution. These data were then tested for statistical significance using a two-way repeated measures ANOVA with a Bonferroni adjustment. P-values below 0.05 were considered as statistically significantly different.

Chapter 3: Quantification and validation of survival signalling proteins during postnatal development using proteomic and molecular biological techniques.

3.1 Introduction

In order to address our first aim and establish whether differences in the expression and phosphorylation state of RISK-SAFE proteins in control hearts – known to play crucial roles in the reduction of cardiac injury following I/RI (**Section 1.4** and **1.5**) – as well as those known to cross-talk with these signalling pathways, may exist at different developmental stages, proteomic and phosphoproteomic analysis was utilised. An existing proteomic output from Dr Martin Lewis with samples from 14-day old, 28-day old and adult rat hearts was used as an initial proof of concept that age-dependent changes in such proteins existed, and these samples were subsequently used for western blot validation of these trends in protein expression. Proteins of interest were identified through literature searches and signalling pathway maps, before statistical analysis to highlight those of which that showed a significantly greater expression in samples from 14-day old hearts in comparison with adult thus indicating potentially better resistance to cardiac insults for us to test our hypothesis. Of these, key proteins were selected for further validation using western blotting.

3.2 Materials & Methods

3.2.1 Animal groups & sample extraction

Proteomic and phosphoproteomic analysis was conducted with samples taken from 14-day old (n = 3), 28-day old (n = 3) and adult (n = 4) rats. Rats were culled as outlined in **Section 2.2**, hearts excised, and the apex removed for flash freezing in liquid nitrogen. Tissue then underwent protein extraction and quantification as described in **Sections 2.4.1** and **2.4.2**.

3.2.2 Proteomic and Phosphoproteomic Analysis

The full process of proteomic and phosphoproteomic analysis has been described in **Section 2.4.3**, but can be summarised as the dilution of the quantified samples mentioned in **Section 3.2.1** with double distilled water to adjust the protein concentration of each sample to 2mg/ml for sending to the University of Bristol Proteomics Facility, in order for samples to undergo Tandem Mass Tag (TMT) analysis (ThermoFisher Scientific, UK). For phosphoproteomic analysis, samples underwent an additional phosphopeptide enrichment step using a TiO_2 column (**Section 2.4.3**).

The resulting output came in the form of a *Proteome Discoverer* file with the abundance of each protein in each sample as a ratio to the pooled sample, from which proteins selected from the existing literature and signalling pathway database searches as relating to cell survival processes were identified (see **Section 2.4.4**). These proteins then underwent statistical analysis in order to identify those that showed significant changes in expression between age groups concordant with the cardiac vulnerability profile during postnatal development (see **Section 2.8**). Selected proteins displayed in **Section 3.3** are given as a 'mean ratio' per age group, referring to the abundance of protein in each individual sample relative to the pooled sample (abundance in individual sample/abundance in pooled sample), from which an average of all samples for each age group was calculated.

3.2.3 Western blot validation

The full western blotting methodology has been described in **Section 2.5**. To summarise, remaining sample from tissue extraction and quantification outlined in **Section 3.2.1** that was not sent for proteomic analysis was instead used to prepare a sample of 0.15mg of

protein in a final volume of 100µl, prepared for gel electrophoresis with the addition of an equal volume of loading buffer (Laemmli buffer + βME). Protein samples were run on a Mini-PROTEAN® TGX™ precast gels and transferred to a PVDF membrane, which in later experiments were subsequently stained with Ponceau S solution to produce full lane bands (see **Section 2.5.4** and **Appendix, Figures 103-108**), before blocking with milk. Membranes were then incubated with antibodies for HSP90, Caveolin-1, Caveolin-3, 14-3-3η, AKT, pAKT, β-Catenin, and pβ-Catenin (see table of antibodies in **Section 2.1.2**), washed with TBST, incubated with a secondary antibody, and visualised using the Enhanced ChemiLuminescence system. Initial experiments used a GAPDH loading control for normalisation of protein bands, but this was subsequently replicated using whole lane intensities as identified by Ponceau S staining.

3.3 Results

The first proteomics study involved the analysis of extracted proteins from 14-day, 28-day and adult rats, before undergoing proteomic and phosphoproteomic analysis (**Section 3.2**). The results collected from the proteomic and phosphoproteomic output will be presented separately in **Sections 3.3.1** and **3.3.2** below. For figure clarity, P14 and P28 were used to represent postnatal day 14 and 28, respectively.

3.3.1. Effect of postnatal development on survival signalling proteome

59 proteins were identified and extracted from the proteomic output due to their previously reported roles in survival signalling or the apoptotic process. Of these, 32 were found to show a statistically significant change in expression with age, 6 of which increased with increasing age, with the remaining 26 proteins decreasing with increasing age, as summarised in **Figures 12** and **13**.

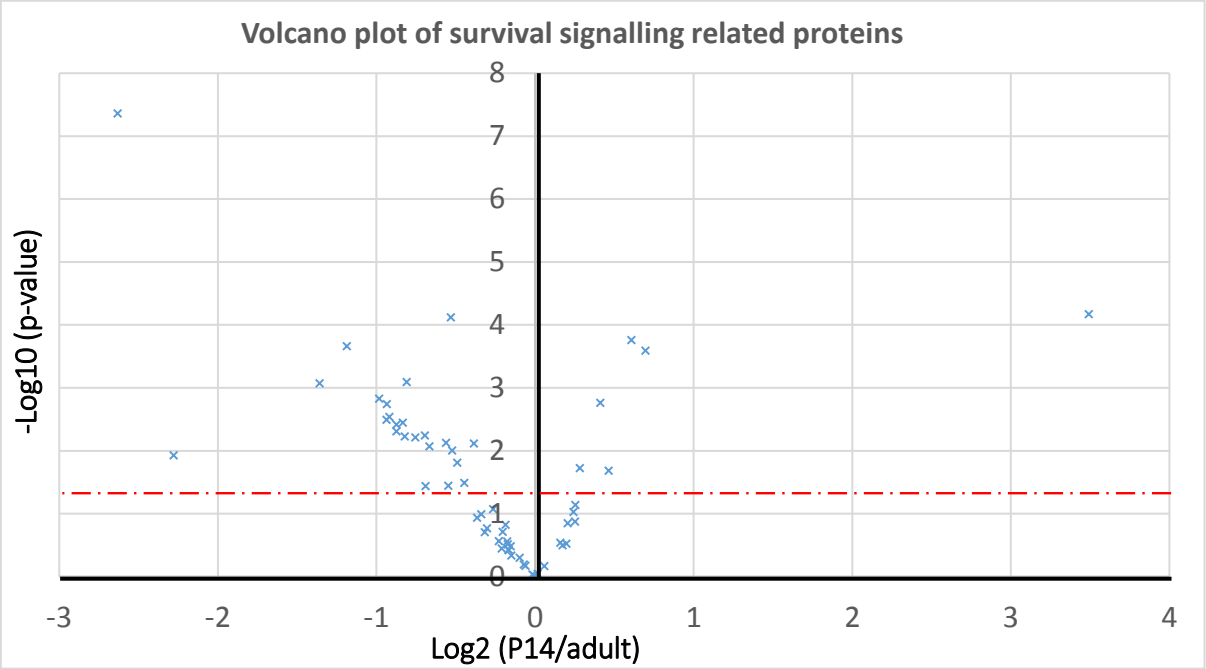

Figure 12. Volcano plot of all survival signalling proteins identified in the proteomics, comparing fold difference (FD) between the average protein expressions in 14-day old and adult heart samples expressed as log2 (x-axis), against the p-value expressed as –log10 (y-axis). The red line indicates a cut-off point for statistical significance (p = 0.05).

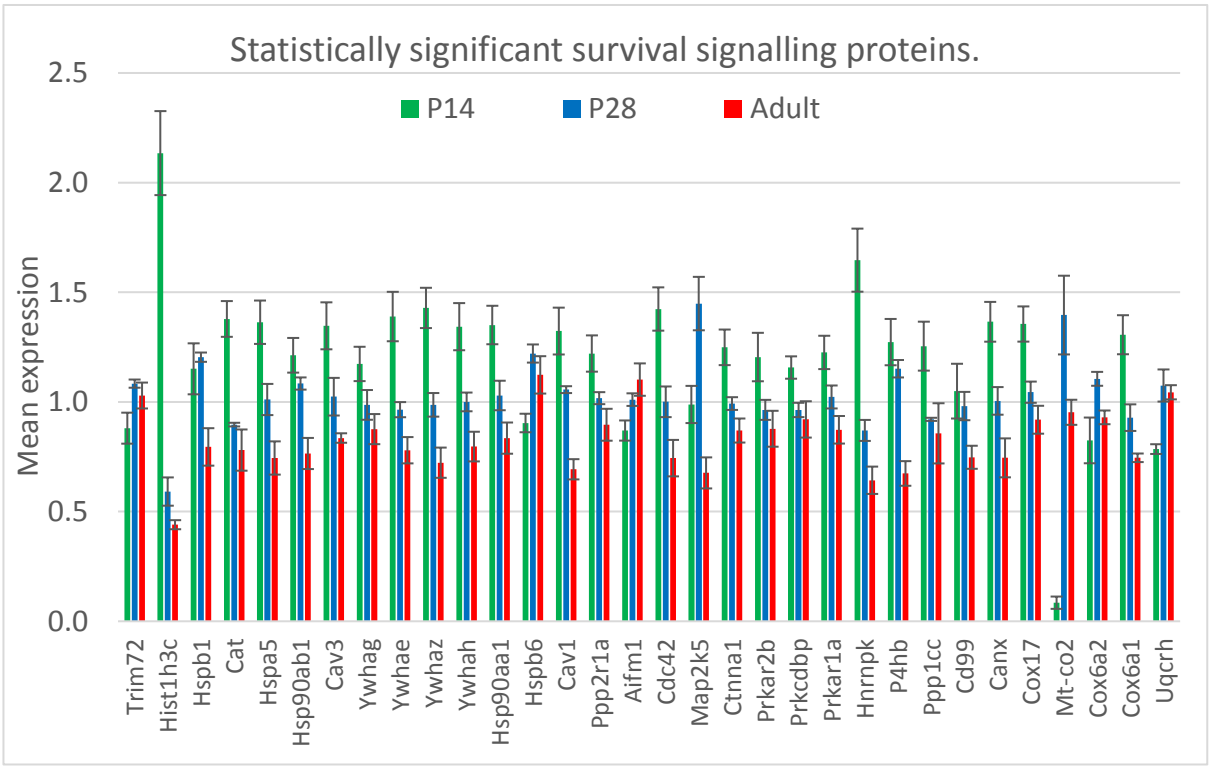

Figure 13. Survival signalling related proteins found to change significantly with age. Data are presented as Mean ± SE (n = 3 for P14, n = 3 for P28 and n = 4 for adult).

3.3.2 Validation of significantly different survival signalling proteins using western blotting

In order to validate the results of this proteomic output, western blotting was run on the same samples, targeting some of the key proteins identified – HSP90, caveolin-1, caveolin-3, and 14-3-3η. These proteins were selected in part due to previous use and testing of the antibodies in our research group, in addition to their reported links to survival signalling pathways. Both HSP90 and 14-3-3η have been linked to the stabilisation of Akt and augmentation of its activity, with subsequent cardioprotection following I/RI (Wang et al. 2009, Gurusamy et al. 2006). Caveolins have similarly been linked to cardioprotection and the promotion of Akt activity (Tsutsumi et al. 2008, Horikawa et al. 2011), in addition to their upstream roles in coordinating the activation of survival signalling pathways at the cell membrane (Das et al. 2007).

Initial western blotting was performed using an antibody for traditional housekeeping protein, GAPDH, as the loading control. However, it was found that GAPDH expression changed during postnatal development both in the proteomic output and using western blot analysis (**Appendix**, **Figures 103-105**). An additional housekeeping protein, β-actin also yielded the same results (**Appendix, Figures 106-107**). Therefore, Ponceau S staining was used instead as a loading control, as analysis found that the intensity of full lane bands did not change significantly between the three age groups (**Appendix, Figure 108**). Each protein tested with western blotting alongside the corresponding results from proteomic analysis are shown below (**Figures 14-18**). The data collected for both the use of GAPDH and full lane Ponceau S staining have been shown for comparison.

3.3.2.1 Validation of the expression of HSP90

HSP90 expression detected by western blotting showed the same pattern of expression across the three age groups, with statistically significant differences between 14-day old samples and adult samples both with correction using GAPDH and Ponceau S.

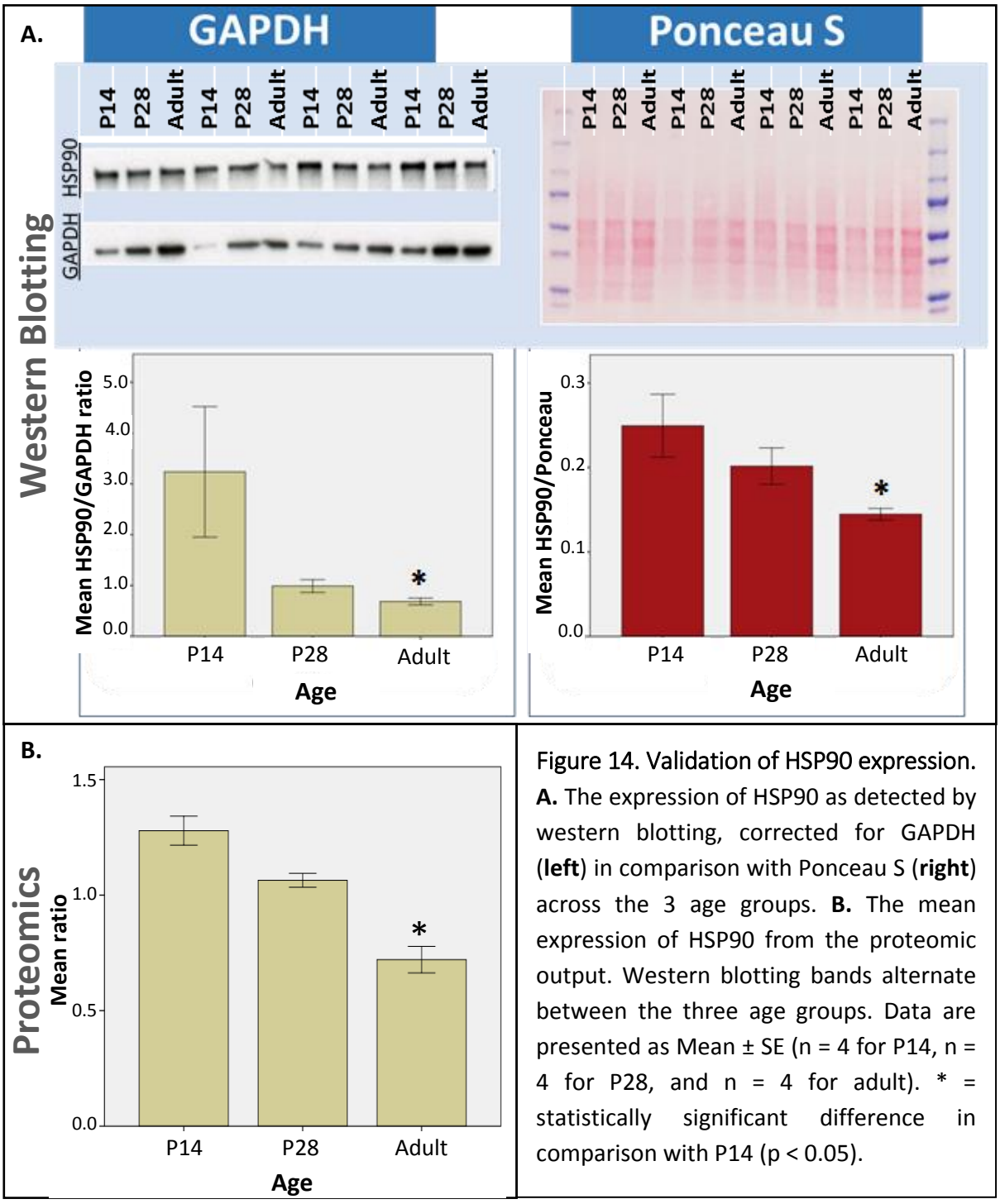

Figure 14. Validation of HSP90 expression. **A.** The expression of HSP90 as detected by western blotting, corrected for GAPDH (**left**) in comparison with Ponceau S (**right**) across the 3 age groups. **B.** The mean expression of HSP90 from the proteomic output. Western blotting bands alternate between the three age groups. Data are presented as Mean ± SE (n = 4 for P14, n = 4 for P28, and n = 4 for adult). * = statistically significant difference in comparison with P14 ($p < 0.05$).

3.3.2.2 Validation of the expression of caveolin-1 (Cav-1)

While the same overall trend in expression of Cav-1 as detected in the proteomic output was seen both with correction using GAPDH expression and correction using whole lane Ponceau S intensity, statistical significance was only seen between 14-day old samples and adult samples when a GAPDH correction was applied.

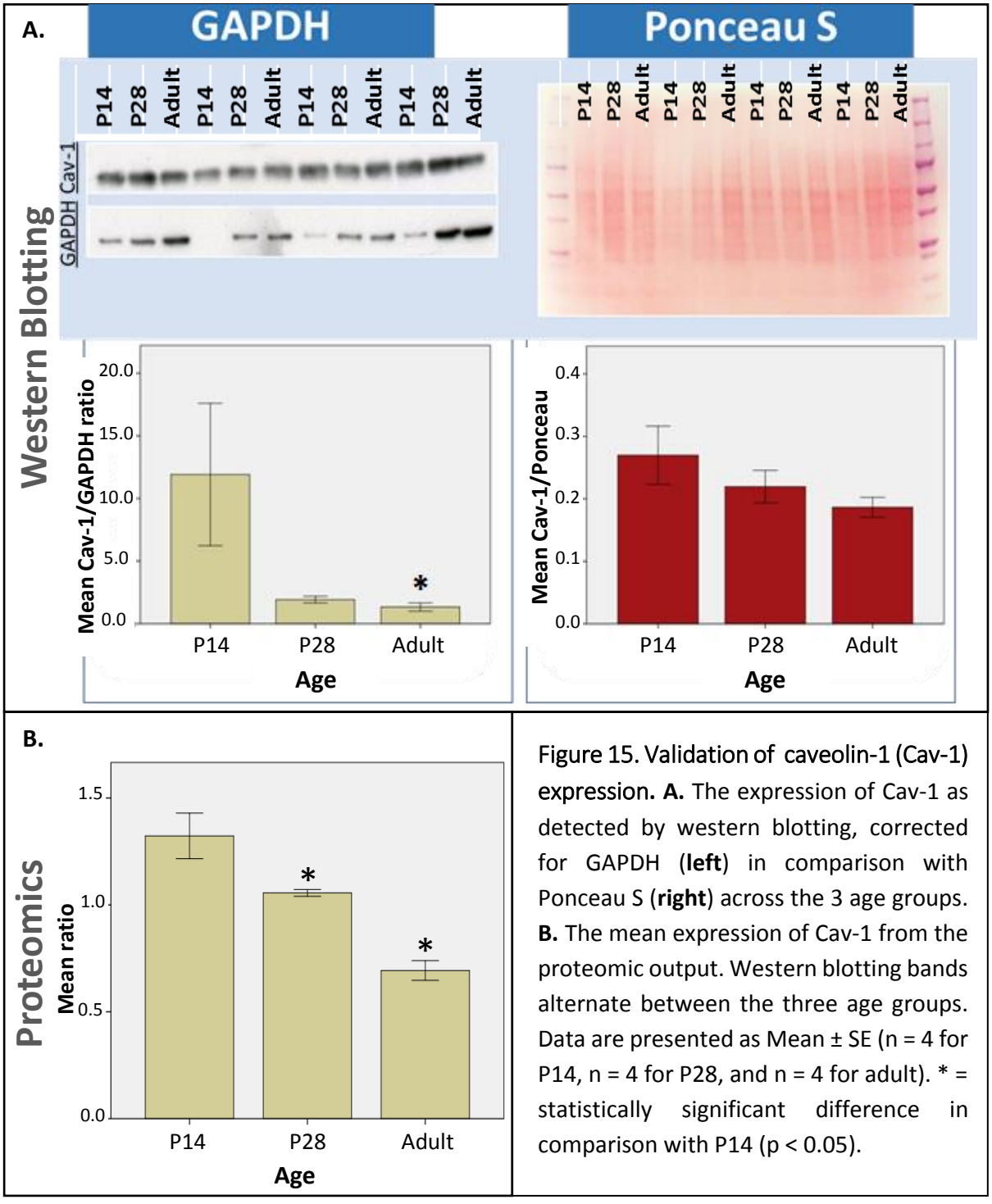

Figure 15. Validation of caveolin-1 (Cav-1) expression. **A.** The expression of Cav-1 as detected by western blotting, corrected for GAPDH (**left**) in comparison with Ponceau S (**right**) across the 3 age groups. **B.** The mean expression of Cav-1 from the proteomic output. Western blotting bands alternate between the three age groups. Data are presented as Mean ± SE (n = 4 for P14, n = 4 for P28, and n = 4 for adult). * = statistically significant difference in comparison with P14 ($p < 0.05$).

3.3.2.3 Validation of the expression of caveolin-3 (Cav-3)

While Cav-3/GAPDH mimicked the trend in expression across the three age groups seen in the proteomic output, albeit with statistical significance only between 14-day old and 28-day old samples, this trend was not seen when Cav-3 expression was corrected for using Ponceau S staining. This may result from the quality of the Cav-3 bands produced.

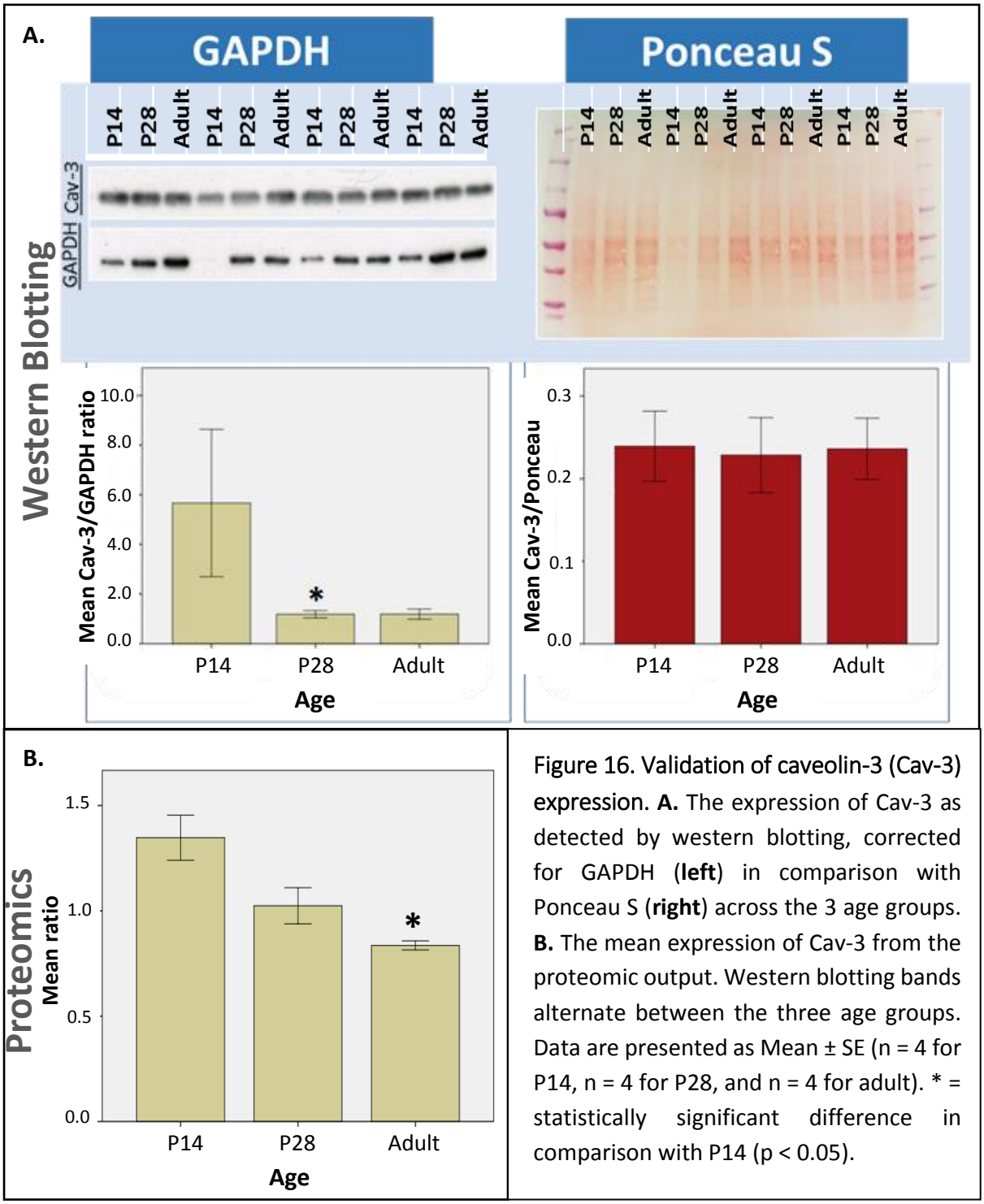

Figure 16. Validation of caveolin-3 (Cav-3) expression. **A.** The expression of Cav-3 as detected by western blotting, corrected for GAPDH (**left**) in comparison with Ponceau S (**right**) across the 3 age groups. **B.** The mean expression of Cav-3 from the proteomic output. Western blotting bands alternate between the three age groups. Data are presented as Mean ± SE (n = 4 for P14, n = 4 for P28, and n = 4 for adult). * = statistically significant difference in comparison with P14 ($p < 0.05$).

3.3.2.4 Validation of the expression of 14-3-3η

The trend in expression of 14-3-3η seen in the proteomic output was replicated both with GAPDH correction and Ponceau S correction. However, correction using GAPDH produced statistically significant differences between 14-day old and 28-day old samples not seen in the proteomic output. It is likely that this discrepancy results from the baseline differences in GAPDH expression between the three age groups.

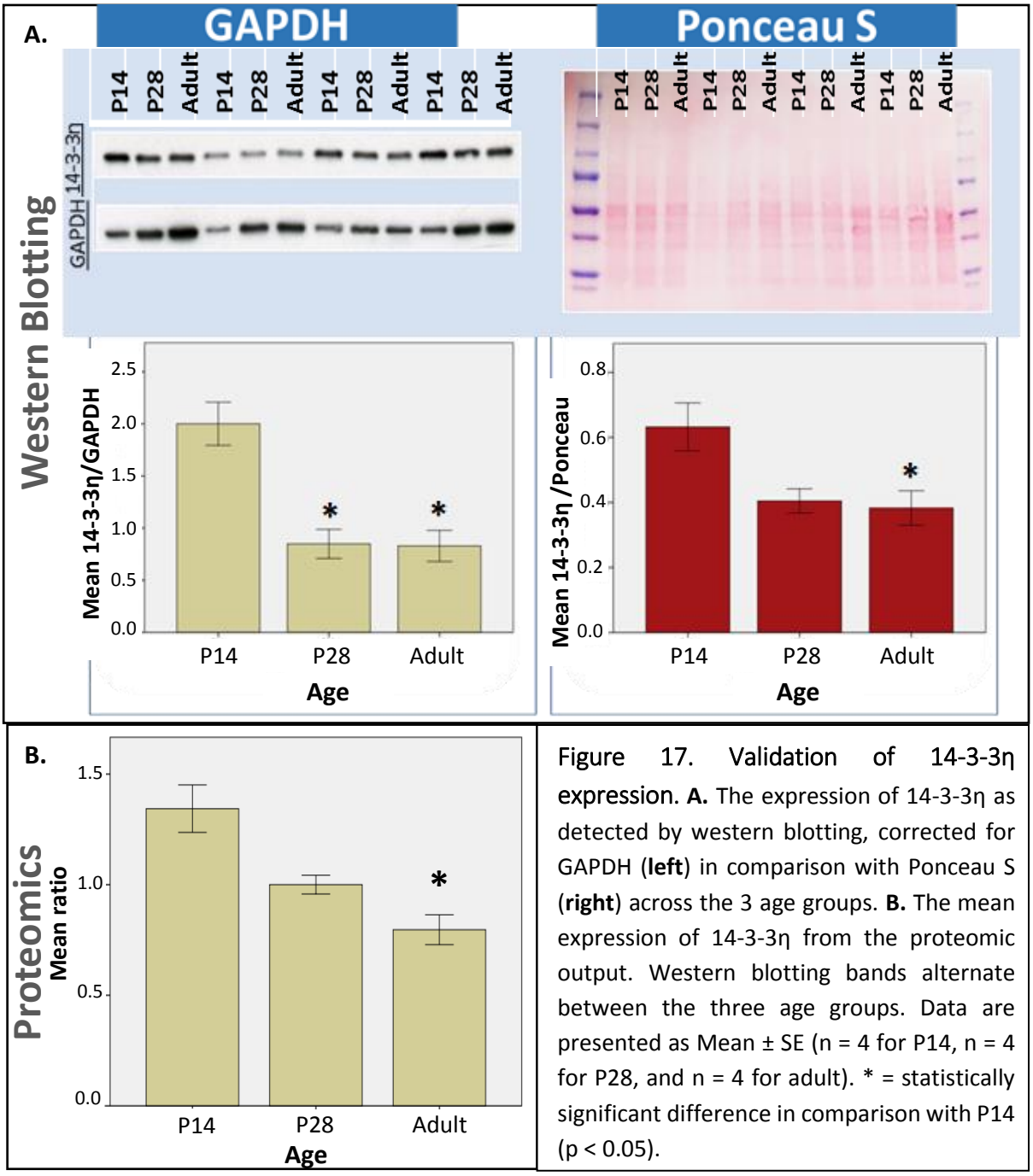

Figure 17. Validation of 14-3-3η expression. **A.** The expression of 14-3-3η as detected by western blotting, corrected for GAPDH (**left**) in comparison with Ponceau S (**right**) across the 3 age groups. **B.** The mean expression of 14-3-3η from the proteomic output. Western blotting bands alternate between the three age groups. Data are presented as Mean ± SE (n = 4 for P14, n = 4 for P28, and n = 4 for adult). * = statistically significant difference in comparison with P14 ($p < 0.05$).

3.3.3 Postnatal development and the survival phosphoproteome

3.3.2.1 Total phosphorylation of select/relevant proteins

Of an original 53 identified, 35 phosphoproteins linked with survival signalling or apoptosis were found to show a statistically significant change in expression with age. Of these, 2 proteins were found to increase with increasing age, with the remaining 33 proteins decreasing with increasing age, as summarised in **Figures 18** and **19**.

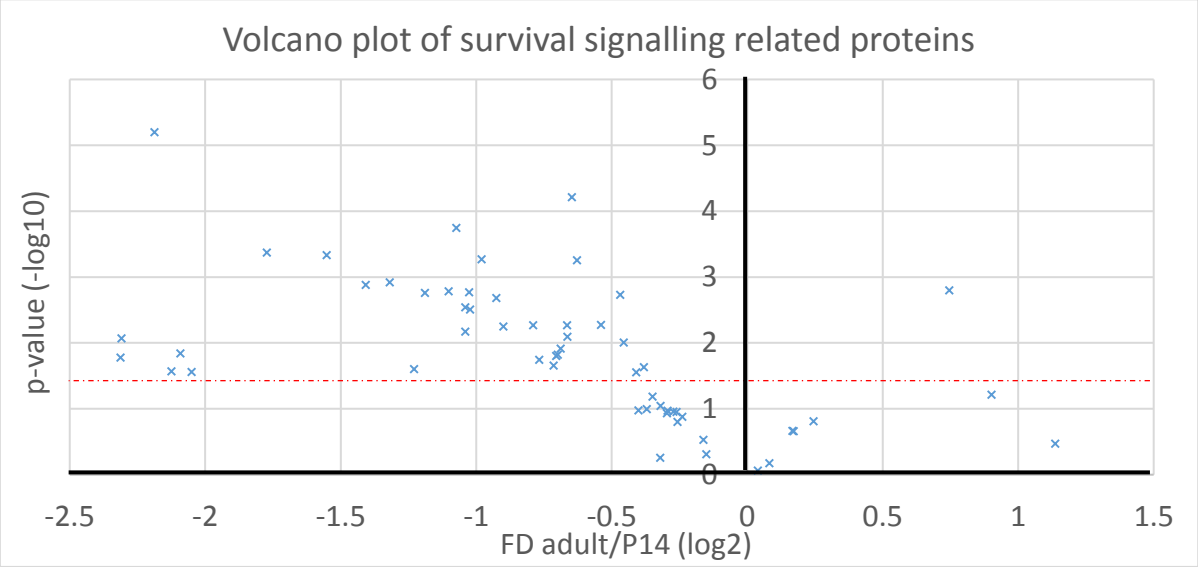

Figure 18. Volcano plot of all survival signalling or apoptosis related phosphoproteins expressed as the fold difference (FD) in the expression of each phosphoprotein in adult samples/14-day old samples identified in the phosphoproteomic output (with log2 transformation for proportional representation of both increased or decreased expression), displaying each phosphoprotein on an axis of fold difference in mean phosphoprotein expression between adults and P14 by the p-value (-log10 transformation), denoting statistical significance of this difference. The red line indicates a cut-off point for statistical significance, with those above the red line displaying statistically significant differences between the 2 age groups.

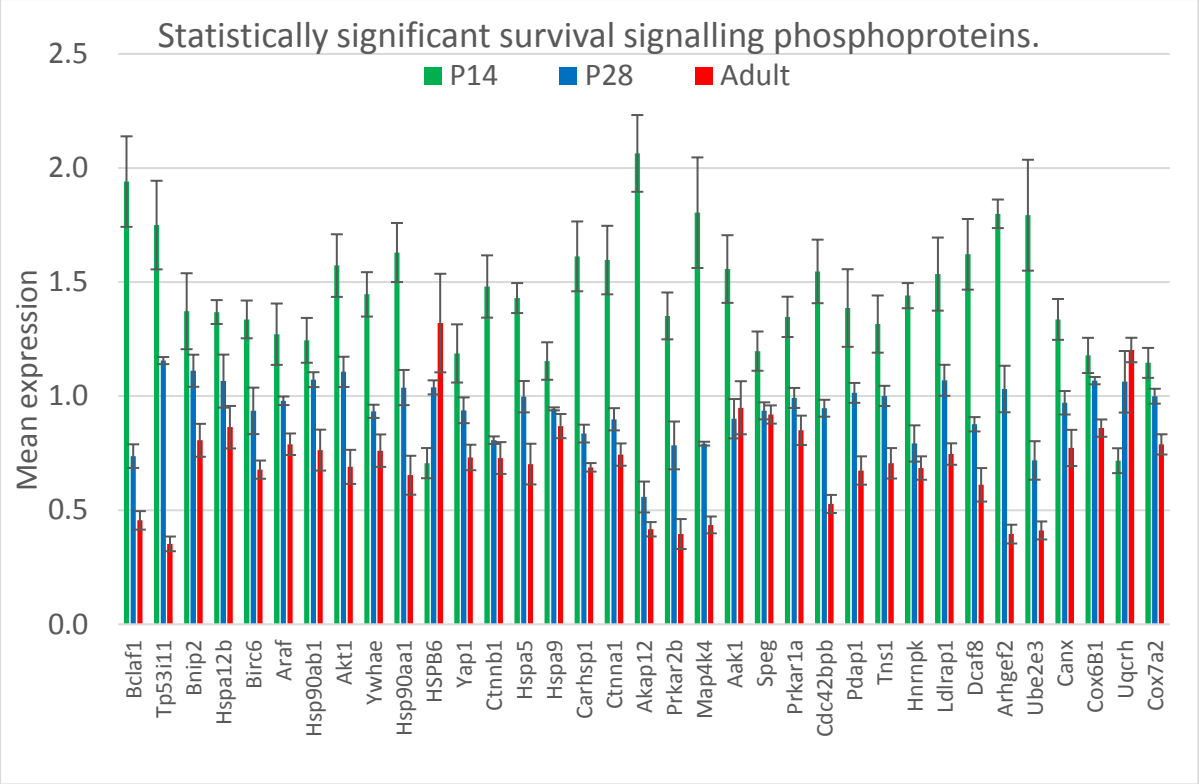

Figure 19. Survival signalling related phosphoproteins found to change in a statistically significant manner with age. Data are presented as Mean ± SE (n = 3 for P14, n = 3 for P28 and n = 4 for adult).

3.3.2.2 Detection of specific phosphorylation sites of select proteins

For each statistically significant protein found, the individual phosphosites were extracted from Proteome Discoverer as outlined in **Section 2.4**, excluding those with low confidence ratings or that were not present in samples from each group. Each phosphosite was subsequently analysed for changes with age, as displayed in **Figures 20-25** below. All those shown in **Figure 21** showed statistically significant changes with age.

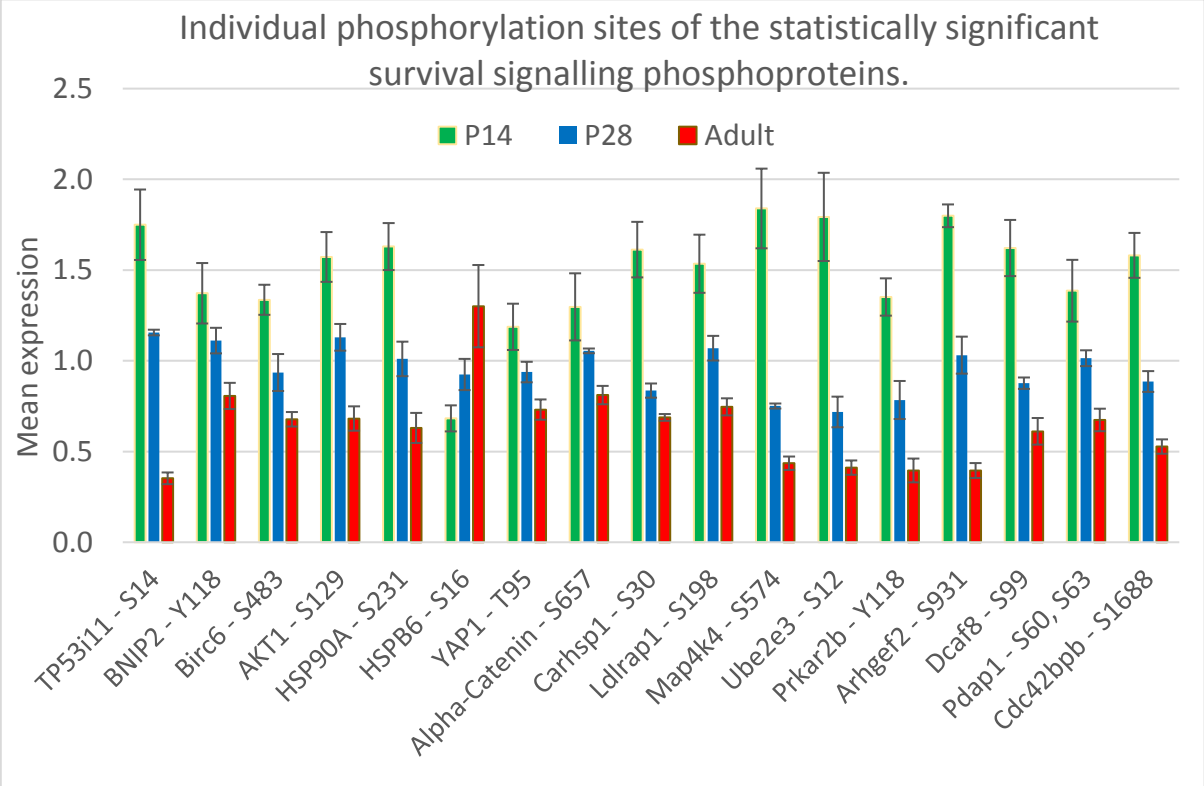

Figure 20. Proteins with only one phosphorylation site detected showing statistically significant differences with age (P14 vs Adult). Data are presented as Mean ± SE (n = 3 for P14, n = 3 for P28 and n = 4 for adult.)

The majority of phosphorylation sites detected in the phosphoproteomic output followed the overall trend in change with age as that of the total phosphorylated protein, as shown in **Figures 21- 23** below.

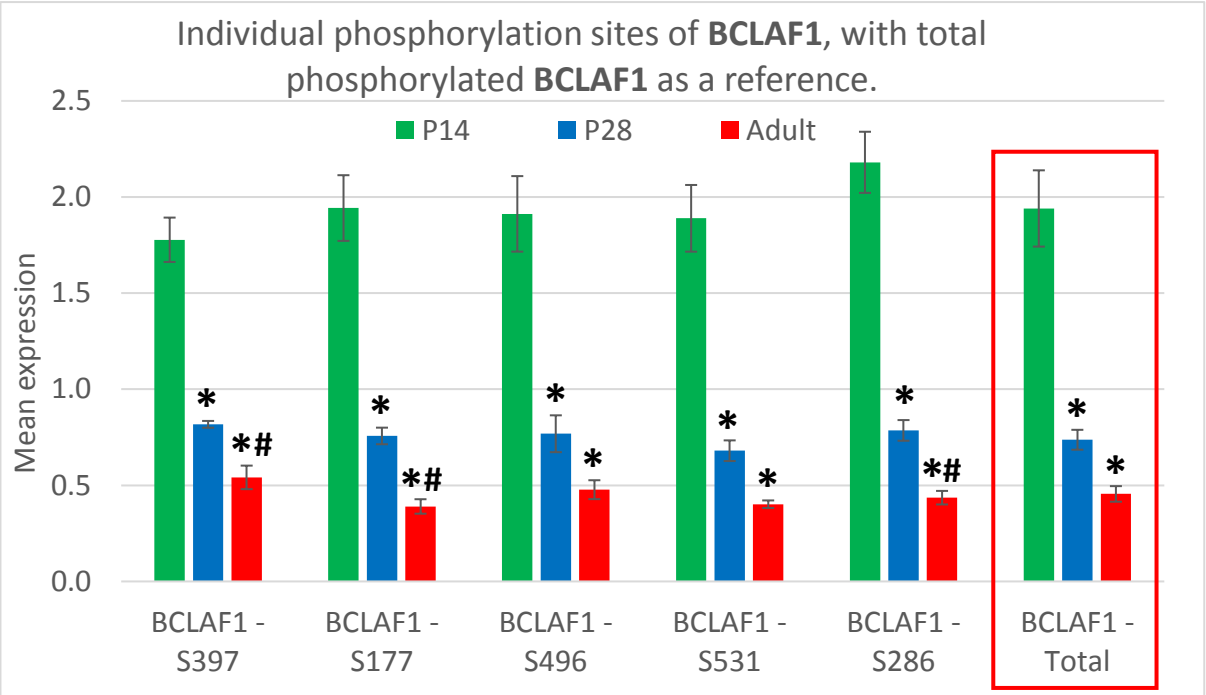

Figure 21. The individual phosphorylation sites detected with proteomic analysis and their pattern of change with age in comparison with the total phosphorylated protein for BCLAF1. Data are presented as Mean ± SE (P14 n = 3, P28 n = 3 and adult n = 4.) * = statistically significant difference compared to P14 ($p < 0.05$). # = statistically significant difference compared to P28 ($p < 0.05$).

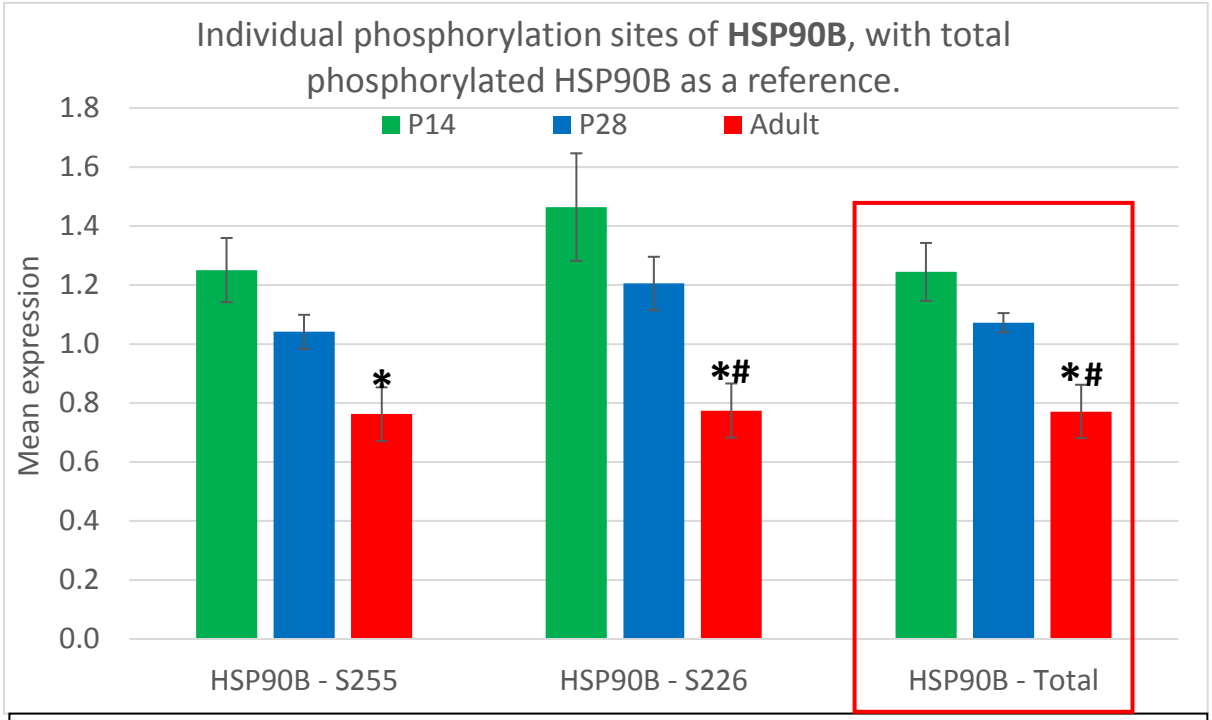

Figure 22. The individual phosphorylation sites detected with proteomic analysis and their pattern of change with age in comparison with the total phosphorylated protein for HSP90-β. Data are presented as Mean ± SE (P14 n = 3, P28 n = 3 and adult n = 4.) * = statistically significant difference compared to P14 ($p < 0.05$). # = statistically significant difference compared to P28 ($p < 0.05$).

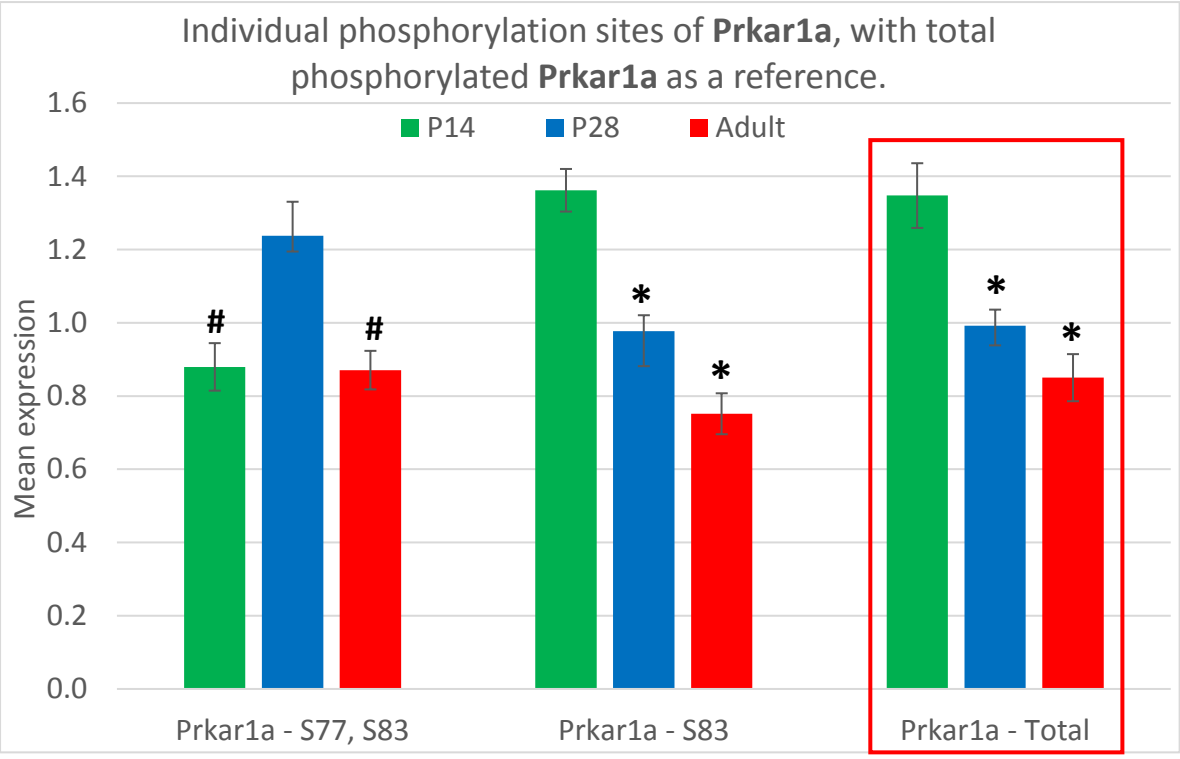

Figure 23. The individual phosphorylation sites detected with proteomic analysis and their pattern of change with age in comparison with the total phosphorylated protein for Prkar1a. Data are presented as Mean ± SE (P14 n = 3, P28 n = 3 and adult n = 4.) * = statistically significant difference compared to P14 ($p < 0.05$). # = statistically significant difference compared to P28 ($p < 0.05$).

In the case of Hspa12b, the two separate runs of phosphoproteomics identified exclusively either phosphorylation at Ser44 or Ser46. As the only other phosphorylation site present in both runs involved dual phosphorylation at both Thr42 and Ser44, which did not fit the overall pattern of change with postnatal development seen in the total phosphoprotein, analysis was run combining the data for Ser44 and Ser46 from the two runs under the possibility that, due to their proximity, this was actually data for the same phosphorylation site. The resulting pattern of change in phosphorylation at this site over the course of postnatal development did indeed match that shown by the total phosphoprotein.

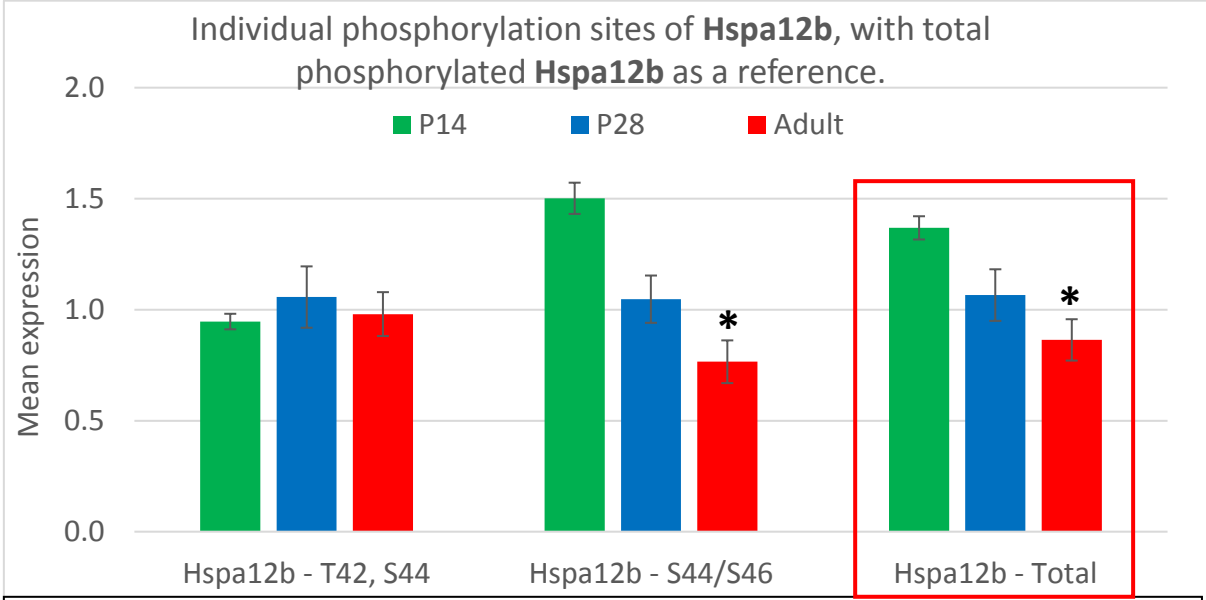

Figure 24. The individual phosphorylation sites detected with proteomic analysis and their pattern of change with age in comparison with the total phosphorylated protein for Hspa12b. Data are presented as Mean ± SE (P14 n = 3, P28 n = 3 and adult n = 4.) * = statistically significant difference compared to P14 ($p < 0.05$).

However, in some cases where multiple phosphorylation sites were detected for a single protein, not all were concordant with the overall protein, for example, Ser794 of Tensin 1 (**Figure 25**). The significance of this will be discussed further in **Section 3.4**

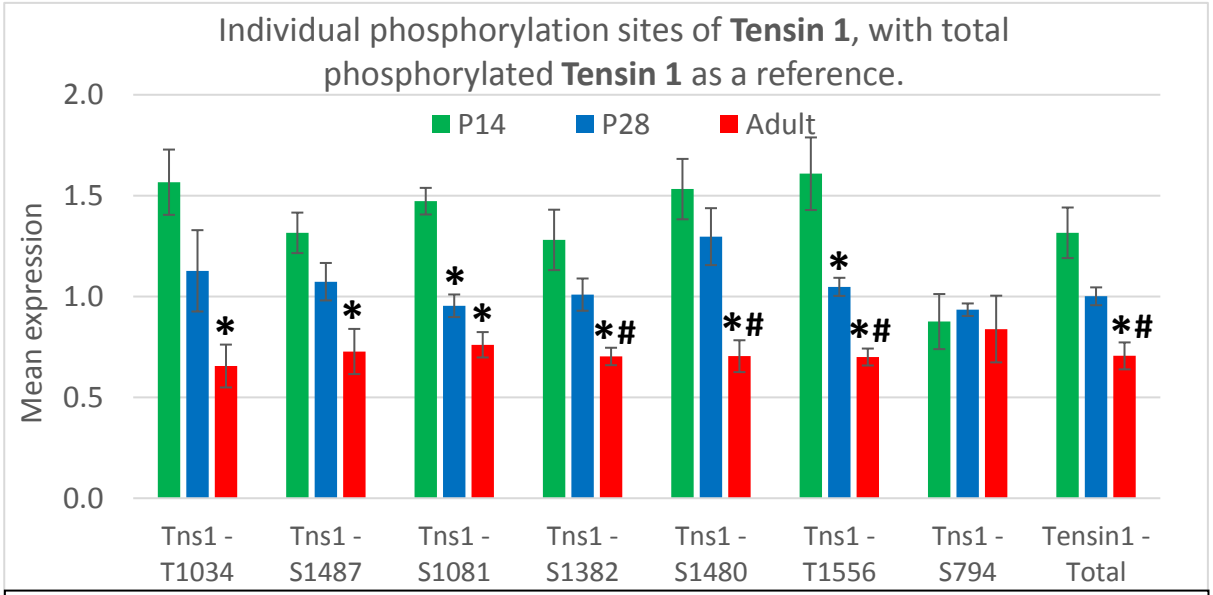

Figure 25. The individual phosphorylation sites detected with proteomic analysis and their pattern of change with age in comparison with the total phosphorylated protein for Tensin 1. Data are presented as Mean ± SE (P14 n = 3, P28 n = 3 and adult n = 4.) * = statistically significant difference compared to P14 ($p < 0.05$). # = statistically significant difference compared to P28 ($p < 0.05$).

3.3.2.3 Validation of significantly different survival signalling phosphoproteins using western blotting

In order to validate the phosphoproteomic output, western blot analysis was run on the same samples to check the trend in expression across the 3 age groups for selected proteins.

Statistical analysis using Kruskal-Wallis detected significant differences in distribution with age for both pβ-catenin normalised with GAPDH and β-catenin normalised with GAPDH, but not for pβ-catenin normalised with β-catenin (**Figure 26**). However, analysis using one-way ANOVA (Bonferroni), following confirmation of normal distribution of the samples using the Shapiro-Wilk test for normality, did in fact show a statistically significant difference in pβ-catenin/β-catenin levels between 14-day old and 28-day old samples. This trend correlates with that seen in the phosphoproteomic output for pβ-catenin.

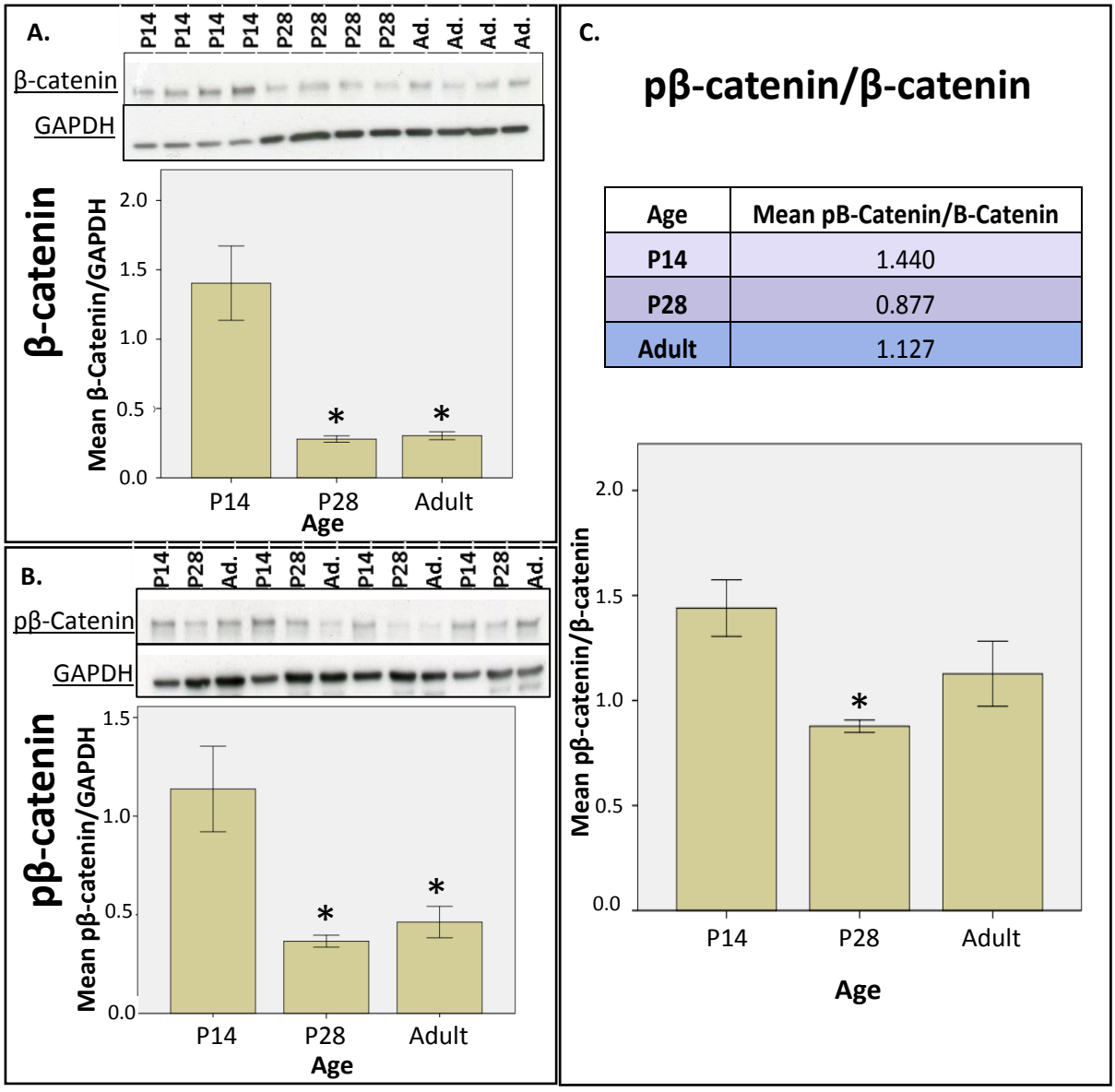

Age	Mean pB-Catenin/B-Catenin
P14	1.440
P28	0.877
Adult	1.127

Figure 26. Comparison of the mean levels of expression of β-catenin (A.) and pβ-catenin (B.) between age groups as measured by western blotting, in addition to the mean ratio of pβ-catenin/β-catenin (**C.**). Data are presented as Mean ± SE (n = 4 for each group). Antibody used was specific for phosphorylation at Ser552. * = statistically significant difference in comparison with P14 samples ($p < 0.05$).

Analysis of the western blotting data for Akt and pAkt (**Figure 27**) using Kruskal-Wallis showed that there was a statistically significant difference between the age groups for Akt normalised with GAPDH, pAkt normalised with Akt, but not pAkt normalised with GAPDH. Following a Shapiro-Wilk test for normal distribution of the data, leading to the exclusion of

one outlier from the 14-day old group for Akt/GAPDH, one-way ANOVA (Bonferroni) was run. Statistical significance was identified in this case only for Akt/GAPDH, therefore conflicting with the phosphoproteomic data for pAkt. It is important to note, however, that the antibody used in this case, as well as in most pre-existing research, targets phosphorylation at Ser473.

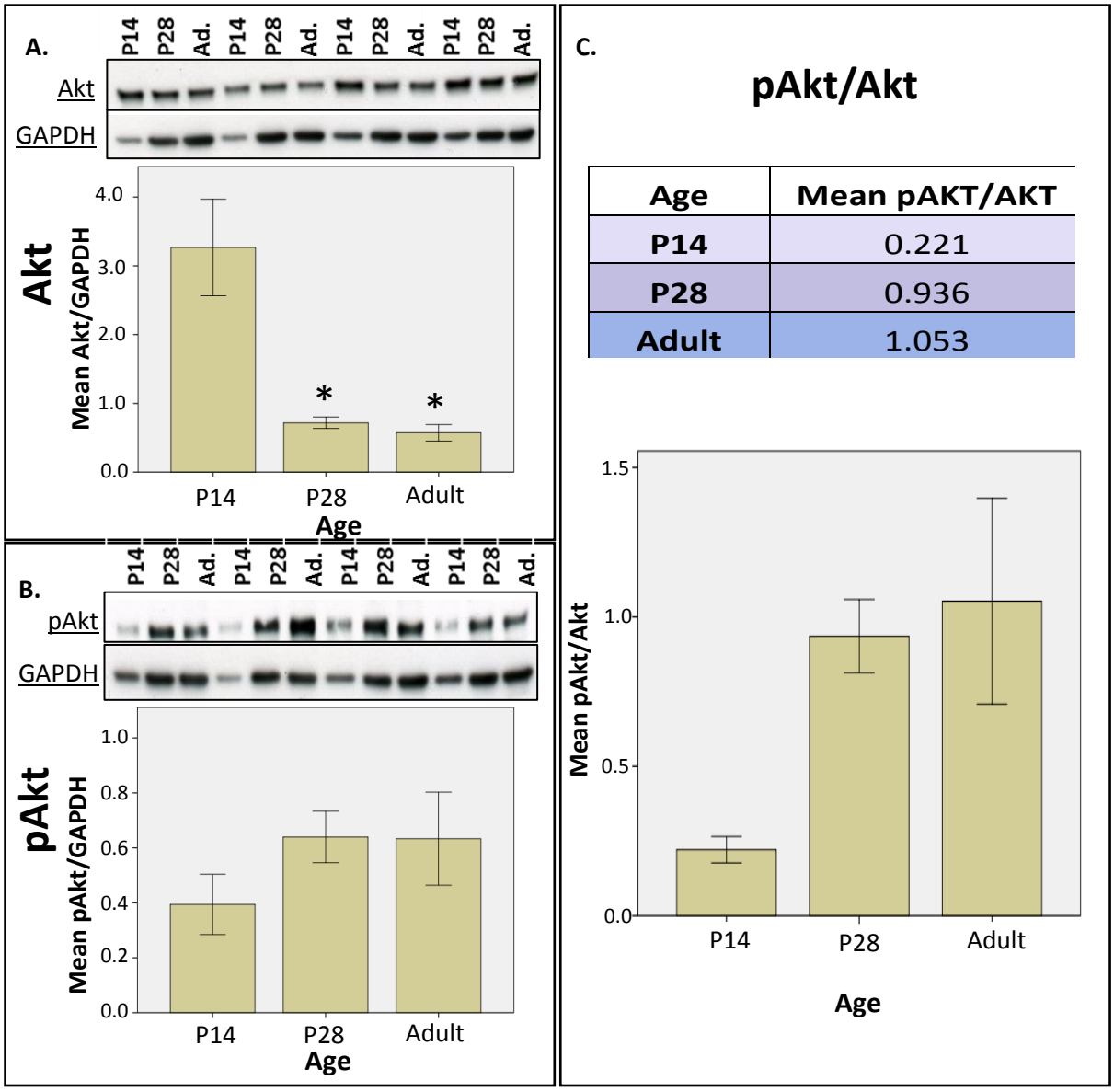

Figure 27. Comparison of the mean levels of expression of Akt (A.) and pAkt (B.) between age groups as measured by western blotting, in addition to the mean ratio of pAkt/Akt (**C.**). Data are presented as Mean ± SE (n = 4 for each group). Antibody used was specific for phosphorylation at Ser473. * = statistically significant difference in comparison with P14 ($p < 0.05$).

However, our phosphoproteomic analysis identified phosphorylation only at Ser129. Subsequently, western blot analysis was conducted with an antibody specific for phosphorylation at Ser129, as shown in **Figure 28** below.

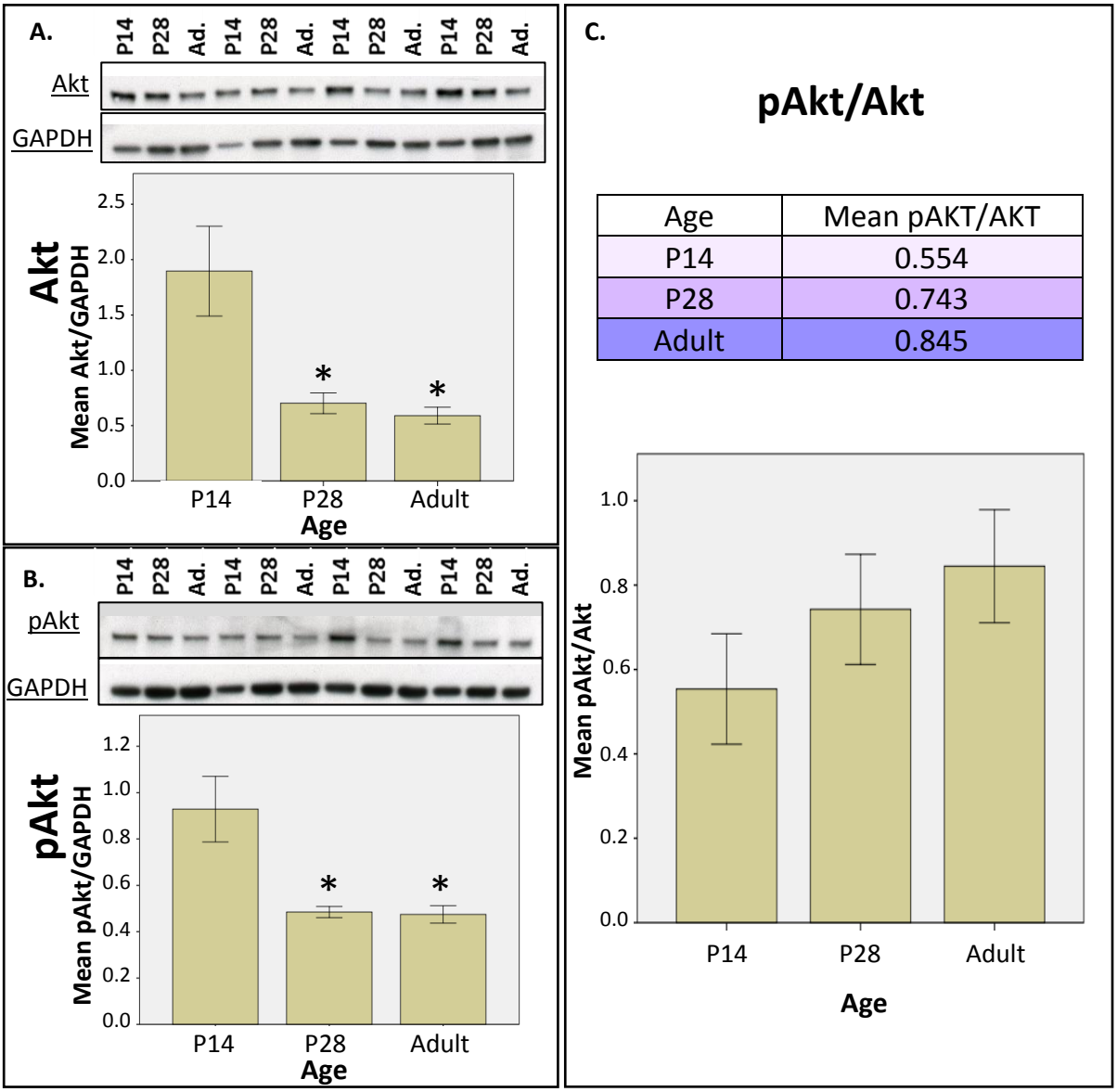

Figure 28. Comparison of the mean levels of expression of Akt (A.) and pAkt (B.) between age groups as measured by western blotting, in addition to the mean ratio of pAkt/Akt (**C.**). Data are presented as Mean ± SE (n = 4 for each group). Significant p-values labelled (One way-ANOVA, Bonferroni). Antibody used was specific for phosphorylation at Ser129. * = statistically significant difference compared with 14-day old samples ($p < 0.05$).

As with previous western blotting for Akt/GAPDH expression, 14-day old samples showed statistically significantly higher expression than both 28-day old and adult samples. In agreement with the phosphoproteomic output, pAkt/GAPDH expression was also higher in 14-day old samples in comparison with both 28-day old and adult samples. However, correction of pAkt expression with Akt expression removed these differences. As multiple phosphorylation sites are required for full activation, it may be that western blot analysis using antibodies targeting specific sites does not reflect what is seen in total phosphoproteomic output, and does not take into account the additive effects of phosphorylation at multiple sites. Discrepancies between the western blot data and phosphoproteomic output may also result from the fact that the phosphoproteomics only looks at phosphorylation level without taking into account a correction for the total protein. In this instance, the greater levels of phosphorylation detected at Ser129 in 14-day old samples was also found in our western blot data when looking at the expression of pAkt/GAPDH alone. The overall lack of difference in pAkt levels when corrected for Akt is likely due to fact that samples are from control hearts prior to any injury that would trigger the activation of survival signalling pathways, and this trend may indeed change following I/R.

3.4 Discussion

This pilot study – using a small number of cardiac samples to measure the survival signalling proteome and phosphoproteome – provided evidence that the trends in expression can, for the majority of proteins, be confirmed using a totally different technique involving antibodies. Furthermore, the analysis found that patterns of change in expression during development for the majority of proteins aligned with what would be expected from their reported roles in survival signalling and apoptosis in the literature, and the differences in vulnerability to I/R injury. It should be noted that the statistical power of this study was low (observed power = 0.612) due to the small sample sizes, but was repeated with greater n-numbers and an additional age group in **Chapter 4**.

3.4.1 Expression of survival signalling proteins tends to be higher in 14-day compared to adults

3.4.1.1 Target proteins of the RISK pathway show trends in expression with either a peak or trough at 14-days of age.

The majority of proteins found to change significantly in expression over the course of postnatal development displayed concordance between their expected role in pro-survival or apoptotic signalling events. Some of the most notable proteins identified in the proteomic output were those linked to the RISK signalling pathways, including HSP90, which acts as a cardioprotective inhibitor of apoptosis following I/R through its upstream regulatory action upon the PI3K/Akt pathway (Wang, Peng et al. 2009, Li, Luo et al. 2013), and shows a corresponding decrease in expression during postnatal development. Similarly, 14-3-3η, the knockout of which leads to GSK3β activation and decreased Akt phosphorylation (Gurusamy, Watanabe et al. 2006), caveolin-3, which causes elevated Akt and GSK3β phosphorylation

with associated improved recovery and reduced apoptosis following I/R (Tsutsumi, Horikawa et al. 2008, Horikawa, Panneerselvam et al. 2011), and HSP27 (HSPB1), a cardioprotective protein that results in reduced H_2O_2 and I/R-induced injury, as well as decreased ROS production and increased Akt activity when overexpressed in rat cardiomyocytes (Liu, Zhang et al. 2007), all show the highest expression at 14-days of age. Similarly, proteins linked to ERK signalling – another component of the cardioprotective RISK pathway – were found to be expressed at a greater level in immature hearts, including 14-3-3ζ as well as caveolin-1. Caveolin-1 has been shown to dissociate from pro-survival signalling ERK1/2 and associate with pro-death signalling p38MAPKα and JNK in angiotensin II pre-conditioned hearts in order to sequester a greater level of death promoting pathway components, whilst making a greater level of survival signalling components available to the cell (Das, Das et al. 2007). 14-3-3ζ knockout was found to result in increased mortality and cardiomyocyte apoptosis, with an associated inhibition of ERK activation and increased pro-apoptotic JNK and p38MAPK activation (Xing, Zhang et al. 2000). MEK5 expression was also shown to be greatest in the immature heart, correlating with its pro-survival activity through activation of anti-apoptotic ERK5 (Shishido, Woo et al. 2008), and its apparent link to caspase 3 activity, which increases following MEK5 deletion (Wang, Merritt et al. 2005). Interestingly, protein kinase C delta-binding protein – also known as cavin-3 – was found to be most highly expressed at 14-days of age, the biological significance of which raises conflict in terms of the involvement of RISK pathway components in the resistance to I/RI seen at this age. Whilst non-cardiac-specific papers have demonstrated cavin-3 to be a negative regulator of Akt activity through the action of EGR1 and PTEN, it has also been shown to act as a positive regulator of ERK signalling at the expense of Akt signalling through the anchoring of caveolae to the plasma membrane and subsequently allowing the transduction of activated ERK

signalling (Hernandez, Weng et al. 2013). However, it is likely that the Akt-inhibiting action of cavin-3 is the more significant in the context of cell survival, as studies have shown that knockout of the protein results in increased cell proliferation and increased resistance to apoptosis (Hernandez, Weng et al. 2013), as well as the attenuation of pro-apoptotic p53 signalling (Lee, Byun et al. 2008). The greater expression of cavin-3 at 14-days compared to adult hearts therefore shows discordance between its role in apoptosis and the differences in vulnerability to I/RI in these age groups. Subsequent monitoring of any changes in its expression in samples extracted from hearts following I/R, and the effect of its selective inhibition or overexpression on recovery following I/RI, will therefore be required.

3.4.1.1.2 Higher expression of ETC components in 14-day hearts

Conflicting roles of the Electron Transport Chain (ETC) component, Cytochrome c oxidase (COX), on cell survival have been reported in the literature (Schull, Gunther et al. 2015, Hütteman, Helling et al. 2012). It has been stated that deficiency of the protein results in the increased activation of ceramide synthase 6, causing the build-up of pro-apoptotic $C_{16:0}$ ceramide, which leads to accelerated mitochondrial apoptosis following oxidative stress and implicates it as an anti-apoptotic protein (Schull, Gunther et al. 2015). However, a contrasting role has been described in a study by Hütteman et al. (2012) in which the role of COX, due to its importance as the rate-limiting step of the ETC, was described as pro-apoptotic. Following ischemia, increased intracellular Ca^{2+} results in hyperactivation of COX via loss of allosteric inhibition by ATP and changes in the protein's phosphorylation state, which in turn leads to pathological high mitochondrial membrane potentials, excessive reactive oxygen species (ROS) production, release of cytochrome c, and finally apoptosis through the subsequent activation of caspases (Hüttemann, Helling et al. 2012). Finally,

mitochondrial dysfunction and secondary energy failure occurs as a result of COX and ETC hypoactivity during reperfusion, leading to cell death (Hüttemann, Helling et al. 2012). Whilst this study was conducted in the brain and not the heart, this mechanism of COX's role in apoptosis fits with our proteomic output for two of the three subunits detected, and may indicate that the higher expression of COX in mature hearts in comparison with immature hearts results in the greater vulnerability to ischemia/reperfusion injury seen, as these hearts are primed for hyperactivation of the ETC and greater levels of subsequent apoptosis. However, it is not certain if our findings of a higher expression of subunits such as Mt-co2 and Cox6a2 in 28-day old and adult hearts in comparison with 14-day old hearts reflects a corresponding higher level of activity of the protein, as others have reported greater activity of the ETC and COX in immature compared to adult hearts to compensate for the increasing energy demands following birth (Johnson and Brown-Borg 2006). It may be that, although activity is higher in the immature heart, the lower expression in comparison with adults may mean that the mature heart has a greater reserve of inactive protein that can be hyperactivated following I/RI, resulting in the greater vulnerability seen. Future steps will therefore be required in order to check if these expression levels correspond with activity of the protein, and with these changes following simulated I/RI. Alternatively, these contrasting reports of COX's role in apoptosis following I/R may in fact reflect subunit-specific roles, as four of the five subunits detected to change significantly in the proteomic output – subunits 2, 6A1 and 6A2 – and phosphoproteomic output – subunits 6B1 and 7A2 – have been described in the literature to contribute to apoptotic or survival pathways. For example, subunit 2 is responsible for the transfer of electrons from cytochrome c to the catalytic subunit 1 of COX, and has been shown to be upregulated in association with apoptosis-inducing cytochrome c as well as being induced in HIV infected T cells, with silencing of the

subunit leading to decreased levels of apoptosis (Tripathy and Mitra 2010). Similarly, subunit 6A2 has been linked to the oxidative stress response, associated with increased levels of pro-apoptotic Bax, and has been suggested to potentially lead to necrosis or apoptosis following a cytokine stress response (Adler-Wailes, Guiney et al. 2008). In apparent accordance with their pro-apoptotic roles, both subunits were shown to increase in expression over the course of postnatal development. In contrast, subunit 6A1 and 6B1 have both been indicated to have pro-survival roles (Eun, Woo et al. 2008, Kim, Mori et al. 2015), and were subsequently shown to decrease during postnatal development in the proteomic and phosphoproteomic output. Subunit 6A1 has been shown to suppress the death-inducing activity of Bax, with overexpression of the subunit resulting in decreased Bax-induced apoptosis, as well as the generation of ROS, release of cytochrome c, and activation of caspase 3 (Eun, Woo et al. 2008). Subunit 6B1 overexpressing cells were shown to have greater basal levels of ROS, but greater cell viability following oxidative stress than control cells (Kim, Mori et al. 2015). These studies highlight the importance of COX activity, as well as that of the individual subunits, to the degree of cardiac injury following I/R as a result of their effect on the levels of ROS production and oxidative stress – key mediators of I/RI and subsequent cell death. The differential expression of these proteins at different stages of development therefore identifies the need for further study into any correlating differences in their expression, as well as whether these trends mimic the biphasic profile of cardiac vulnerability, and how this effects the degree of cardiac injury in the context of I/RI at different ages.

3.4.1.1.3 Changes in the expression of HSPB6, TRIM72, Prkcdbp and Cd99 are not consistent with their reported role in survival signalling

Exceptions to the overall concordance of the change in protein expression with postnatal development and their role in survival signalling within the proteomic data are HSPB6 and TRIM72, which increase with increasing age despite being pro-survival proteins (Fan, Chu et al. 2005, He, Tang et al. 2012), in addition to Prkcdbp and Cd99, which are both implicated in pro-apoptotic processes and decrease with increasing age (Sohn, Choi et al. 1998, Hernandez, Weng et al. 2013). In the case of TRIM72, this may be linked to its apparently crucial role in preconditioning. As TRIM72 levels have been shown to decrease following I/R or hypoxia/oxidative stress, an effect that has been shown to be prevented following IPC, Cao et al. (2010) aimed to address the importance of TRIM72 in IPC. It was found that TRIM72 interacts with caveolin-3 and PI3K to activate the RISK pathway, leading to a reduction in cell death following I/R or hypoxia/oxygenation, and that deficiency or knockdown of the protein resulted in heightened damage, as well as the loss of the cardioprotective effects provided by IPC (Cao, Zhang et al. 2010). The lower expression of TRIM72 seen in immature hearts in comparison with mature hearts in our proteomic data may therefore correlate with the lack of efficacy of IPC in young hearts (Doul, Charvatova et al. 2015).

3.4.1.1.4 PRKAR1A is highly expressed in the young heart

An additional confounding factor in the comparison between our proteomic data and the supposed roles of the identified proteins in the literature is the fact that, in some cases, reports as to the effects of these proteins on apoptosis and the response to I/RI are conflicting. For example, the cAMP-dependent protein kinase type I-alpha regulatory

subunit (PRKAR1A) has been described as having a pro-apoptotic role due to its regulatory effects on PKA activity, an important regulator of cell growth and function (Yin, Pringle et al. 2011). The study showed that knockout of this regulatory subunit resulted in excessive PKA activity and tumorigenesis, a finding supported through demonstration that depletion of the subunit resulted in increased BCL-XL expression, resistance to apoptosis, and increased PKA and MEK/ERK signalling (Basso, Rocchetti et al. 2014). However, knockdown of this protein, whilst increasing PKA activity, has also been shown to result in decreased cardiomyocyte proliferation and downregulation of key transcription factors required for cardiogenesis (Yin, Jones et al. 2008), as well as an increase in the transcription of pro-apoptotic proteins, such as members of the BCL-2 family, and increased apoptosis (Gangoda, Doerflinger et al. 2014).

Alternatively, PKA has been demonstrated to have an effect on sympathetic stimulation via phosphorylation of ryanodine receptors and other Ca^{2+}-cycling proteins, with subsequent alterations to Ca^{2+}-cycling, increased NCX currents, increased sinoatrial node (SA) node firing rate, and therefore increased heart rate (Larsson 2010). As mentioned in **Section 1.1.1**, neonatal heart rates are lower than that of adult rats, with slower Ca^{2+}-cycling and greater action potential durations. It is therefore possible that the greater expression of PKA-regulating PRKAR1A in 14-day old hearts is a reflection of the lower heart rates in this age group. Moreover, due to the fact that immature hearts show a greater reliance on Ca^{2+}-influx from extracellular sources and the action of the NCX to control Ca^{2+}-cycling, due to the underdevelopment of the SR and relatively small contribution of Ca^{2+}-channels at this stage of development (**Section 1.1.1**), high levels of PRKAR1A may also present a protective mechanism by which PKA activity is reduced to prevent Ca^{2+}-overload. PKA has been suggested to increase NCX activity via upstream phosphorylation targets (Yaniv, Juhaszova

et al. 2011), and thus high levels of PRKAR1A may be expressed in order to reduce excessive NCX activity in 14-day old hearts.

The uncertainty as to the exact role of some of the identified proteins makes a definitive connection between the levels of their expression with the vulnerability profile to I/RI difficult to elucidate, with studies often highlighting tissue-specificity for the role of these proteins. In order to address this issue, further work will be required to look at expression levels in hearts that have undergone ischemia/reperfusion in order to form a comparison with their expression in control hearts, in addition to experiments looking at the activity of these proteins and the result of selective inhibition.

3.4.1.2 Phosphorylated survival signalling and cardioprotection related proteins change in expression during development

3.4.1.2.1 Cardioprotective pHSPB6 expression increases during postnatal development

Whilst most proteins identified in the phosphoproteomic output also correlated with their expected role in survival signalling, a notable exception was HSPB6, which was shown to increase during postnatal development, a similar trend to that displayed in the non-phosphorylated proteomic data. This is unexpected, as HSPB6 has been described within the literature as possessing a pro-survival and anti-apoptotic role (Fan, Chu et al. 2005, Gusev, Bukach et al. 2005), therefore suggesting it should show greater expression in cardiac samples taken from 14-day old rats, which show the greatest resistance to I/R injury. Furthermore, HSPB6 phosphorylation at Ser16 was shown to increase over the course of postnatal development, again contradicting its reported role in the literature, as phosphorylation of this site by PKA has previously been shown to be the phosphorylation

event required for the cardioprotective effects of HSPB6, with inhibition of Ser16 phosphorylation resulting in the loss of HSPB6's cardioprotective effects (Nicolaou, Knoll et al. 2008, Qian, Ren et al. 2009). The low levels of phosphorylation at this site in 14-day old hearts is further confounded by the detection of phosphorylated AKAP12 in the phosphoproteomics, which is reportedly activated to enhance its scaffolding ability by PKA (Tao, Wang et al. 2010), and is a member of a protein family suggested to be cardioprotective through its vital role in localising PKA within certain regions of the cell in order to direct its phosphorylation of substrates such as HSPB6 at Ser16 (Edwards, Scott et al. 2012). However, previous research has shown that HSPB6 levels, in addition to levels of Ser16 phosphorylation, are higher specifically within the ischemic myocardium, with cardiac-specific overexpression resulting in decreased infarct size and improved recovery of contractile performance following I/R, due to the protein's ability to reduce necrosis and apoptosis in cardiomyocytes (Edwards, Scott et al. 2012). This suggests that, as our samples were taken from control hearts, the simulation of I/R may result in a reversal of the trend detected in the proteomic and phosphoproteomic output, with greater expression of Ser16 phosphorylated HSPB6 in immature hearts correlating with decreased cell death and increased recovery following ischemic insult. It is therefore possible that, as is the case for pAkt (Liaw, Hoe et al. 2013), basal levels of the active protein are low in immature hearts, allowing for subsequent activation and thus a protective response following damage which cannot be mimicked in mature hearts due to baseline high levels. HSPB6 is therefore a protein of interest for future experiments, to examine the differences between these age groups with samples that have undergone I/R in comparison with those that have not.

3.4.1.2.2 Phospho-Cytochrome b-c_1 increased in expression during development

HSPB6 comprised one of only two phosphoproteins that increased in expression during the course of postnatal development, the other being cytochrome b-c_1 subunit 6. However, unlike HSPB6, this pattern of change with age does fit with the protein's reported role in the apoptotic process. Cytochrome b- c_1 has been implicated as a component of the intrinsic apoptotic pathway, triggering this process in order to drive the removal of cells containing mitochondria that have begun to produce ROS following an event inducing irreparable damage (Dibrova, Cherepanov et al. 2013), in addition to enhancing cytochrome c release from the mitochondria in order to accelerate the apoptotic process (Okazaki, Ishibashi et al. 1998). However, a potentially conflicting role for the protein, as studies looking at the cardioprotective effects of preconditioning (PC) and pharmacological inhibition of GSK3β via their effect on the mitochondria found that cytochrome b-c_1 subunit 6 levels were increased, with decreased levels of cytochrome c, suggesting PC results in alteration of ETC components that result in cardioprotective effects on mitochondrial function (Wong, Aponte et al. 2010). While the low expression of this protein in 14-day old hearts and its apparent link to PC may correlate with the lack of efficacy of PC in immature hearts, this study did not provide a true cause and effect relationship between cytochrome b-c_1 levels and mitochondrial function or recovery of the heart post-I/R. Moreover, the biological significance of phosphorylation has not yet been reported, meaning it is uncertain as to whether the protein has been detected in its active or inactive state.

3.4.1.2.3 RISK pathway targeted phosphoproteins change during postnatal development

As with the total proteomic output, several proteins associated with members of the cardioprotective RISK pathway were found to change significantly with age during postnatal development. For example, HSPA12B has been shown to result in decreased infarct size, as well as improved cardiomyocyte survival and cardiac function following I/RI when overexpressed or upregulated, with an associated enhancement of PI3K/Akt pathway activation (Ma, Lu et al. 2013, Kong, Dai et al. 2016), and abolition of its cardioprotective properties following the pharmacological inhibition of PI3K/Akt (Zhou, Qian et al. 2011, Kong, Dai et al. 2016). YAP1 (Lin, Zhou et al. 2015), HSPA9 (Li, Yang et al. 2011, Na, Kaul et al. 2016), and hNRNP-K (Hutchins, Belrose et al. 2015) have also been implicated as mediators or downstream targets of the PI3K/Akt or ERK1/2 signalling within the RISK pathway.

3.4.1.2.4 Pro-apoptotic phospho-proteins decrease in expression during development

Unexpectedly, several reportedly pro-apoptotic proteins displayed greater levels of expression at 14-days of age than in adults. For example, BCLAF1 is a transcriptional repressor that leads to increased apoptosis and cell death (Kasof, Goyal et al. 1999, Haraguchi, Holaska et al. 2004, Wessely, Seidl et al. 2005, Sarras, Alizadeh Azami et al. 2010, Berk, Tifft et al. 2013), Tp53i11 is a p53 target gene that promotes apoptosis following cellular stress (Liang, Cao et al. 2004, Ise, Han et al. 2005), and Dcaf8, as well as other members of its protein family, has been described as a mediator of apoptosis (Tsunekawa, Kondo et al. 2013, NCBI 2016). Similarly, ARHGEF2 has been implicated as death promoting

through activation of RhoA/ROCK signalling in cardiomyocytes (Chang, Lee et al. 2006, Chang and Lee 2006, Huang, Chen et al. 2014, Meiri, Marshall et al. 2014), and MAP4K4 reportedly activates the TAK1, JNK and mitochondrial death pathways (Xie, Zhang et al. 2007), in addition to mediating pro-apoptotic TNF-α action and inhibiting pro-survival protein YAP via phosphorylation of LATS (Meng, Moroishi et al. 2015). In the case of ARHGEF2, phosphorylation has been suggested to hold an inactivating effect on functional activity (Meiri, Marshall et al. 2014), suggesting it may be highly expressed in its inactive state at 14-days of age. However, the functional significance of ARHGEF2's individual phosphosite detected by phosphoproteomics is not yet known, an issue that is seen with many of these phosphoproteins. As a result, it is uncertain as to whether the data produced involves proteins that are functionally active or inactive, making correlation with an effect on cell survival and the vulnerability profile to I/RI difficult to determine.

3.4.1.2.5 Changes in specific phosphorylation sites correlate with total phosphoprotein sites

As mentioned in **Section 3.4.2.2**, individual phosphorylation sites displayed a predominantly concordant pattern of change over the course of postnatal development to that seen in the total phosphorylated protein. An exception to this involved a protein for which multiple phosphorylation sites were detected; Ser794 of Tensin 1. Whilst these differences may be due to interference from other modifications present within the detected peptides, or due to differences in confidence ratings, the functional roles of this phosphorylation site has not previously been described in the literature. Potentially, those which do not fit the pattern of change seen in the total phosphorylated protein, or indeed the other phosphorylation sites detected, may do so as a result of a conflicting functional role. As most of the detected

phosphorylation sites are more greatly enriched in 14-day old rat hearts, it may be that phosphorylation sites such as Ser794 of Tensin 1, which do not follow this pattern of expression, are not involved in the protein's survival signalling activities, or may even be repressors of this activity. Further work will be needed to investigate the functional roles of such phosphorylation sites.

3.4.1.2.6 Phospho-Akt levels measured using proteomics did not correlate with western blot analysis

Analysis of the phosphoproteomic output also identified that phosphorylation of the pro-survival signalling protein, Akt1, at Ser129 was shown to be greater at 14-days, a phosphorylation site reported to be phosphorylated by the anti-apoptotic kinase, Casein Kinase 2 (CK2) (Di Maira, Salvi et al. 2005), subsequently promoting the catalytic activity of Akt1. It should be noted that the pattern of change in pAkt/Akt expression over the course of postnatal development obtained from the western blot data showed a complete reversal to that seen in the phosphoproteomic output, with the highest levels of pAkt expression in adult samples. The reason for this discrepancy between our proteomic data and the western blot trends in pAkt expression during postnatal development is uncertain, but may be a result of the non-specificity of the antibody to Akt1, which was the isoform detected by phosphoproteomic analysis, in addition to the fact that phosphoproteomics only detected phosphorylation at Ser129, whereas the antibody used in initial experiments was specific to Ser473. Subsequent testing with an antibody specific for phosphorylation at Ser129 did in fact show statistically significant changes in abundance across the three age groups that was concordant with that seen in the phosphoproteomic output, with the greatest levels of pAkt-Ser129 in 14-day old samples compared with both 28-day olds and adults. However,

correction for total Akt expression removed any statistically significant differences between the three age groups. It is therefore likely that discrepancies between the western blotting data and phosphoproteomic output result from the fact that phosphoproteomic analysis did not account for total protein expression, only looking at the raw abundance of phosphorylation at each site to the pooled sample. This correlates with previous reports that neonates exhibiting a greater tolerance to I/R also possess a large pool of inactive, non-phosporylated Akt in comparison with adults, and that adults show greater damage following I/R that correlates with decreased expression of Akt (Liaw, Hoe et al. 2013). The authors suggest that this "Akt reserve" allows immature hearts to produce a powerful pro-survival response following I/R through phosphorylation and activation of the inactive Akt pool, resulting in a greater tolerance to I/RI than that seen in mature hearts. However, the specific phosphorylation site used in this study was not reported by the authors, making exact comparison between our findings and their data difficult.

Antibodies targeting Ser473 are the most predominantly utilised in the literature, with phosphorylation at Ser473 often being reported as the key step for Akt activation, whereas our phosphoproteomic output did not detect any phosphorylation at Ser473. This apparent difference in phosphorylation levels between two reportedly activating phosphosites of Akt during postnatal development raises the possibility that it is in fact Ser129 phosphorylation that is the more important modification in the context of developmental-related differences in survival signalling. However, it will be necessary to further investigate the reason for the complete lack of Ser473 detection in the phosphoproteomic output, and whether this is merely a reflection of the fact that samples tested were taken from non-stressed hearts which likely would not have any need for the activation of survival signalling pathways.

3.4.2 Summary & Conclusion

Proteomic and phosphoproteomic analysis identified a number of proteins linked to survival signalling and apoptosis that showed statistically significant changes in expression over the course of postnatal development. The trend in expression of the majority of these proteins was consistent with their reported roles in cell survival, with most pro-survival proteins showing their greatest levels of expression at 14-days of age, and most of those that promote cell death showing their greatest levels of expression in adults. Western blot validation of selected proteins demonstrated patterns of expression that were by and large concordant with that seen in the proteomic output. However, this work does not address the biphasic (bell-shaped) profile in response to I/R which involves including younger age group compared to 14-day old. Therefore, further proteomic/phosphoproteomic work was undertaken to further explore the expression patterns of survival-related proteins in order to identify those displaying biphasic profiles of expression, as will be described in **Chapter 4**.

Chapter 4: Developmental Changes in the Cardiac Survival Signalling Proteome in relation to vulnerability to cardiac insults

4.1 Introduction

As discussed in **Sections 1.4** and **1.5**, pro-survival and anti-apoptotic signalling pathways such as RISK-SAFE play a crucial role in the reduction of cell death and subsequent cardiac injury following I/RI. Our hypothesis states that, due to their importance in the I/RI response, underlying differences in the abundance and activity of these proteins may exist between age groups, contributing to the differences in cardiac vulnerability identified over the course of postnatal development. In order to address whether differences in the expression and phosphorylation state of RISK-SAFE proteins, as well as those known to cross-talk with these signalling pathways, may exist at different developmental stages, proteomic and phosphoproteomic analysis was utilised using age groups that are known to result in the bell-shaped vulnerability profile. Potential proteins of interest were identified through literature searches and signalling pathway maps, before statistical analysis to highlight those that showed a significant peak or nadir in expression at 14-days of age, coinciding with the peak in cardiac resistance to I/RI at this age. Identification of any survival related proteins with a pattern of postnatal expression mimicking the profile of cardiac vulnerability would therefore provide promising targets for further experimentation as to the effect of their inhibition on cardiac injury, and potential differences in the response of hearts from different age groups.

4.2 Materials & Methods

4.2.1 Animal groups & sample extraction

Proteomic and phosphoproteomic analysis was conducted with samples taken from 7-day old (n = 4), 14-day old (n = 8), 28-day old (n = 8) and adult (n = 7) rats. Rats were culled as outlined in **Section 2.2**, hearts excised, and the apex removed for flash freezing in liquid nitrogen. Tissue then underwent protein extraction and quantification as described in **Sections 2.4.1** and **2.4.2**.

4.2.2 Proteomic and Phosphoproteomic Analysis

The full process of proteomic and phosphoproteomic analysis has been described in **Section 2.4.3**, but can be summarised as the dilution of the quantified samples mentioned in **Section 4.2.1** with double distilled water to adjust the protein concentration of each sample to 2mg/ml for sending to the University of Bristol Proteomics Facility, in order for samples to undergo Tandem Mass Tag (TMT) analysis (ThermoFisher Scientific, UK). For phosphoproteomic analysis, samples underwent an additional phosphopeptide enrichment step using a TiO_2 column (**Section 2.4.3**).

The resulting output came in the form of a *Proteome Discoverer* file with the abundance of each protein in each sample as a ratio to the pooled sample, from which proteins selected from the existing literature and signalling pathway database searches as relating to cell survival processes were identified (see **Section 2.4.4**). These proteins then underwent statistical analysis in order to identify those that showed significant changes in expression between age groups concordant with the cardiac vulnerability profile during postnatal development (see **Section 2.8**).

4.3 Results

An initial run of proteomic analysis was conducted for survival signalling proteins, with western blot validation of the proteomic data, using only 3 age groups; 14-day old, 28-day old and adult hearts (**Chapter 3**). A younger age group is important for testing and comparison to the biphasic profile of vulnerability to I/RI. Therefore, protein was extracted from the cardiac tissue of 4 age groups, 7-day (n = 4), 14-day (n = 8), 28-day (n = 8) and adult (n = 7) rats, and used for proteomic analysis (as described in **Section 2.4**). From this data, we identified relevant proteins presenting with a similar biphasic profile expression mirroring that of vulnerability to I/RI for future targeting. For figure clarity, P7, P14 and P28 were used to represent postnatal day 7, 14 and 28, respectively.

4.3.1 Comparison of trends in key survival signalling protein expression between the original proteomic output and the new proteomic output.

Proteins from the original proteomic output were identified in the new proteomic output in order to determine which of these – selected for being most highly expressed in 14-day old hearts in comparison with adult hearts – also showed a biphasic pattern of expression in the new proteomic output. Of the original 59 proteins selected for their role in survival signalling – 33 of which showed statistically significant differences in expression between 14-day old and adult samples in the first run of proteomics (**Section 3.3.1**) – only 14 had an overall biphasic trend in expression, with only 5 of these showing a statistically significant difference in comparison to both 7-day old and adult samples. This new run of proteomic analysis has subsequently allowed us to exclude a large number of proteins of interest identified from the original proteomic output from further investigation and study, as they do not fit the biphasic profile seen in cardiac vulnerability over the course of postnatal development.

4.3.2 Do changes in survival signalling proteins during postnatal development follow a biphasic profile?

We identified 659 proteins that were related to survival signalling, either directly within the RISK-SAFE pathways or within peripheral/interconnected pathways in all age groups. Comparing the 14-day old and adult proteome, we found 468 proteins were expressed at a higher level in 14-day old samples, with 37 proteins showing significantly lower expression in 14-day old samples (**Figure 29**).

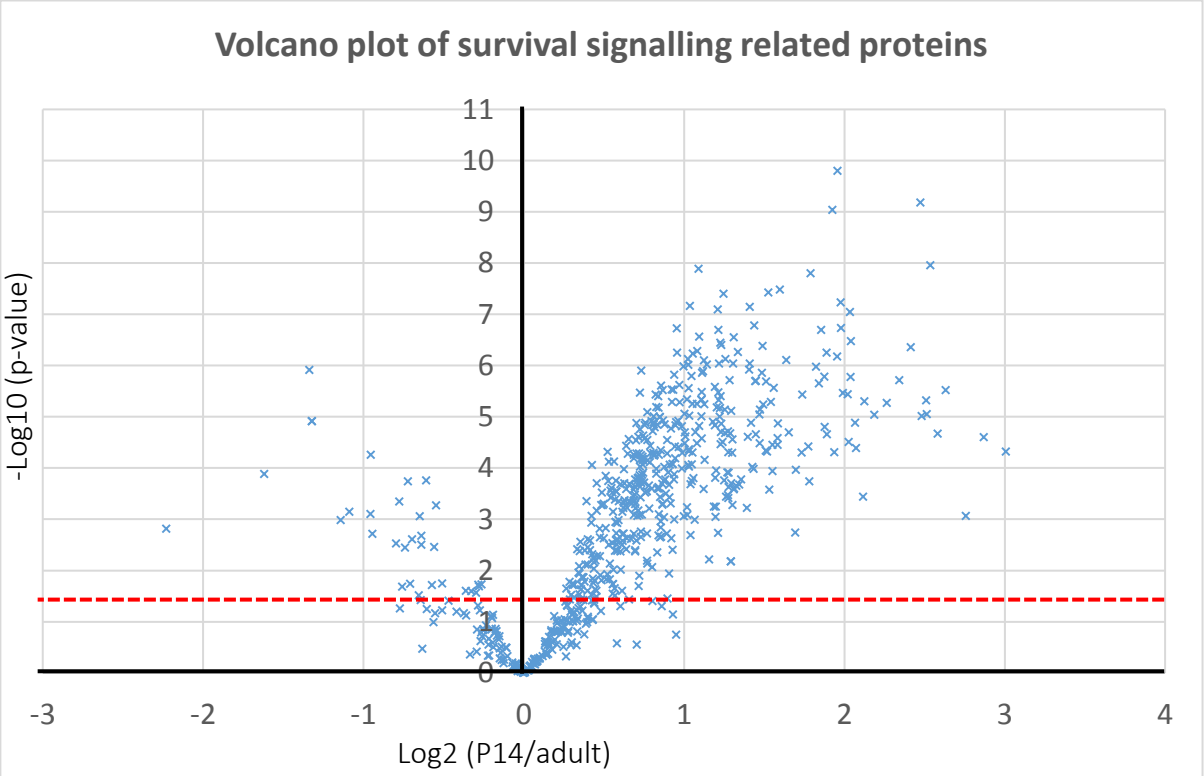

Figure 29. Volcano plot of all survival signalling proteins identified in the proteomics (n = 659), comparing fold difference (FD) between the average protein expressions in 14-day old and adult heart samples expressed as log2 (x-axis), against the p-value expressed as –log10 (y-axis). The red line indicates a cut-off point for statistical significance (p = 0.05) for change in expression between adult and 14-day old hearts.

However, to match the biphasic profile of vulnerability to I/RI, we focused on proteins which also displayed a biphasic profile of expression with age including 7- and 28-days old. The

original proteomic output identified a total of 10,453 proteins, 412 of which demonstrated a biphasic profile of expression across the four age groups. Of the 659 survival signalling-related proteins previously described, 346 were found to exhibit a profile with a peak or nadir of protein expression at 14-days, with statistically significant differences between 14-day old and adult samples. However, of these, only 86 proteins also showed statistically significantly differences between 14-day and 7-day old samples. For the purposes of this work, only key proteins strongly involved with the RISK-SAFE pathways specifically, exhibiting biphasic profiles of expression, are presented in **Figure 30**.

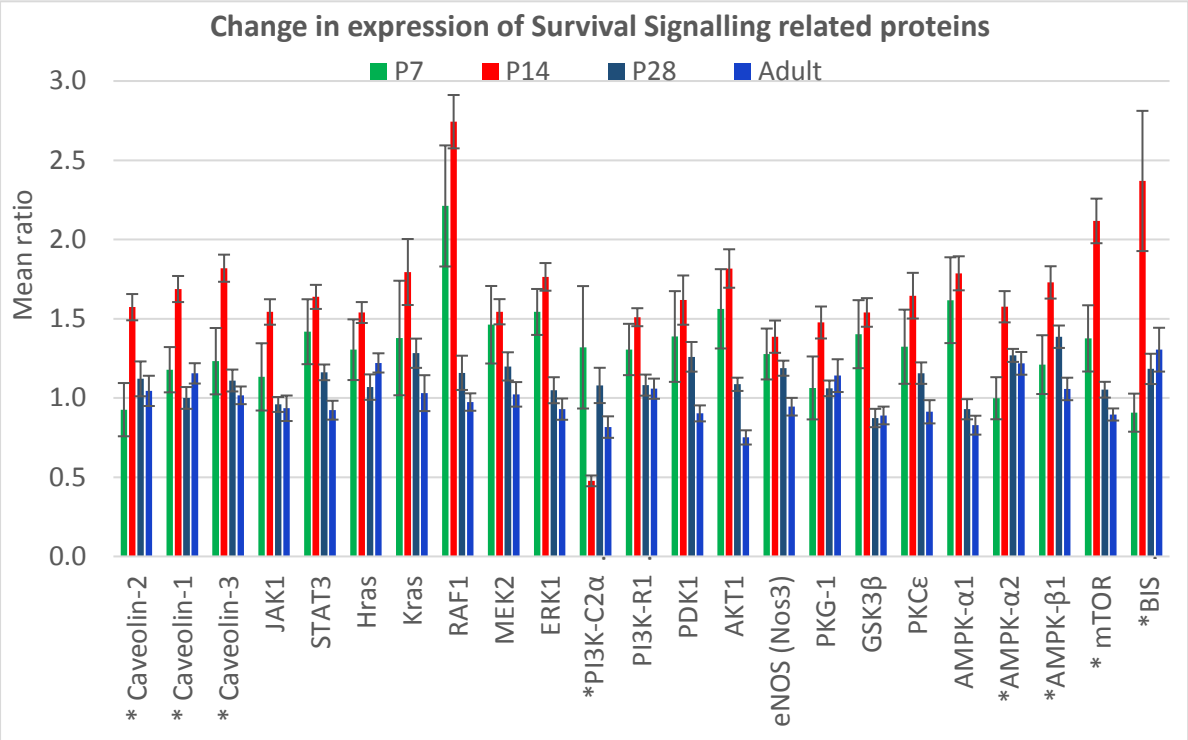

Figure 30. Biphasic profile of key survival signalling related protein expression in the proteomic output. All proteins show statistically significant difference between 14-day old and adult samples. Proteins with (*) also show statistically significant difference between 14-day old and 7-day old samples. Data for adult and 28-day old tend to follow similar pattern. Data expressed as Mean ± SE.

4.3.3 Phospho-proteomic Output

As described in **Section 2.4**, samples also underwent phosphoproteomic analysis. Of the original proteins of interest, selected due to their central role in RISK-SAFE and survival signalling and displayed in **Section 4.3.2**, complete sets of phosphoproteomic data – i.e. detected in all three sets and thus all four age groups – were only identified for two proteins; Akt1 and AMPK-β1 (**Figures 31** and **32**).

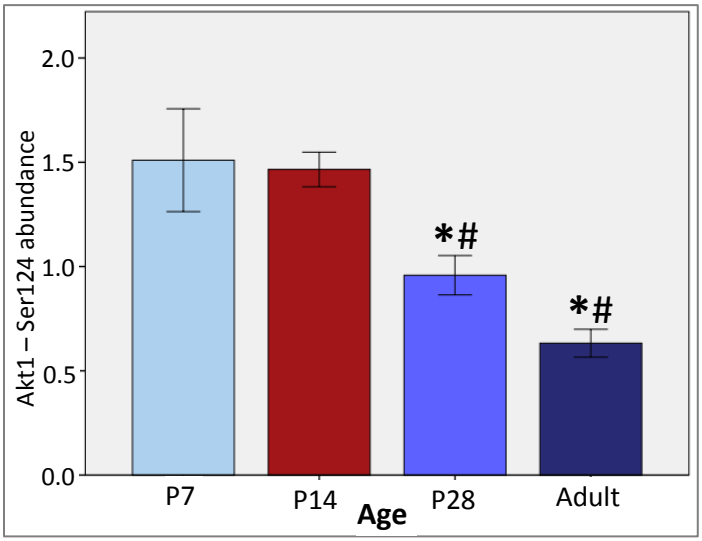

Figure 31. The abundance of Akt phosphorylation at Ser124 across the 4 age groups (7-day (n = 4), 14-day (n = 8), 28-day (n = 8) and adult (n = 7)). * = Statistically significant difference in comparison with 7-day old samples ($p < 0.05$). # = Statistically significant difference in comparison with 14-day old samples ($p < 0.05$). Data presented as Mean ± SE.

Whilst both 7-day old and 14-day old samples showed statistically significantly higher levels of pAkt phosphorylation at Ser124 than both 28-day old and adult, no significant difference was seen between 7-day old and 14-day old samples.

Two separate phosphorylation sites were detected for pAMPK-β1, as shown in **Figure 32** below, both of which showed markedly differing trends of abundance between the four age groups. Phosphorylation at Ser24 followed the expected trend of statistically significantly greater levels in 14-day old samples in comparison to both 28-day old and adult samples. Phosphorylation at Ser108 showed statistically significantly greater levels in 28-day old

samples in comparison to all of the other three age groups. The significance of these phosphosites is discussed in further detail in **Section 4.4.3**.

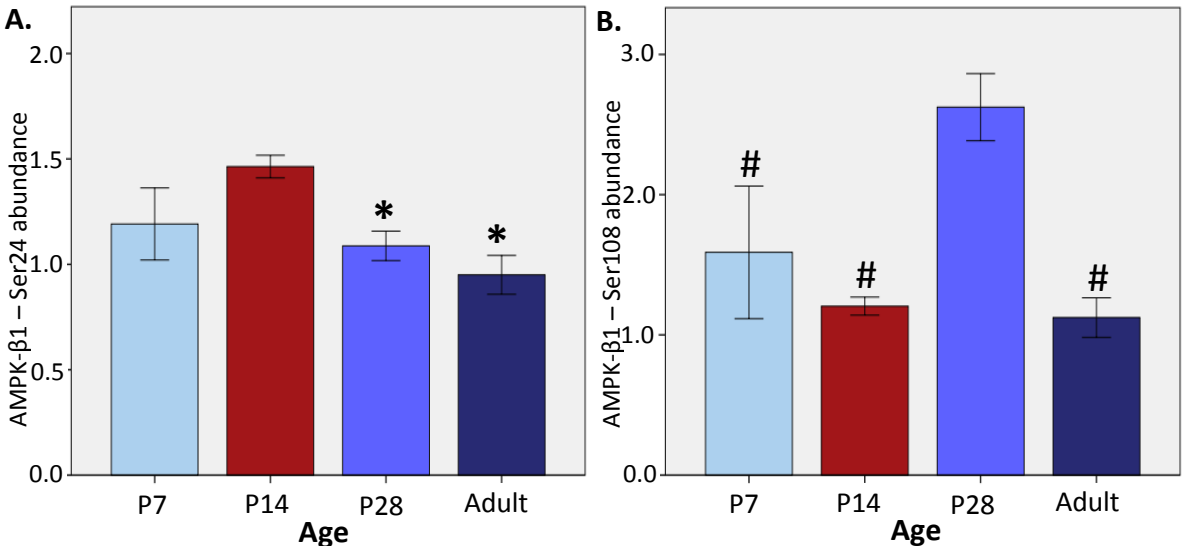

Figure 32. Relative abundance of AMPK-B1 phosphorylation at **A.** Ser24 and **B.** Ser108 across the 4 age groups (7-day (n = 4), 14-day (n = 8), 28-day (n = 8) and adult (n = 7)). * = Statistically significant difference in comparison with 14-day old samples ($p < 0.05$). # = Statistically significant difference in comparison with 28-day old samples ($p < 0.05$). Data presented as Mean ± SE.

4.4 Discussion

Proteomic and phosphoproteomic analysis show that patterns of change in expression during development for the majority of proteins aligned with what would be expected from their reported roles in survival signalling and apoptosis in the literature, and the differences in vulnerability to I/R injury. A number of key and peripheral survival signalling proteins were identified in an initial run of proteomic analysis with only 3 age groups as displaying a gradual decrease or increase in expression from 14-days of age to adult (**Chapter 3**). A second run of proteomic analysis including a fourth age group – 7-day old rats – as well as a larger number of samples per age group (**Section 4.3**), switching from the use of the TMT-6plex to TMT-10plex kit and from the LTQ-Orbitrap Velos Mass Spectrometer (Thermo Fisher) to the Orbitrap Fusion Tribid Mass Spectrometer (Thermo Fisher) with greater sensitivity, identified a greater number of proteins that are more central to the RISK-SAFE survival signalling pathways than those identified in the initial run of proteomics. The addition of the fourth age group also allowed for biphasic trends in expression analogous to the cardiac vulnerability profile to be identified, with the subsequent exclusion of a number of proteins from the initial run that showed a gradual change in expression with postnatal development, but not the characteristic biphasic profile of interest.

4.4.1 RISK-SAFE pathways proteins displayed age-related biphasic changes in expression

As discussed in **Section 1.5**, the RISK-SAFE signalling pathways play a key role in cell survival following ischemic insult, in addition to other overlapping cardioprotective pathways. A number of these proteins were subsequently found to display an overall biphasic pattern of expression during postnatal development, and for the purposes of this work, **Section 4.3**

focuses on those that either function directly within the RISK-SAFE pathways, or which have high degrees of overlap and strong statistical significance (i.e. statistical significance both between 14-day old and adult samples, as well as 14-day old and 7-day old samples).

Members of the RISK pathway with overall biphasic changes in expression included ERK1, MEK2, Raf1, H-ras, and K-ras, as well as PI3K subunits, PDK1, Akt1, eNOS, PKG-1, GSK3β and PKCε. Similarly, JAK1 and STAT3 of the SAFE pathway also showed a biphasic profile of expression. These proteins, while displaying biphasic expression, did not show statistical significance between 14-day and 7-day old samples. However, it is uncertain whether this is due to the fact that only four 7-day old samples were run, and as a result there was often scatter between samples. The apparent overall peak in expression at 14-days of these survival signalling proteins supports the hypothesis that they play a causal role in improved cardiac vulnerability in this age group.

The exception to this, however, is GSK3β, which is a known anti-survival signalling protein via opening of the mPTP during I/RI (Juhaszova, Zorov et al. 2004, Lal, Ahmad et al. 2015), phosphorylation at Serine 9 by Akt and subsequent inactivation of which is believed to be required for cardioprotection (Gomez, Paillard et al. 2008). The peak in its expression at 14-days of age therefore seems to contradict its functional role in cell survival. However, work by Zhai et al. (2011) showed that GSK3β had distinct effects on myocardial injury depending on which phase of I/R it was activated at. During prolonged ischemia, inhibition of GSK3β was found to exacerbate injury, whereas activation lead to suppression of mTOR activity and increased autophagy, resulting in decreased infarct sizes. In contrast, GSK3β inhibition during reperfusion lead to increased activation of mTOR, decreased autophagy, and a subsequent reduction in reperfusion injury (Zhai, Sciarretta et al. 2011). It is therefore

possible that 14-day old hearts have a high reserve of GSK3β that can be activated during ischemia to reduce ischemic injury, and is subsequently inhibited by other survival signalling proteins, such as Akt, during reperfusion for cardioprotection. Further work will be needed to look at the expression and phosphorylation states of GSK3β in 14-day old compared with adult samples taken following ischemia alone and following reperfusion.

Upstream of these signalling pathways, caveolins play an important role in co-ordinating survival signalling at the cell membrane, and have previously been shown to exert cardioprotective roles through knockout and overexpression studies (Das, Das et al. 2007). In keeping with this, three isoforms of caveolin (-1, -2 & -3) all displayed a biphasic profile of expression, with statistically significant differences between 14-day and both 7-day and adult samples. It is therefore possible that enrichment of survival signalling begins even at the initial stages of these pathways and their activation via caveolins, or that the caveolins themselves may play a direct role in the reduction of I/RI through actions such as binding and inhibition of caspase-3 (Sharma et al. 2011), increased association of caveolin-1 with pro-apoptotic p38MAPK-α, or decreased association of caveolin-3 with anti-apoptotic p38MAPK-β (Das, Gherghiceanu et al. 2008). Moreover, caveolin-3 has also been reported to exert cardioprotective effects via the regulation of autophagy during Ischemia and I/R (Kassan et al. 2016). In this study, caveolin-3 overexpressing cells were found to have a much greater autophagic response during ischemia following treatment with traditional autophagy inducing compounds, in addition to co-immunoprecipitation with and upregulated expression of autophagic markers such as beclin-1 in comparison with wild type, with associated cardioprotection and preservation of mitochondrial function. Knockdown of caveolin-3 was subsequently demonstrated to result in a reduction of autophagic marker expression following simulated ischemia and I/R, increased apoptosis and apoptotic protein

expression, and greater mitochondrial dysfunction (Kassan et al. 2016). This link of caveolin-3 to autophagy, shared by GSK3β and further proteins to be discussed, indicate the potential that this process may be of particular importance in 14-day old hearts.

As mentioned in **Section 1.5.3**, AMPK is a cardioprotective protein that monitors cellular stress and acts as a subsequent regulator of metabolism, for example through increased glucose uptake via GLUT4 (Moussa and Li 2012), the inactivation of which has been shown to increase ROS production during reperfusion and decrease resistance of mitochondria to mPTP opening, in addition to reduced JNK signalling and increased necrosis (Zaha et al. 2016). In addition to this, AMPK is believed to play a role in autophagy, which could result in a pro-survival response during ischemia via removal of damaged cellular components in the stressed environment, and subsequent freeing of nutrients and energy (Paiva et al. 2011). Paiva et al. (2011) also report that AMPK activation may preserve both post-reperfusion cardiac function and mitochondrial integrity as a result of increased glycolysis, and subsequently raised ATP levels in the cell once reperfusion begins. Our proteomic output found that both AMPK-α2 and AMPK-β1 were more highly expressed at 14-days of age in comparison with both 7-day old and adult samples. AMPK could therefore potentially play a role in the decreased vulnerability of this age group to cardiac insult through its range of cellular functions, or through its links to members of the RISK-SAFE pathways. Indeed, work by Chen et al. (2017) found that Lysophosphatidic Acid (LPA) treatment of 14-day old Langendorff perfused hearts resulted in significant improvements in cardiac function and infarct size, with decreased CK-MB release and apoptosis, and an associated increase in the expression of survival signalling proteins such as Akt, BCL-2, and AMPK. However, previous work has also described AMPK activation as being detrimental during reperfusion (Paiva et al. 2011). Therefore, similarly to GSK3β, it will be necessary to look at the differential

expression and activation of AMPK in 14-day old and adult samples both post-ischemia and post-reperfusion.

Finally, mTOR showed statistically significant biphasic expression in the proteomic output between 14-day old and both 7-day old and adult samples. As previously discussed, mTOR activity is reportedly suppressed during ischemia by proteins such as GSK3β and AMPK, in order to upregulate autophagy and confer cardioprotection to the heart. However, mTOR is also known to be both an upstream activator of and downstream target for activation by Akt (Tao et al. 2010), which also displayed an overall biphasic trend in expression in the proteomic output. In a study by Kong et al. (2016), overexpression of HSPA12B – which although not included in this chapter, also showed a statistically significant biphasic peak in expression at 14-days of age in comparison with all other age groups in the proteomic output – was shown to reduce infarct size and cardiac dysfunction, with increased cardiomyocyte survival. These cardioprotective effects were associated with increased pAkt/Akt, pGSK3β/GSK3β, and pmTOR/mTOR ratios, all of which were abolished by the inhibition of upstream PI3K activity (Kong et al. 2016). It is therefore possible that the high expression of mTOR at 14-days of age could indicate a reserve of the protein kept inactive during ischemia by AMPK and GSK3β, and is subsequently activated by Akt during reperfusion. Expression and phosphorylation status of mTOR will consequently be tested in post-ischemic and post-I/R samples in order to further elucidate these potential interactions, as well as any differences between 14-day old and adult samples.

4.4.2 Phosphoproteomic analysis did not identify biphasic changes in the phosphorylation status of survival signalling proteins

Analysis of the phosphoproteomic output detected only a few proteins with phosphosites common across all 4 age groups examined. Firstly, phosphorylation of Akt was detected at Ser124, with significant differences only between 28-day old and adult samples in comparison with 7-day old and 14-day old samples, therefore showing an overall decrease during postnatal development, but not a biphasic change. Ser124 has been reported to be constitutively phosphorylated (Iacovides, Johnson et al. 2013), unaffected by pharmaceutical inhibition of PI3K and thus independent of the classic phosphorylation axis associated with RISK-SAFE signalling (Liao and Hung 2010). It is therefore unlikely that differences in levels of Ser124 phosphorylation relate to differences in cardioprotective signalling between these age groups, and instead reflect the greater expression of total Akt in 7-day old and 14-day old samples, as shown in **Section 4.3.1.** Indeed, tissue was extracted from control hearts in their non-stressed states, and therefore it is not unexpected that abundant levels of Akt activating phosphorylation, e.g. at Ser473, were not detected. It should be noted that Akt phosphorylation in the first run of phosphoproteomic analysis (**Chapter 3**) identified phosphorylation only at Ser129, not Ser124. The fact that samples from both runs of phosphoproteomic analysis were taken from hearts in their control state, in addition to the fact both Ser129 detected in the first run and Ser124 detected in the second showed the same trends in abundance across the three common age groups tested – with 14-day olds showing significantly greater levels of phosphorylation at both sites in comparison with 28-day olds and adults – is consistent with these data representing phosphorylation at the same site in both runs of analysis. Indeed, previous papers have

suggested that current phosphoproteomic methods are limited by the ionisation and behaviour of phosphopeptides and phosphate groups during the MS/MS process, with subsequent inaccuracies and impairment of the correct identification of individual phosphorylation sites (Solari et al. 2015). It is therefore possible that, due to the close proximity of the two residues (Ser129 and Ser124), such issues during the process of phosphoproteomic analysis itself may have resulted in their incorrect identification, with both runs having actually identified phosphorylation at the same site. However, it is not possible to say for certain whether this was indeed the case, and which, if either, was incorrectly identified. On the other hand, the fact that previously described western blotting experiments for Akt phosphorylation at Ser129 (**Section 3.3.2.3**) did mimic the trend seen in the phosphoproteomic output may indicate that phosphorylation at this site was correctly identified.

Similarly, phosphorylation was detected for AMPK at Ser24, but was only significantly different between 28-day old and adult samples in comparison with 14-day old samples. Ser24 has been shown to be one of several sites involved in the "autophosphorylation cascade" triggered by the AMPK-α1 (Mitchelhill, Michell et al. 1997), and whilst not involved in the enzymatic activity of AMPK, its phosphorylation is linked to cellular distribution of the protein and required for its exportation from the nucleus (Sanz, Rubio et al. 2013). Similarly to Akt, it is therefore likely that the trend in abundance of phosphorylation at this site reflects the trend in total AMPK-β1 expression shown in **Section 4.3.1**, as opposed to an association to cardioprotective mechanisms in these control hearts. However, it is possible that the role of phosphorylation at Ser24 in the cellular localisation of AMPK means that the greater levels of phosphorylation at this site in 14-day old samples suggests a larger pool of

protein primed for full activation in the event of cellular stress and cardiac injury in this age group.

Phosphorylation of AMPK was also detected at Ser108, again subverting the expected biphasic trend in abundance and instead peaking at 28-days of age, with statistically significantly greater levels than all 3 of the other age groups. Ser108 has been shown to be a target of autophosphorylation located in the glycogen binding region of AMPK-β1 (Iseli, Walter et al. 2005), and whilst studies have shown that mutation at this site confers only partial disruption of glycogen binding (Polekhina, Gupta et al. 2003), it has also been shown that mutation results in a 60% reduction in enzymatic activity of the protein (Warden, Richardson et al. 2001). However, due to the pattern of abundance of phosphorylation at Ser108 found in the phosphoproteomic output, peaking at 28-days of age, it is unlikely that phosphorylation at Ser108 is mechanistically significant to the biphasic differences in cardiac vulnerability seen across these four age groups.

4.4.3 Summary & Conclusion

A number of RISK-SAFE pathway and survival signalling proteins were identified in the proteomic output that demonstrated a pattern of expression consistent with both their reported roles in cell survival, and with the biphasic profile of cardiac resistance to I/RI. As a result, three key proteins – PKCε, GSK3β, and AMPK – were selected from this data for further investigation into the effects of their inhibition on isolated cardiomyocyte vulnerability to simulated I/RI, as will be described in **Chapter 5**.

Chapter 5: Targeting of signalling pathways to assess the response of isolated cardiomyocytes to cardiac insult

5.1 Introduction

Analysis of proteomic data (**Section 4.3**) identified a number of key survival signalling proteins that demonstrated an overall biphasic pattern of expression across the four age groups (7-day old, 14-day old, 28-day old, and adult rats) concordant with the differences in cardiac vulnerability to I/RI seen. Having thus addressed the first aim of this work – the identification of "any changes that occur in survival signalling through changes in the expression of pro-survival and apoptosis-related proteins during development" – work to address the second aim was subsequently undertaken; "To see if specific inhibition of the identified proteins affects the vulnerability to ischemia/reperfusion injury during postnatal development in isolated cardiomyocytes."

As described in **Section 1.5**, PKCε and GSK3β are important downstream targets of RISK-SAFE signalling, both demonstrating an overall biphasic trend of expression during the course of postnatal development in the proteomic output (**Section 4.3.1**), as shown in **Figures 33** and **34** below. As statistically significant differences in the expression of these two proteins was not seen between 7-day old and 14-day old samples, the scatter plots of individual data points are included to highlight the overall trend in expression, and the uncertainty introduced by the fact that only 4 samples from 7-day old hearts were included in the proteomic analysis. In the case of GSK3β particularly, a clear outlier in the 7-day old group of samples was identifiable (indicated by a red circle). However, its removal did not alter findings of significance between the age groups. An outlier was also detected for PKCε in the 14 day old samples, removal of which did not affect findings of statistically significant differences in expression between 14-day old and both 28-day old and adult samples.

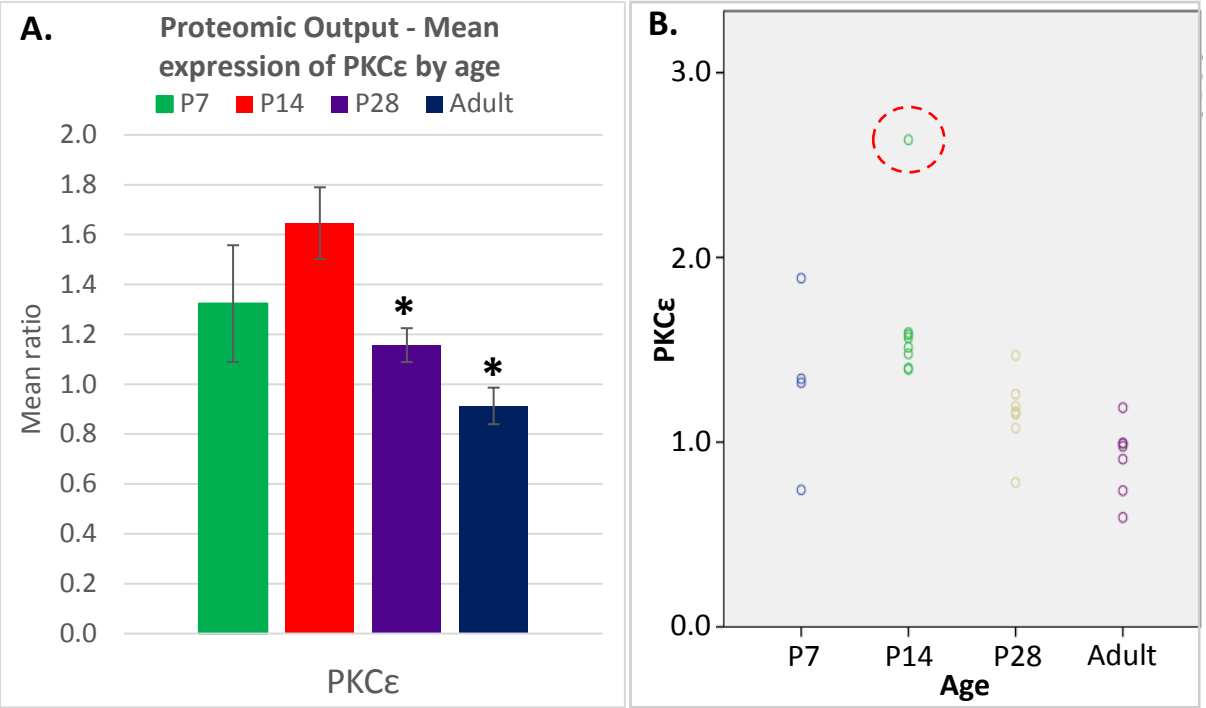

Figure 33. A. Biphasic profile of PKCε expression in the proteomic output. * = statistically significant difference with P14 ($p < 0.05$). Data presented as Mean ± SE. **B.** Plot of PKCε expression for each individual sample. The dotted red circle indicates a likely outlier.

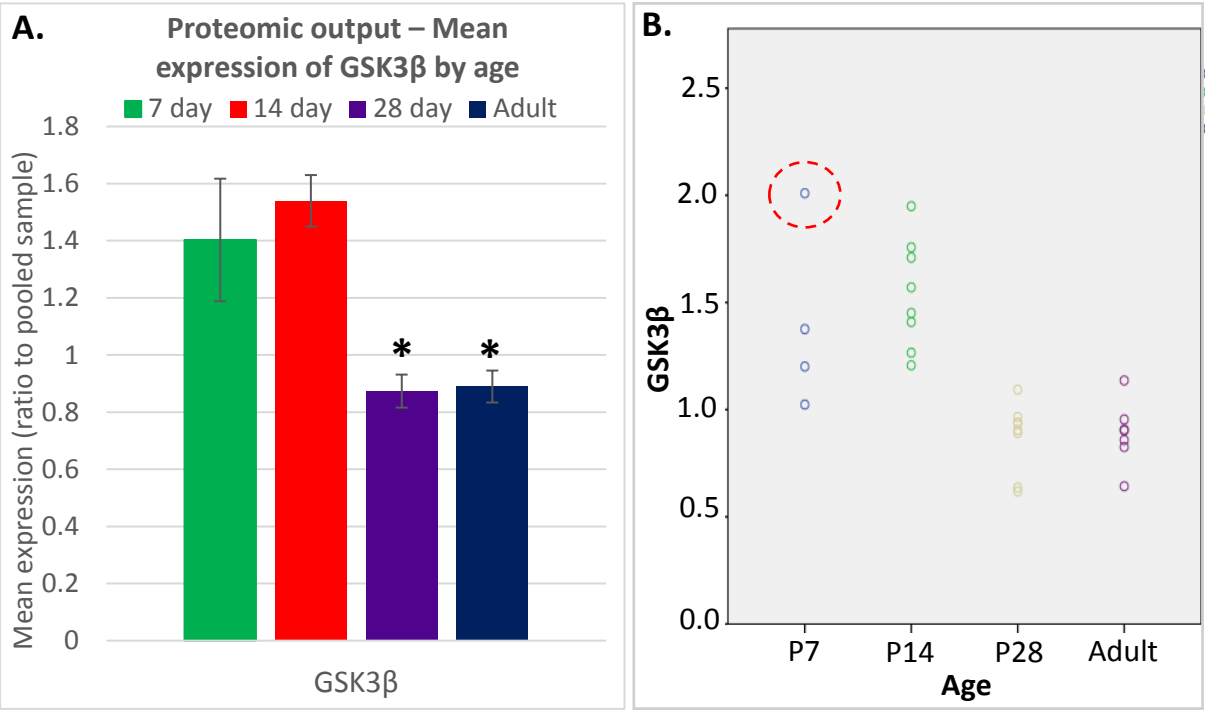

Figure 34. A. Biphasic profile of GSK3β expression in the proteomic output. * = statistically significant difference with P14 ($p < 0.05$). Data presented as Mean ± SE. **B.** Plot of GSK3β expression for each individual sample. The dotted red circle indicates a likely outlier.

Analysis of the proteomic output (**Section 4.3.1**) identified a biphasic trend in the expression of AMPK with statistically significant differences between 14-day old samples and all 3 of the remaining age groups, therefore showing a strong correlation with the biphasic pattern of cardiac resistance to I/RI across these 4 age groups, as shown in **Figure 35** below. AMPK has an important role in reducing cardiac injury during ischemia and reperfusion, as described in **Section 1.5.3**, combining with its strong biphasic profile of expression to make it a key target for further investigation alongside PKCε and GSK3β. Although both PKCε and GSK3β did not show statistically significant differences in expression between 7-day old and 14-day old samples, the previously discussed limitation of having only 4 samples for the 7-day old group, the overall biphasic profile, the importance of both proteins as end targets of survival signalling pathways in addition to their links to AMPK in terms of both signalling and autophagy (Nishino et al. 2004, Sciaretta et al. 2014), and the availability of previously tested inhibitors highlighted them as important targets for these initial studies.

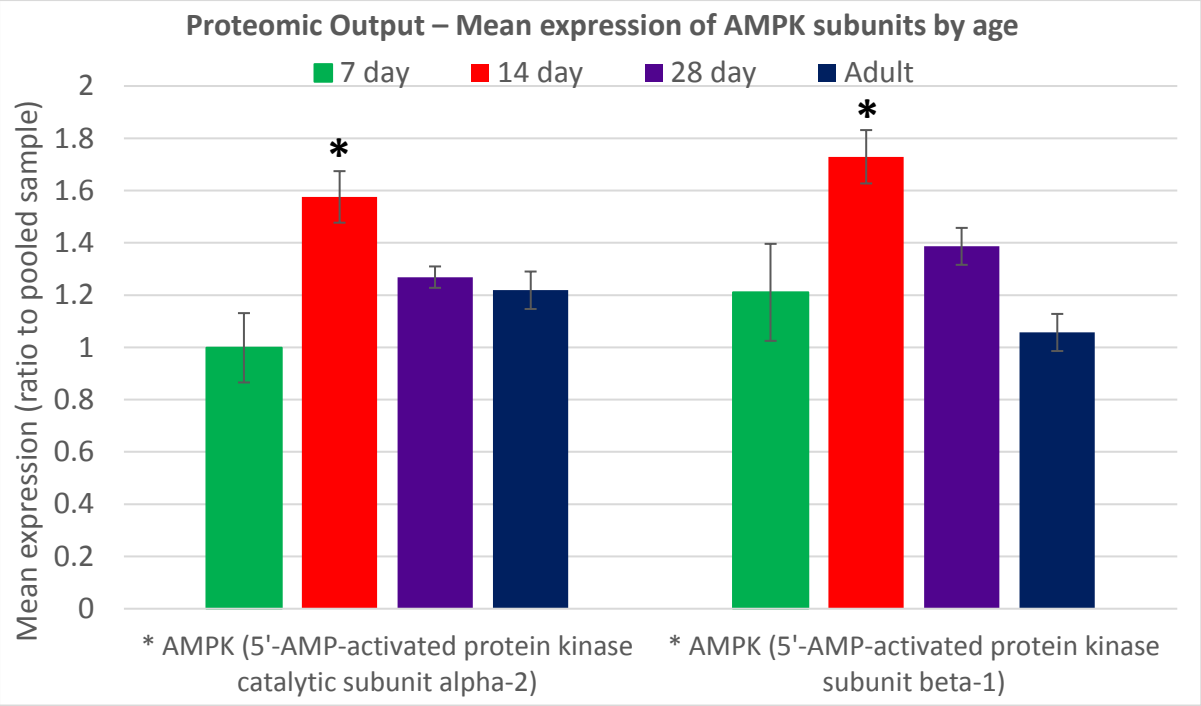

Figure 35. Biphasic profile of AMPK subunit expression in the proteomic output. * = significantly different from all other age groups ($p < 0.05$). Data presented as Mean ± SE.

As a result of these findings, PKCε, GSK3β and AMPK were targeted using the inhibitors chelerythrine (Huang, Liu et al. 2010), TWS119 (Jiang, Xiao et al. 2016) and dorsomorphin dihydrochloride (Konishi, Haraguchi et al. 2011), respectively, for cell viability studies into the potential differential effects of their inhibition on cardiomyocytes isolated from different age groups.

5.2 Materials & Methods

5.2.1 Cardiomyocyte isolation

Cardiomyocyte isolation was performed as outlined in **Section 2.3**, using hearts extracted from 14-day old (n = 6), 28-day old (n = 4), and adult (n = 3) rats. As previously described, hearts were perfused with an initial buffer containing 750 µM Ca^{2+} to optimise circulation and wash out any remaining blood or clots. This was switched to perfusion with an EGTA containing solution to remove any remaining Ca^{2+}, followed by freshly made enzyme solution until an optimal softness of the heart was reached, indicating sufficient digestion to provide a good yield of isolated cardiomyocytes. Calcium was then gradually reintroduced into cells through perfusion with a buffer of 150 µM Ca^{2+}, and sequential addition of 0.5 mM and 1 mM Ca^{2+} solutions. The resulting cell solution was separated into two groups; control and simulated I/R, the latter receiving an additional 3 mM Ca^{2+} (for a final concentration of 4 mM), as well as 20 mM KCl and 0.5 mM H_2O_2. Cell viability was subsequently measured using Trypan Blue from the total cell solution as a start viability, then every hour for 2 hours for each group.

5.2.2 Protocol for investigating the effect of drugs in an injury model of cardiomyocyte suspension

Cardiomyocyte isolation was performed as outlined in **Section 2.3** and **5.2.1** above, using hearts extracted from 14-day old (n = 5) and adult (n = 4) rats, and with some changes to the protocol. Firstly, solutions B, C and enzymatic solution D were all made from a stock solution A containing glucose, as previously described. However, solutions used following enzymatic digestion – i.e. solutions E, F and G – were made using a stock of solution A containing no glucose. This exclusion of glucose was made as initial experiments demonstrated that the presence of glucose in these solutions aided cardiomyocyte survival even in cells undergoing simulated I/R, resulting in relatively low drops in cell viability over the 2 hour experimental period (see **Section 5.3.1** and **Figure 36**) which subsequently made measurements for changes in viability difficult. Previous studies have also discussed the potential issue that glucose inclusion in the final solution may affect isolated cardiomyocyte studies due to the uptake of glucose by cells and subsequent changes in metabolism (Voigt et al. 2015). Secondly, the cell suspension of isolated cardiomyocytes was divided into three groups; one as a control group with no further treatments, one as a simulated I/R group (0.5 mM H_2O_2 + an additional 3 mM Ca^{2+}), and one with both simulated I/R and treatment with a specific inhibitor selected based on proteomic analysis (5 µM chelerythrine, 5 µM TWS119 or 1 µM dorsomorphin dihydrochloride). Elevated K^+ concentrations (20 mM) were not used for simulated I/R in these experiments in order to limit the effects to the key mechanisms of injury traditionally described – oxidative stress and calcium overload. Both TWS119 (Jiang et al. 2016) and dorsomorphin dihydrochloride (Konishi et al. 2011, Chen et al. 2010) have been tested in cardiomyocytes and Langendorff perfused hearts in previous studies, which successfully demonstrated the effective and specific inhibition of our proteins of interest at

the concentrations used in these experiments. Similarly, chelerythrine has been demonstrated to inhibit PKCε activity in rat hearts at the 5 μM concentration used, as determined by the decreased PKCε translocation and abundance in mitochondrial fractions (Nunez et al. 2017). However, it is important to note that this inhibitor and concentration is not specific for PKCε, and also inhibits other PKC isoforms (Huang et al. 2010), an issue that will be discussed further in **Chapter 9**. Finally, for these experiments, cell viability was measured using Trypan blue from the total cell solution as a start viability, then every 30 minutes for 2 hours.

5.2.3 Western blot analysis of protein extracted from isolated cardiomyocytes

The full western blotting methodology has been described in **Section 2.5**. To summarise, samples of the isolated cardiomyocyte suspension (**Section 5.2.2**) from the starting solution and from the final solutions of the experimental groups following 2 hours incubation were flash frozen in liquid nitrogen at the end of the experiment. Protein was subsequently extracted and quantified as outlined in **Sections 2.4.1.2** and **2.4.2**, and used to prepare a sample of 0.15mg of protein in a final volume of 100μl. These samples were then prepared for gel electrophoresis with the addition of an equal volume of loading buffer (Laemmli buffer + βME), before being run on a Mini-PROTEAN® TGX™ precast gels and transferred to a PVDF membrane, which was subsequently stained with Ponceau S solution to produce full lane bands (see **Section 2.5.4**), before blocking with milk. Membranes were then incubated with antibodies for PKCε, pPKCε, GSK3β or pGSK3β (see table of antibodies in **Section 2.1.2**), washed with TBST, incubated with a secondary antibody, and visualised using the Enhanced ChemiLuminescence system. Ponceau S staining was used as a loading control for normalisation of protein bands.

5.3 Results

5.3.1 Vulnerability of isolated cardiomyocytes to simulated I/R in the presence of glucose

Cardiomyocytes were isolated from rat hearts of ages 14-days (n = 6), 28-days (n = 4) and adult (n = 3), and viability was measured for each as a percentage of cells without Trypan blue staining at each time point (as outlined in **Section 2.1**). Solutions used for these experiments were as described in Section 5.2.1, with inclusion of glucose in the final solutions, as well as elevated K^+ concentrations in the simulated I/R groups.

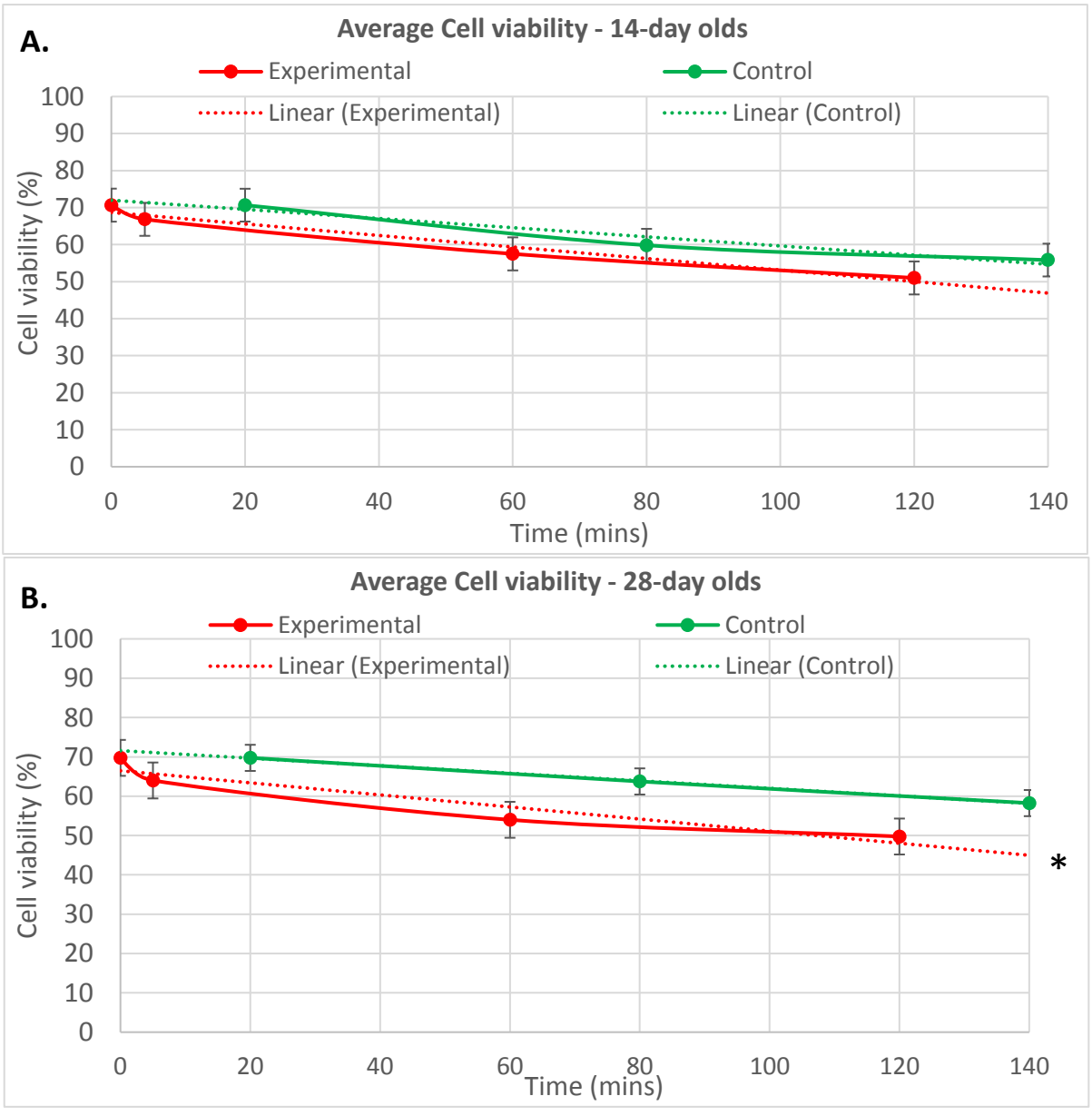

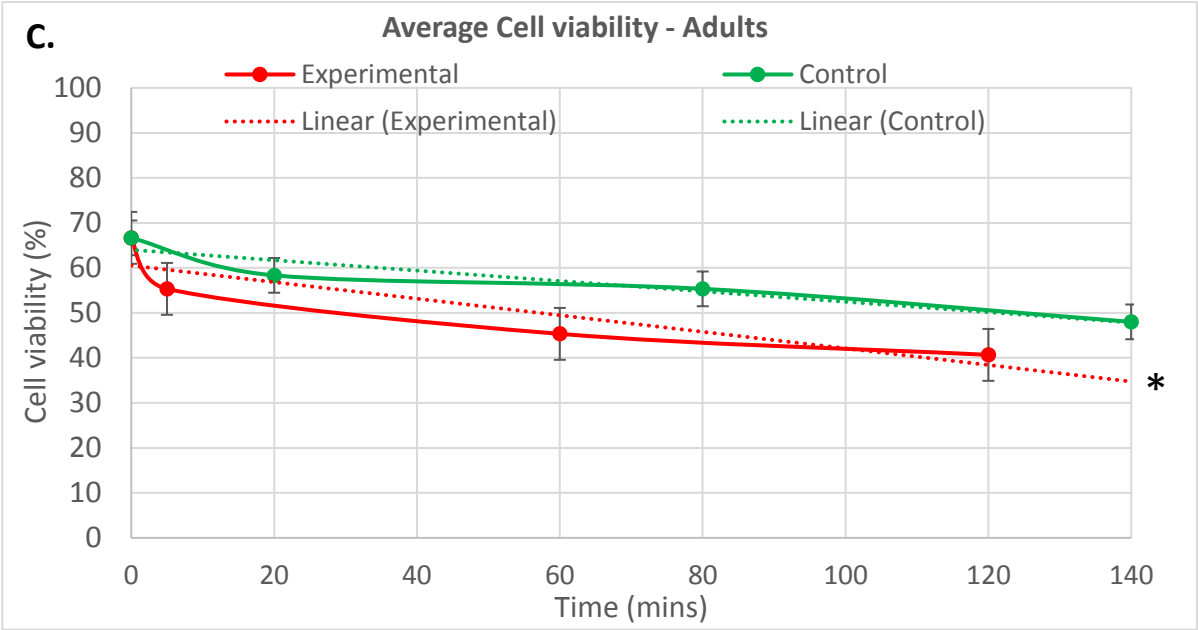

Figure 36. The mean percentage of viable cells over time for control cells compared to cells that underwent simulated I/RI by age (**A.** 14-days, **B.** 28-days, **C.** Adult). Data are presented as mean ± SE (n = 6 for P14, n = 4 for P28 and n = 3 for adult). * = statistically significant difference in cardiomyocyte viability in comparison with control group ($p < 0.05$).

The mean percentage of viable cells for each group is displayed in **Figure 36**. These data show a greater decrease in the mean percentage of viable cells over time in the experimental group undergoing simulated I/RI (0.5 mM H_2O_2, 20 mM KCl, 4 mM Ca^{2+}) in comparison with the control group at each age group. However, this difference is not statistically significantly different at 14-days of age. In 28-day old and adult hearts, however, the difference in the percentage of viable cells between experimental and control groups was shown to be statistically significant.

5.3.2 Effect of inhibition of selected survival signalling proteins on cardiomyocyte viability following simulated I/R at different stages of postnatal development.

Three proteins were selected based on proteomic analysis for further investigation – PKC & GSK3β, which are key end effectors of RISK-SAFE signalling, and AMPK, which showed strong statistical significance between 14-day old samples and all other age groups – as discussed in **Section 5.1**. Therefore, three selective inhibitors of these proteins were used: chelerythrine (5 μM), TWS119 (5 μM) & dorsomorphin dihydrochloride (1 μM). For these experiments, the data for which are presented in **Figures 37-44**, glucose was absent from the final solutions, and elevated K^+ was not used in the simulated I/R groups (see **Section 5.2.2**). The effects of these drugs on cell viability were investigated using a suspension of cardiomyocytes (as described in **Section 2.3**).

5.3.2.1 Effect of survival signalling protein inhibition on cardiomyocyte viability following simulated I/R injury.

5.3.2.1.1 Differential effects of PKCε inhibition on isolated cardiomyocytes from 14-day old and adult hearts.

5.3.2.1.1.1 Effect of chelerythrine treatment on percentage change in cardiomyocyte viability.

The percentage change of viable cardiomyocytes – defined as cells that have not taken up trypan blue staining, and expressing the initial viability as 100% – was measured every 30 minutes for 2 hours in each experimental group, and the results for both 14-day old and adult cells are displayed in **Figure 37** below. Whilst cardiomyocyte suspensions from adult hearts displayed statistically significant differences in viability only between the control group (green) in comparison with both the simulated I/R (blue) and simulated I/R with PKC

inhibition (red) groups, 14-day old cells showed additional statistically significant differences in viability between the simulated I/R and PKC inhibited groups. This shows that inhibition of PKC only had an effect on cell viability in cardiomyocytes taken from 14-day old hearts, whereas adult cells were unaffected by PKC inhibition.

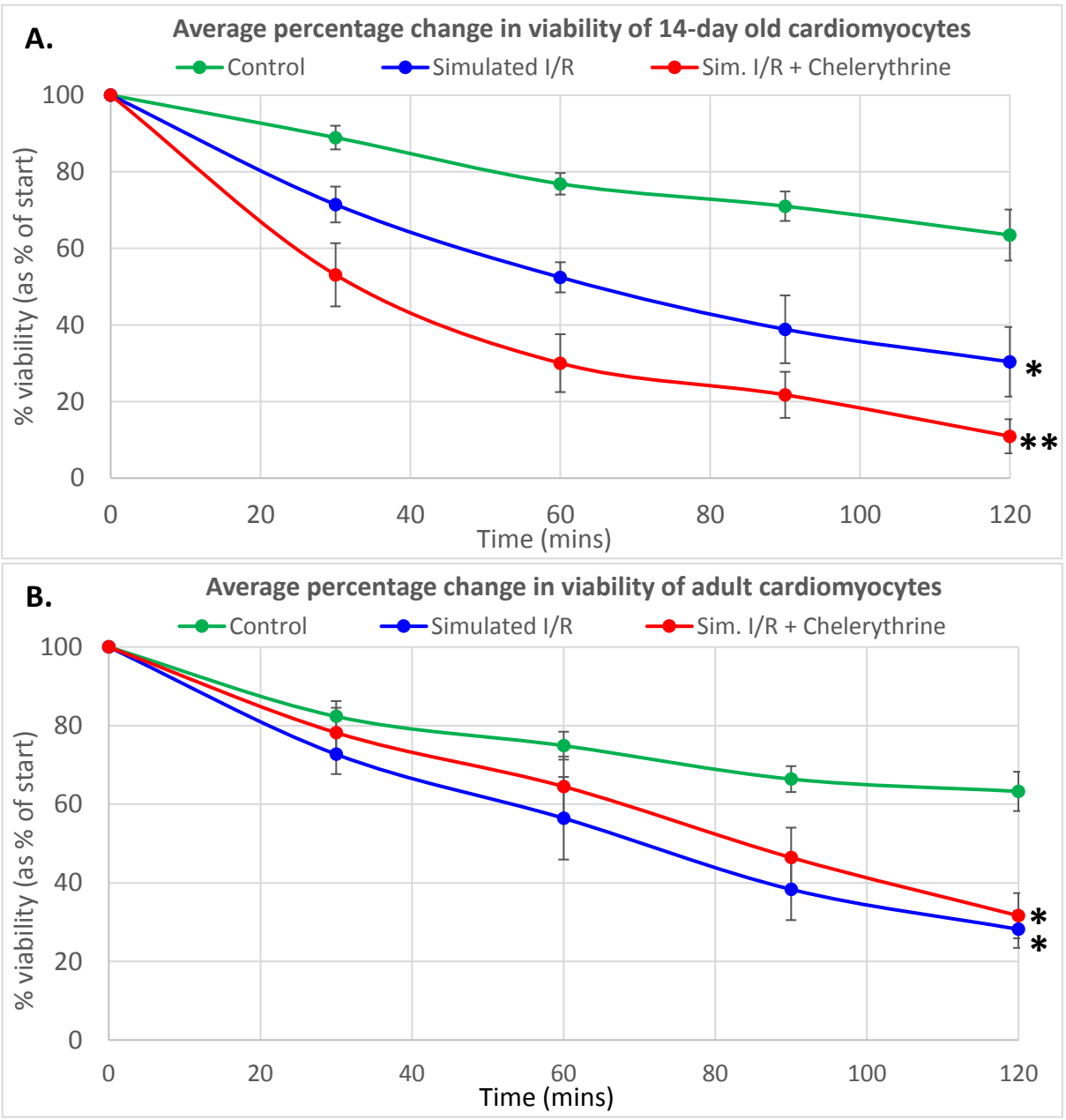

Figure 37. Time-dependent changes in percentage change of viability of cardiomyocytes isolated from 14-day (A) old and adult (B) rat heart incubated in the presence or absence of H_2O_2 or H_2O_2 + chelerythrine; **A.** 14-day old hearts (n = 5 per group), control vs. simulated I/R, control vs. chelerythrine, simulated I/R vs. chelerythrine. **B.** Adult hearts (n = 4 per group), control vs. simulated I/R, control vs. chelerythrine. * = statistically significant difference with control ($p < 0.05$). ** = statistically significant difference with control & simulated I/R ($p < 0.05$).

5.3.2.1.1.2 Effect of chelerythrine treatment on percentage change of rod-shaped cardiomyocytes.

Counts were also taken at each time point for the percentage of rod-shaped cardiomyocytes alone, treating all rounded cells as no longer viable regardless of staining with trypan blue. Calculation of the percentage change in rod-shaped cardiomyocytes showed statistically significant differences between experimental groups only in adult cells, with a higher percentage retaining their rod-shaped structure in the control (green) group in comparison with both the simulated I/R (blue) and I/R + PKC inhibition (red) groups.

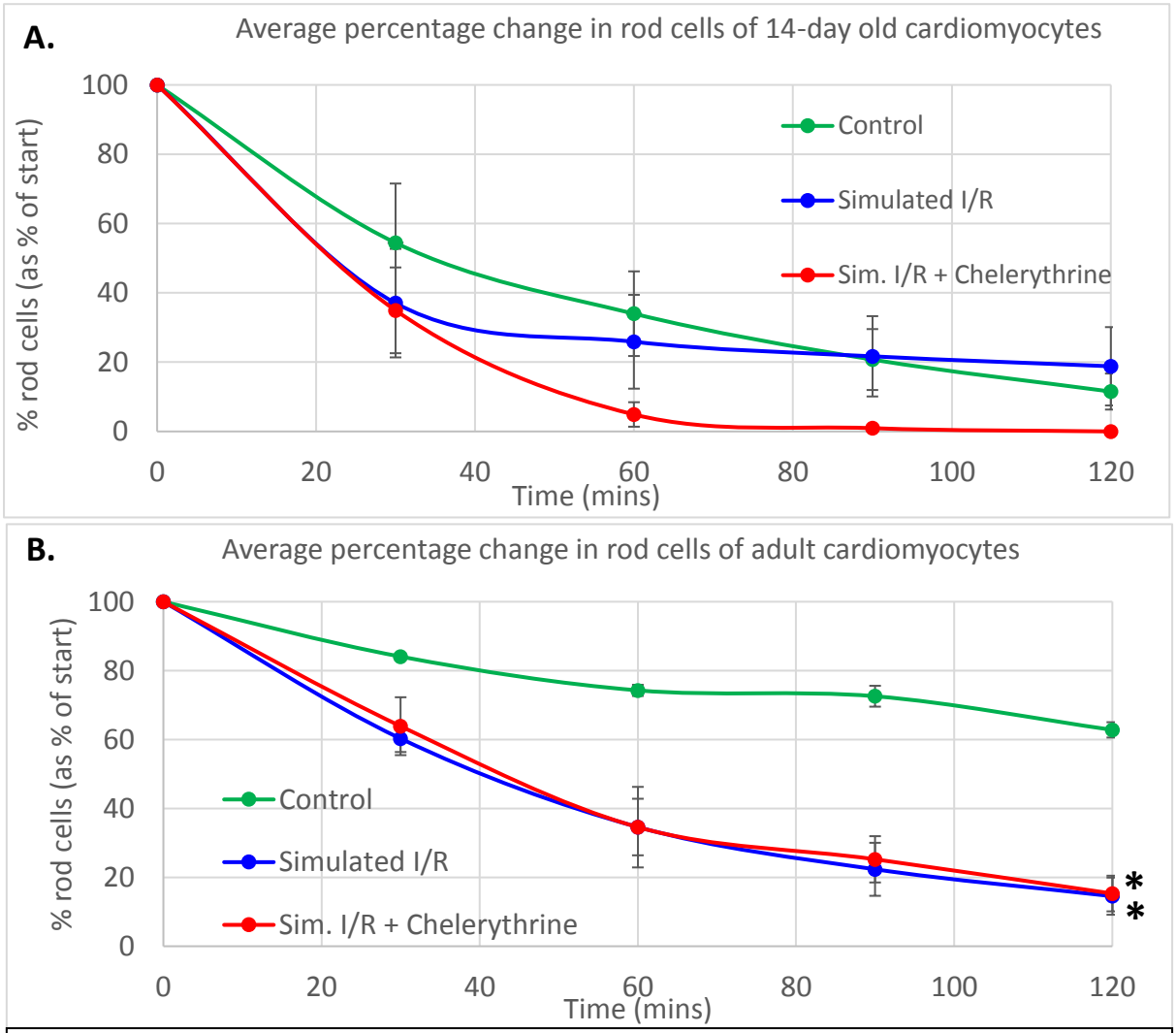

Figure 38. Percentage change in rod-shaped cardiomyocytes over the course of 120 minutes in 14-day old and adult rat heart derived cardiomyocytes; control vs. simulated I/R vs. chelerythrine treated cardiomyocytes. **A.** 14-day old hearts (n = 5 per group). **B.** Adult hearts (n = 4 per group), control vs. simulated I/R, control vs. chelerythrine. * = statistically significant difference with control ($p < 0.05$).

5.3.2.1.1.3 Effect of chelerythrine treatment on the expression and phosphorylation state of PKCε

Samples were collected from the cell suspension at the start of the experiment, and again at the end for each of the three experimental groups (control, simulated I/R, and simulated I/R + chelerythrine), in the form of a cell pellet spun down through microcentrifugation. Protein was extracted from these pellets and samples were prepared for western blotting as outlined in **Section 2.5**. These samples were then tested for pPKCε expression, before the membrane was stripped and reprobed with an antibody for PKCε, in order to compare the effects of simulated I/R as well as treatment with chelerythrine on the expression and phosphorylation status of PKCε between the two age groups (**Figure 39**.)

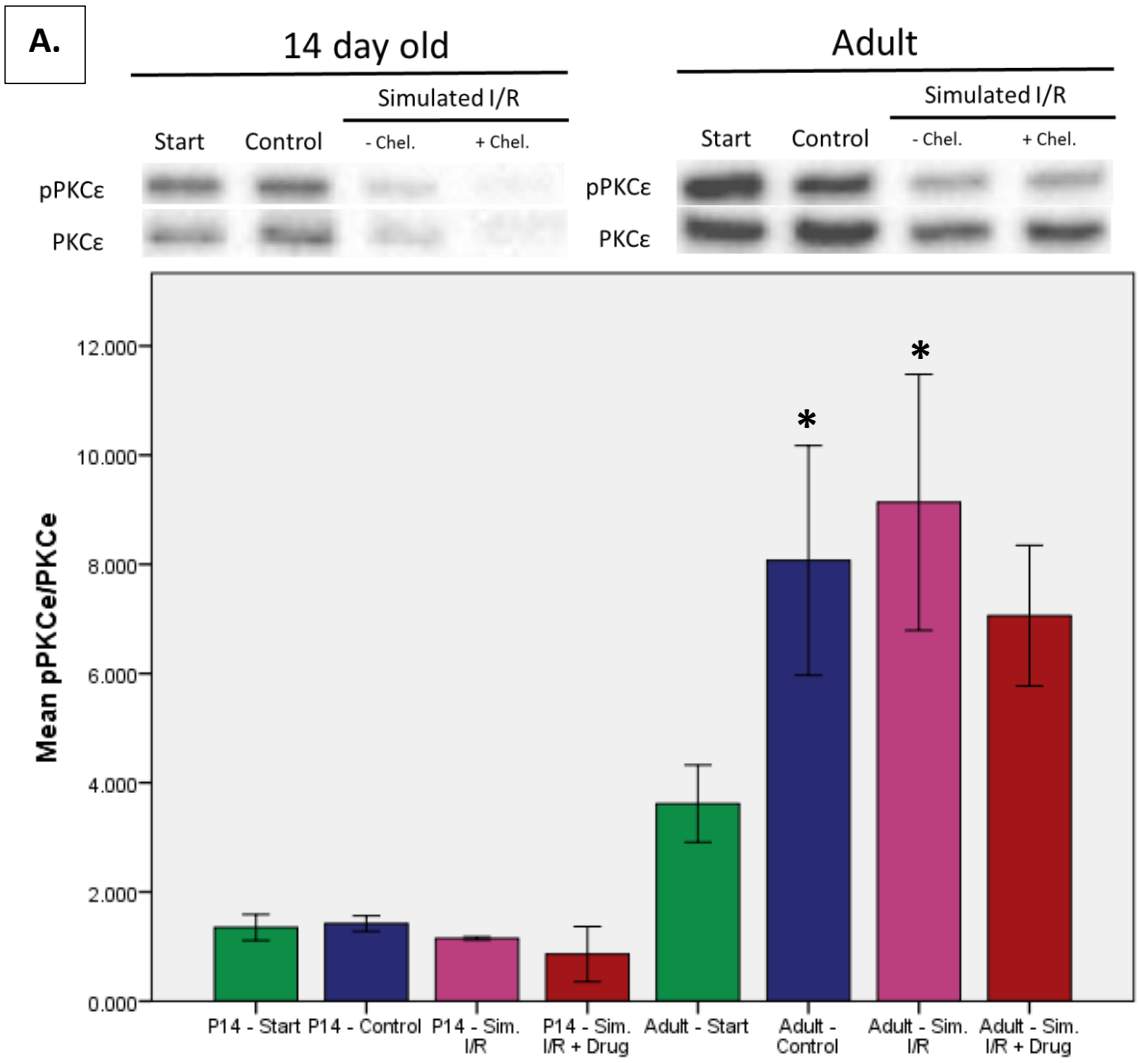

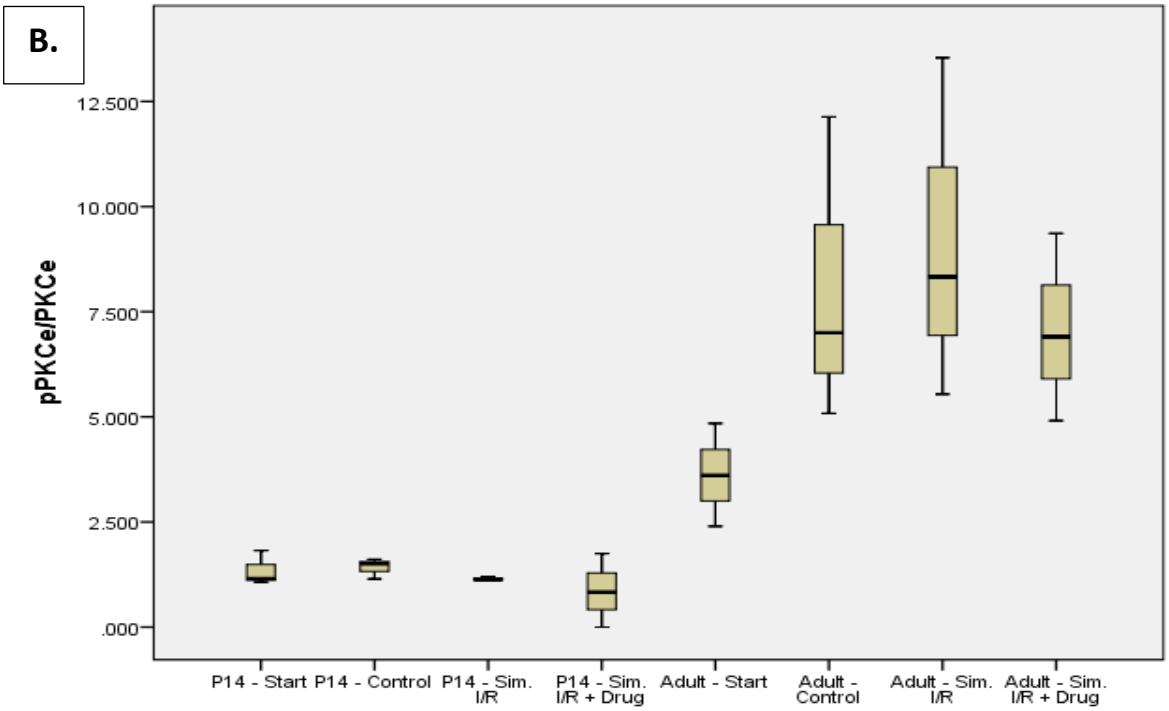

Figure 39. A. Representative western blot bands for pPKCε and PKCε for each experimental group from both 14-day old and adult cardiac samples, with a graph depicting the average ratio of pPKCε/PKCε for each age and experimental group. (n = 3 for each group). Data presented as mean ± SE. ***** = statistically significant difference in comparison with corresponding 14-day old group ($p < 0.05$). **B.** Boxplot representation of the pPKCε/PKCε for each age and experimental group.

No statistically significant differences were seen in pPKCε/PKCε expression between the experimental groups of cells isolated from either 14-day old hearts or adult hearts. However, between the two age groups, pPKCε/PKCε was significantly higher in adults than 14-day old cells both in the control and simulated I/R groups. The significance of this is unclear, but may reflect the overall higher viability in adult cells than 14-day old cells following isolation. It is also important to note that other studies have looked at the translocation of PKC or have conducted analysis of protein activity as opposed to phosphorylation state in order to examine the efficacy of the drug's inhibitory effect. In addition to the fact that chelerythrine is not a PKCε specific inhibitor, this may explain why no significant differences were detected by western blotting. However, the concentration used here has been shown in previous studies to be effective in the inhibition of PKCε.

5.3.2.1.2 Effects of GSK3β inhibition on cardiomyocytes from 14-day old and adult hearts

5.3.2.1.2.1 Effect of TWS119 treatment on percentage change in cardiomyocyte viability.

As seen in **Figure 40,** cardiomyocyte suspensions from adult hearts displayed statistically significant differences in percentage change in viability only between the control (green) group in comparison with both the simulated I/R (blue) and simulated I/R with TWS119 (red) groups. However, 14-day old cells showed additional statistically significant differences in viability between the simulated I/R and GSK3β inhibited groups. This shows that inhibition of GSK3β only had an effect on cell viability in cardiomyocytes taken from 14-day old hearts, whereas adult cells were unaffected by GSK3β inhibition.

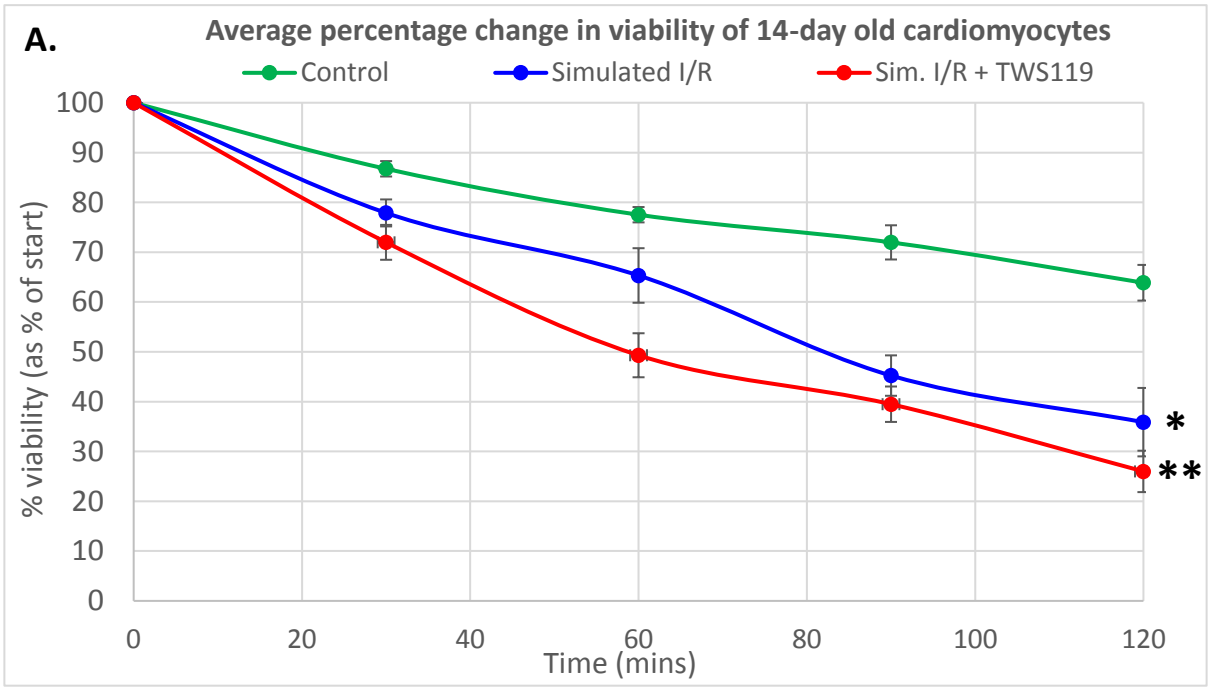

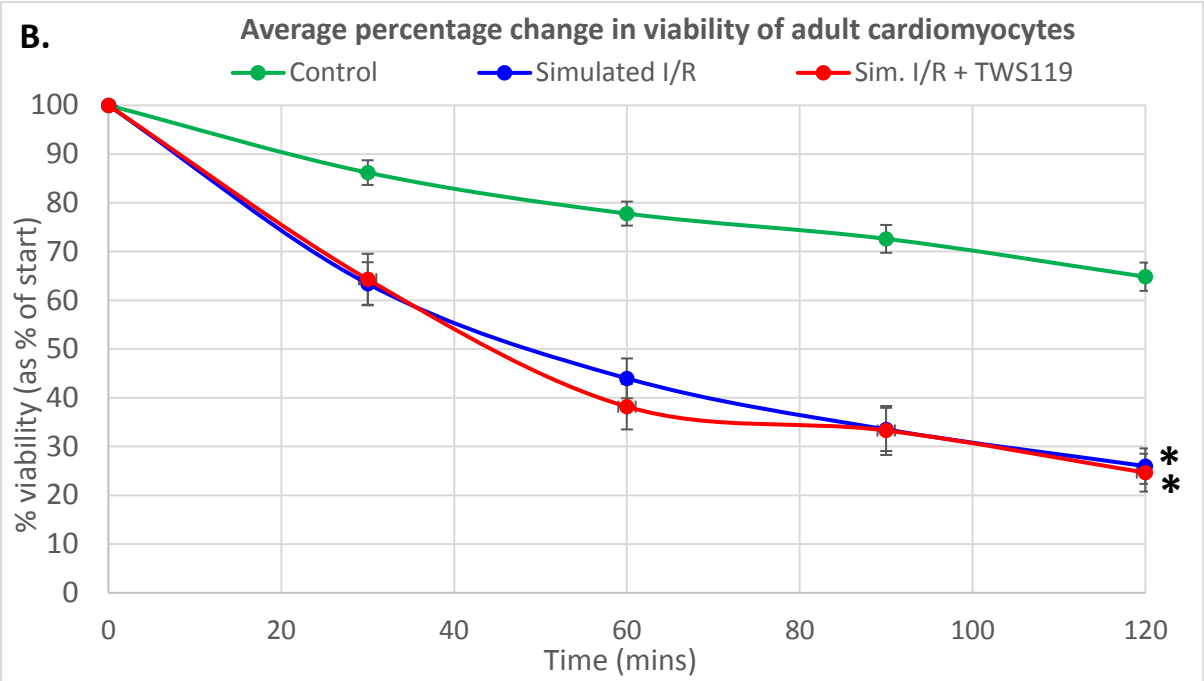

Figure 40. Percentage change in viability over the course of 120 minutes in 14-day old and adult rat cardiomyocytes; control vs. Simulated I/R vs. TWS119 treated cardiomyocytes. A. 14-day old hearts (n = 5 per group), control vs. simulated I/R, control vs., simulated I/R vs. TWS119. **B.** Adult hearts (n = 4 per group), control vs. simulated I/R, control vs. TWS119. * = statistically significant difference with control ($p < 0.05$). ** = statistically significant difference with control & simulated I/R ($p < 0.05$).

5.3.2.1.2.2 Effect of TWS119 treatment on percentage change of rod-shaped cardiomyocytes

The percentage of rod-shaped cardiomyocytes was significantly different between control and TWS119 treated cells, as well as between simulated I/R and TWS119 treated cells, whereas there was no difference between Control and simulated I/R cells in 14-day olds. In adults, however, only the Control group showed differences to both the simulated I/R and TWS119 groups, indicating GSK3β inhibition effected the percentage of rod cells only in 14-day olds.

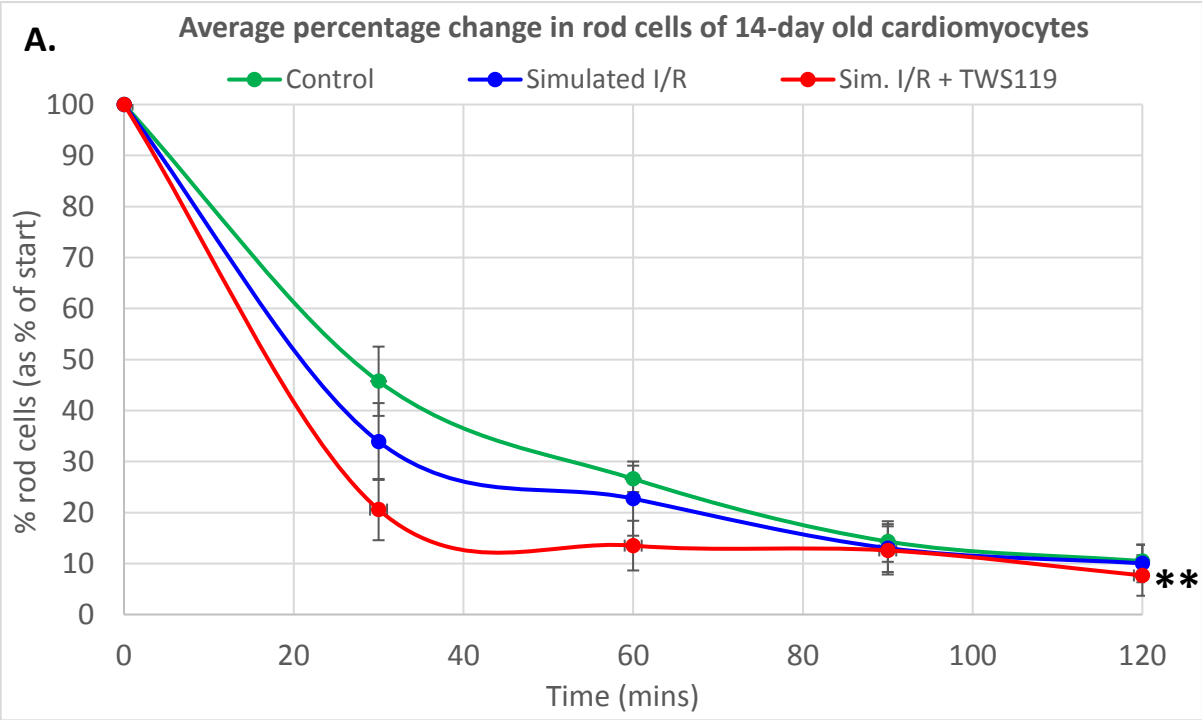

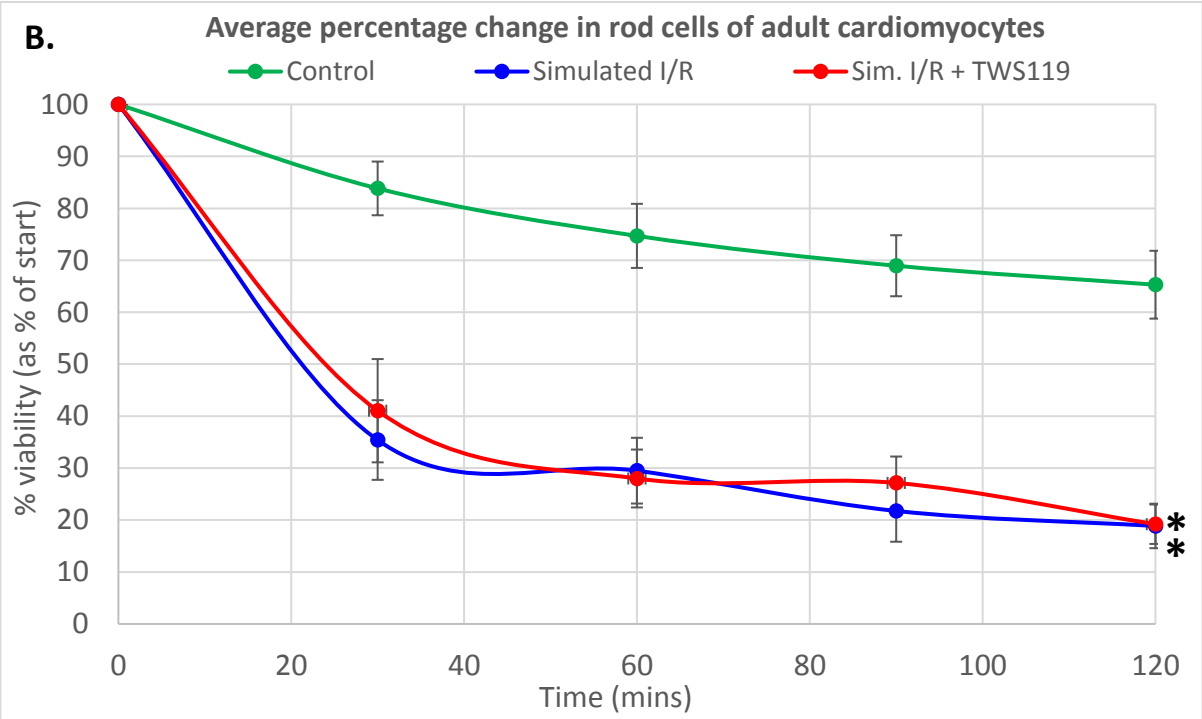

Figure 41. Percentage change of rod-shaped cardiomyocytes over the course of 120 minutes in 14-day old and adult rat cardiomyocytes; control vs. simulated I/R vs. TWS119 treated cardiomyocytes. **A.** 14-day old hearts (n = 5 per group), control vs. TWS119, simulated I/R vs. TWS119. **B.** Adult hearts (n = 4 per group), control vs. simulated I/R, control vs. TWS119. * = statistically significant difference with control ($p < 0.05$). ** = statistically significant difference with control & simulated I/R ($p < 0.05$).

5.3.2.1.2.3 Effect of TWS119 treatment on the expression and phosphorylation state of GSK3β.

Samples were collected from the cell suspension at the start of the experiment, and again at the end for each of the three experimental groups (Control, Simulated I/R, and Simulated I/R + TWS119), in the form of a cell pellet spun down through microcentrifugation. Protein was extracted from these pellets and samples were prepared for western blotting as outlined in **Section 2.5**. These samples were then tested for pGSK3β expression, before the membrane was stripped and reprobed with an antibody for GSK3β, in order to compare the effects of simulated I/R as well as treatment with TWS119 on the expression and phosphorylation status of GSK3β between the two age groups (**Figure 42**.)

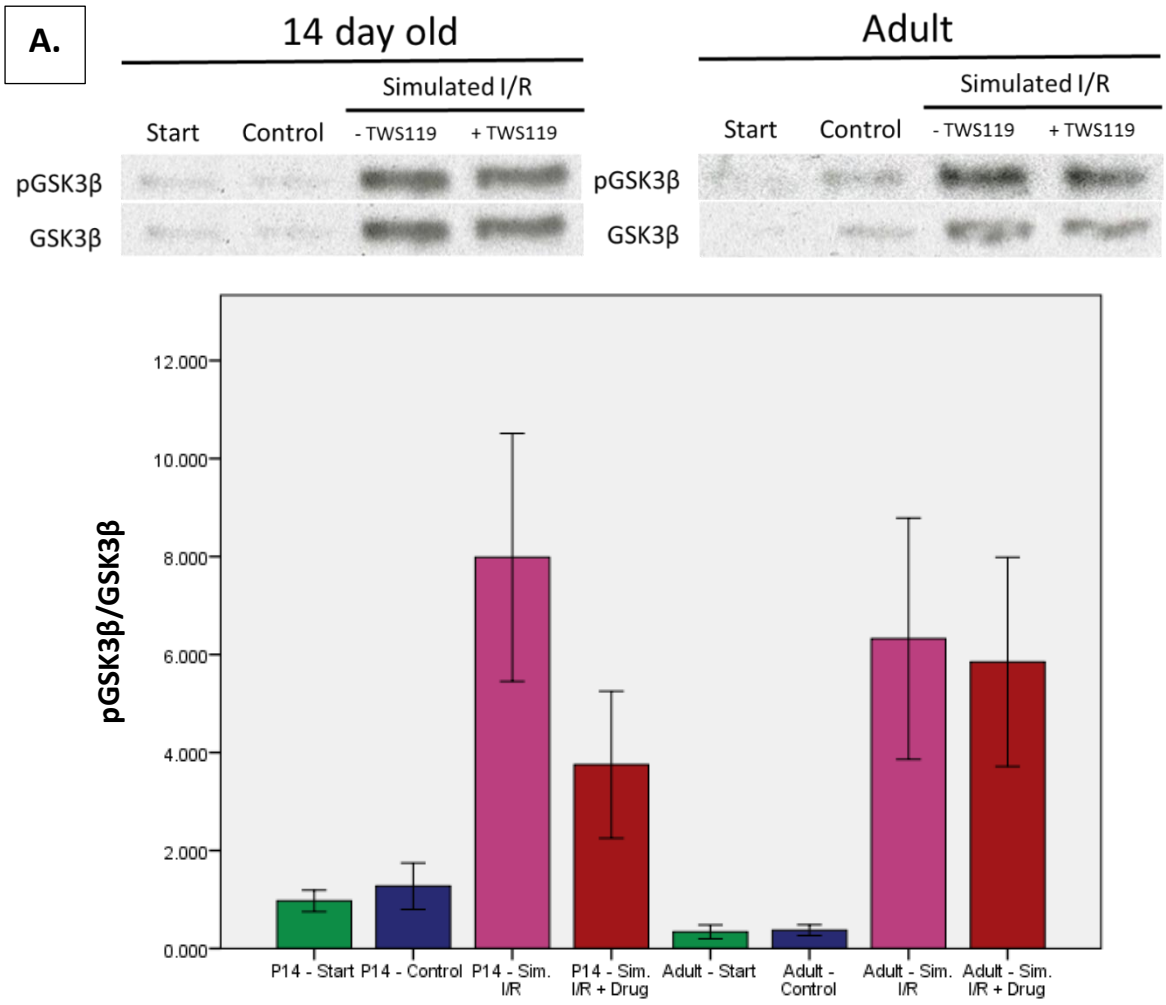

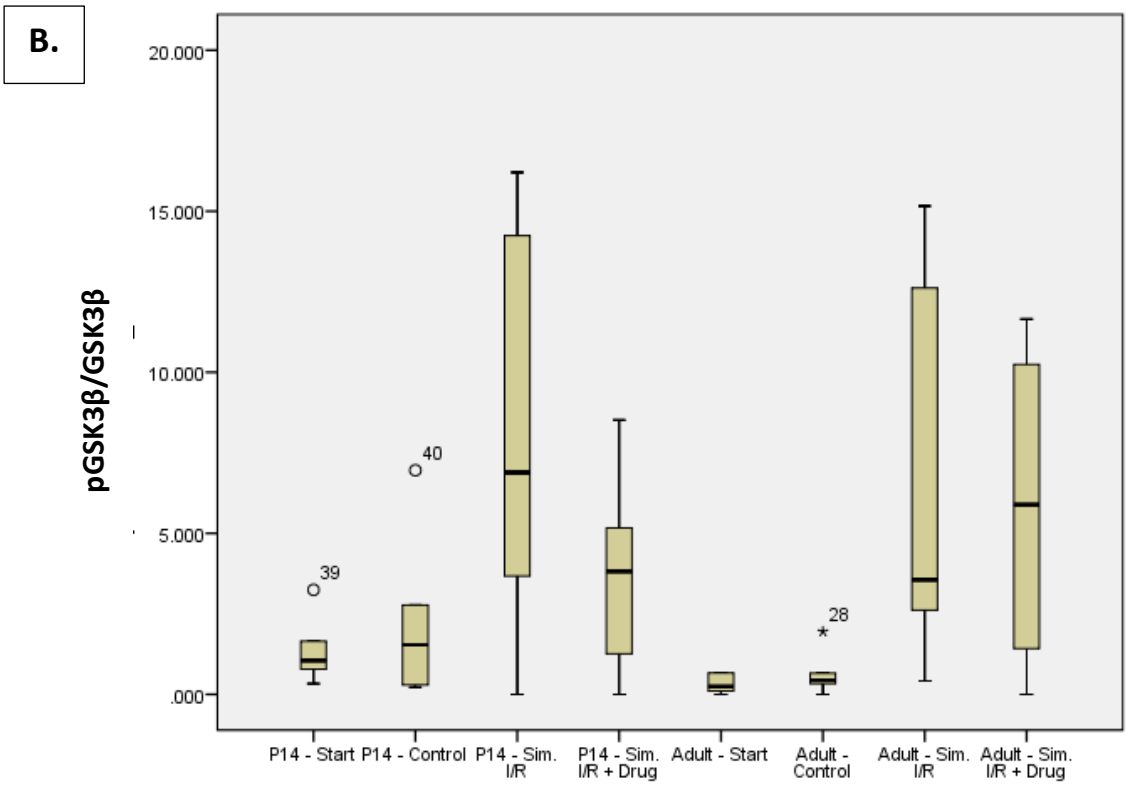

Figure 42. A. Representative western blot bands for pGSK3β and GSK3β for each experimental group from both 14-day old and adult cardiac samples, with a graph depicting the average ratio of pGSK3β /GSK3β for each age and experimental group. (n = 3 for each group). Data presented as mean ± SE. **B.** Boxplot representation of the pGSK3β /GSK3β for each age and experimental group.

No statistically significant differences were detected between any age or experimental groups. This likely results from the need for splitting and running samples on two separate gels, and resulting scatter in results, in addition to issues with the collection of cell pellets and subsequent extraction of proteins from these samples at the end of the experiment when cell viability is very low. Protein concentration in these samples was low, and subsequently produced weak bands which may not have provided sufficient resolution to identify differences in expression, particularly when attempting to detect phosphorylated proteins. However, the concentration of inhibitor used in these experiments has been demonstrated to effectively inhibit GSK3β in previously published works.

5.3.2.1.3 Differential effects of AMPK inhibition on isolated cardiomyocytes from 14-day old and adult hearts.

5.3.2.1.3.1 Effect of dorsomorphin dihydrochloride treatment on percentage change in cardiomyocyte viability.

As seen in **Figure 43**, cardiomyocyte suspensions from adult hearts displayed statistically significant differences in percentage change in viability only between the control (green) group in comparison with both the simulated I/R (blue) and simulated I/R with dorsomorphin (red) groups. However, 14-day old cells showed additional statistically significant differences in viability between the simulated I/R and AMPK inhibited groups. This shows that inhibition of AMPK only had an effect on cell viability in cardiomyocytes taken from 14-day old hearts, whereas adult cells were unaffected by AMPK inhibition.

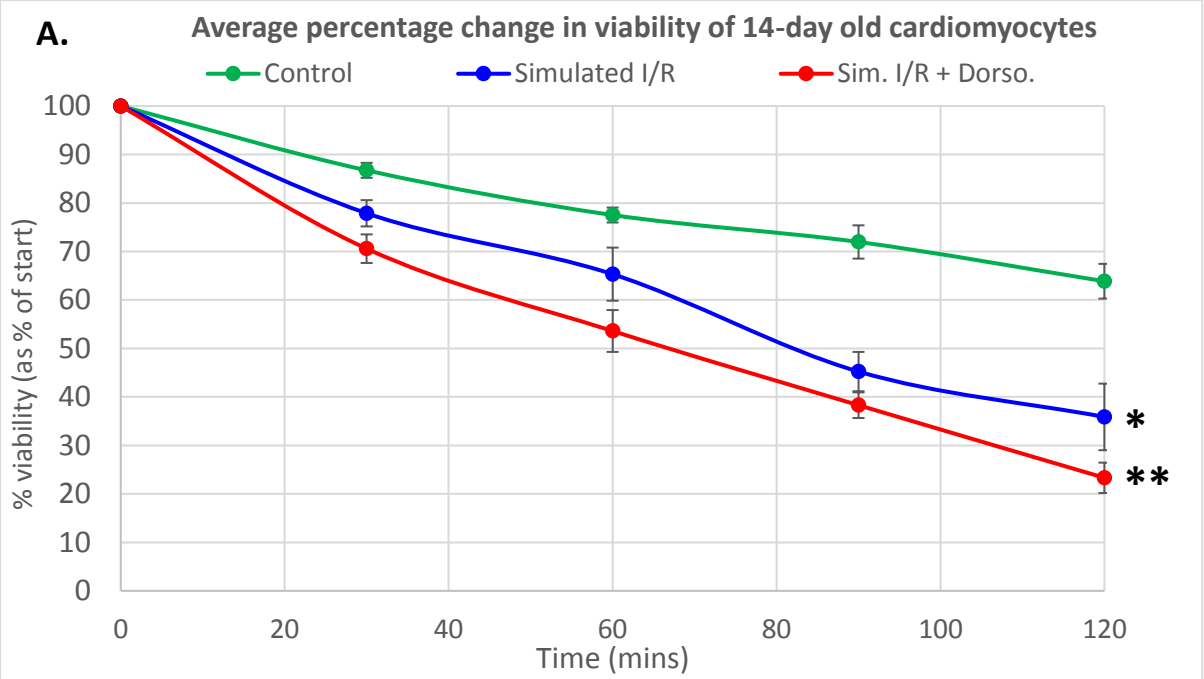

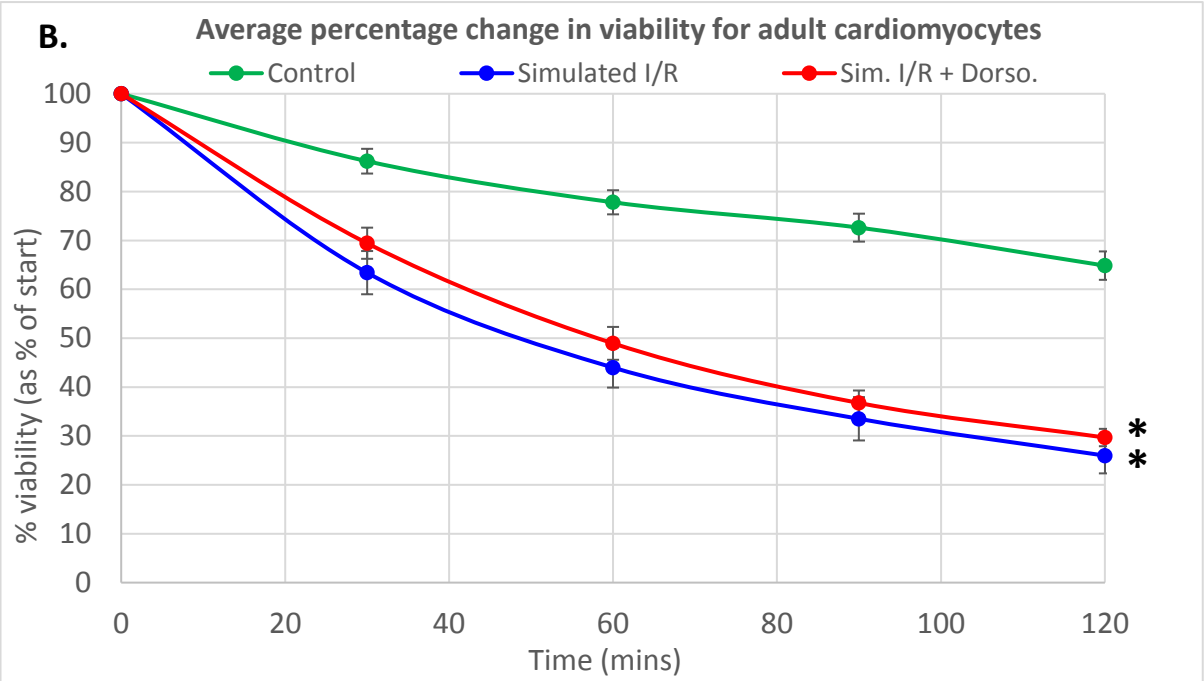

Figure 43. Percentage change in viability over the course of 120 minutes in 14-day old and adult rat heart derived cardiomyocytes; control vs. simulated I/R vs. dorsomorphin treated cardiomyocytes. **A.** 14-day old hearts (n = 5 per group), control vs. simulated I/R, control vs. dorsomorphin, simulated I/R vs. dorsomorphin. **B.** Adult hearts (n = 4 per group), control vs. simulated I/R, control vs. dorsomorphin. * = statistically significant difference with control ($p < 0.05$). ** = statistically significant difference with control & simulated I/R ($p < 0.05$).

5.3.2.1.3.2 Effect of dorsomorphin dihydrochloride treatment on percentage change of rod-shaped cardiomyocytes.

The percentage change of rod-shaped cardiomyocytes was significantly different between control and dorsomorphin treated cells, as well as between simulated I/R and dorsomorphin treated cells, whereas there was no difference between control and simulated I/R cells in 14-day olds. In adults, however, only the control group showed differences to both the simulated I/R and dorsomorphin groups, indicating AMPK inhibition effected the percentage of rod cells only in 14-day olds.

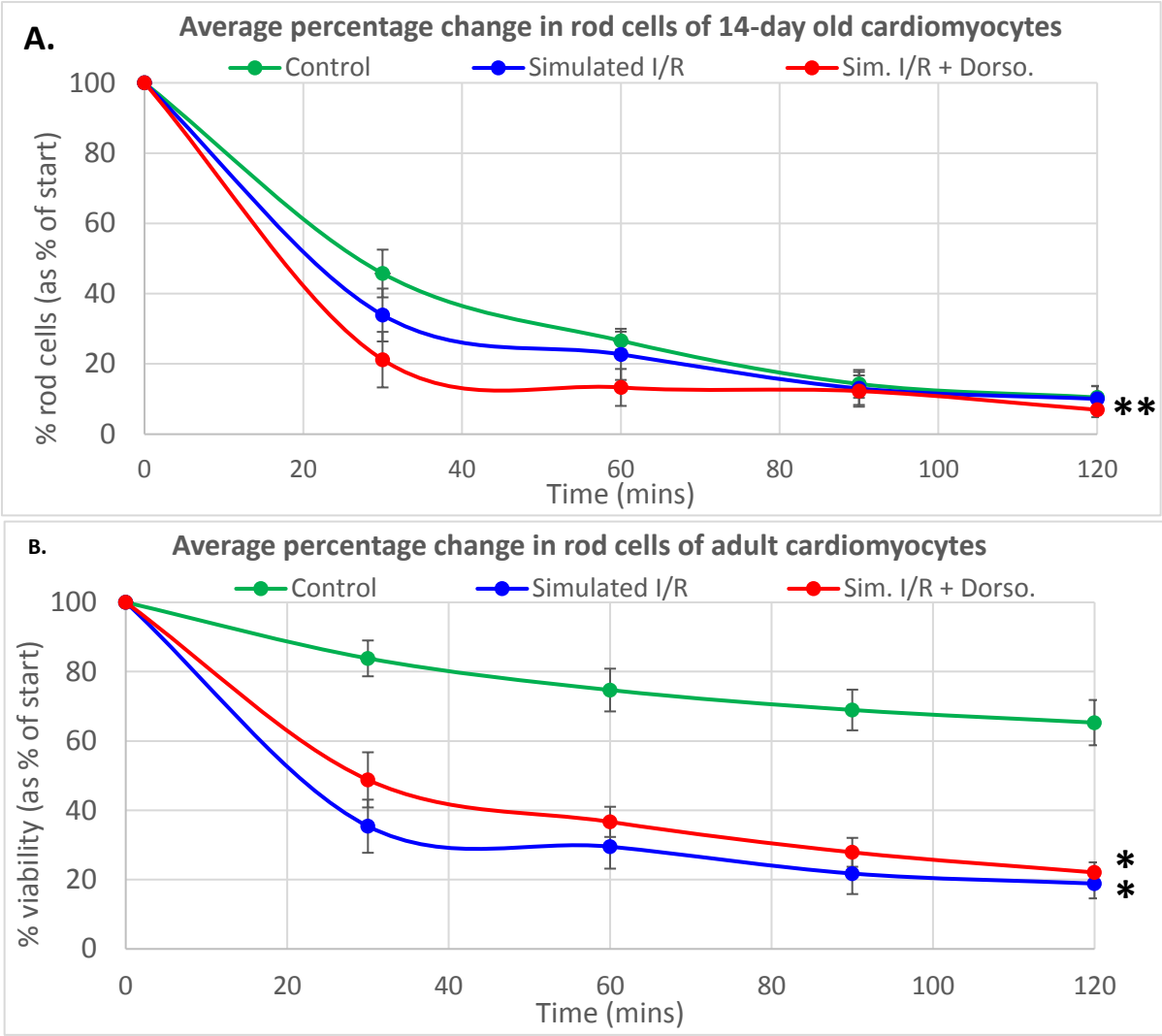

Figure 44. Percentage change of rod-shaped cardiomyocytes over the course of 120 minutes in 14-day old and adult rat heart derived cardiomyocytes; control vs. simulated I/R vs. dorsomorphin treated cardiomyocytes. **A.** 14-day old hearts (n = 5 per group), control vs. dorsomorphin, simulated I/R vs. dorsomorphin. **B.** Adult hearts (n = 4 per group), control vs. simulated I/R, control vs. dorsomorphin. * = statistically significant difference with control ($p < 0.05$). ** = statistically significant difference with control & simulated I/R ($p < 0.05$).

As previously mentioned, difficulty in collecting sufficient cells to form a pellet as a result of the very low cardiomyocyte viability at the end of incubation, often meant having an insufficient protein concentration for detection in western blotting. However, previous studies have demonstrated the efficacy of this concentration of dorsomorphin dihydrochloride in inhibiting AMPK activity (Konishi, Haraguchi et al. 2011). Western blotting data for this experiment was therefore not included.

5.4 Discussion

5.4.1 Simulated I/R decreases viability in adult & 28-day old, but not 14-day old cardiomyocytes

Simulation of ischemia/reperfusion injury in isolated cardiomyocytes found that there was no statistically significant difference in the resulting percentage cell viability between the experimental and control groups in 14-day old cardiomyocytes, whereas a statistically significant change was found in both 28-day old and adult cardiomyocytes. The absence of a statistically significant difference at 14-days is consistent with previous reports of a greater resistance to injury from I/RI injury at this age (Modi and Suleiman 2004). Moreover, the bell-shaped pattern of resistance reported – in which recovery following I/R markedly decreases at 28-days, and subsequently further in adults – appears to be mimicked in this data. As previous work into differences in resistance to I/RI have predominantly been conducted in whole hearts, the fact that a similar vulnerability profile can be seen in isolated cardiomyocyte samples that do not contain the same interacting factors found in the whole heart is significant. It should be noted that for direct statistical comparison of the viabilities of the experimental and control groups at the end of the experimental procedure, viability counts were treated as having been taken at exactly the same time point, whereas in reality there was a 20 minute delay between the measurements taken for the experimental group to those of the control group. It is therefore possible that the degree and significance of the differences as reported by statistical analysis have been underestimated.

5.4.2 Inhibition of differentially expressed proteins altered vulnerability of 14-day old, but not adult cardiomyocytes to simulated I/R

5.4.2.1 Inhibition of PKC

As previously mentioned, PKC was chosen for targeting in isolated cardiomyocyte viability studies due to its overall biphasic pattern of expression with postnatal development in the proteomic output, and due to the fact that it is a key end effector of survival signalling pathways such as RISK-SAFE. Inhibition of PKC with chelerythrine had a statistically significant effect on percentage viability of cardiomyocytes in 14-day old hearts only, but not in percentage rod-shaped cells in either age group. The fact that inhibition of PKC only seemed to effect 14-day old cardiomyocytes, at which age expression was greatest over the course of postnatal development, indicates that there is a potential causative mechanism linking the action of PKC and its greater expression to the associated greater resistance to cardiac insult at this age.

Active PKCε is known to translocate to the sarcolemma and mitochondria from the cytosol, an effect seen following preconditioning in both the whole heart and in cultured neonatal rat cardiomyocytes (Inagaki et al. 2006). It is believed that this translocation allows PKCε to interact with K_{ATP}-channels present at both sites, although the mitochondrial form is believed to be more relevant in cardioprotection (Gross and Peart 2003, Light et al. 1996). Work has shown that in rabbit hearts, treatment with a PKC activator resulted in reduced infarct size, an effect that was lost with use of a K_{ATP}-channel inhibitor (Miura et al. 2000). However, similarly to our findings and those of others on the effect of chelerythrine in adult hearts, Miura et al. (2000) found that the use of a PKC inhibitor, in this case calphostin, did not affect infarct size.

PKCε has also been shown to interact with the mPTP, preventing its opening and subsequent water and solute entry, mitochondrial swelling, outer membrane rupture, release of intermembrane cytochrome c, and apoptosis (Inagaki et al. 2006). Baines et al. (2003) demonstrated that PKCε is able to directly interact with components of the mPTP, for example, through phosphorylation of VDAC1 and the resulting inhibition of pore opening (Kerner et al. 2014). While incubation of isolated cardiomyocytes with PKCε and cardiac specific expression of active PKCε resulted in greater interaction between PKCε and mPTP components, as well as inhibition of mPTP opening and reduced Ca^{2+}-induced mitochondrial swelling, expression of inactive PKCε did not have an effect on pore opening (Baines et al. 2003). This mimics the lack of effect seen with PKC inhibition via chelerythrine treatment frequently reported, but whether such findings would be the same in the more injury resistant 14-day old heart is uncertain. Our findings in isolated cardiomyocytes showed that chelerythrine did indeed have a negative effect on cell viability, and may indicate that the greater expression of PKCε in 14-day old hearts correlates with a greater dependence on PKCε activity. Interestingly, three isoforms of VDAC (-1, -2, and -3) were all found to be most highly expressed in 14-day olds, with statistically significant differences compared to both 7-day old and adult hearts. This presents the possibility that a greater expression of VDAC in these hearts makes them more reliant on the activity of PKCε to phosphorylate and inhibit pore opening. Indeed, Zhang et al. (2012) showed that the cardioprotective effects of urantide following I/RI, associated with increased pAkt levels and BCL-2:Bax ratios, were lost following treatment with either chelerythrine or the PI3K-Akt inhibitor, LY294002. As their previous work had demonstrated no effect on I/RI with chelerythrine treatment alone (Zhang et al. 2005), it is possible that PKC inhibition and thus the effect of chelerythrine only effects survival and the response to cardiac insult in a situation where PKC expression or

activity is already elevated, which may provide an explanation as to why the drug was only effective in 14-day old hearts. Further work will be required to examine the effects of chelerythrine in 14-day old, Langendorff-perfused whole hearts.

5.4.2.2 Inhibition of GSK3β

GSK3β was chosen for targeting in isolated cardiomyocyte viability studies due to its overall biphasic pattern of expression with postnatal development, in addition to its role as a key end effector of survival signalling pathways such as RISK-SAFE. TWS119 treatment resulted in a statistically significant drop in cardiomyocyte percentage viability in 14-day olds, an effect that was also seen in the percentage of rod-shaped cells. However, this occurred in neither percentage viability nor percentage rod-shaped cells in adults. These results therefore demonstrate a putative link between the greater expression of GSK3β in 14-day olds in comparison with adult hearts, implicating GSK3β as a potentially causal protein in the greater resistance to cardiac insult seen in 14-day old hearts. Whilst this may appear surprising due to previous reports that GSK3β activity is detrimental to cardiomyocytes following I/RI, and that inhibition via pharmacological means or via phosphorylation by Akt is cardioprotective (Das et al. 2008), the majority of these studies have been focused on the adult heart, or in neonatal cardiomyocytes cultured prior to the 14-day peak in resistance to cardiac injury. As GSK3β is known to actually provide a cardioprotective effect during ischemia (discussed in **Section 1.5.3**), it is possible that this ischemia-specific role is more prominent in 14-day old hearts, and that inhibition of GSK3β results in the loss of this protection, leading to decreased cardiomyocyte viability in this age group. However, targeting of GSK3β in our isolated cardiomyocyte work employs chronic inhibition, as TWS119 is added to the cell suspension and left to incubate, whereas Langendorff studies

will wash out the drug, usually prior to ischemia. It will therefore be necessary to investigate the effect of GSK3β inhibition in the whole heart, and to examine the expression and phosphorylation states of samples taken from Langendorff perfused hearts following ischemia alone and following I/R.

5.4.2.3 Inhibition of AMPK

AMPK was chosen for targeting in isolated cardiomyocyte viability studies due to its strong biphasic pattern of expression, with statistical significance between 14-day old and both 7-day and adult hearts, as well as its previously discussed cardioprotective properties (**Section 5.1.3**), and overlap with RISK-SAFE signalling pathways. Inhibition of AMPK with dorsomorphin dihydrochloride resulted in a statistically significant drop in both cardiomyocyte percentage viability and the percentage of rod-shaped cells in 14-day olds, but not adults. Furthermore, the percentage of rod-shaped cells was found not to differ between control and simulated I/R cardiomyocytes in 14-day olds, whereas cells with simulated I/R in addition to dorsomorphin treatment had a significantly lower percentage than both. In adults, however, the percentage of rod-shaped cells was significantly lower in both the simulated I/R alone and simulated I/R with dorsomorphin groups compared to control, whereas these groups did not differ from one another. This supports the hypothesis that a greater expression of survival signalling related proteins in the 14-day old hearts confers greater resistance to cardiac insult, as inhibition of such proteins appears to confer a negative effect on viability not seen in adult hearts where basal AMPK expression is lower. Of particular interest is AMPK's link to PKCε – the result of inhibition of which is discussed in **Section 5.4.2.1** – in the setting of iPreC. Nishino et al. (2004) found that iPreC resulted in increased AMPK activity following translocation of PKCε to the cell membrane, and that this

effect of iPreC on AMPK activity was lost following pre-treatment with PKC inhibitors, including chelerythrine. This study implies that AMPK-mediated cardioprotection is PKCε-dependent, and may be a contributing factor to our findings that chelerythrine treatment effected cardiomyocyte viability only in 14-day old cells, but not adults. However, whilst PKCε was found to translocate from the cytosol even in non-iPreC regions of the heart, these regions did not display greater AMPK activity (Nishino et al. 2004). The authors suggest that this may be due to the lack of the elevated AMP levels that accompany iPreC required for AMPK activation, raising interesting implications in the context of immature hearts. It has previously been reported that there is a lack of efficacy of iPreC in neonatal hearts (Doul et al. 2015, Schmidt et al. 2014), which may suggest that 14-day old hearts have an additional mechanism or signalling influence that allows for elevated AMPK activity, thus rendering iPreC redundant. Whether these findings hold true in the whole heart requires further investigation.

5.4.3 Isolated cardiomyocytes respond differently to stress than intact hearts

Contrary to what is seen in the whole heart, cardiomyocytes isolated from 14-day old hearts with simulated I/RI appeared to have a similar, if not greater, drop in percentage viability over the 2 hour experimental procedure in comparison with adults, in addition to a very dramatic decrease in the percentage of rod-shaped cells. While this seems to contradict reports that 14-day old hearts have a greater resistance to cardiac insult than adults, it is likely that these differences are due to the process of enzymatic digestion itself, which may be more harmful to 14-day old cardiomyocytes and indeed tended to yield a smaller number of cells that would quickly lose their rod shaped morphology and become rounded, but remain viable. Furthermore, this transition from a rod to rounded morphology seemed to

be exacerbated by the process of filtering the cardiomyocyte suspension and the subsequent stepwise increase of Ca^{2+} concentration in these 14-day old cells, suggesting the digestion process may have increased their sensitivity to Ca^{2+} loading.

Initial proof of model studies (**Section 5.3.1**) actually found that, in comparison with 28-day olds and adults, 14-day old cardiomyocytes were the only age group not to show a statistically significant difference in viability over the two-hour experimental period between control and simulated I/RI groups. However, as the decrease in cell viability following simulated I/RI across all three age groups was not very dramatic, our standard laboratory protocol for cardiomyocyte viability studies subsequently switched to perfusion with a non-glucose or sodium pyruvate containing solution following enzymatic digestion. This may have had a greater effect on 14-day olds, especially as it is known that hearts switch from predominantly glycolysis based metabolism during the neonatal period to predominantly β-oxidation based as they transition into adulthood (Lopaschuk and Jaswal 2010), and may therefore contribute to these differences in response to insult seen between isolated 14-day old cardiomyocytes and the intact 14-day old heart.

5.3.4 Summary & Conclusion

Inhibition of PKCε, GSK3β and AMPK – which showed biphasic patterns of expression in the proteomic output correlating with the cardiac vulnerability profile to I/RI – all resulted in significant decreases to cardiomyocyte viability following I/RI in 14-day old, but not adult hearts. This is consistent with our hypothesis that these proteins, due to their role in cell survival and peak expression at 14-days of age, may play an important part in the underlying mechanism conferring heightened cardiac resistance to I/RI in this age group. Further work

was therefore undertaken to see if such age-dependent effects of inhibition on cardiac injury could be replicated in the whole heart, as will be described in **Chapter 6**.

Chapter 6: Targeting survival signalling pathways and vulnerability of intact adult and neonatal hearts to I/R

6.1 Introduction

A number of key survival signalling proteins that demonstrated an overall biphasic pattern of expression across the four age groups, concordant with the differences in cardiac vulnerability to I/RI, were identified in the proteomic analysis (**Section 4.3**). One of the key proteins found was AMPK, which demonstrated a biphasic trend in expression with statistically significant differences between 14-day old samples and all 3 of the remaining age groups. As AMPK has an important role in reducing cardiac injury during ischemia and reperfusion (**Section 1.5.3**), a biphasic profile of expression that correlates with changes cardiac resistance to I/RI, as well as having demonstrated the effect of its inhibition on isolated cardiomyocytes from different age groups (**Section 4.3.3.1.3**), the two first aims of this work have already been addressed:

1. "To identify any changes that occur in survival signalling through changes in the expression of pro-survival and apoptosis-related proteins during development."
2. "To see if specific inhibition of the identified proteins affects the vulnerability to ischemia/reperfusion injury during postnatal development in isolated cardiomyocytes."

This chapter therefore looks to address the third and fourth aims of this work; "To see if specific inhibition of the identified proteins affects the vulnerability to ischemia/reperfusion injury during postnatal development in whole hearts" and "To identify any changes that may subsequently occur in terms of survival signalling protein expression or activity following ischemia/reperfusion injury."

6.2 Materials & Methods

6.2.1 Protocol for ischemia/reperfusion experiments in the whole heart

Langendorff perfusion was performed as described in **Section 2.6**, using 14-day old (n = 6), adult (n = 6) rats. Hearts were removed, cannulated on a Langendorff apparatus and perfused with Krebs-Henseleit solution for a period of stabilisation, prior to a 30 minute period of global ischemia, and 60 minutes of reperfusion. Effluent was collected before ischemia and at 1, 5, 10, 20, 30 and 60 minutes of reperfusion for use in creatine kinase measurements. As tissue was taken from the left ventricular wall and processed for electron microscopy (**Section 8.3**), TTC staining for infarct sizes was not performed. The creatine kinase data for these experiments are presented in **Section 6.3.1** below.

6.2.2 Protocol for ischemia/reperfusion experiments with drug wash-out prior to ischemia

Langendorff perfusion was performed as described in **Section 2.6** and **6.2.1** above, using 14-day old (control n = 5, dorsmorphin dihydrochloride n = 5) and adult (control n = 5, dorsmorphin dihydrochloride n = 5) rats. However, for these experiments, a control heart and dorsomorphin dihydrochloride treated heart were perfused simultaneously for comparison. Inhibitor treated hearts were stabilised for 5 minutes, followed by 15 minutes of perfusion with Krebs-Henseleit buffer containing dorsomorphin dihydrochloride (1µM), before switching back to non-drug treated Krebs-Henseleit buffer to wash-out any remaining drug prior to ischemia. The full protocol for both experimental groups is shown in **Figure 45** below.

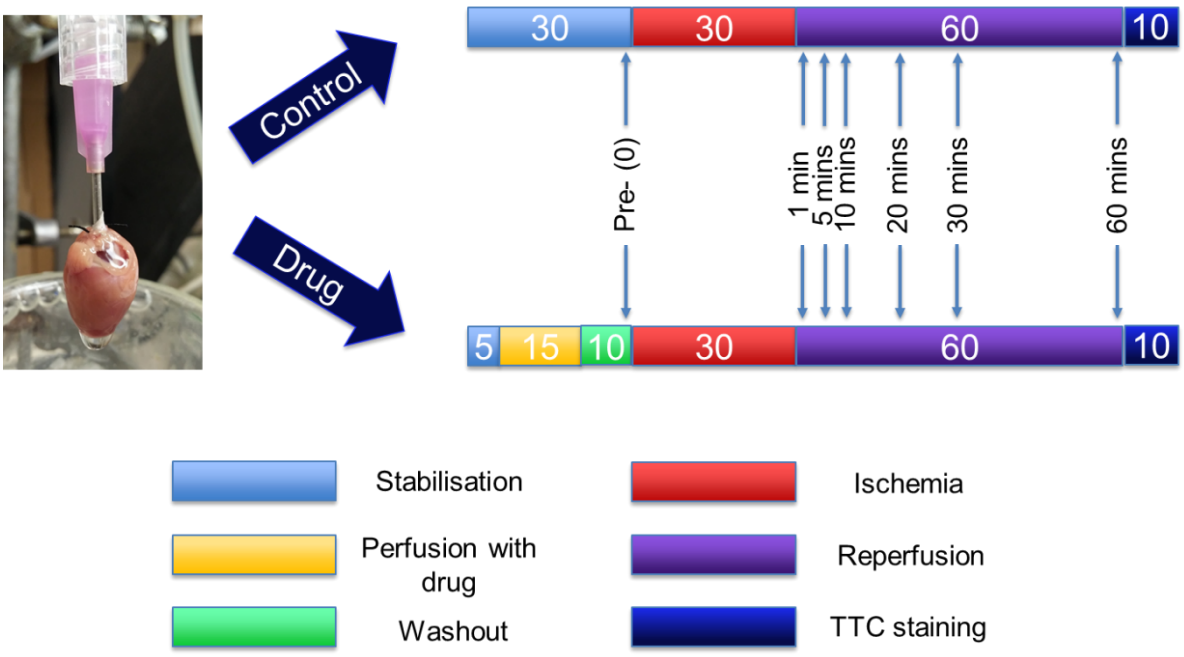

Figure 45. Experimental design for ischemia/reperfusion experiments with dorsomorphin **dihydrochloride** treatment.

As previously described, effluent was collected prior to ischemia and at 1, 5, 10, 20, 30 and 60 minutes of reperfusion for use in creatine kinase measurements. Following the final effluent collection, perfusion of the heart was switched to TTC solution (**Section 2.6.4**) for 10 minutes in order to stain for regions of infarction. Hearts were then incubated at 37°C in PBS for 5 minutes, frozen for 20 minutes, and cut into thin cross-sectional slices. These slices were stored at 4°C in 4% formalin overnight, before transfer into PBS to be stored until scanning. Slices were scanned, dried and weighed, then analysed for percentage infarct size as described in **Section 2.6.4**. The data for these experiments are presented in **Section 6.3.2.1**.

6.2.3 Protocol for experiments with drug present throughout ischemia

Langendorff perfusion was performed as described in **Section 2.6** and **6.2.2** above, using 14-day old (control n = 5, dorsomorphin dihydrochloride n = 4) and adult (control n = 3,

dorsomorphin dihydrochloride n = 4) rats. However, for these experiments, dorsomorphin dihydrochloride was not washed out prior to ischemia. Instead, inhibitor-treated hearts underwent a 10 minute period of stabilisation before perfusion with a Krebs-Henseleit solution containing 1µM dorsomorphin dihydrochloride for 5 minutes. Flow was then halted for 30 minutes of global ischemia as previously described, and the rest of the experiment conducted as described in **Section 6.2.2** above. The full protocol for both experimental groups is outlined in **Figure 46** below.

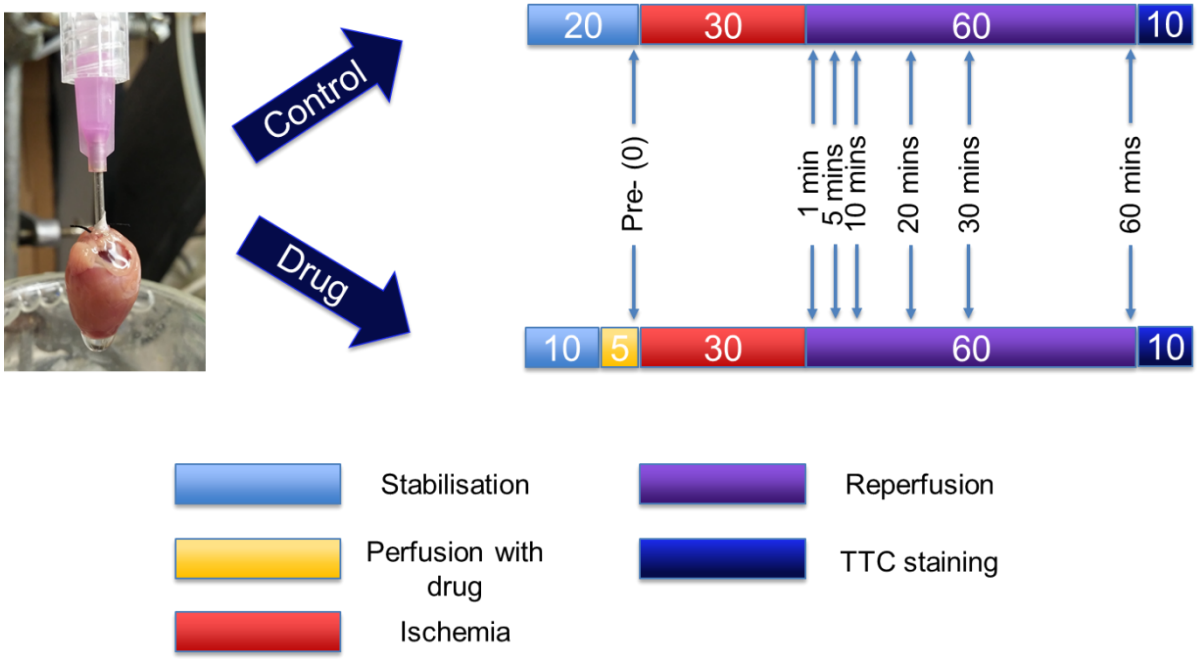

Figure 46. Overview of the experimental design for ischemia/reperfusion experiments with dorsomorphin **dihydrochloride** treatment.

6.2.4 Western blot analysis of extracted tissue

The full western blotting methodology has been described in **Section 2.5**. To summarise, protein samples were extracted and quantified (**Sections 2.4.1.1** and **2.4.2**) from the apex of control hearts and hearts that had been treated with dorsomorphin dihydrochloride following the ischemia/reperfusion protocol outlined in **Figure 46** above. Samples were

appropriately diluted to a final concentration of 0.15mg protein in a final volume of 100µl with double distilled water, and prepared for gel electrophoresis with the addition of an equal volume of loading buffer (Laemmli buffer + βME). These samples were loaded onto a Mini-PROTEAN® TGX™ precast gels and transferred to a PVDF membrane, stained using Ponceau S solution to produce full lane bands (see **Section 2.5.4**), before blocking with milk. Membranes were then incubated with antibodies for AMPK, pAMPK, mTOR, pmTOR, Akt, pAkt, PKCε, pPKCε, GSK3β, pGSK3β, BAC, BCL-2, or Mfn1 (see table of antibodies in **Section 2.1.2**), washed with TBST, incubated with a secondary antibody, and visualised using the Enhanced ChemiLuminescence system. The resulting blots were analysed using ImageJ or Image Studio Lite as described in **Section 2.5.6**, and corrected using full lane intensities obtained from Ponceau S staining as a loading control.

6.3 Results

6.3.1 Effect of I/R injury on isolated hearts from 14-day old and adult rats

In order to examine the differences in the degree of cardiac injury during reperfusion following ischemia during postnatal development, hearts from 14-day old (n = 6) and adult (n = 6) rats were extracted, cannulated, and perfused with Krebs-Henseleit solution, as described in **Section 2.6**. Effluent was collected during the reperfusion period for measurements of creatine kinase release, small sections of the apex were taken at 20 minutes for later protein extraction.

Creatine kinase release was measured in effluent samples collected pre-ischemia, following stabilisation (0 minutes), then at 1, 5, 10, 20, 30, and 60 minutes into reperfusion. Absorbance for each sample was measured using a spectrophotometer (**Section 2.6.3**) and converted into units/L, as plotted in **Figure 47A** below. From this, a corrected value from the wet weights of the hearts were calculated (**Figure 47B**), as well as a corrected area under the curve (**Figure 47C**).

In order to assess the differences in cardiac injury between the two age groups, statistical analysis was performed for creatine kinase released at each time point in 14-day old samples compared with adult samples. 14-day old samples were shown to have peak creatine kinase release at 1 minute reperfusion, higher than that seen in adults, both uncorrected and corrected for wet heart weight. However, this difference was only statistically significant following correction for weight. In both the corrected and uncorrected (age: $p < 0.05$, time: $p < 0.05$, age*time: $p < 0.05$ for both) data, creatine kinase levels were then shown to increase to levels significantly higher in adults than in samples collected from 14-day olds

over the remaining course of reperfusion. Statistically significant differences following post hoc tests with a Bonferroni correction are indicated in **Figures 47A** and **47B** (* = $p < 0.05$). Area under the curve was significantly higher in adults than 14-day olds. The lower creatine kinase released following 1 minute of reperfusion in 14-day olds, and the subsequently higher levels in adult samples from 5 minutes reperfusion onwards, indicates a greater degree of cardiac injury in the adult hearts in comparison with 14-days old.

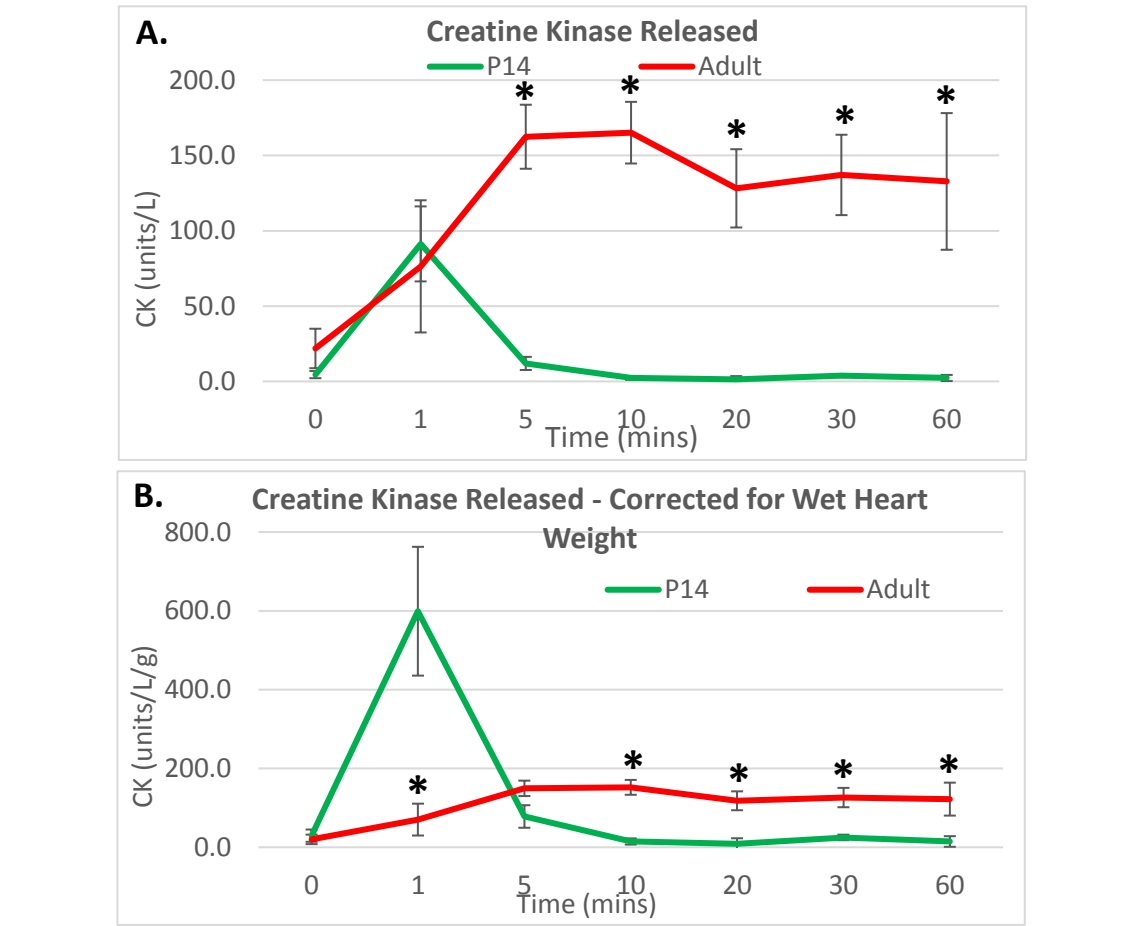

Figure 47. Time-dependent CK release during reperfusion from 14-day old and adult hearts shown as absolute values (**A**), corrected for weight (**B**) and total release (AUC) (**C**). Data shown as Mean ± SE (n=6/group). * = statistical significance compared with 14-day old hearts ($p < 0.05$).

6.3.2 Effect of selected survival signalling proteins inhibition on injury following I/R in adult and 14-day old hearts.

A statistically significant biphasic change in AMPK expression was detected by proteomic analysis (**Section 4.3**), thus highlighting this protein as a potential component of the underlying mechanism behind biphasic changes in resistance to cardiac injury seen during postnatal development. Following experiments to identify any effects of AMPK inhibition on cell viability in isolated cardiomyocytes (**Section 5.3.2**), further experiments were undertaken to examine the effects of inhibiting this protein using dorsomorphin dihydrochloride in the whole heart, to better take into account additional factors that are excluded when looking at individual cardiomyocytes.

6.3.2.1 Effect of pre-ischemic treatment with an AMPK inhibitor on whole hearts

In order to test the effect of AMPK inhibition on whole hearts, 14-day old and adult rats were culled, hearts excised and subsequently cannulated onto a Langendorff setup (**Section 2.6**). Non-control group hearts were perfused with dorsomorphin dihydrochloride for 5 minute before washout with Krebs-Henseleit buffer prior to ischemia, as outlined in **Section 6.2.2.**

6.3.2.1.1 AMPK inhibition and creatine kinase release post I/R

As previously described in **Section 6.3.1**, effluent was collected at set time points during reperfusion (**Section 6.2.2**) and creatine kinase levels at each timepoint were measured for both control and dorsomorphin dihydrochloride treated hearts in order to compare the degree of cardiac injury between the two groups.

14-day old

Tests of Within-Subjects Effects showed that the difference between the means is not statistically significant (treatment: $p > 0.05$, time: $p < 0.05$, treatment*time: $p > 0.05$), indicating creatine kinase release was not significantly altered by treatment of hearts with dorsomorphin dihydrochloride, as shown in **Figure 48.**

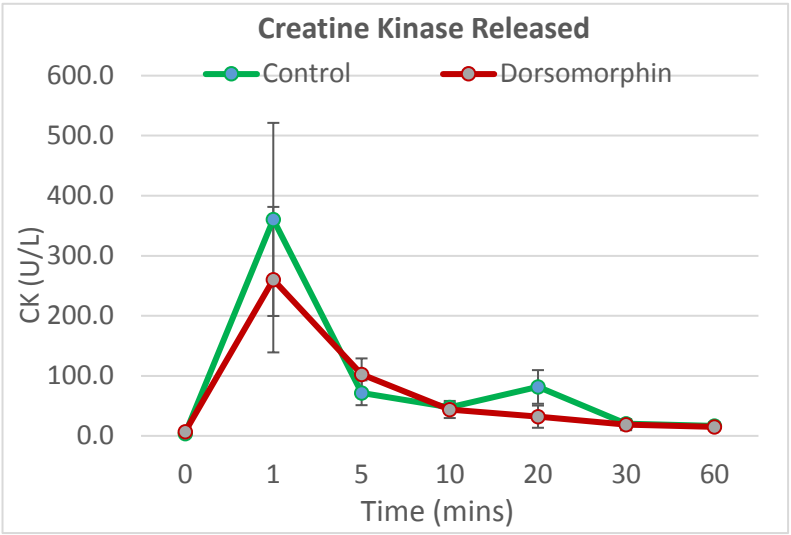

Figure 48. CK release during reperfusion following 30 minutes ischemia in 14-day old hearts ± pre-treatment with dorsomorphin dihydrochloride, corrected for wet weight of the heart. Data presented as Mean ± SE. (n = 5/group).

Adult

Tests of Within-Subjects Effects showed that the difference between the means is not statistically significant (treatment: $p > 0.05$, time: $p < 0.05$, treatment*time: $p > 0.05$), indicating creatine kinase release was not significantly altered by treatment of hearts with dorsomorphin dihydrochloride.

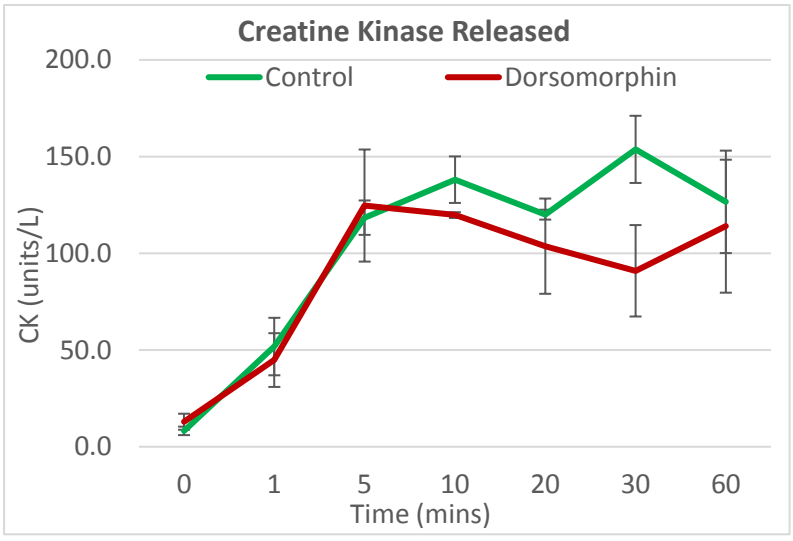

Figure 49. CK release during reperfusion following 30 minutes ischemia in adult hearts ± pre-treatment with dorsomorphin dihydrochloride, corrected for wet weight of the heart. Data presented as Mean ± SE. (n = 5/group).

6.3.2.1.2 AMPK inhibition and infarct size post I/R

Cardiac injury was assessed in both age groups using TTC staining (**Section 2.6.4**), with any regions lacking brick red staining measured as areas of infarction. **Figure 50** below shows that in 14-day old hearts, dorsomorphin dihydrochloride treatment followed by drug wash out prior to ischemia did not produce a statistically significant difference in infarct size in comparison with the control group, indicating inhibition of AMPK did not result in a significant increase in cardiac injury in 14-day old hearts.

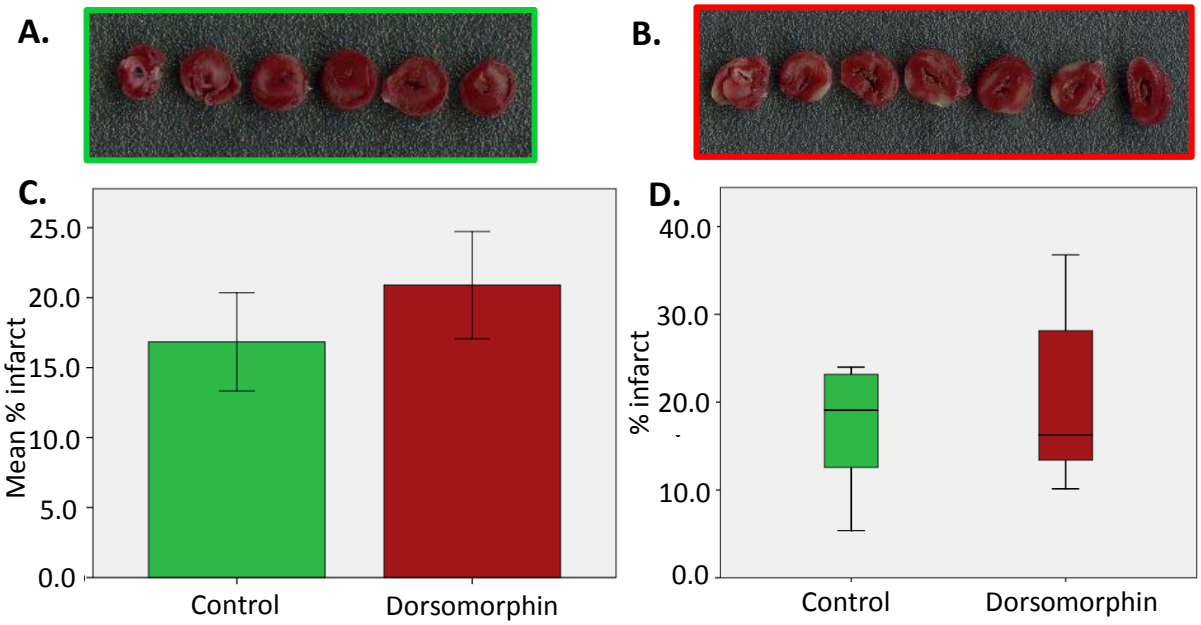

Figure 50. Infarct size measurements in 14-day old hearts following I/RI with or without AMPK inhibitor pre-treatment. **(Top)** Representative example images of control (**A**) and dorsomorphin dihydrochloride (**B**) treated hearts stained with TTC. **(Bottom)** The differences in infarct size between 14-day old hearts following I/R with or without dorsomorphin dihydrochloride pre-treatment. Data presented as mean ± SE (**C**) and boxplot (**D**). (n = 5/group)

This was also the case in adult hearts (**Figure 51**), where no statistically significant difference was seen between the mean infarct sizes of the control group and dorsomorphin treated group.

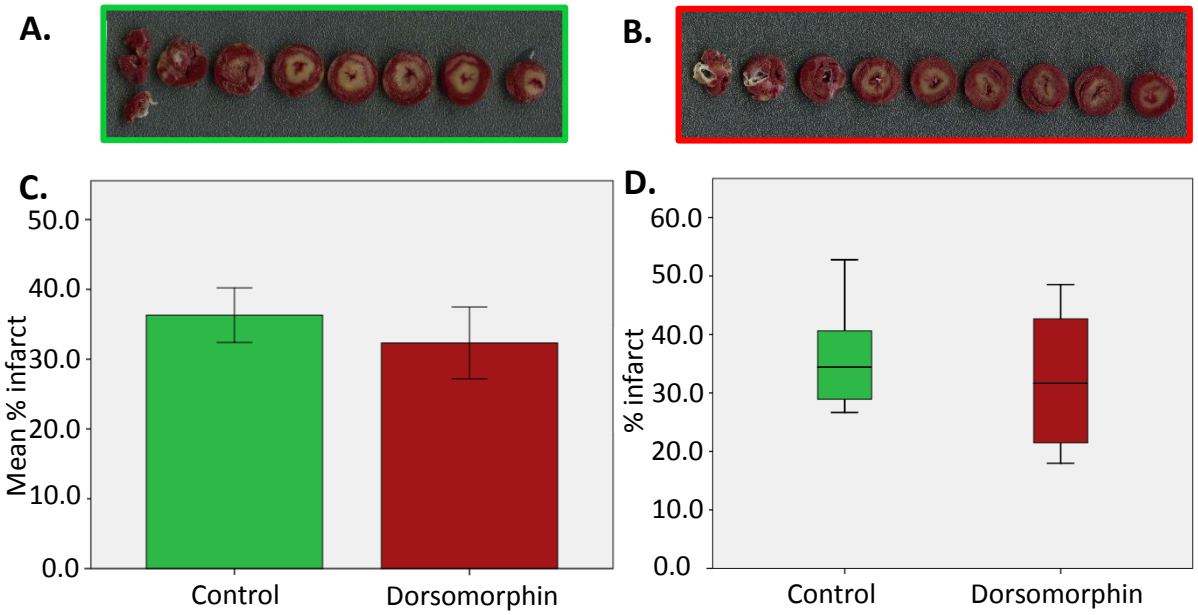

Figure 51. Infarct size measurements in adult hearts following I/RI with or without AMPK inhibitor pre-treatment. **(Top)** Representative example images of control (**A**) and dorsomorphin dihydrochloride (**B**) treated hearts stained with TTC. **(Bottom)** The differences in infarct size between adult hearts following I/R with or without dorsomorphin dihydrochloride pre-treatment. Data presented as mean ± SE (**C**) and boxplot (**D**). (n = 5/group)

6.3.2.2 Effect of AMPK inhibition during ischemia on reperfusion injury

The data above showed no statistically significant differences in injury when hearts were treated with AMPK inhibitor, dorsomorphin dihydrochloride, when added and washed out prior to ischemia. Therefore, these experiments were repeated, without washout of the drug prior to ischemia, as outlined in **Section 6.2.3**.

6.3.2.2.1 Effect of AMPK inhibition during ischemia on creatine kinase release.

As previously described, effluent was collected at set time points during reperfusion (**Section 6.2.3**) and creatine kinase levels at each timepoint were measured for both control and dorsomorphin dihydrochloride treated hearts in order to compare the degree of cardiac injury between the two groups.

14-day old: Creatine kinase Release Corrected for Heart Weight

While peak creatine kinase levels and Area Under Curve (AUC) values were not significantly different between the two groups, creatine kinase released over the course of reperfusion was shown to be statistically significantly different between control and dorsomorphin dihydrochloride treated hearts by two-way repeated measures ANOVA analysis (age: $p < 0.05$, time: $p < 0.05$, age*time: $p < 0.05$). Subsequent post hoc tests with a Bonferroni correction showed significant differences between control and dorsomorphin dihydrochloride treated hearts only at 10 minutes ($p < 0.05$).

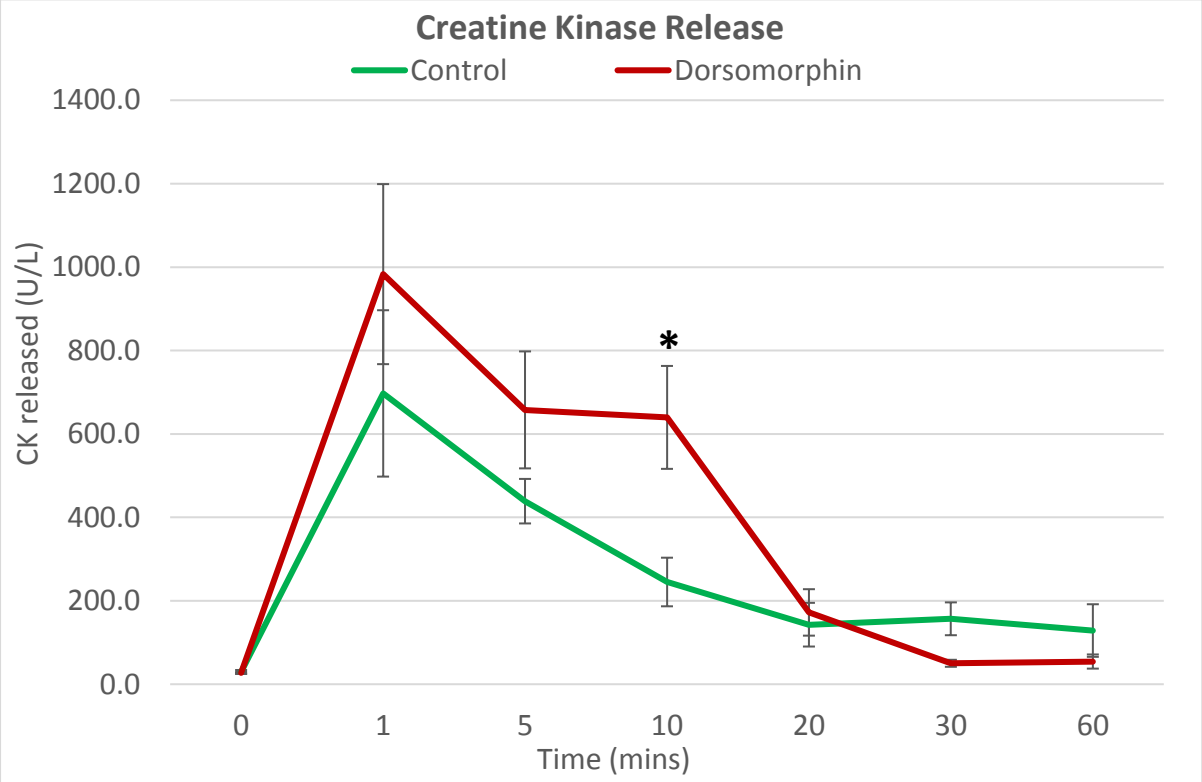

Figure 52. CK release from 14-day old hearts during reperfusion following 30 minutes ischemia with or without dorsomorphin dihydrochloride treatment during ischemia, corrected for wet weight of the heart. Data presented as mean ± SE. (control: n = 5. dorsomorphin: n = 4). * = statistically significant difference in comparison with control group ($p < 0.05$).

Adult: Creatine kinase release corrected for heart weight

No statistical significance was seen between control and dorsomorphin treated hearts in terms of peak creatine kinase release, AUC values, two-way repeated measures ANOVA analysis of creatine kinase released over the 60 minute course of reperfusion, as well as comparison of creatine kinase levels at each time point between the two experimental groups. Whilst this suggests that perfusion of hearts with dorsomorphin dihydrochloride does not make a difference to the degree of injury seen in adult hearts, it is important to note that, as mentioned previously, a large degree of variation was seen between measurements due to the reagent used to measure creatine kinase, which may have affected these results. This will be further discussed in **Section 6.4**.

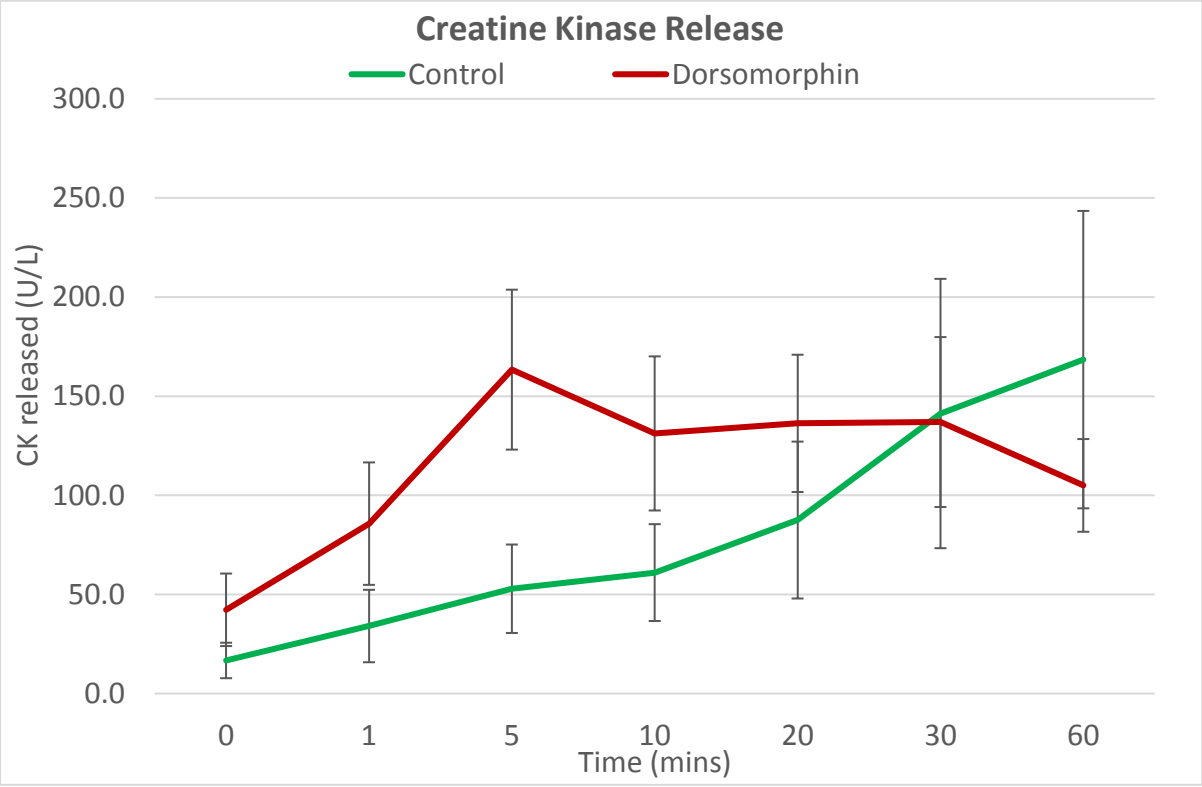

Figure 53. CK release from adult hearts during reperfusion following 30 minutes ischemia with or without dorsomorphin dihydrochloride treatment during ischemia, corrected for wet weight of the heart. Data presented as mean ± SE. (Control: n = 3. Dorsomorphin: n = 4).

6.3.2.2.2 Effect of AMPK inhibition on infarct size

Cardiac injury was assessed in both age groups using TTC staining (**Section 2.6.4**), with any regions lacking brick red staining measured as areas of infarction. In 14-day old hearts (**Figure 54**), a statistically significant difference was seen between the mean infarct sizes of the control group and dorsomorphin treated group ($p = 0.005$), indicating inhibition of AMPK throughout ischemia did result in a significant increase in cardiac injury in 14-day old hearts. In adult hearts (**Figure 55**), however, no statistically significant difference was seen between the mean infarct sizes of the control group and dorsomorphin treated group ($p = 0.253$), indicating inhibition of AMPK throughout ischemia did not result in a significant increase in cardiac injury in adult hearts. It should be noted, however, that infarct was measured as any region of the heart without "brick-red" staining, and it may be that measurement of more extremely infarcted regions of tissue – i.e. those stained white – separately may show a significant difference between the two experimental groups in adults.

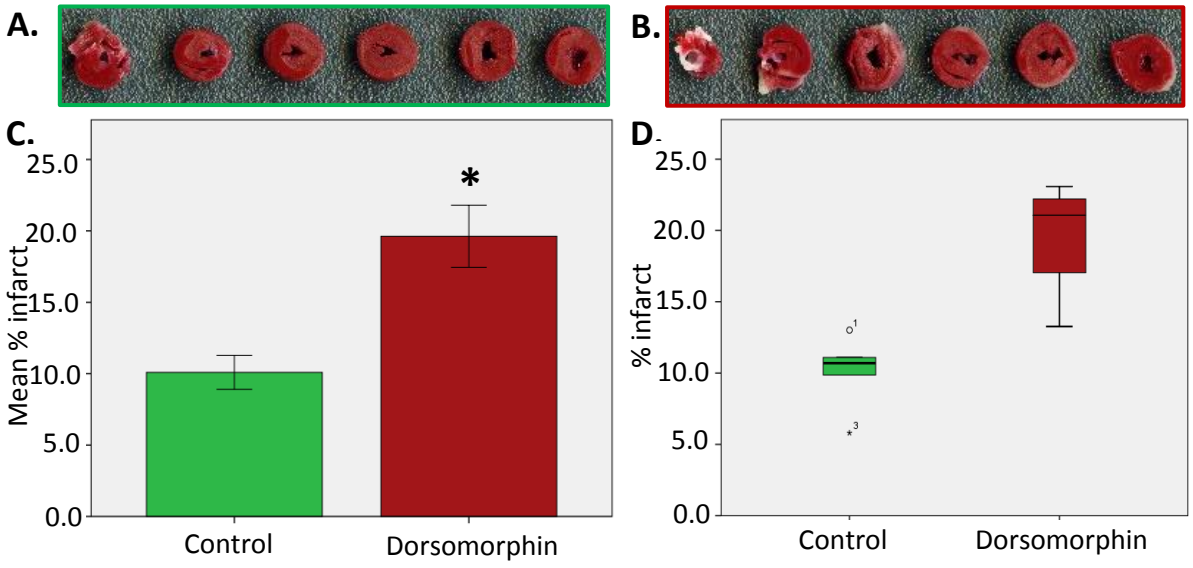

Figure 54. Infarct size measurements in 14-day old hearts following I/RI with or without AMPK inhibitor treatment during ischemia. **(Top)** Representative example images of control (**A**) and dorsomorphin dihydrochloride (**B**) treated hearts stained with TTC. **(Bottom)** The differences in infarct size between 14-day old hearts following I/R with or without dorsomorphin dihydrochloride treatment. Data presented as mean ± SE (**C**) and boxplot (**D**). * = statistically significant difference in comparison with control ($p < 0.05$). (Control: n = 5. Dorsomorphin: n = 4).

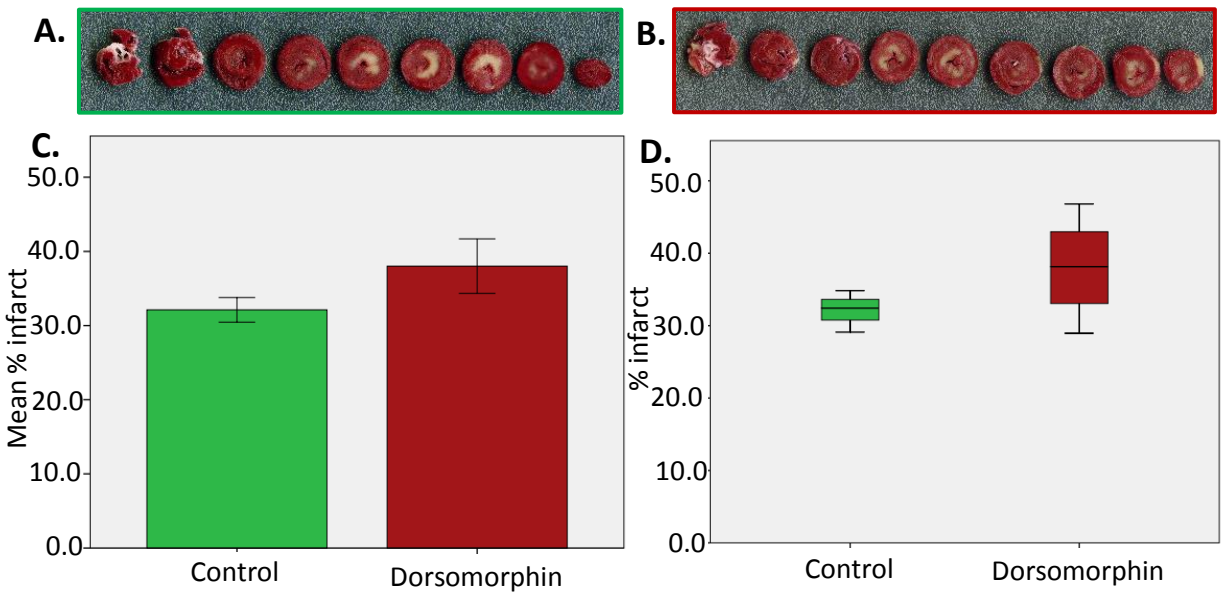

Figure 55. Infarct size measurements in adult hearts following I/RI with or without AMPK inhibitor treatment during ischemia. **(Top)** Representative example images of control (**A**) and dorsomorphin dihydrochloride (**B**) treated hearts stained with TTC. **(Bottom)** The differences in infarct size between adult hearts following I/R with or without dorsomorphin dihydrochloride treatment. Data presented as mean ± SE (**C**) and boxplot (**D**). (Control: n = 3. Dorsomorphin: n = 4).

6.3.2.2.3 Effect of AMPK inhibition during ischemia on the expression and phosphorylation state of key survival signalling proteins.

In order to further investigate the signalling mechanisms underlying differences in the degree of cardiac injury seen in 14-day old and adult hearts following ischemia/reperfusion Injury, and the specific effect of AMPK inhibition on these two age groups, the apex of control, post-ischemia, post-ischemia/reperfusion, and post-ischemia/reperfusion + dorsomorphin dihydrochloride perfused hearts were collected. Tissue was homogenised and quantified as described in **Section 2.4.1 and 2.4.2** before preparation for western blotting (**Section 2.5**). Due to the number of experimental groups required to be run simultaneously for each age group, and limitations in the number of samples that could be run per gel due to lane configurations, two separate gels had to be run for each protein tested. Each gel was

also run with a pooled reference sample to act as a standard between each run, which was used to produce a ratio of sample/pooled sample for each.

6.3.2.2.3.1 Effect of AMPK inhibition on pAMPK & AMPK expression

To ensure the efficacy of dorsomorphin dihydrochloride inhibition of AMPK, samples were tested for phosphorylation of AMPK.

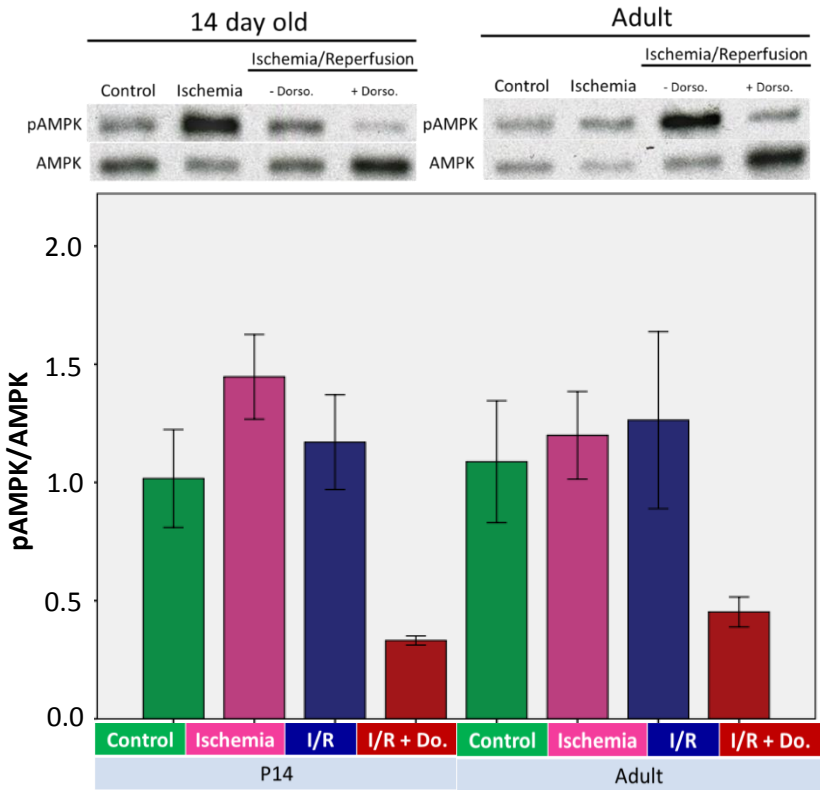

Figure 56. Effect of AMPK inhibition on pAMPK/AMPK. Mean pAMPK/AMPK levels in 14-day old and adult rat hearts either in control, following ischemia, I/R, or I/R + dorsomorphin dihydrochloride treated groups. Data presented as mean ± SE (n = 6/group)

While no statistically significant differences were seen between corresponding experimental groups, a clear trend demonstrating the expected drop in pAMPK detection in the dorsomorphin dihydrochloride treated group was seen in comparison to all other experimental groups in both 14-day old and Adult samples. Effective inhibition of AMPK in this experimental group can thus be inferred. Furthermore, as expected due to the reported cardioprotective signalling properties of active AMPK during ischemia and cardiotoxic properties during reperfusion, the bands show that in 14-day old samples, there is an overall higher level of phosphorylated and active AMPK in the ischemic group than the reperfused

group. In adults, however, stronger bands for phosphorylated AMPK were seen in the reperfused group than ischemic groups. The lack of statistical significance likely results from technical restrictions in terms of the number of samples that could be run per gel and subsequent comparison of protein expression between gels, thus resulting in substantial scatter of values. This will be discussed further in the limitations section (**Section 9.2**).

6.3.2.2.3.2 Effect of AMPK inhibition on pmTOR & mTOR expression

Due to the known role of AMPK as an upstream regulator of mTOR via inhibition of other members of the mTORC1 complex, samples were analysed using western blot to assess any changes to mTOR expression or phosphorylation following AMPK inhibition.

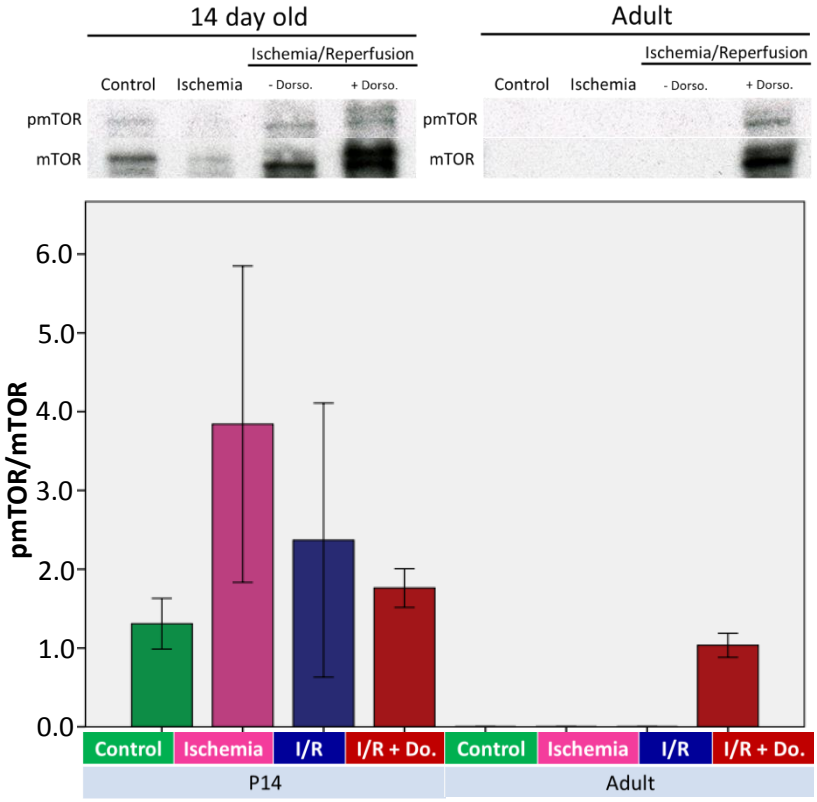

Figure 57. Effect of AMPK inhibition on pmTOR/mTOR. **(Top)** Representative western blot bands for each experimental and age group. **(Bottom)** Mean pmTOR/mTOR levels in 14-day old and adult rat hearts either in control, following ischemia, I/R alone, or I/R + dorsomorphin dihydrochloride treated groups. Data presented as mean ± SE (n = 3/group).

Similarly to pAMPK expression, no statistically significant changes in pmTOR/mTOR levels were detected by western blot, likely due to a large scatter in values resulting from the necessity of running multiple gels, as will be discussed in limitations (**Section 9.2**). However,

as can be seen from the images themselves, pmTOR levels appear to be greater in the dorsomorphin dihydrochloride treated group, particularly in adult samples where no protein was detected in control, ischemia or I/R groups. This greater expression in the dorsomorphin dihydrochloride treated groups correlates with inhibition of AMPK, which usually works to inhibit the action of mTOR during ischemia in a cardioprotective manner. The importance of this will be further discussed in **Section 6.4.3**.

6.3.2.2.3.3 Effect of AMPK inhibition on pAKT & AKT expression

As a key component of the survival signalling related RISK pathway, as well as its link to AMPK activity and signalling, the expression and phosphorylation state of AKT was measured by western blotting from samples to identify any changes caused by AMPK inhibition.

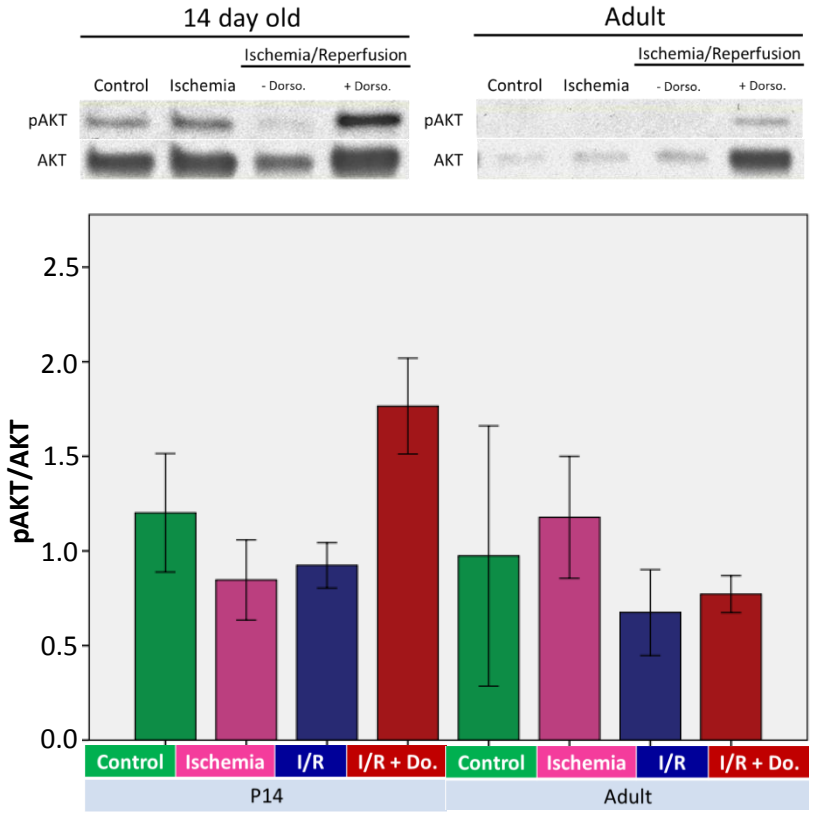

Figure 58. Effect of AMPK inhibition on pAKT/AKT. **(Top)** Representative western blot bands for each experimental and age group. **(Bottom)** Mean pAKT/AKT levels in 14-day old and adult rat hearts either in control, following ischemia, I/R alone, or I/R + dorsomorphin dihydrochloride treated groups. Data presented as mean ± SE (n = 3/group).

No statistically significant difference was seen in pAKT/AKT expression. However, blots showed visually that both pAKT and AKT levels were greater in 14-day old samples in comparison with adult samples, and that in AMPK inhibited dorsomorphin dihydrochloride treated groups in both 14-day old and adult hearts showed particularly high levels of both protein forms across the four experimental groups.

6.3.2.2.3.4 Effect of AMPK inhibition on pPKCε & PKCε expression

PKCε is an important endpoint of the survival signalling related RISK pathway, as well as closely linked to AMPK activity and signalling. Therefore, the expression and phosphorylation state of PKCε was measured by western blotting from samples to identify any changes caused by AMPK inhibition.

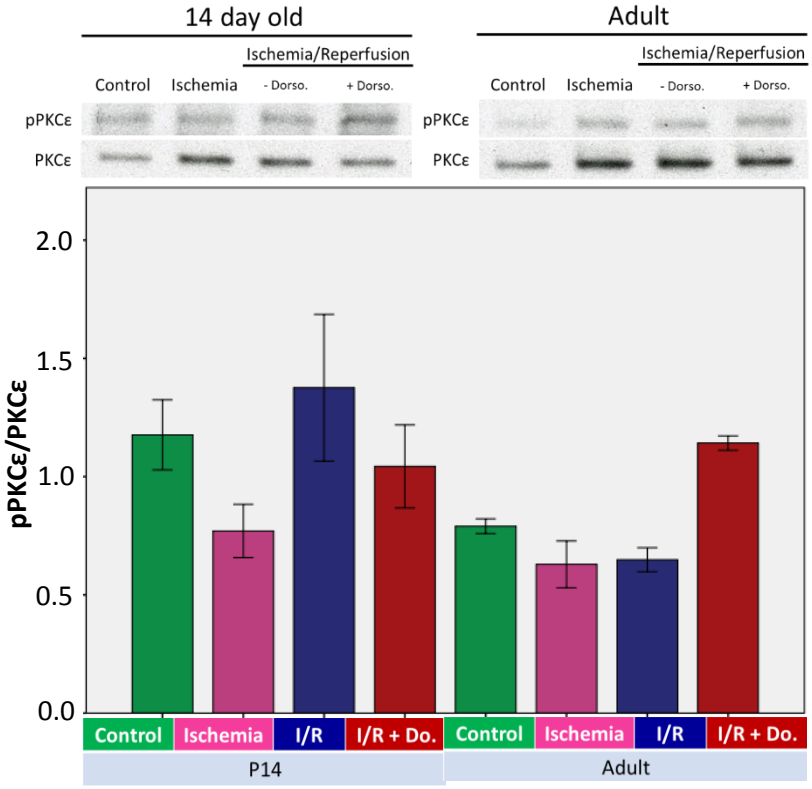

Figure 59. Effect of AMPK inhibition on pPKCε/PKCε. **(Top)** Representative western blot bands for each experimental and age group. **(Bottom)** Mean pPKCε/PKCε levels in 14-day old and adult rat hearts either in control, following ischemia, I/R alone, or I/R + dorsomorphin dihydrochloride treated groups. Data presented as mean ± SE (n = 3/group).

However, no statistically significant differences were seen in pPKCε/PKCε expression between age groups or experimental groups.

6.3.2.2.3.5 Effect of AMPK inhibition on pGSK3β & GSK3β expression

GSK3β is an important endpoint of the survival signalling related RISK pathway, in addition to being a cardioprotective protein when active during ischemia, whilst being cardiotoxic during reperfusion in a similar mechanism to AMPK. Therefore, the expression and phosphorylation state of GSK3β was measured by western blotting to identify any changes caused by AMPK inhibition.

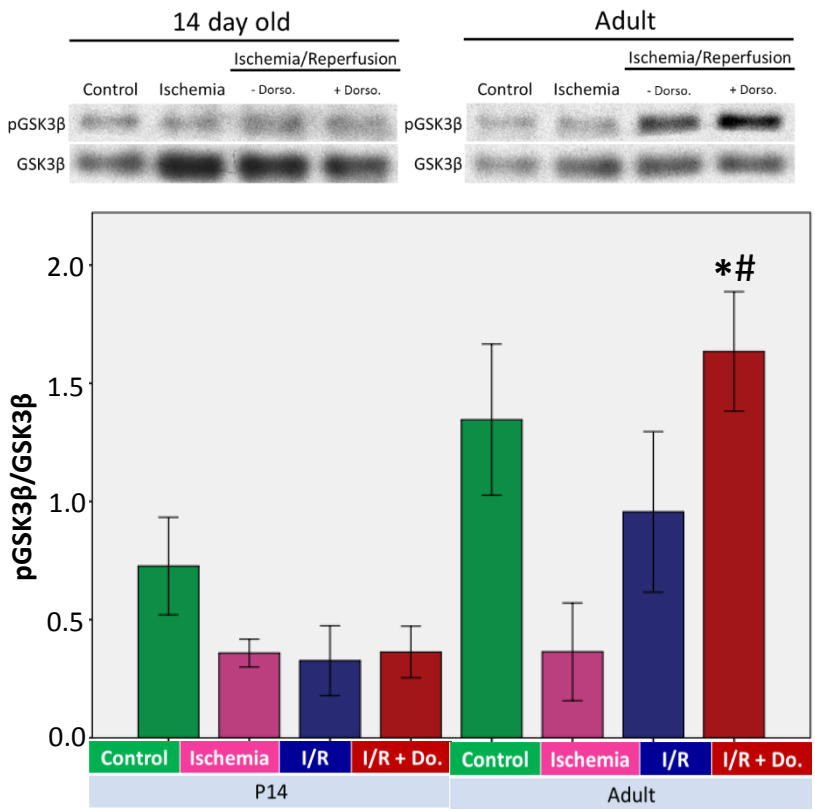

Figure 60. Effect of AMPK inhibition on pGSK3β/GSK3β. **(Top)** Representative western blot bands for each experimental and age group. **(Bottom)** Mean pGSK3β/GSK3β levels in 14-day old and adult rat either in control, following ischemia, I/R alone, or I/R + dorso. dihydrochloride treated groups. Data presented as mean ± SE (n = 3/group). Statistically significant difference in comparison with; * = corresponding 14-day old group ($p < 0.05$). # = Adult_Ischemia ($p < 0.05$).

Statistically significant differences in pGSK3β/GSK3β were seen only between dorsomorphin dihydrochloride treated adult hearts and dorsomorphin dihydrochloride treated 14-day old hearts ($p < 0.05$), as well as inhibitor treated adult hearts and adult hearts that had undergone ischemia alone ($p < 0.05$). As phosphorylation at Ser9 indicates inactivation of the protein, this suggests that AMPK inhibition results in the inhibition of GSK3β in adult hearts, but not 14-day old hearts. The importance of this will be discussed further in **Section 6.4.5**.

6.3.2.2.3.6 Effect of AMPK inhibition on BAX & BCL-2 expression

BAX and BCL-2 are commonly used measures of cell death and therefore indicators of the degree of cardiac injury. The expression and ratio of these two proteins was therefore analysed by western blot in order to identify any potential changes following the inhibition of AMPK. The data for BAX and BCL-2 as corrected by Ponceau S staining are shown below in **Figure 61** & **Figure 62** respectively. **Figure 63** shows representative examples of western blot bands for both proteins by age and experimental group, as well as a graphical representation of the mean BAX/BCL-2 ratios.

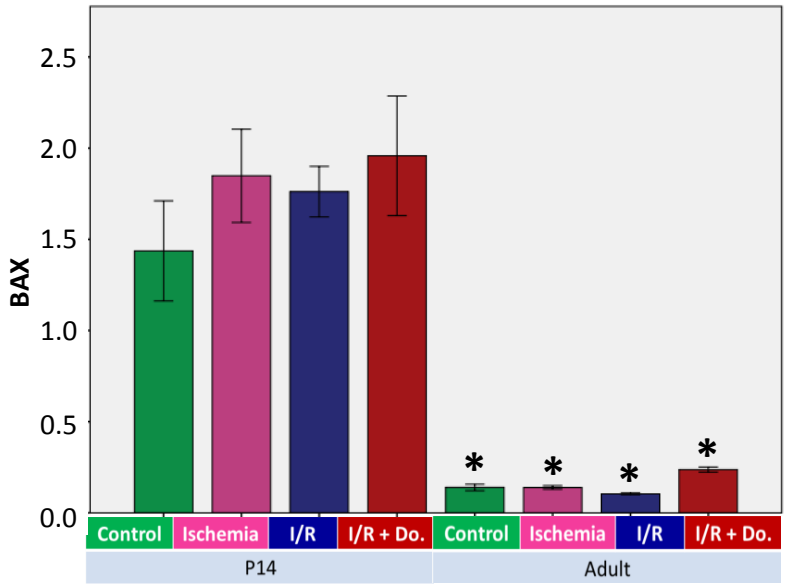

Figure 61. Mean BAX levels in 14-day old and adult rat hearts either in control, following ischemia, I/R, or I/R + dorsomorphin dihydrochloride treated groups. Data presented as mean ± SE (n = 3/group). * = statistically significant difference in comparison with corresponding 14-day old group ($p < 0.05$).

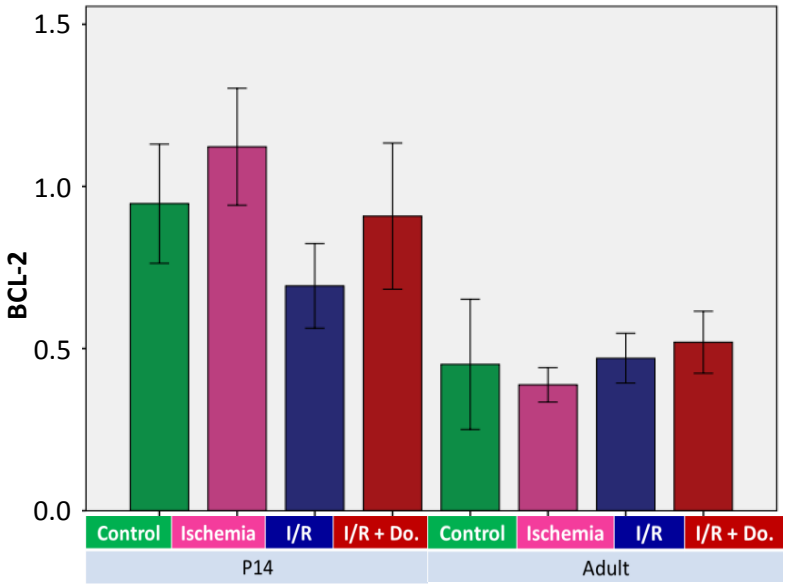

Figure 62. Mean BCL2 levels in 14-day old and adult rat hearts either in control, following ischemia, ischemia/reperfusion, or ischemia/reperfusion + dorsomorphin dihydrochloride treated groups. Data presented as mean ± SE (n = 3/group).

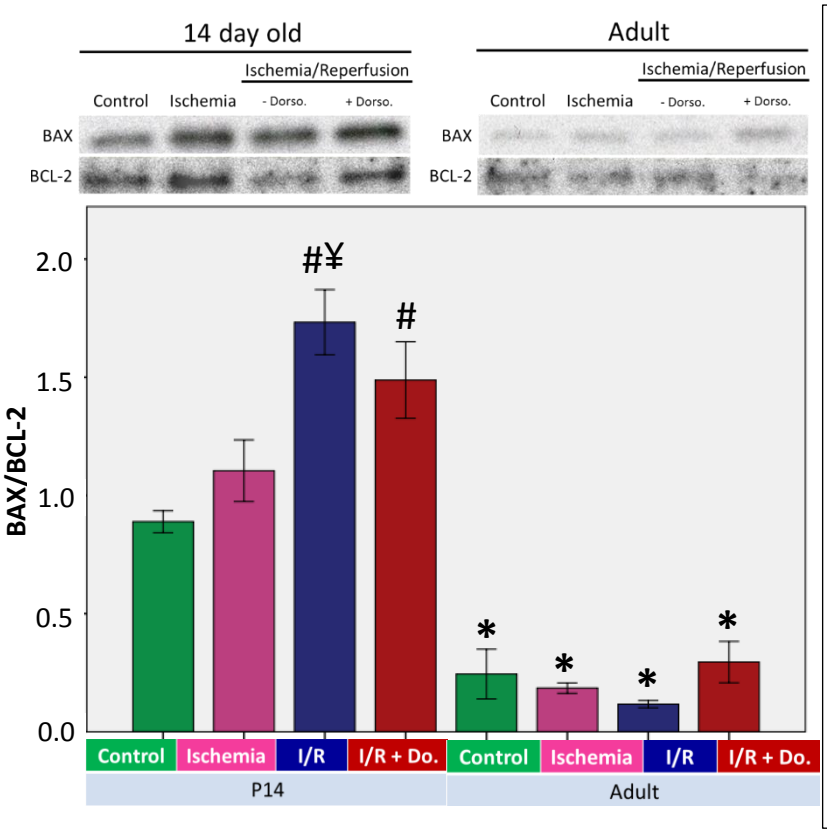

Figure 63. Effect of AMPK inhibition on BAX/BCL-2. **(Top)** Representative western blot bands for each experimental and age group. **(Bottom)** Mean BAX/BCL2 levels in 14-day old and adult rat either in control, following ischemia, I/R alone, or I/R + dorsomorphin dihydrochloride treated groups. Data presented as mean ± SE (n = 3/group). Statistically significant difference in comparison with; * = corresponding 14-day old group ($p < 0.05$). # = P14_Control ($p < 0.05$). ¥ = P14_Ischemia ($p < 0.05$).

Both BAX and BCL-2 expression, as well as BAX/BCL-2 ratio, were visibly greater in 14-day old samples than adult samples across all four experimental groups. Statistical significance was seen in BAX expression between all 14-day old experimental groups in comparison with all adult groups ($p < 0.05$), in addition to greater BAX/BCL-2 ratios in all 14-day old samples in comparison with their corresponding experimental group in adults ($p < 0.05$), i.e. P14_Control vs. Adult_Control. This greater expression of both proteins in 14-day olds was also seen in the proteomic output of control samples, and suggests that this overall higher expression of pro-apoptotic BAX and cardiotoxic higher BAX/BCL-2 ratio seen in all 14-day old groups in comparison with adults may not allude to a physiologically relevant to the response to ischemia and reperfusion and subsequent increased cardiac injury in this age group, as it is already seen in control, non-stressed hearts. This will be further discussed in **Section 6.4.6**.

Whilst no differences could be seen between the experimental groups in terms of BAX/BCL-2 levels in adult samples, which may result from overall low expression and weak bands of BAX and BCL-2 in these samples, 14-day old samples showed an expected higher pro-apoptotic BAX/BCL-2 level in samples from hearts that underwent I/R both with ($p < 0.05$) and without ($p < 0.01$) dorsomorphin dihydrochloride perfusion than control hearts. Hearts that underwent ischemia alone, however, showed no statistically significant increase in BAX/BCL-2 levels in comparison to control.

6.3.2.2.3.7 Effect of AMPK inhibition on Mfn1 expression

Mfn1 was identified in the proteomic output as showing an overall biphasic profile of expression during postnatal development, and is an important component of the mitochondrial fusion process (**Sections 7.3.4** & **7.1.2.3**). Due to the importance of mitochondrial fusion and fission in cardiomyocyte injury and cell death, in addition to Mfn1's biphasic pattern of expression, western blot analysis was undertaken in order to identify any changes in expression that occurred following inhibition of AMPK.

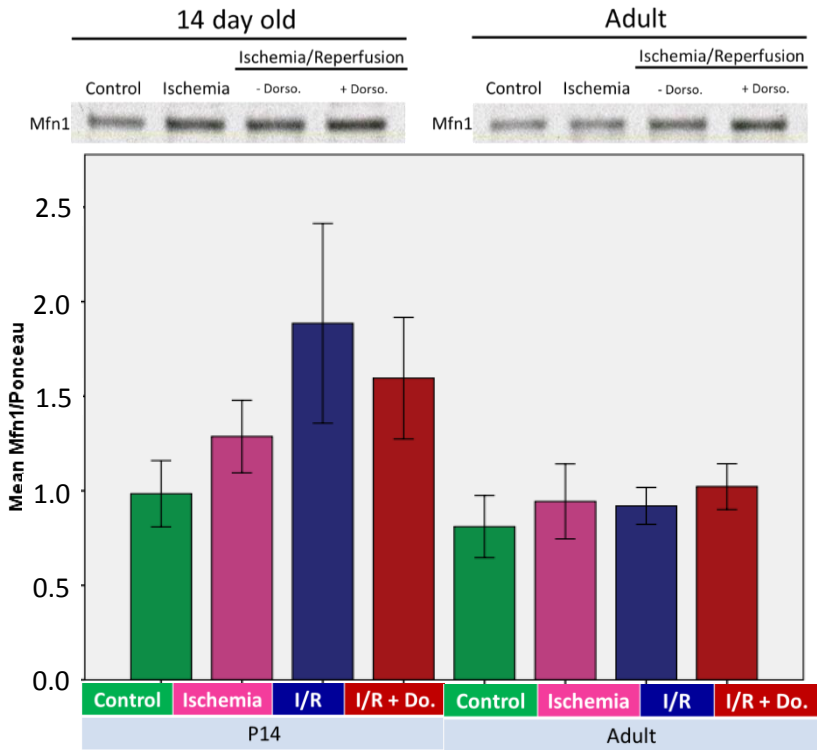

Figure 64. Effect of AMPK inhibition on Mfn1. **(Top)** Representative western blot bands for each experimental and age group. **(Bottom)** Mean Mfn1 levels in 14-day old and adult rats either in control, following ischemia, I/R alone, or I/R + dorsomorphin dihydrochloride treated groups. Data presented as mean ± SE (n = 3/group).

Whilst no statistically significant differences were seen in Mfn1 expression between either the experimental groups or age groups, bands were visually consistently weaker in the adult groups – as supported by the lower expression of Mfn1 in adult samples in the proteomic output (**Section 7.3.4**) – and also appeared to be weaker in the 14-day old control groups. The significance of this will be further discussed in **Section 6.4.7**.

6.4 Discussion

Initial studies into differences in the response to I/RI of Langendorff perfused 14-day old and adult hearts, using the measurement of creatine kinase (CK) release, found that, despite an initial peak at 1 minute of reperfusion, 14-day old hearts had statistically significantly lower levels of CK released over the course of reperfusion than adults. This was seen both using values for AUC, an indicator of total CK release, as well as with direct comparisons of CK concentration at each time point between the two age groups. Following the initial peak in CK release at 1 minute in 14-day olds, there was a subsequent decrease over the course of reperfusion, with levels returning to those seen pre-I/RI by approximately 10 minutes of reperfusion. In adults however, despite showing significantly lower levels of CK than 14-day olds at 1 minute of reperfusion, there was a subsequent increase in CK concentration peaking at approximately 5-10 minutes of reperfusion, remaining at this level for the duration of the reperfusion period. This indicates a greater degree of injury in adults than 14-day olds by the end of the reperfusion period, correlating both with the greater infarct size seen in adult control compared to 14-day old control hearts in subsequent TTC staining experiments (**Section 6.3.2.1.2** and **6.3.2.2.2**), as well as the greater resistance of 14-day olds to I/RI seen in the postnatal vulnerability profile (**Section 1.4.2**). The reason behind the initial peak in 14-day CK levels is uncertain, but may indicate an initial stress response at the

early stages of reperfusion which trigger survival signalling mechanisms in order to subsequently protect the heart from injury.

6.4.1 AMPK inhibition increased the vulnerability of 14-day old, but not adult hearts, to I/RI

Perfusion of whole hearts with AMPK inhibitor, dorsomorphin dihydrochloride, had no effect on the degree of cardiac injury in either age group when washed out prior to ischemia (**Section 6.3.2.1**). However, when left in hearts for the duration of ischemia, a statistically significant increase in infarct size was seen in 14-day old, but not adult hearts, in concordance with the age dependent differences on the effect of AMPK inhibition seen in isolated cardiomyocytes (**Section 5.3.3.1.3**). These findings therefore support the hypothesis that AMPK, which displayed a statistically significant biphasic peak in expression at 14-days of age in the proteomic output, may play a role in the resistance to ischemia/reperfusion injury seen in this age group. Due to the importance of AMPK activity to cardioprotection specifically during ischemia (**Section 1.5.3**), it is possible that the mechanism underlying the decreased vulnerability of 14-day old hearts to cardiac injury focuses upon signalling events that occur prior to reperfusion, priming the heart to reduce cell death upon the restoration of blood flow. The lower expression of AMPK in adult hearts may therefore reflect the lack of efficacy of AMPK inhibition in increasing infarction size in comparison with 14-day olds, as it does not play as important a role in cardioprotection in this age group.

However, creatine kinase levels showed no statistically significant changes in either age group following treatment with dorsomorphin dihydrochloride. It should be noted that the original creatine kinase experiments in **Section 6.3.1** were performed using a subsequently discontinued form of reagent (see **Section 2.1.1**), and subsequent creatine kinase

measurements (**Section 6.3.2**) were performed with a supposedly equivalent product (see **Section 2.1.1**) provided in smaller bottles. These bottle sizes meant that multiple bottles had to be made up for each round of measurements, and appeared to result in a greater variation in creatine kinase values than those seen with the original product. This may contribute to the lack of statistical significance seen. As a result of this, the determination of cardiac injury has focused on infarct sizes, as determined by TTC staining. However, previous studies have shown that dorsomorphin dihydrochloride does in fact result in the attenuation of cardioprotective methods through the inhibition of AMPK and AMPK-dependent autophagy in adult rat hearts (Kosuru, Cai et al. 2018, Zeng, He et al. 2018), in conflict with our data. This may be due to the fact that, in contrast to these studies, work in this project was conducted on hearts that had not undergone any other treatments or cardioprotective measures. Alternatively, it may result from the methodology of infarct determination used, as in this work, any areas not stained a brick red colour were measured as infarcted regions in order to be able to compare with 14-day old hearts, which do not tend to produce the clear white regions of infarcted tissue often reported, and instead a light pink, likely due to the resistance hearts of this age group have to ischemia/reperfusion injury. It is possible that measurements of the white regions of infarcted tissue alone may in fact show a significant difference in infarct size between control and dorsomorphin dihydrochloride treated hearts. Due to these difficulties in quantification and comparison between the two age groups, future work may benefit from expanding the determination of cardiac injury to include measurements of functionality, alternate assays for apoptosis, or other methods of histological staining.

6.4.2 AMPK inhibition does not cause significant changes in pAMPK expression

No statistically significantly significant changes in AMPK phosphorylation were seen following treatment with AMPK inhibitor, dorsomorphin dihydrochloride, between 14-day old and adult samples, or between samples taken at different experimental points. However, it is likely that this is due to expected variance and scatter resulting from the need to run samples on two separate gels. Indeed, as previously mentioned (**Section 6.3.2.2.3.1**), a clear difference in band intensity could be seen visually between experimental groups, supported by differences in the mean levels of pAMPK/AMPK, with lower levels of phosphorylated and thus active AMPK in dorsomorphin treated groups demonstrating successful inhibition of the protein and efficacy of the inhibitor. Moreover, a higher overall level of pAMPK/AMPK was seen in the 14-day old ischemic group in comparison with the reperfused group. This corresponds with the reported cardioprotective role of AMPK during ischemia specifically, and its damaging effects during reperfusion. Conversely, adult samples showed stronger bands for pAMPK in the reperfused group in comparison with samples taken from hearts that had undergone ischemia alone. This may suggest that these adult hearts display a pattern of AMPK activation over the course of ischemia and reperfusion that is actually detrimental to the heart and increases cardiac injury, whereas 14-day old hearts do in fact follow the cardioprotective process of AMPK activation. It is also possible that an additional pro-survival protein or proteins may act to promote activation of AMPK during ischemia, and subsequently deactivate it during reperfusion in 14-day old hearts.

6.4.3 AMPK inhibition does not cause significant changes in mTOR and AKT phosphorylation levels

While no statistically significant differences were seen in pmTOR/mTOR levels between any of the experimental or age groups, clear differences could be seen in band intensities between these groups. Notably, adult samples showed no detectable mTOR or pmTOR bands, except for in hearts treated with dorsomorphin dihydrochloride. The absence of detectable bands in the control, post-ischemic, and I/R groups of adult hearts could relate to the fact that proteomic analysis indicated low levels of mTOR expression in adults, especially compared to 14-day olds, coupled with the fact that successful detection of both the total and phosphorylated forms of the protein in these western blot experiments was difficult, requiring long exposure times and often producing high levels of background. Indeed, antibody reviews from the manufacturer's (CST) website discussed difficulties in obtaining bands when loading 20 µg of protein, only detecting clear bands when using 30 µg of protein. However, these factors do not account for the fact that treatment with dorsomorphin dihydrochloride appeared to increase the actual expression of mTOR, with detectable bands only in these treated hearts. While AMPK is known to inhibit mTOR activity via phosphorylation of its mTORC1 binding partners (Shaw 2009), the ability of AMPK to effect mTOR expression is uncertain. However, studies have demonstrated that inhibition of AMPK in the context of tumour cells – where its antagonism of mTOR activity is again a critical component of suppressing tumour cell growth – does in fact result in alterations in the gene expression of a range of proteins, indicating an important role for AMPK in transcription (Zhou et al. 2009). It is therefore possible that AMPK has an inhibitory role on mTOR gene expression in adult rat hearts that is alleviated upon AMPK inhibition with dorsomorphin dihydrochloride.

As mentioned in **Section 6.3.2.2.3.2**, pmTOR bands were visually much stronger in samples taken from hearts that had undergone AMPK inhibition throughout ischemia. Most notably, protein bands were detected very faintly if at all in control, ischemia and I/R groups, but showed clear bands in dorsomorphin dihydrochloride treated groups. This is concordant with the fact that AMPK is a known inhibitor of the mTORC1 complex, of which mTOR is a key component, in order to promote cellular energy conserving processes such as autophagy and thus increase ATP availability, leading to reduced cardiac injury during ischemia (Moussa and Li 2012). While AMPK is not reported to directly interact with mTOR itself, it is known to phosphorylate other members of the mTORC1 signalling pathway, including mTORC1 inhibitor TSC2 (Gwinn and Shaw 2010) and mTOR binding partner, Raptor (Shaw 2009). The phospho-site, Ser2481, targeted by western blotting in **Section 6.3.2.2.3.2** is an autophosphorylation site commonly used to demonstrate an intact mTOR signalling pathway, meaning the greater levels of pmTOR/mTOR in AMPK inhibited hearts may represent an alleviation of AMPK-mediated inhibition of mTOR and mTORC1 activity. However, this difference was not as distinct between 14-day old experimental groups, with bands for pmTOR & mTOR detectable in all four experimental groups, and the mean levels of pmTOR/mTOR displaying no clear trends across the four experimental groups. As previously mentioned, this may result from the large scatter of data points due to the running of samples on separate gels, as visually stronger bands were seen in AMPK inhibited hearts in a similar manner to adult samples. It is also important to note that blots using these pmTOR and mTOR antibodies (**Section 2.1.2**) consistently presented with non-specific bands and high levels of background noise, meaning the accuracy of measured band intensities may also have been negatively affected by the quality of the blots themselves.

Conversely to AMPK, Akt is a known activator of mTOR and mTORC1 signalling through the phosphorylation and inactivation of mTOR inhibitors TSC2 and PRAS40 (Hahn-Windgassen, Nogueira et al. 2005), and through promotion of IKKα-mediated phosphorylation and activation of mTOR (Dan, Ebbs et al. 2014). Again, contrary to AMPK, Akt has been shown to work during reperfusion as opposed to ischemia, inhibiting "deleterious autophagy" (Panisello-Roselló, Lopez et al. 2018) and subsequent apoptosis via activation of mTORC1 during this stage of I/RI, conferring cardioprotection. This role of AKT would therefore suggest that changes in pAkt/Akt levels would correlate with pmTOR/mTOR following inhibition of AMPK. However, our data showed that pAkt/Akt was greater in 14-day old hearts treated with dorsomorphin dihydrochloride, whereas there was no clear difference in adult dorsomorphin dihydrochloride treated hearts in comparison to the other experimental groups, contrasting the trends seen in pmTOR/mTOR levels. The importance of this remains uncertain, as despite these overall trends in differences in phosphorylation state were seen, with visually clear differences in band intensities between these groups, no statistically significant difference was seen in pAkt/Akt expression, again likely due to the large scatter resulting from the need to separate the samples into two gels.

Studies have traditionally reported opposing mechanisms of cardioprotection by AMPK and Akt dependent on the phase of I/RI during which they are active, in addition to reports that Akt actually functions to inhibit AMPK via phosphorylation of its α1 subunit at Ser458 and its α2 subunit at Ser491 with subsequent inhibition of AMPK-activating phosphorylation at Thr172 (Qi and Young 2015). However, recent studies investigating the underlying signalling mechanisms of cardioprotective compounds such as PLCA and activation of the κ-opioid receptor have shown that AMPK and Akt are actually both activated and work synergistically in order to confer cardioprotection (Lee, Ku et al. 2015, Zhang, Zhou et al. 2018). It is possible

that the greater levels of pAkt/Akt in 14-day old dorsomorphin dihydrochloride treated hearts may reflect an attempt to compensate for inhibition of AMPK. Further work will be needed to examine the full mechanisms and interactions between AMPK and Akt specifically during cardiac I/RI, as existing publications often discuss conflicting reports as to whether these two proteins work upstream or downstream of one another (Qi and Young 2015, Zhang, Zhou et al. 2018), as well as whether they function synergistically or during different phases of I/RI in order to confer cardioprotection (Lee, Ku et al. 2015, Panisello-Roselló, Lopez et al. 2018).

Finally, it is important to note that previously published work has in fact shown that dorsomorphin dihydrochloride actually inhibits Akt and mTOR, inducing autophagy in treated cells despite inhibition of AMPK (Vucicevic, Misirkic et al. 2011, Liu, Chhipa et al. 2014), which appears to directly contradict our findings. However, these studies were all conducted in cancer cell lines, meaning tissue and cell-type specific differences may account for the contrasting effects of dorsomorphin dihydrochloride on Akt and mTOR activation.

6.4.4 AMPK inhibition does not cause significant changes in PKCε phosphorylation

Similar to AMPK, mTOR and Akt, the levels of pPKCε/PKCε did not show any statistically significant changes following AMPK inhibition, nor between the other experimental or age groups. However, some clear differences could be identified between the experimental and age groups based on their means. For example, levels of phosphorylated PKCε appeared to be greater in 14-day old hearts following I/R than adult hearts following I/R, which correlates with the cardioprotective role of PKCε and the greater resistance of 14-day old hearts to I/RI than adults. pPKCε expression also appeared to be greater in adult hearts treated with

dorsomorphin dihydrochloride than the other three adult experimental groups. This apparent increase in active PKCε in AMPK inhibited groups is somewhat unexpected, as PKCε is reported to function upstream as an activator of AMPK, for example, during IpreC ((Jackson, Escobar et al. 2018)(Nishino et al., 2004)), and would therefore be unaffected by AMPK inhibition. The reason for this apparent increase is therefore uncertain, but may suggest a mechanism by which there is an increase in PKCε activity as an attempt to compensate for the loss of AMPK activity. Further investigation of this issue will be required in future work in order to elucidate the reason for these differences, as well as to examine changes in the localisation of PKCε within the cell.

6.4.5 AMPK inhibition induces changes in GSK3β phosphorylation only in adult hearts

Inhibition of AMPK resulted in statistically significant differences in pGSK3β/GSK3β levels only in adult hearts, with dorsomorphin dihydrochloride treated hearts showing significantly higher levels of pGSK3β/GSK3β in comparison with dorsomorphin dihydrochloride treated 14-day old hearts, as well as in comparison with adult hearts that had undergone ischemia alone. As the phosphosite examined by these western blotting experiments (Ser9) is known to indicate an inactive form of the protein (Lal, Ahmad et al. 2015), it is possible that this indicates a mechanism by which inhibition of AMPK inhibition results in a correlating inhibition of GSK3β in adult, but not 14-day old hearts. While 14-day old hearts did show a statistically significant increase in infarct size following dorsomorphin dihydrochloride treatment not seen in adult hearts, the overall infarct size did remain significantly lower in both control and inhibitor treated 14-day old hearts in comparison with adults (**Section 5.3.2.1.2**). The activity of both AMPK and GSK3β are reported to be cardioprotective during

ischemia via inhibition of mTORC1 (Gwinn and Shaw 2010), which may suggest that, while AMPK is an important protein in mediating cardioprotection in 14-day old hearts, activation of GSK3β may in fact help to compensate for the loss of AMPK-induced autophagy during ischemia, maintaining the relatively low infarct sizes seen in this age group in comparison with adult hearts. This correlates with previous experiments looking at the inhibition of GSK3β in isolated cardiomyocytes (**Section 5.3.2.1.2**), in which cardiomyocyte viability was only decreased by TWS119 treatment in 14-day old hearts, with adults showing no change in viability. This highlights the importance of GSK3β to cardioprotection in 14-day old hearts, and therefore may support a potential mechanism by which it works synergistically with AMPK in this age group. The significantly higher levels of phosphorylated and inactivated GSK3β in dorsomorphin dihydrochloride treated adult hearts compared to 14-day old hearts may indicate that any potential compensatory activity is not present in this age group, or that in adult hearts, AMPK may in fact have an activating role that is lost following dorsomorphin treatment, leading to the greater levels of Ser9 phosphorylation. Notably, phosphorylated Akt – which is known to phosphorylate and thus inhibit GSK3β at Ser9 – did not appear to be significantly higher in adult hearts treated with dorsomorphin dihydrochloride (**Section 6.3.2.2.3.3**), indicating the higher levels of Ser9 phosphorylation in this group did not result from greater Akt activity. Conversely, PKCε phosphorylation did appear to be higher in adult hearts following AMPK inhibition, which was not seen in 14-day old hearts, which may suggest that greater PKCε activity in this group resulted in increased phosphorylation of GSK3β. Indeed, previous work has stated that PKCε works upstream of GSK3β in a complimentary manner to Akt (Hunter et al. 2007). However, these relationships are currently only correlative, and further work will be needed in order to establish whether they do indeed represent a novel mechanism by which GSK3β remains active in the absence

of AMPK activity only in 14-day old hearts, or whether it merely pertains to the fact that phosphorylation and inactivation of GSK3β at Ser9 by Akt during reperfusion has previously been shown to be cardioprotective (Lal, Ahmad et al. 2015), alongside the correlating lack of a statistically significant increase in infarct size in adult hearts following dorsomorphin dihydrochloride treatment.

6.4.6 BAX expression and BAX/BCL-2 was higher in 14-day olds compared to adults

BAX expression was found to be statistically significantly greater in 14-day old samples from all four experimental groups in comparison with corresponding adult groups, a trend that was also seen in the proteomic output from control hearts. BCL-2 expression showed no statistically significant differences between any age or experimental groups, but had clearly stronger bands in all four 14-day old experimental groups in comparison with adults. As could be seen in the representative blots presented in **Section 6.3.2.2.3.6**, the BCL-2 antibody was relatively weak, producing a high degree of background that may have affected the accuracy of these measurements. As with previously discussed proteins, these samples were run on two separate gels, which likely further affected the accuracy of these measurements and contributed to the scatter of data points seen for BCL-2.

A commonly used measure of cardiac injury and cell death is the ratio of BAX/BCL-2 to indicate the relative levels of pro-apoptotic to pro-survival protein. Western blotting showed that all four experimental groups had statistically significantly greater levels of BAX/BCL-2 in 14-day olds in comparison with their corresponding adult groups. Whilst no significant differences were seen between adult experimental groups, 14-day old samples showed greater levels of BAX/BCL-2 in both hearts that underwent I/R alone and in hearts that

underwent I/R with the addition of AMPK inhibition compared to control hearts. Furthermore, hearts that underwent I/R alone also showed statistically significantly higher levels of BAX/BCL-2 in comparison with hearts that had undergone ischemia alone. These differences in comparison with both control and ischemic hearts correlates with the fact that the majority of cardiac injury and cell death is triggered upon reperfusion. The lack of difference between adult experimental groups appears to contradict the large infarct sizes seen in adult hearts following I/RI, but may once again relate more to the methodology and quality of the bands produced, as both BAX and BCL-2 bands were very weak in adult samples, with high degrees of background for BCL-2 in particular. This may also explain the lack of statistically significant differences in BAX/BCL-2 between I/R alone and I/R with dorsomorphin dihydrochloride treatment, despite significantly higher percentage infarct sizes in dorsomorphin dihydrochloride treated hearts in 14-day olds.

Whilst high BAX expression and BAX/BCL-2 levels are traditionally used as indicators of cell death and cardiac injury (Shen, Zhou et al. 2017, Liu 2018), our data have shown that in both proteomic analysis and western blotting, control levels of BAX expression and BAX/BCL-2 are already elevated in 14-day old hearts with statistical significance in comparison with adult hearts. Previous work by Liaw et al. (2013) showed a similar change in the expression of BAX, BCL-2 and BAX/BCL-2 levels from neonatal to adult hearts that correlates with biphasic changes in resistance to I/RI. Whilst the authors also noted these paradoxically high levels of BAX in 14-day old hearts with the greatest resistance to cardiac injury, they suggested that this is merely balanced out by correlating high levels of BCL-2 (Liaw, Hoe et al. 2013). However, in both data presented by Liaw et al. and data presented in this work, adult hearts were found to show significantly lower levels of both BAX and BAX/BCL-2 than 14-day old

hearts. The reason behind these greater levels of pro-apoptotic protein even in control hearts is uncertain, possibly suggesting an alternate mechanism by which BAX primes the immature heart for I/RI, and will require further investigation. Future work may benefit from examining any differences in 14-day old BAX and BAX/BCL-2 levels compared to adult samples using alternate assays in order to confirm this significantly higher level present in control hearts is consistent across several different methodologies.

6.4.7 AMPK inhibition does not alter Mfn1 expression

No statistically significant differences were seen in the expression of Mfn1 between the two age groups or four experimental groups. However, western blotting bands showed visually stronger Mfn1 bands in 14-day old samples, with proteomic analysis showing a similarly higher expression of Mfn1 in 14-day old hearts compared to adults (**Section 6.3.6**). Control hearts also appeared to display weaker bands than both hearts undergoing I/R and I/R with dorsomorphin dihydrochloride treatment in particular, a trend that appeared to be stronger in 14-day old samples than adult samples. Skewing of the balance between mitochondrial fusion and fission towards fusion is known to be cardioprotective (Ong, Kalkhoran et al. 2015), with overexpression of fusion proteins Mfn1 and Mfn2 in cardiac cell lines that have undergone simulated I/RI resulting in reduced cell death, and an associated inhibition of mPTP opening (Ong, Subrayan et al. 2010). Whilst the higher expression of Mfn1 seen in 14-day old hearts both in proteomic and western blot analysis correlate with the reported cardioprotective effects of mitochondrial fusion and Mfn1 overexpression, no clear difference was seen in hearts treated with an AMPK inhibitor. It is therefore unlikely that any cardioprotective mechanisms provided to 14-day old hearts by AMPK involve direct effects on mitochondrial fusion or Mfn1.

6.4.8 Summary & Conclusion

Inhibition of AMPK showed significant effects on cardiac infarct size in 14-day old, but not adult hearts, and only when inhibition was sustained throughout ischemia. These findings support the hypothesis that the biphasic peak in expression of AMPK at 14-days of age in the proteomic output reflects a key role of the protein in the mechanism that confers greatest resistance to I/RI to 14-day old hearts. The lack of such an effect in hearts that underwent AMPK inhibitor pre-treatment, with washout of the drug prior to ischemia, highlights the importance of AMPK activity specifically during ischemia, and correlates with previous reports of its cardioprotective function (**Section 1.5.3**). Whilst western blot analysis did not identify any statistically significant changes in related survival signalling proteins, overall trends and visible differences in band intensities were present, and it is likely that the lack of significance was due to experimental limitations in the number of samples that could be run concurrently. These data implicate AMPK as a potentially causal protein to the biphasic cardiac vulnerability profile seen in rat hearts, and therefore highlight it as a target for future research and investigation.

Having identified AMPK and a number of other survival signalling related proteins as biphasically expressed during postnatal development, and therefore potentially linked to the mechanism underlying the biphasic pattern of cardiac resistance to I/RI in rat hearts, the next section of work looks to identify any correlating changes in other survival signalling related structures. To do this, differences in the morphology of mitochondria – a critical end target of survival signalling pathways – and their response to I/RI in 14-day old and adult hearts will be examined, as well as any differences in other structures linked to survival signalling, such as caveolae and MVBs.

Chapter 7: Structural cardiac differences during development: implications for cardioprotection

7.1 Introduction

Thus far, the first four aims of this work have been addressed, with the identification of proteins showing biphasic patterns of expression during postnatal development, as well as testing the effects of targeted inhibition of such proteins during I/RI and the effect of this on the expression of other survival signalling related proteins. This chapter therefore focuses on the fifth aim:

To identify differences in cardiomyocyte structure and ultrastructure that may influence the response to I/RI at different stages of development, including:

iv. blood vessel dimensions, cardiomyocyte hypertrophy and sarcomere lengths

v. caveolae, multivesicular body (MVB) and exosome abundance

vi. mitochondrial subpopulation morphology and distribution

These changes will be investigated for specific comparison of 14-day old with adult hearts in order to address this fifth aim, and to provide data on control hearts with which to make comparisons with post-ischemic and post-I/R hearts for the sixth aim (**Chapter 8**).

7.1.1 Key cardiac structures implicated in survival signalling

As discussed in **Chapter 1**, multiple changes occur in the structure of cardiac tissue over the course of postnatal development. This includes growth via hypertrophy of existing myocytes as opposed to growth via hyperplasia over the course of development (**Section 1.2**), with an associated switch from dependence on extracellular sources in early stages of development – for example, a reliance on Ca^{2+} influx via the NCX – to intracellular sources in adult cardiomyocytes – for example, Ca^{2+}-cycling dependent on SR. The development of cardiac t-

tubules during postnatal development are understood to facilitate signalling to inner regions of the cardiomyocyte as hypertrophic growth occurs (Hong and Shaw 2017), and perfusion to these regions from extracellular sources is no longer as effective as it is in the smaller and narrower cells seen in early stages of development. However, it is possible that these changes in cardiomyocyte morphology also leave them more vulnerable to ischemic insult, as blood supply and the perfusion of nutrients and signalling molecules to and throughout cells may be decreased as a result of this hypertrophy. We therefore examined the characteristics of blood vessels in 14-day old and adult hearts, as well as the morphology of isolated cardiomyocytes from different age groups, in order to determine whether hypertrophic changes are accompanied by an associated increase in blood vessel sizes to support the greater supply needs of the adult myocardium.

7.1.2 Key cardiac ultra-structures implicated in survival signalling

7.1.2.1 Caveolae

Caveolin-1, -2 and -3 were all found to show biphasic profiles of expression during postnatal development in the proteomic output (**Section 4.3.1**), peaking at 14-days of age. As discussed in **Section 4.4.2**, these proteins play an important role in cardioprotection, in addition to being important components of the structure of the membrane subcompartments, caveolae (Couet, Belanger et al. 2001). Caveolae play important roles in cell signalling, both through the roles of Caveolins – which are able to interact with other intracellular signalling molecules to promote cell survival (Sharma et al. 2011, Das, Gherghiceanu et al. 2008) as well as cardioprotective autophagy during ischemia (Kassan et al. 2016) – and through their own ability to compartmentalise and localise key proteins for rapid signal transduction (Lisanti, Scherer et al. 1994). As a result, these structures were

identified in electron micrographs obtained from 14-day old and adult samples (**Section 7.2.3**) in order to compare their abundance between the two age groups, as well as with samples that have undergone ischemia (**Chapter 8**).

7.1.2.2 Exosomes and MVBs

Exosomes, transported in MVBs (**Figure 65**), have been reported to carry a number of microRNAs, signalling molecules and Heat Shock Proteins (HSP) known to promote cardiac survival (Waldenstrom and Ronquist 2014). In particular, research has demonstrated that exosomes trigger protective signalling and reduced cell death through HSP70 carried by exosomes, which in turn activate ERK and p38MAPK via TLR4, resulting in HSP27 phosphorylation and subsequent cardioprotection in rat models of I/RI (Vicencio, Yellon et al. 2015). Due to the apparent importance of these structures in promoting cell survival following I/RI, electron micrographs were checked for the presence and abundance of putative MVBs, in order to identify any differences between 14-day old and adult samples that may reflect differences in cardiac vulnerability to injury between these two age groups. Moreover, the proteomic output was analysed for the presence of commonly used exosome markers, as well as for proteins comprising their signalling pathways.

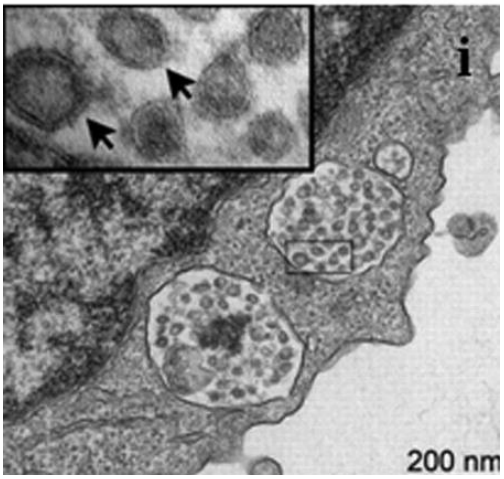

Figure 65. Electron micrograph examples of MVBs containing exosomes (marked with arrows) (image taken from (Sahoo, Klychko et al. 2011))

It should be noted that identification of such vesicles and distinguishing them from other similar structures, such as caveolae and autophagosomes, was difficult when using electron micrographs alone. Due to the visual similarities between such structures, other studies have reported using additional methods such as staining for specific markers of these vesicles in order to definitively and correctly identify them, an additional step that will be necessary in our future work.

7.1.2.3 Mitochondria

In comparison with the typical morphology of mitochondria in control hearts (**Figure 7**, **Section 1.6**), those that have undergone the fusion process possess a much more elongated morphology, whereas those that have undergone fission appear much more fragmented and rounded (**Figure 66**).

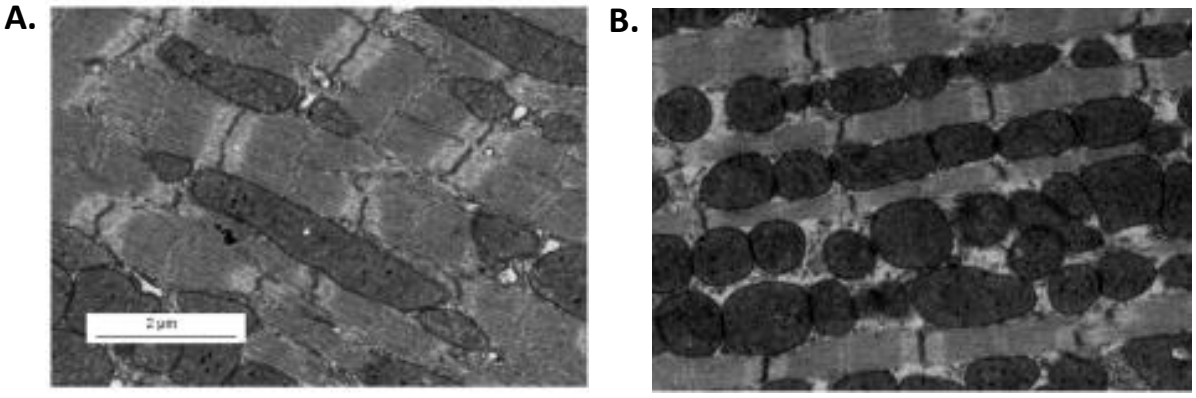

Figure 66. Electron micrograph examples of A. elongated mitochondria characteristic of fusion, and B. fragmented and round mitochondria indicative of fission (following 20 minutes of ischemia). (image taken from (Ong and Hausenloy 2010))

Mitochondrial fusion proteins – Mfn1, Mfn2 and Opa1 – and fission proteins – Drp1 and Fis1 – play central roles in mitochondrial morphology, allowing the switch from elongated networks of mitochondria to the more fragmented phenotype that arises following fission (Ong and Hausenloy 2010). As mentioned in **Section 6.4.7**, skewing the balance between

mitochondrial fusion and fission towards fusion is known to be cardioprotective (Ong, Kalkhoran et al. 2015), with the overexpression of proteins such as Mfn1 and Mfn2 that promote mitochondrial fusion resulting in reduced cell death, and an associated inhibition of mPTP opening (Ong, Subrayan et al. 2010). Furthermore, it has been demonstrated that cellular stress can trigger 'hyperfusion' in order to provide a protective response and reduce injury, requiring Opa1 and Mfn1, and correlating with the increased production of mitochondrial ATP in order to deliver resistance to cellular stress (Tondera, Grandemange et al. 2009). Conversely, excessive mitochondrial fission has been shown to result in the production of unhealthy fragmented mitochondria with reduced function, greater susceptibility to mPTP opening, and subsequent increased cell death (Maneechote, Palee et al. 2017). Studies that have employed inhibitors of fission protein Drp1 in the context of I/RI demonstrated that prevention of its activation resulted in the reduction of mitochondrial fragmentation and swelling, and the prevention of cardiomyocyte death, as well as the reduction of mitochondrial ROS and improvement of LV developed pressure in Langendorff perfused hearts (Sharp, Fang et al. 2014).

Due to the importance of mitochondria as the end target of the RISK-SAFE signalling pathways, the functional differences between the three mitochondrial subpopulations (**Section 1.6**), and the cardioprotective roles of fusion proteins, electron micrographs from 14-day old and adult hearts were used to analyse any potential differences in morphology between the two age groups, as well as any differences in the relative abundance of each mitochondrial subpopulation. Additionally, proteomic data (described in **Chapter 4**) was used to identify any differences in the expression of fusion and fission proteins.

7.2 Materials & Methods

7.2.1 Histology

The full methodology of histological sample preparation and analysis has been described in **Section 2.7.1**. To summarise, hearts from 14-day old (n = 4), 28-day old (n = 5), and adult (n = 5) rats were flushed with Krebs-Henseleit buffer and cut to remove the apex and any excess tissue. The remaining heart sections were placed into tubes of fixative solution for 24 hours, before washing with phosphate buffer and processing. This involved dehydrating the tissue to allow the infiltration of paraffin wax. Processed tissue was then embedded in paraffin wax and placed onto an ice block to solidify the wax. Tissue was then sectioned to a thickness of 5µm and mounted onto a microscope slide. These slides were then left overnight to dry out in a 37°C oven, before staining for blood vessels with Elastic Van Gieson. Images were taken and analysed to obtain measurements for the largest vein and artery present as a complete cross-section in each region of the heart (left ventricle, right ventricle and interventricular septum), for comparison of the size of the largest vessels by age group and localisation.

7.2.2 Cardiomyocyte isolation & cell size determination

A sample of cardiomyocytes isolated in **Section 5.3.1** were taken for the measurement of their widths and lengths, in order to compare the average dimensions of cells between the three age groups – 14-day old (n = 3 hearts and 60 cells), 28-day old (n = 4 hearts and 52 cells) and adults (n = 3 hearts and 97 cells). These sizes were measured using a light microscope with a grid-lined slide. Each cell length and width were measured by the number of squares spanned on the grid, and converted from this number into an actual size in micrometres using the scale 1 square = 0.01mm.

7.2.3 Electron microscopy

The full methodology for preparation and analysis of electron micrographs has been described in **Section 2.7.2**. To summarise, hearts were removed from 14-day old (n = 3) and adult (n = 3) rats and placed directly into ice cold cardioplegic solution, before cannulation via the aorta and perfusion with cardioplegia. This was then repeated with EM fixative solution, following which hearts were cut into small cubes taken from the left ventricular wall, left in the fridge overnight in fixative, and transferred into phosphate buffer to be sent for processing. Images were taken in several regions of each heart at a range of magnifications, from which measurements of mitochondrial area, length, width, as well as the area of cardiomyocyte covered, were taken for each of the three mitochondrial subpopulations. These images were also analysed for the length of sarcomeres, abundance of caveolae, and abundance of putative exosome containing MVBs.

7.2.4 Proteomic Analysis

The full process of proteomic and phosphoproteomic analysis has been described in **Section 2.4.3** and **4.2.2**. From the proteomic output described in **Chapter 4**, with samples from 7-day old (n = 4), 14-day old (n = 8), 28-day old (n = 8) and adult (n = 7) rats, proteins involved in mitochondrial fusion and fission, as well as those linked to exosome signalling or as exosome markers, were extracted. These proteins were then analysed for any statistically significant differences in expression between the four age groups.

7.3 Results

7.3.1 Cardiac structural changes during postnatal development

Hearts from three age groups, 14-day olds (n = 4), 28-day olds (n = 5), and adult (n = 5), were extracted from rats, and processed for histology as outlined in **Section 2.4.1.** The slides produced were analysed, locating the largest veins and arteries in each section of the heart (right ventricle RV, left ventricle LV and interventricular septum IVS), and taking the dimensions and area for each. Representative examples of the largest vessels are given in **Figure 67** & **68** below.

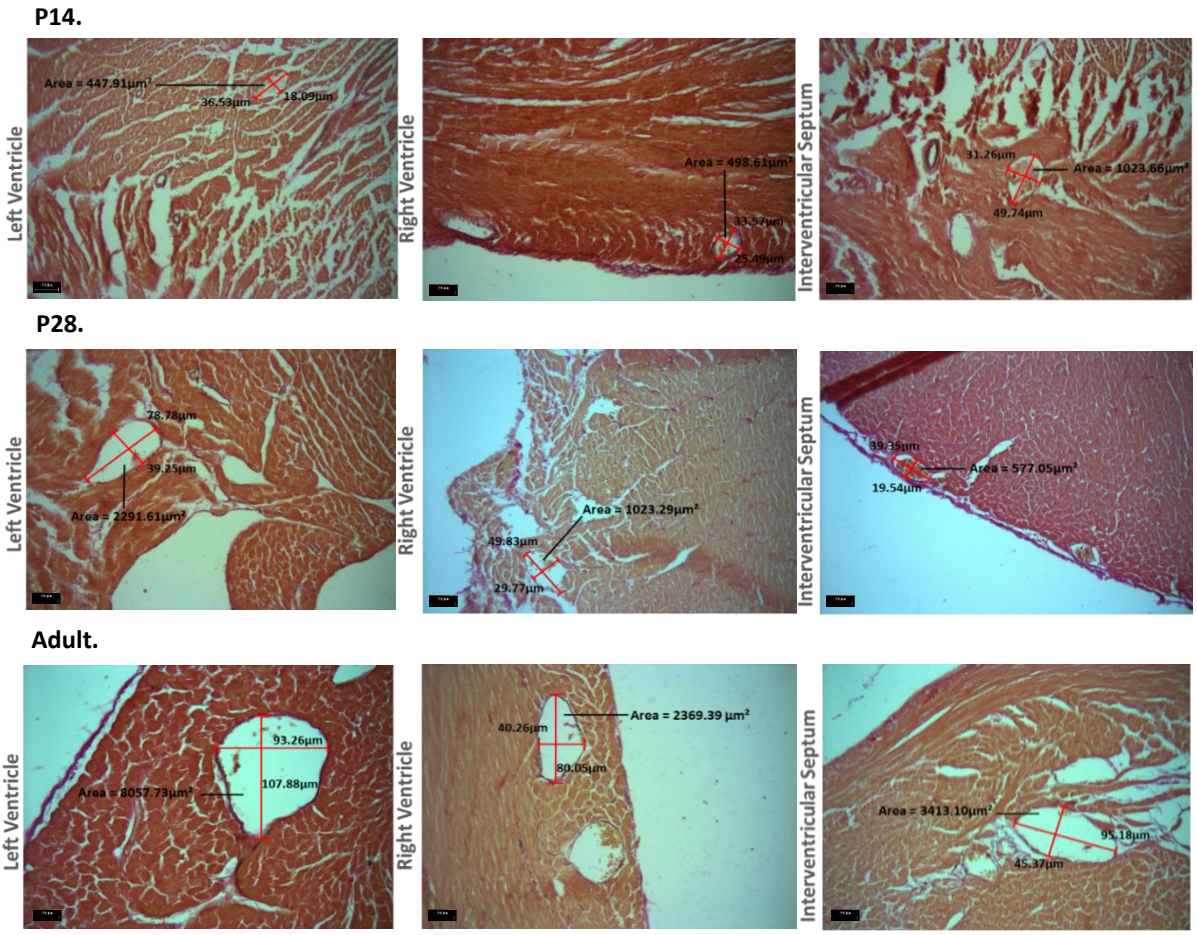

Figure 67. Examples of large veins in each section of the heart by age, labelled for width and length, as well as area in micrometres.

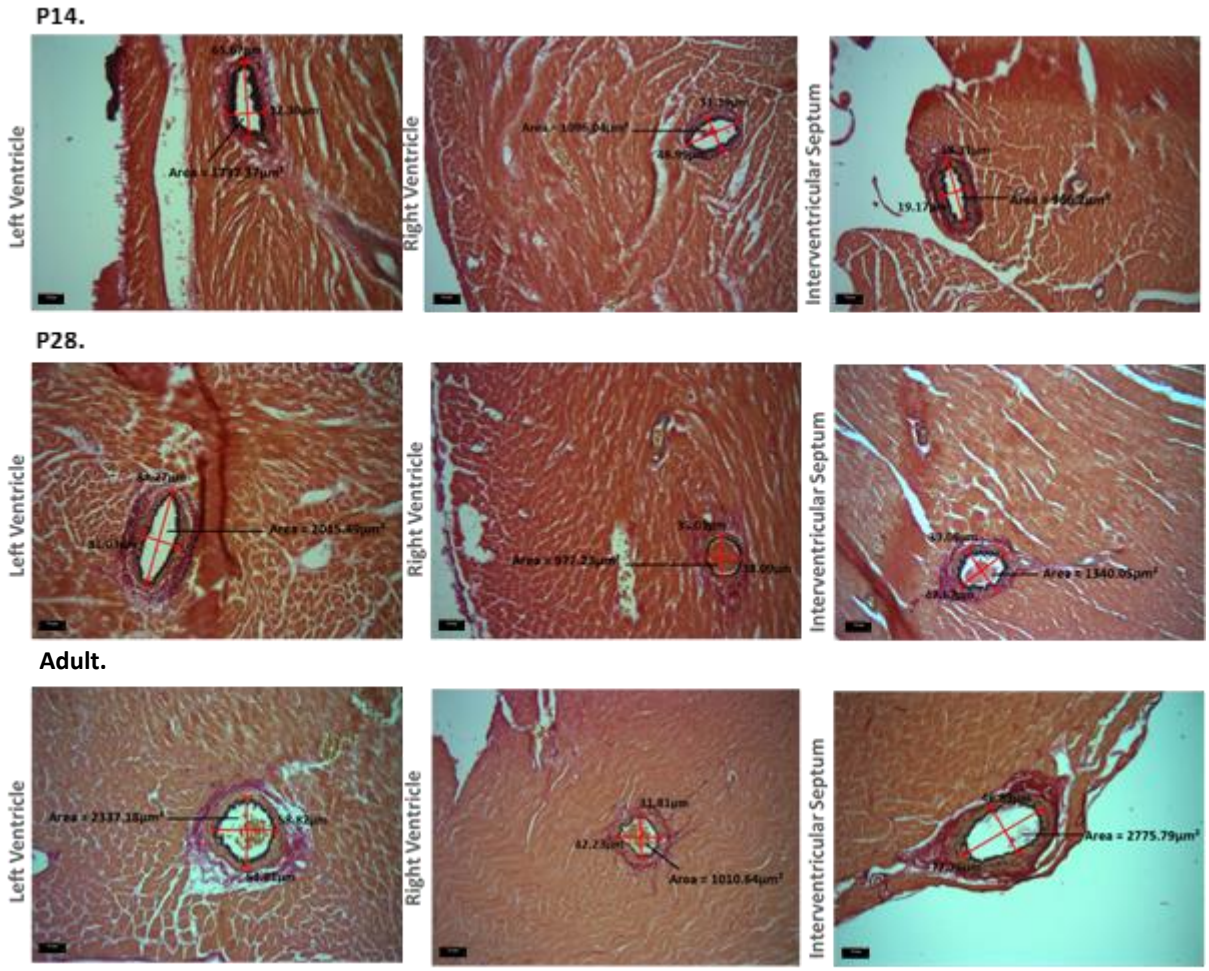

Figure 68. Examples of large arteries in each section of the heart by age, labelled for width and length of the elastic vessel wall, as well as area in micrometres.

The areas of the largest veins in different regions of the heart were measured and the data shown in **Figure 69A**. **Figures 69B & 69C** show the areas of the largest arteries in each region of the heart, as well as the areas of their corresponding lumen. Comparison of these vessel sizes found no statistically significant difference between the three age groups in neither veins, arteries, nor the area of the arterial wall itself.

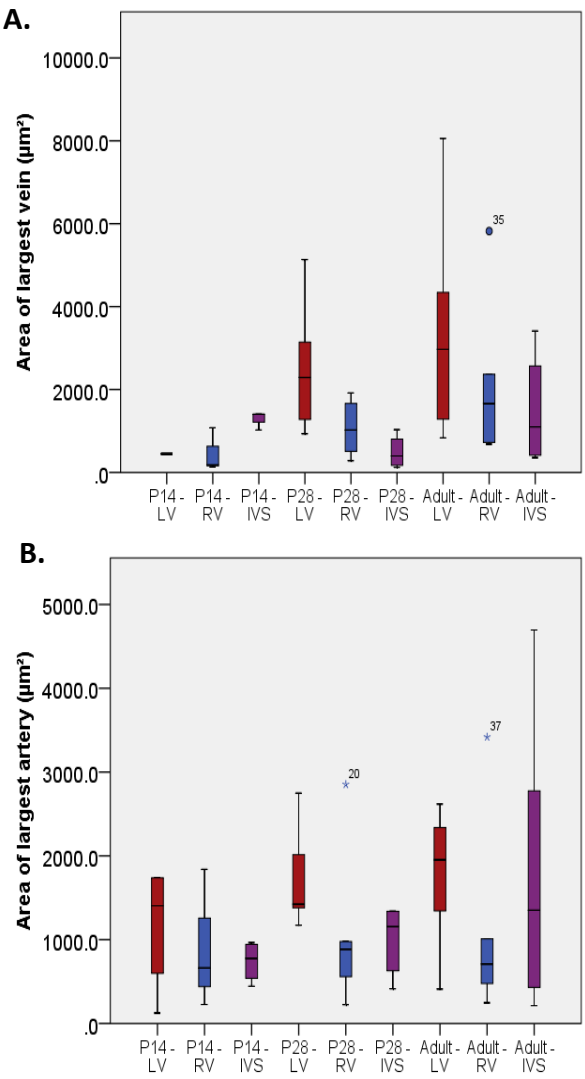

Figure 69. Graphical summary of the mean areas for the largest veins (A), arteries (B) and arterial lumens (C) in each sample, by section of the heart (LV, RV or IVS) and age. Data are presented as Mean ± SE (n = 4 for 14-day old, n = 5 for 28-day olds and n = 5 for adult).

However, statistical significance was found between 14-day old and both 28-day old and adult rats for the ratio between the area of the elastic lamina of the arterial wall and the area of the whole vessel, as shown in **Figure 70A**. Whilst this significance was not found in the right ventricle (not shown), arteries from the interventricular septum did display a statistically significant difference between 14-day old and adult hearts (**Figure 70B**).

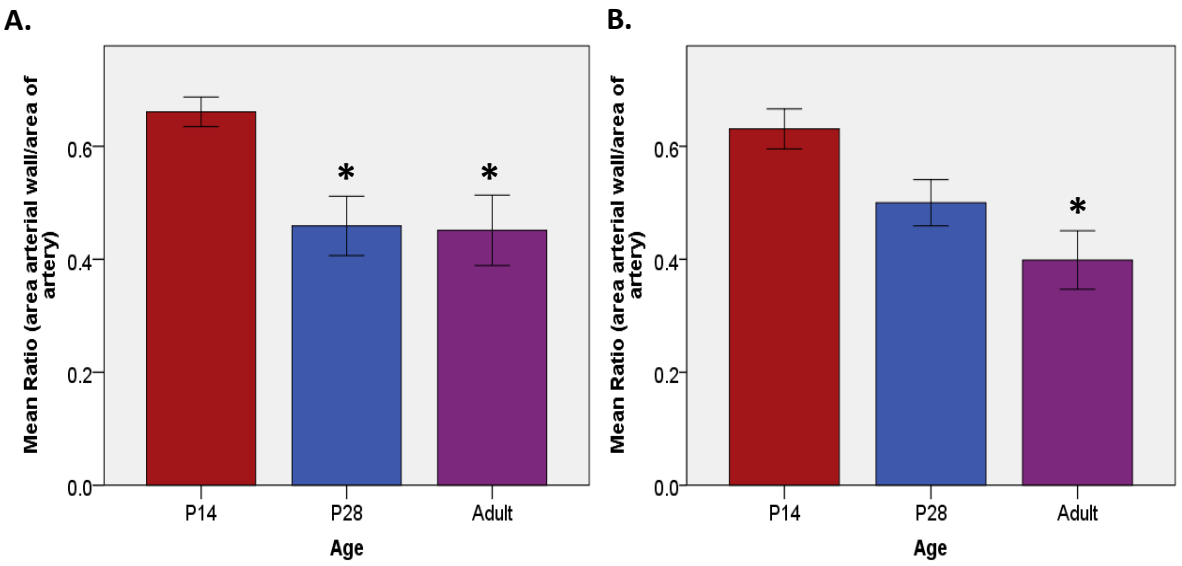

Figure 70. Differences in the elastic layer of the arterial wall/total vessel area ratio between age groups for the left ventricle (**A**) and the interventricular septum (**B**). Significant p-values are labelled. Data are presented as Mean ± SE (n = 4 for 14-day olds, n = 5 for 28-day olds and n = 5 for adult). * = statistically significant difference in comparison with 14-day old samples ($p < 0.05$).

7.3.2 Cardiomyocyte hypertrophy during development

Following the isolation of cardiomyocytes from the hearts of 14-day old, 28-day old, and adult rats, the sizes of these isolated cells were measured using a grid-lined slide (as described in **Section 2.1.5**). Example images of cells isolated from the different age groups are presented in **Figure 71** below.

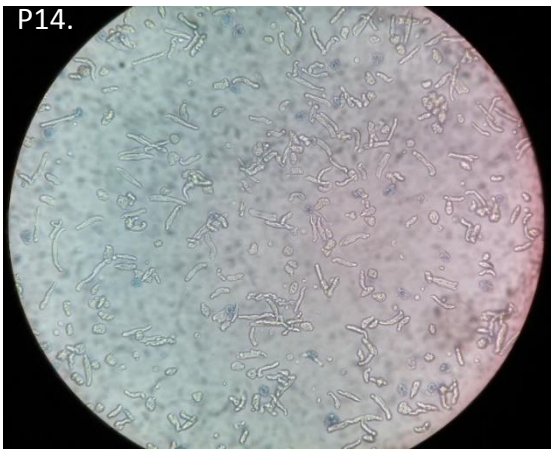

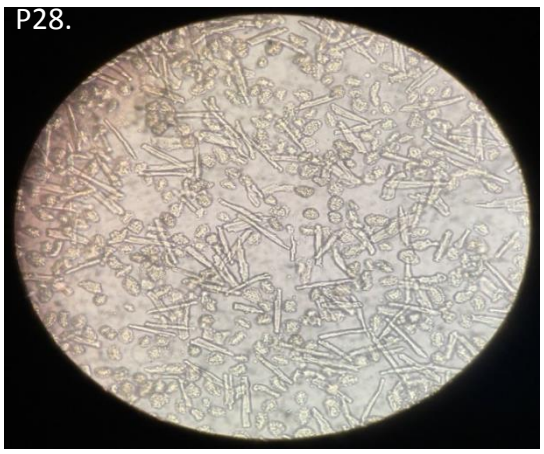

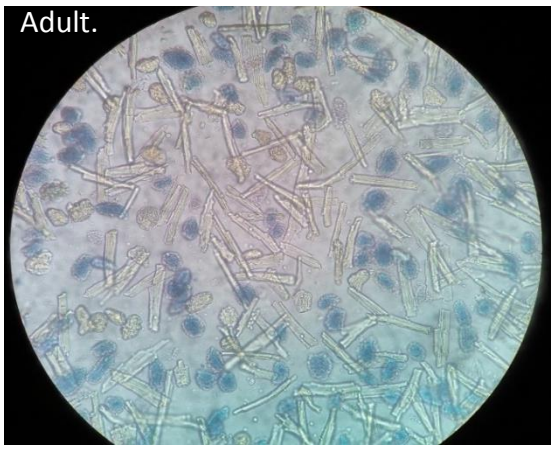

Figure 71. Isolated cardiomyocytes from a 14-day old heart (left), a 28-day old heart (right), and an adult heart (bottom), with non-viable cells stained with Trypan Blue for the 14-day old and adult samples.

Cardiomyocyte dimensions were measured for cells from 3 different hearts for each age group, the averages of which are shown in **Figure 72**. A statistically significant difference was found between the 3 age groups in terms of both the length and width of the isolated cardiomyocytes.

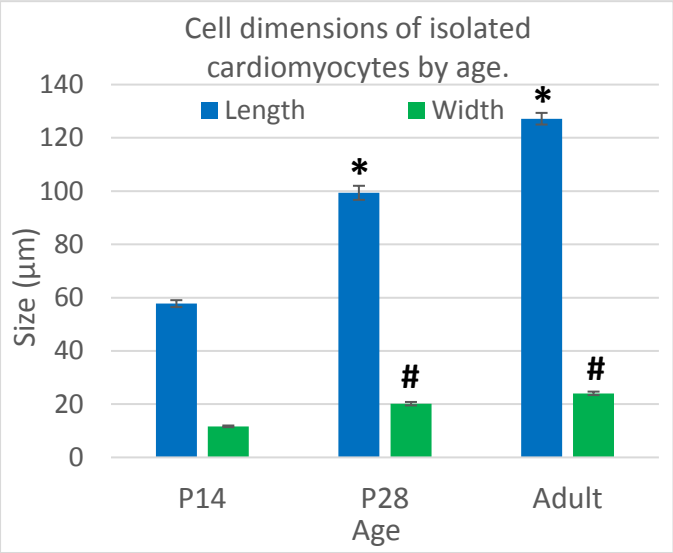

Figure 72. Comparison of the length and width measurements of cardiomyocytes obtained from cell isolation between age groups. Data are presented as Mean ± SE (n = 3 for 14-day old, n = 3 for 28-day old and n = 3 for adult). * = statistically significant difference in comparison with 14-day old average length ($p < 0.05$). # = statistically significant difference in comparison with 14-day old average width ($p < 0.05$).

7.3.3 Changes in cardiomyocyte ultrastructure during development

7.3.3.1 Changes in sarcomere length during postnatal development

Average sarcomere length was statistically significantly lower in 14-day old than adult hearts in control, pre-ischemic samples ($p < 0.05$). This corresponds to the fact that cardiomyocytes undergo hypertrophy of existing cells during postnatal development, with associated increases in the length of sarcomeres.

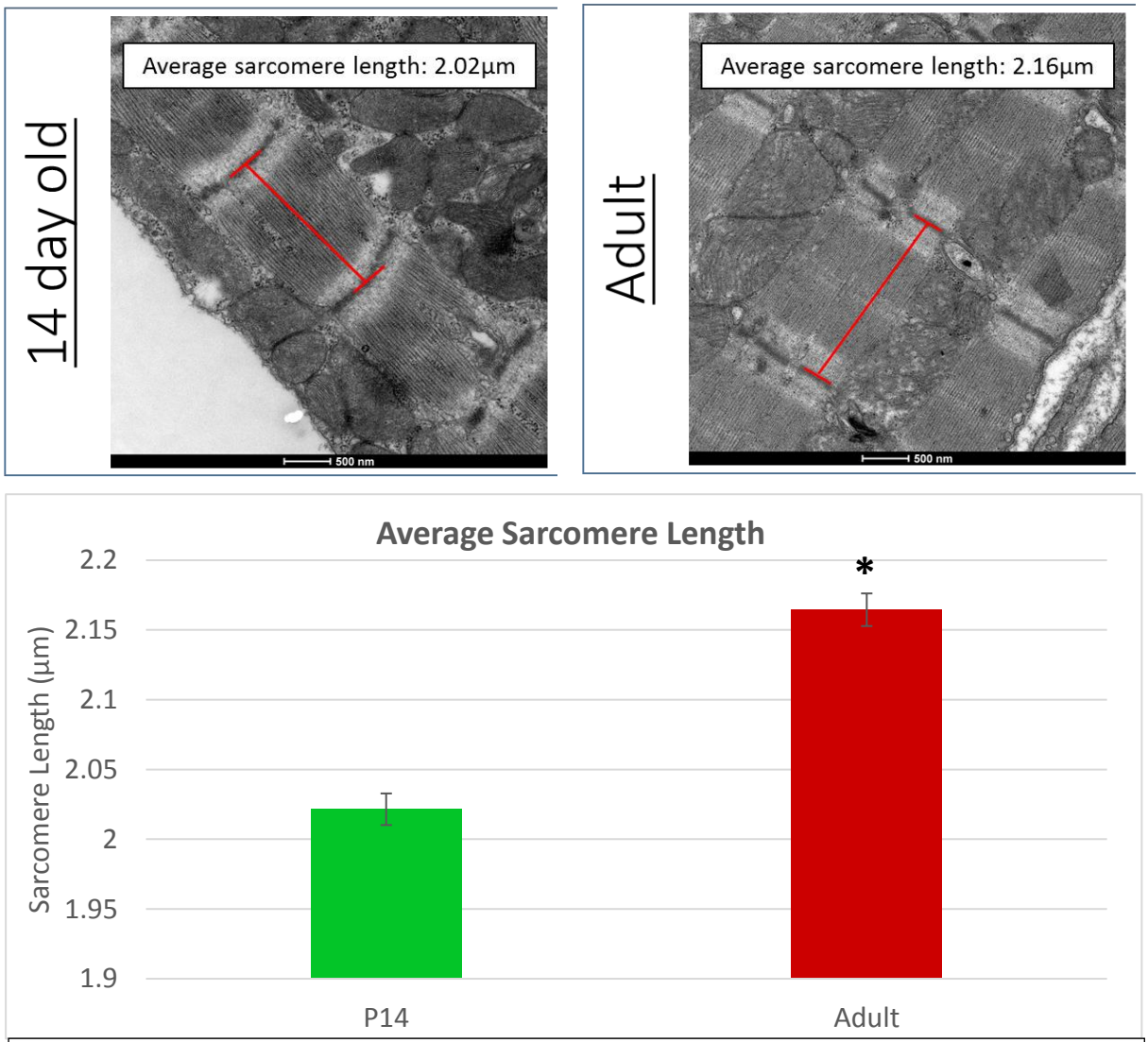

Figure 73. Graph to show average sarcomere length in control 14-day old and adult rat hearts. * = statistically significant difference compared to 14-day old samples ($p < 0.05$). (P14 n = 3 hearts, 475 sarcomeres. Adult n = 3 hearts, 641 sarcomeres) Data presented as Mean ± SE.

7.3.3.2 Changes in the abundance of caveolae during postnatal development

The number of caveolae present at cardiomyocyte membranes per/µm was statistically significantly higher in 14-day old hearts in comparison with adult hearts ($p < 0.0001$). This correlates with the significantly greater expression of Caveolin-1, -2 and -3 in the proteomic output.

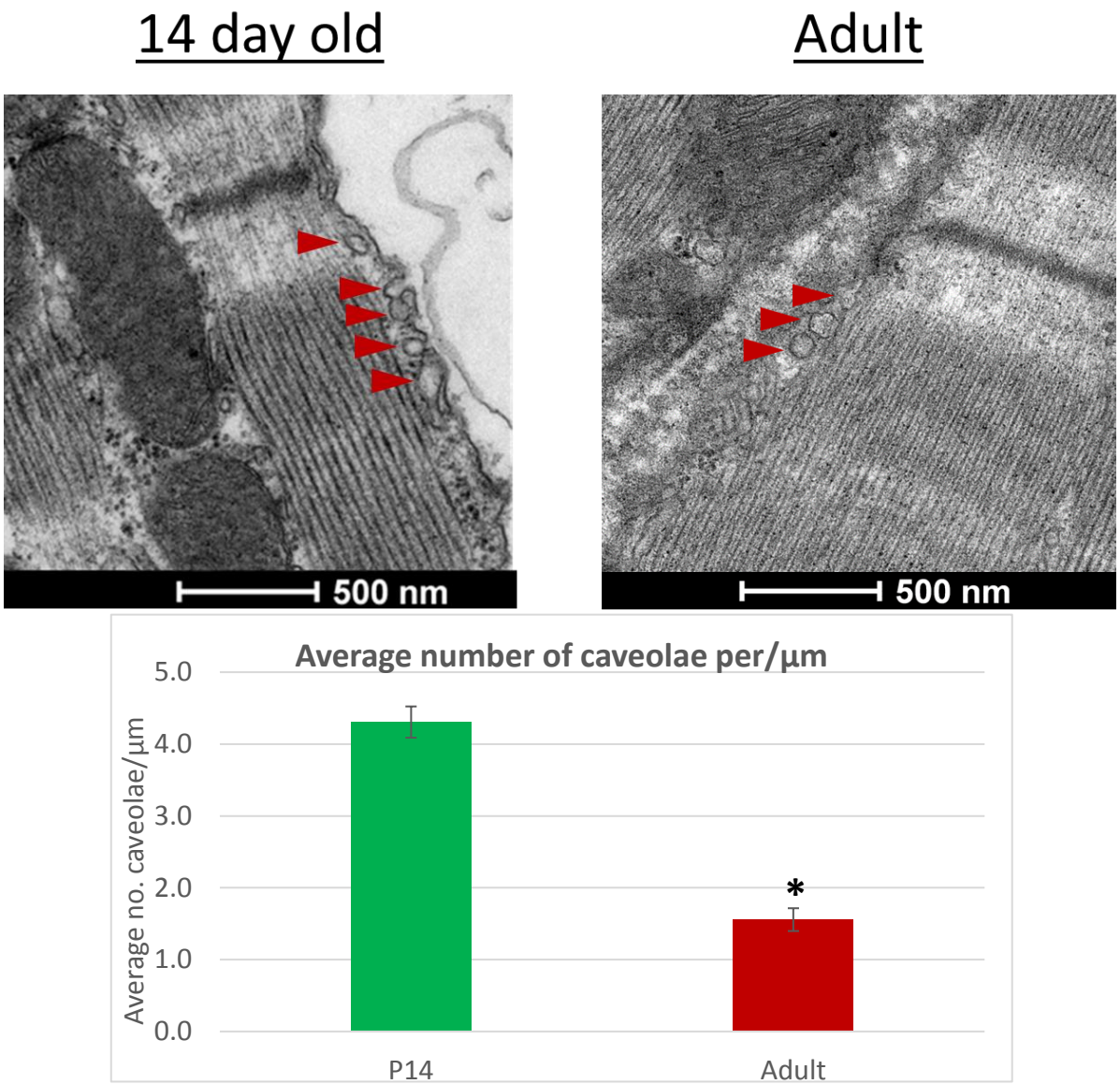

Figure 74. Comparison of caveolae abundance in 14-day old and adult hearts. **(Top)** Representative electron micrographs of caveolae in 14-day old (**right**) and adult (**left**) heart. **(Bottom)** Mean number of caveolae present at the cardiomyocyte cell membrane per/µm in 14-day old and adult rat hearts. * = statistically significant difference in comparison with P14 ($p < 0.05$). Data presented as Mean ± SE (calculated from 35 P14 and 22 adult fields for n = 3 hearts per group).

7.3.3.3 Changes in MVB & exosome abundance during postnatal development

7.3.3.3.1 Proteomics of proteins reported to be involved in exosome signalling

As mentioned in the introduction, MVBs and exosomes are known to be linked to cardioprotective signalling, reducing the degree of myocardial injury seen following ischemia/reperfusion through activation of survival signalling pathways. We therefore examined our proteomic output for proteins involved in these signalling pathways, as well as commonly used exosome markers, CD63 and Tsg101. TLR4 and CD63 were not detected across all 4 age groups of the proteomic output, and subsequently could not be analysed. Results for the remaining proteins with full sets of proteomic data are shown below.

The majority of proteins showed a progressive increase – HSP70-1a & p38MAPK-MAPK12 – or decrease – HSP70-13, HSP70-14, HSP70-4, ERK2 & HSP27 – in expression over the course of postnatal development, as opposed to a biphasic pattern of expression, indicating they are unlikely to play a role in the biphasic changes to cardiac vulnerability seen over these age groups. Conversely, two of the members of the HSP70 family – HSP70-12a & HSP70-12b – believed to be carried by exosomes and stimulate cardioprotective signalling via TLR4 did show a statistically significant biphasic trend in expression, highlighting them as potentially important proteins underlying postnatal changes in response to ischemia/reperfusion injury. The remaining proteins involved in this cardioprotective pathway – ERK1 & p38MAPK-MAPK14 – as well as reported exosome marker TSG101 were also shown to have an overall biphasic trend in expression. However, ERK1 and TSG101 did not show statistically significant differences in expression between 7-day old and 14-day old samples, and p38MAPK-MAPK14 did not show any statistically significant changes in expression between these age

groups. As a result, the importance of these proteins' roles in biphasic cardiac vulnerability changes is uncertain.

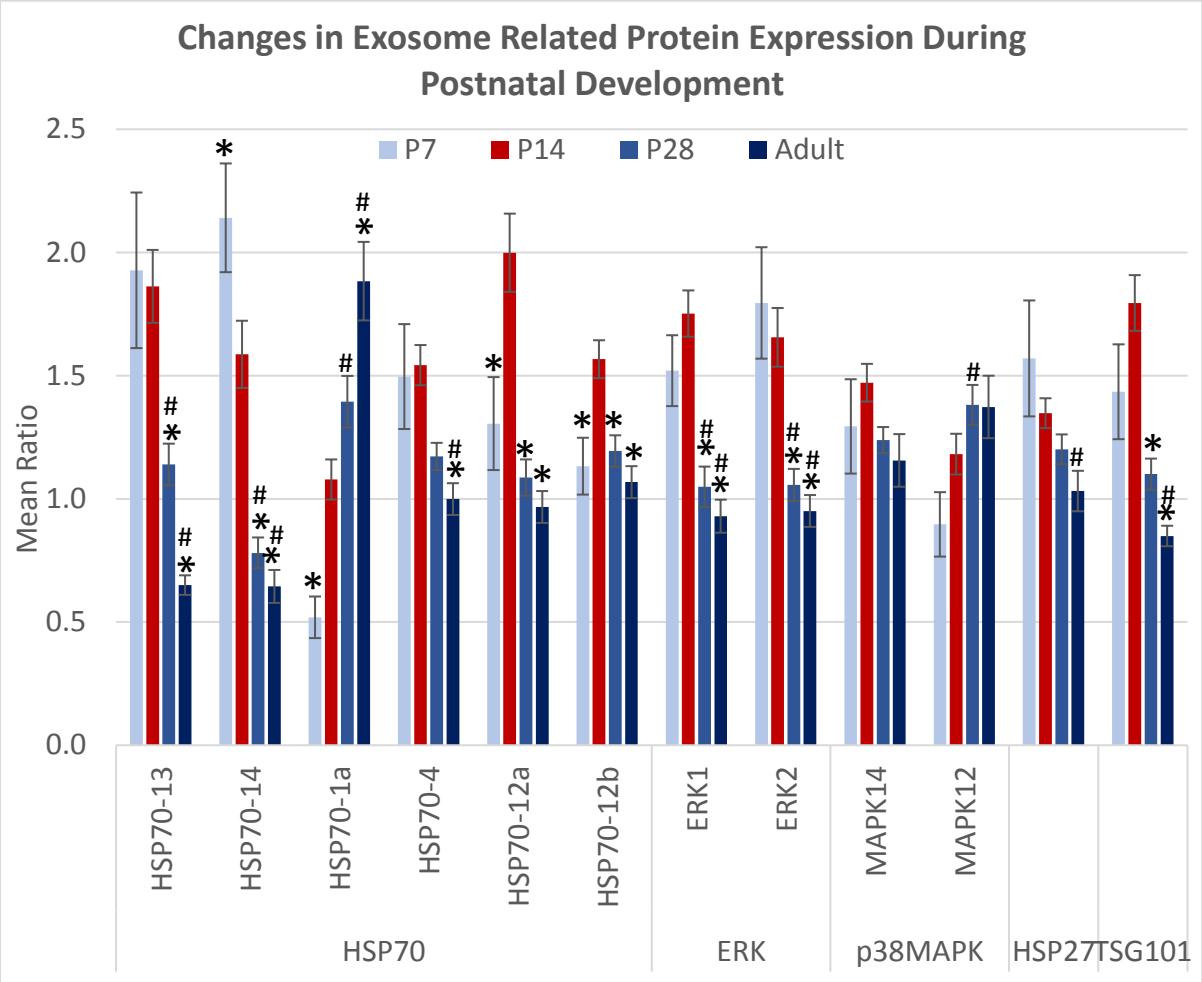

Figure 75. Changes in the expression of key exosome-related proteins and downstream signalling targets during postnatal development, as detected by proteomic analysis. Data are presented as Mean ± SE ((7-day (n = 4), 14-day (n = 8), 28-day (n = 8) and adult (n = 7)) * = statistically significant difference compared to 14-day old samples ($p < 0.05$). # = statistically significant difference compared to 7-day old samples ($p < 0.05$).

As this proteomic output was produced from whole tissue samples, future work will need to further examine the role of these proteins in exosome function and their cardioprotective properties, possibly through staining – IHC or Immunogold staining – in order to establish whether those proteins showing statistically significant biphasic expression specifically do so within or in association with exosomes, or whether they change in cardiac tissue as a whole.

7.3.3.3.2 Effect of postnatal development on the abundance of MVBs & exosomes in control hearts

Examination of Electron Micrographs taken from control hearts found numerous putative MVBs with large circular exosomes in 14-day old hearts, which were much rarer in adult hearts. It is possible that this reflects a greater abundance of these cardioprotective vesicles present in 14-day old hearts prior to injury that primes them for activation of survival signalling pathways upon cardiac insult, corresponding to their greater resistance to ischemia/reperfusion injury. This corresponds to the detection of survival signalling related proteins in the proteomic output from control hearts with a greater expression in 14-day old hearts than adult hearts.

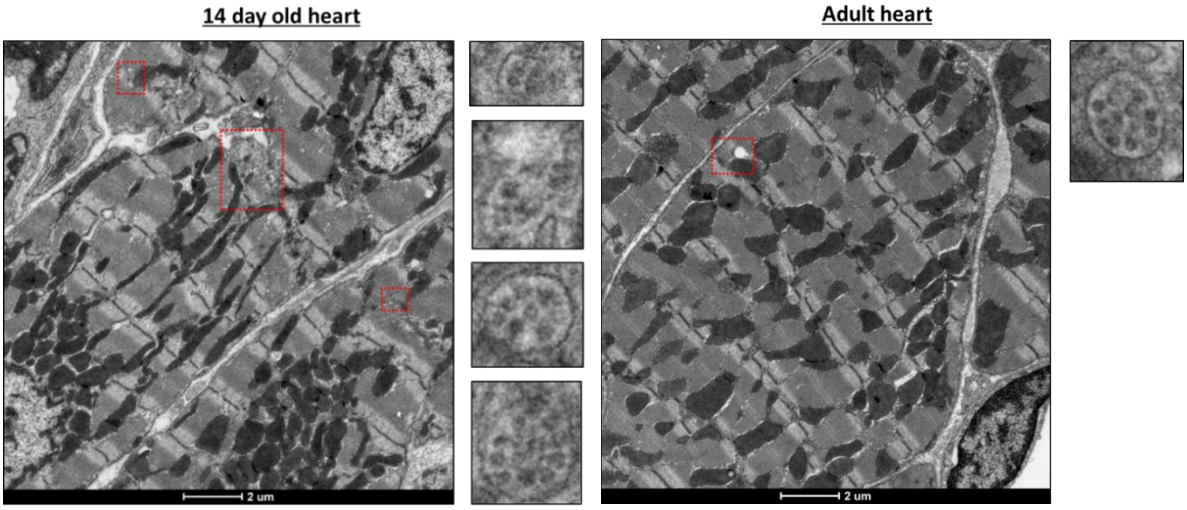

Figure 76. Representative images of putative MVBs containing exosomes in cardiac sections taken from control hearts at 14-days of age (**Left**) and adults (**Right**).

7.3.4 Changes in mitochondrial fission and fusion protein expression during development

As mentioned in **Section 7.1.2.3**, mitochondrial fission and fusion play an important role in the survival of cardiomyocytes following ischemia/reperfusion injury. Therefore, the proteomic output was checked for the presence and expression of proteins related to these processes in control hearts, in order to identify any differences that may exist over the course of postnatal development prior to cardiac insult that could potentially prime hearts and confer greater resistance to injury. The data was checked for commonly reported mitochondrial fission and fusion proteins, and those that had complete sets – i.e. were present across all three runs of proteomic analysis and thus all four age groups – were analysed for statistically significant differences in expression across the four age groups, as shown in **Figure 77** below.

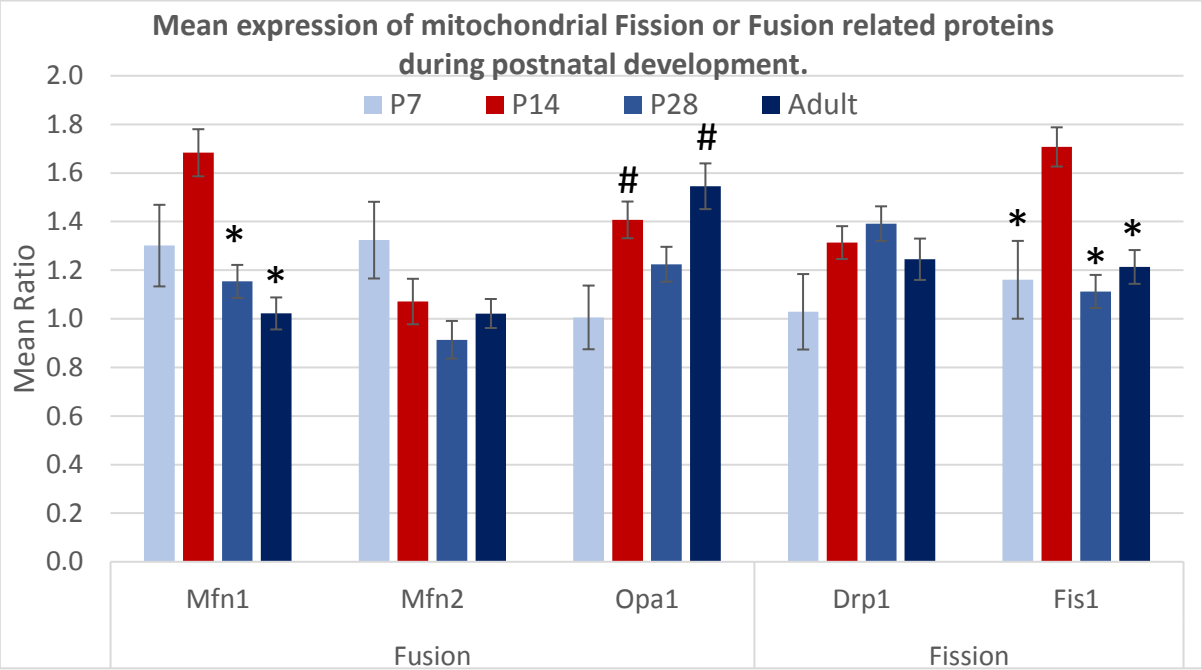

Figure 77. Changes in expression of mitochondrial fission & fusion related proteins at different stages of postnatal development, as detected in the proteomic output. Data are presented as Mean ± SE. (7-day (n = 4), 14-day (n = 8), 28-day (n = 8) and adult (n = 7)) * = statistically significant difference compared to 14-day old samples ($p < 0.05$). # = statistically significant difference compared to 7-day old samples ($p < 0.05$).

No statistically significant differences were seen in the expression of Mfn2 or Drp1 across the four age groups, and differences in Opa1 expression were only seen between 7-day old samples and both 14-day old and adult. As a result, it is likely that these proteins do not play a role in potential differential mitochondrial fission or fusion responses to ischemia/reperfusion injury in 14-day old hearts that may contribute to their improved resistance to cardiac injury. However, a biphasic trend in expression was seen in the fusion protein Mfn1 and fission protein Fis1, with a statistically significant difference between 7-day old and 14-day old samples only in the case of Fis1.

7.3.5 Changes in mitochondrial morphology during postnatal development

The morphological characteristics of each mitochondrial subpopulation are displayed in **Figure 78 & 79**, with statistical analysis conducted for comparison of the subpopulations within each age group. Further statistical analysis was run to compare the morphology of the subpopulations between the age groups, as shown in **Figure 80**.

Statistically significant differences in morphology were seen predominantly between Interfibrillar (IF) mitochondria in comparison with the two other subpopulations in 14-day old hearts, with both a significantly greater area and lower roundness than Perinuclear (PN) and Subsarcolemmal (SSL) mitochondria. All three subpopulations significantly differed in Aspect Ratio (AR), with PN showing a value closest to 1.0, and IF showing a value furthest from 1.0.

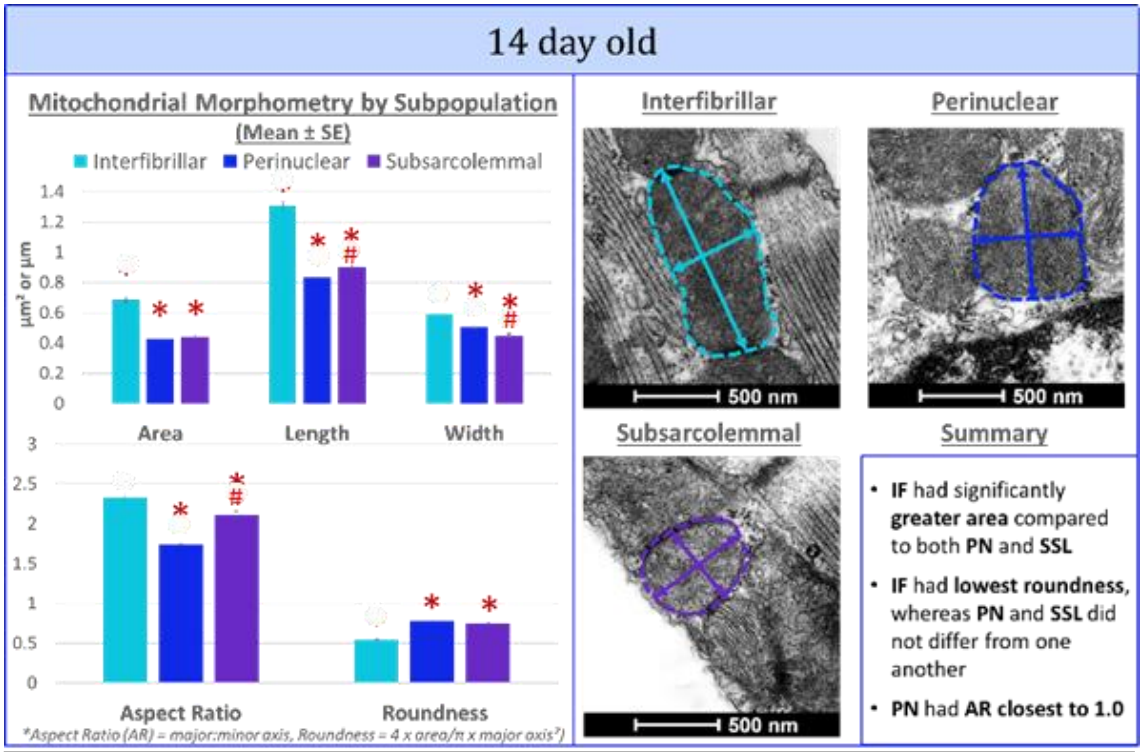

Figure 78. 14-day old cardiac mitochondrial morphometry by subpopulation. * = statistically significant difference in comparison with IF mitochondria ($p < 0.05$). # = statistically significant difference in comparison with PN mitochondria ($p < 0.05$). Turquoise = Interfibrillar (IF), Blue = Perinuclear (PN), Purple = Subsarcolemmal (SSL). **IF** n = 312, **PN** n = 635, **SSL** n = 402.

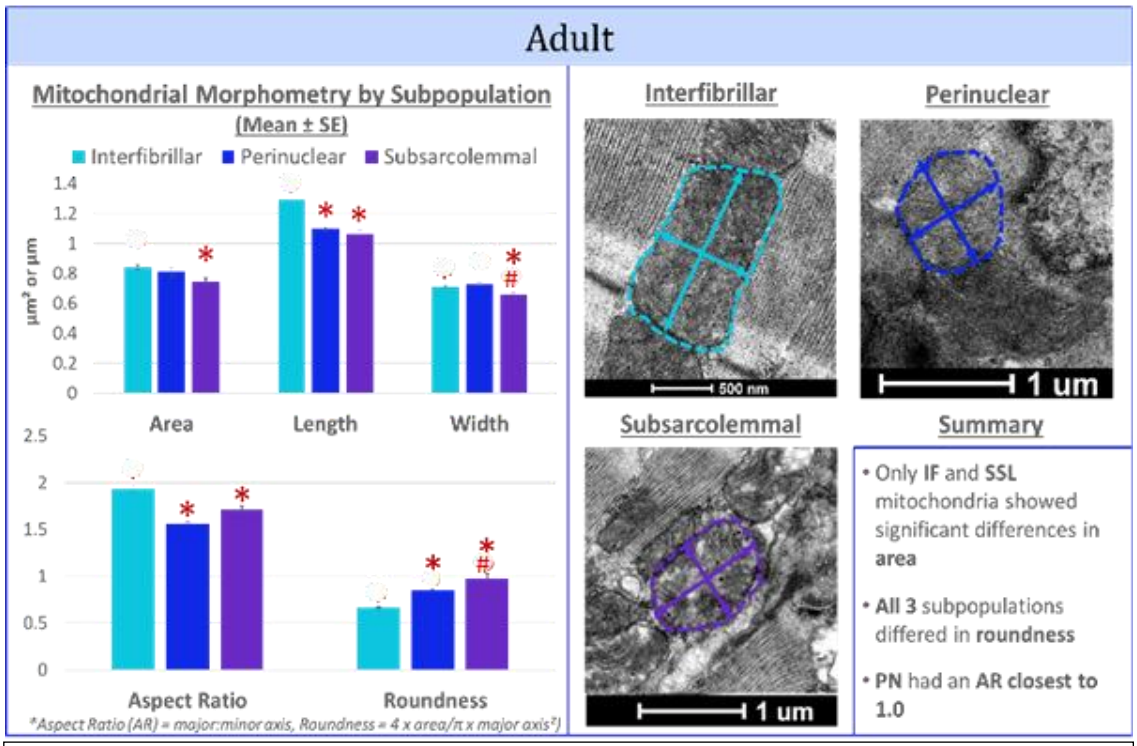

Figure 79. Adult cardiac mitochondrial morphometry by subpopulation. * = statistically significant difference in comparison with IF mitochondria ($p < 0.05$). # = statistically significant difference in comparison with PN mitochondria ($p < 0.05$). Turquoise = Interfibrillar (IF), Blue = Perinuclear (PN), Purple = Subsarcolemmal (SSL). **IF** n = 671, **PN** = 122, **SSL** n = 243.

In adult hearts, statistical significance was only seen between IF and SSL mitochondria in terms of their mean area. Similar to 14-day old hearts, the AR for IF differed from both PN and SSL, with a value furthest from 1.0. All three subpopulations were shown to differ in roundness, with IF showing the lowest measure of roundness of the three subgroups.

Direct comparisons between the two age groups (**Figure 80**) showed that all of the morphological characteristics measured for each of the three subpopulations – with the exception of IF length – were significantly different. In all three subpopulations, adult mitochondria had a greater mean area, as well as both a greater degree of roundness and an AR closer to 1.0 than 14-day olds.

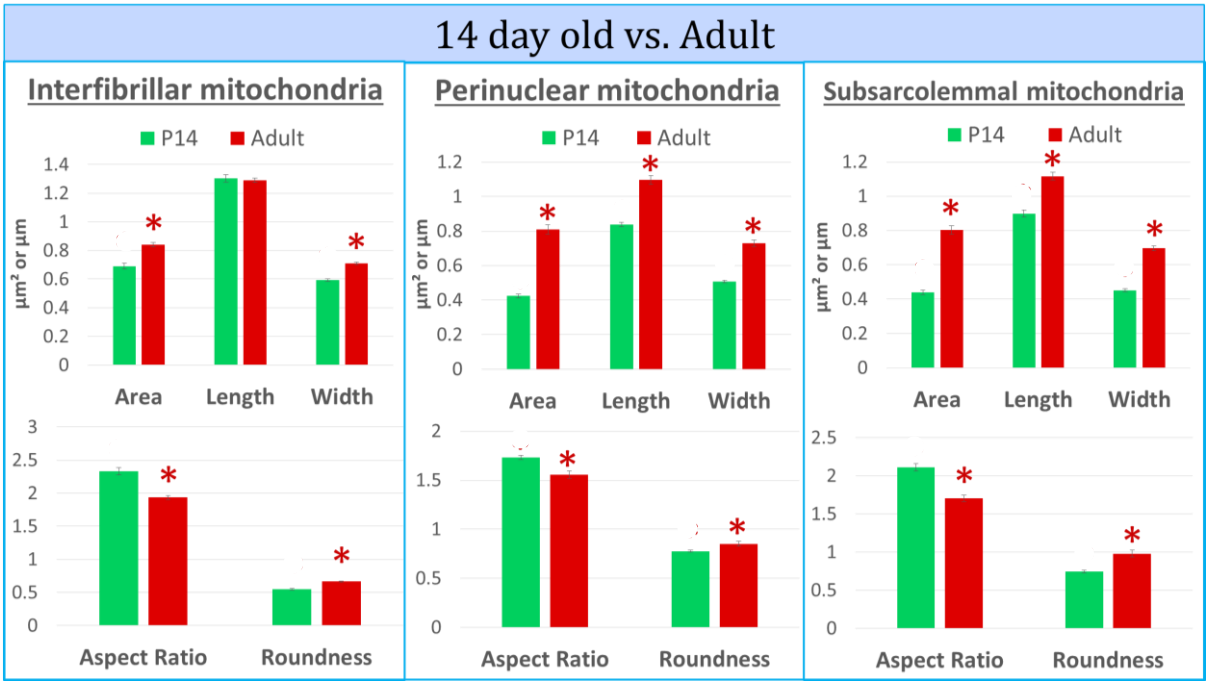

Figure 80. Differences in mitochondrial morphological between 14-day old and Adult hearts, by mitochondrial subpopulation. * = statistically significant difference in comparison with 14-day old hearts ($p < 0.05$). (n = 3 hearts/age group)

7.3.6 Changes in mitochondrial subpopulation distribution during postnatal development.

In order to examine the relative numbers of each mitochondrial subpopulation present in the myocardium, and how this differs between the two age groups, the area of the cardiomyocyte, as well as the collective area of the cardiomyocyte covered by each subpopulation, were measured.

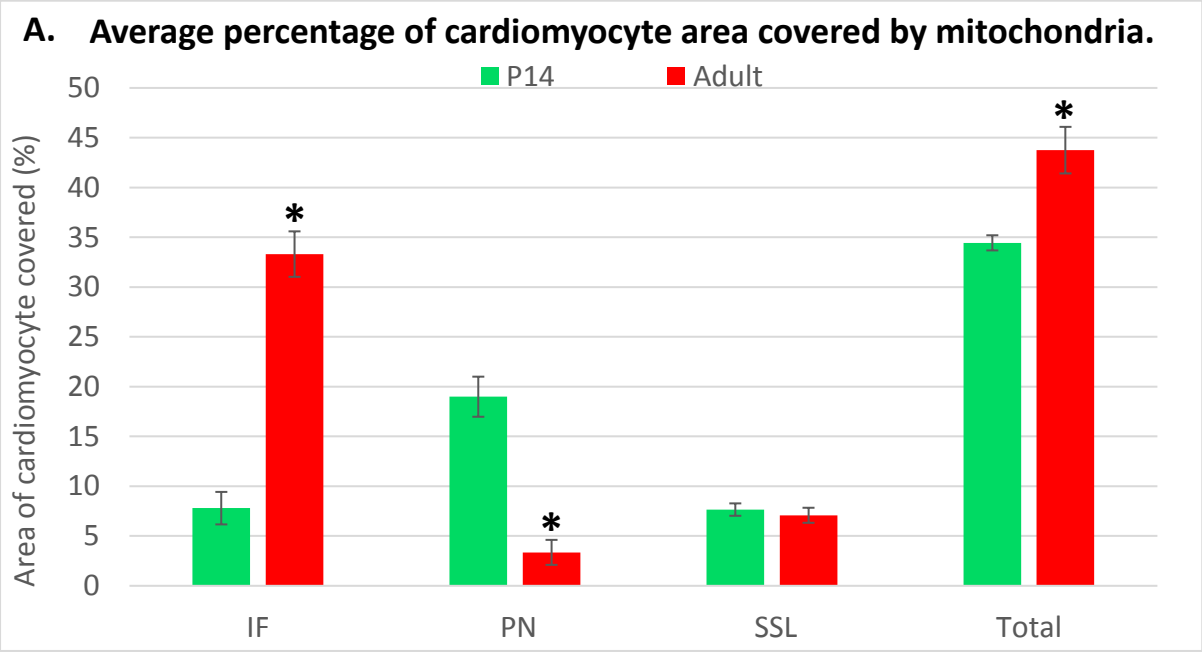

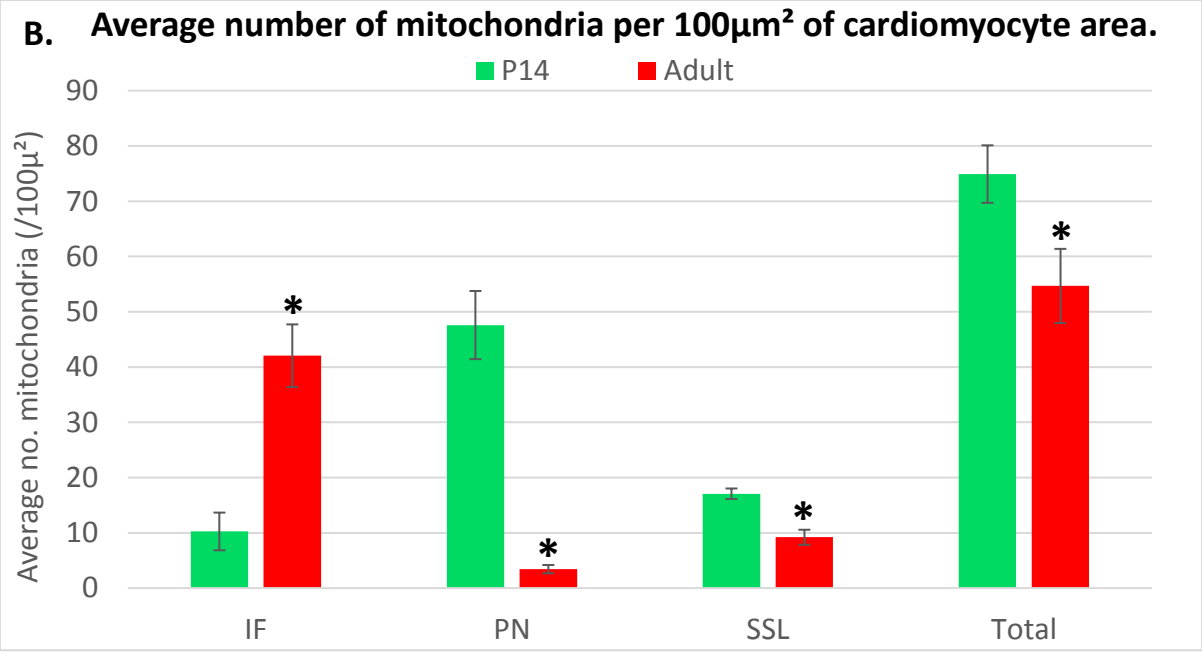

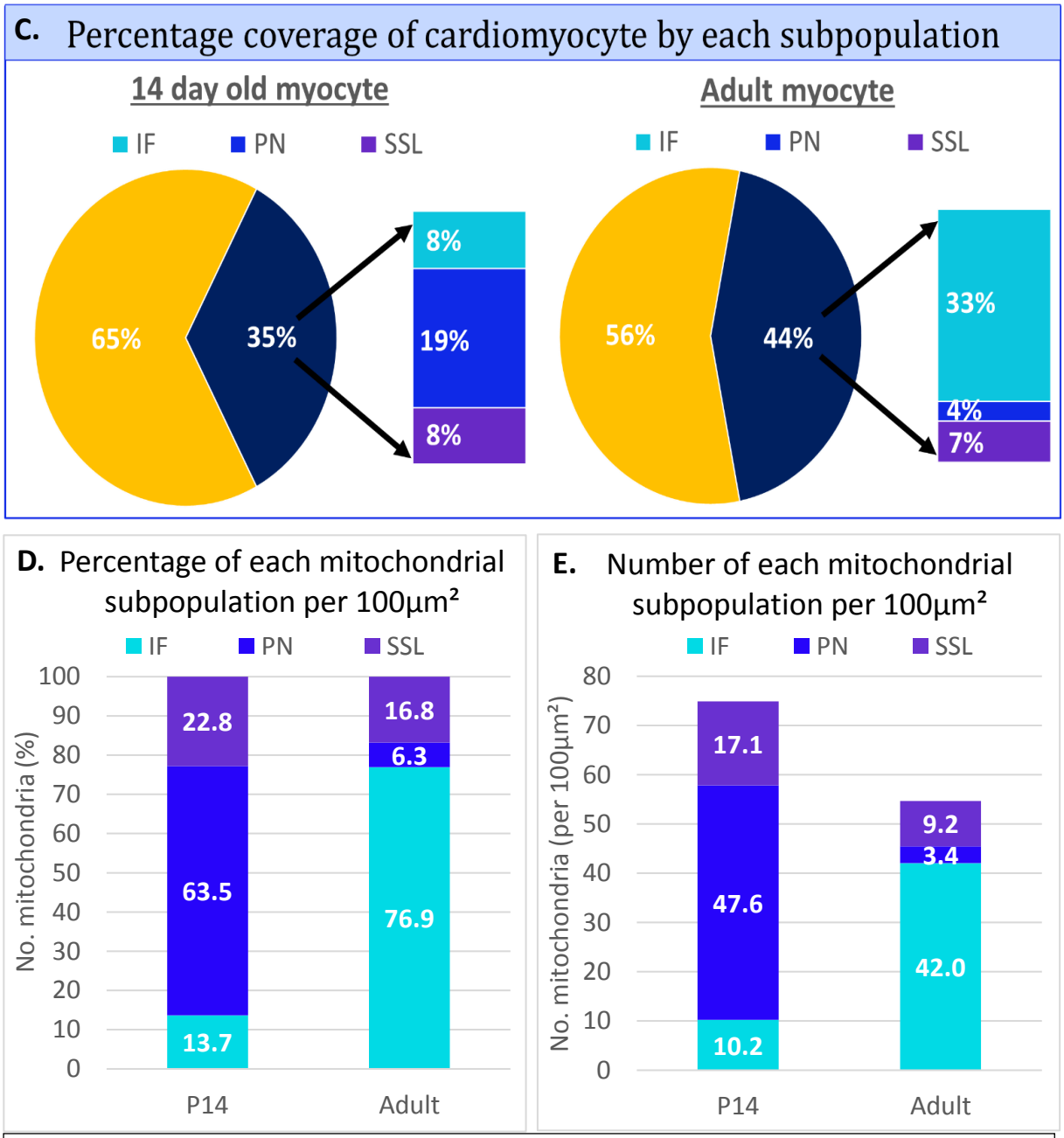

Figure 81. Mitochondrial subpopulation distribution in 14-day old and adult hearts. **A.** Percentage of cardiomyocyte covered by mitochondria and mitochondrial subpopulations. **B.** Average number of each mitochondrial subpopulation in a 100µm² area of cardiomyocyte, calculated as: *area (µm²) of mitochondria subpopulation covering cardiomyocyte/average area of an individual mitochondrion of that subpopulation*. * = statistically significant difference with P14. **C.** Graph comparing the relative percentages of each mitochondrial subpopulation covering a region of cardiac tissue between the two age groups. Yellow segment indicates percentage of the cardiomyocyte area free of mitochondria. **D.** Graph depicting the relative percentages of number of each mitochondrial subpopulation per 100µm² area of cardiomyocyte by age group. **E.** Graph depicting relative numbers of each mitochondrial subpopulation per 100µm² area of cardiomyocyte by age group. (P14 n = 3 hearts, 7 sections. Adult n = 3 hearts, 6 sections)

A greater proportion of the cardiomyocyte was covered by mitochondria in adults (44%) compared with 14-day old (35%). Of these areas, only 8% of the 14-day old cardiomyocyte was comprised of IF in comparison with 33% in adults. However, 14-day olds showed a greater percentage of PN in cardiomyocytes than adults (19% vs. 4%), but a similar proportion of SSL. A similar trend in distribution was seen when calculating the number of each mitochondrial subpopulation, with 14-day olds having the greatest number of PN per 100µm² and adults having the greatest number of IF. In addition to this, 14-day olds were also found to have a greater number of SSL in comparison with adults (17 mitos/100µm² vs. 9 mitos/100µm²). The significance of these differences in distribution will be discussed in **Section 7.4**.

7.4 Discussion

7.4.1 Gross cardiac structural changes during development

Analysis of cell dimensions following isolation of cardiomyocytes from 14-day old, 28-day old and adult rat hearts found a statistically significant increase in both cell length and width during postnatal development ($p < 0.0001$ for both measurements). These findings are consistent with current knowledge of the switch from hyperplasic growth to hypertrophic growth at postnatal day 4 in rats (Olivetti, Anversa et al. 1980), as increasing heart mass is supported by the increasing size of individual, pre-existing cardiomyocytes.

While there does appear to be an upward trend in both vein and artery size during postnatal development, the large range of values of cross-sectional area in each group and within each region of the heart resulted in a large standard error, and the lack of statistical significance between these factors. Whether this lack of statistical significance is due to the small sample numbers used, the fact that only the largest vessel from each sample was measured, or is in

fact of true physiological relevance is uncertain. Previous reports have described that the increasing blood supply needed to support the growing myocardium during postnatal development is supported by the proportional growth of capillaries, whereas the coronaries may not in fact increase with increasing heart size, resulting in increased coronary vascular resistance with age (Hudlicka and Brown 1996).

There also appears to be a non-statistically significant pattern in vessel size between the regions of the heart. Both veins and arteries appear to be largest in the left ventricle (LV) and smallest in the interventricular septum (IVS), with the exception of veins at 14-days of age which are largest in the IVS, and arteries in the adult samples which are again largest in the IVS, although only marginally. This finding correlates with the respective roles of each region of the heart in cardiac function and the circulatory system, as the LV is responsible for sustaining contraction sufficient to pump blood from the heart to the entire body, and as such would require a greater substrate and metabolite supply in order to support the higher muscle mass and energy demands than those required by the IVS or right ventricle (RV). It is likely that the exceptions found are due to methodological issues in terms of selection of the vessels for measurement, in addition to the relatively low sample numbers, as a single anomalous result would be capable of altering the average and pattern of change in vessel size of the whole age group or heart section. Indeed, a full cross-sectional vein could only be found in the LV of one out of the four 14-day old samples. Notably, the ratio of the elastic arterial wall area to total vessel area was statistically significantly higher in 14-day old hearts than adults in the IVS as well as the 28-day old hearts in the LV. The significance of this is uncertain, but may reflect a morphological response of the arteries at this age to the increasing coronary vascular resistance, increasing cardiac output and progression towards functional and structural maturity at 21 postnatal days (Wu and Wu 2009).

7.4.2 Caveolae abundance and caveolin-1, -2 and -3 expression is higher in 14-day old compared to adult hearts

Concordant with the greater expression of caveolin-1, -2 and -3 in the proteomic output (**Section 4.3.2**), the abundance of caveolae was significantly greater in 14-day old hearts than adult hearts. As discussed in **Section 7.1.2.1**, caveolae and caveolins play important cardioprotective roles during I/RI through localisation of important survival signalling proteins at the cell membrane to facilitate faster signal transduction, as well as through the signalling properties of caveolins themselves. Therefore, this greater abundance of caveolae in 14-day old samples therefore suggests a potential underlying contribution of these structures, as well as associated caveolins, to the greater resistance to I/RI seen in hearts of this age group. Future work examining cardiac ultrastructure would be required to see if the abundance of caveolae in 7 day old hearts also mimics the trends of caveolin-1, -2 and -3 expression seen across the four age groups.

7.4.3 MVB and exosome associated protein expression is higher in 14-day old hearts compared to adults

Similar to caveolae, the abundance of putative MVBs was greater in 14-day old hearts than adult hearts. This was supported by proteomic analysis, which found that the expression of commonly used exosome marker, TSG101, had a biphasic profile, peaking at 14-days of age. It should be noted, however, that the difference between 14-day old and 7-day old samples was not statistically significant, but may result from the relatively low number of samples analysed in the 7-day old group. A number of other proteins linked to exosome signalling also showed an overall biphasic profile of expression, including two isoforms of HSP70 – with statistically significant differences between 14-day old samples and all three age groups – as

well as ERK1, which showed statistically significant differences only between 14-day old samples in comparison with 28-day old and adult samples. While this correlates with the greater number of putative MVBs identified in the 14-day old myocardium, these signalling proteins do also play important roles in survival signalling in their own right (**Section 1.5**), and may therefore display this pattern of expression independently of exosomes.

Quantitative analysis of MVB and exosome abundance was not performed in this case, due to the uncertainty in accurately identifying and distinguishing MVBs from other vesicles of a similar morphology and appearance. While the majority had a clear morphology similar to the example given in **Section 7.1.2.2**, with large circular structures located within MVBs, a number had intermediate phenotypes, or ones that appeared similar to structures that have previously been presented as both MVBs/exosomes (Waldenstrom, Genneback et al. 2012) and autophagasomes (Martin, Xu et al. 2011). As a result, future work would benefit from the use of exosome markers in order to conclusively identify MVBs and therefore quantitate potential differences between age groups. Such investigation would also need to apply this to 7-day old samples to confirm that trends in abundance also follow the biphasic profile seen in cardiac vulnerability to I/RI.

7.4.4 Proteomic analysis of fission and fusion proteins showed age-related biphasic changes in both Mfn1 and Fis1 expression

Proteomic analysis of mitochondrial fusion and fission proteins identified only two that showed an overall biphasic profile of expression; Mfn1 and Fis1. Whilst Mfn1 expression only showed statistical significance between 14-day old in comparison with 28-day old and adult samples, statistical significance was seen between 14-day old samples and all three age groups in the case of Fis1. This biphasic expression of both a pro-fusion and pro-fission

protein (**Section 7.1.2.3**) indicates no clear bias in favour of one process over the other in control hearts, but could indicate that there is a balance between the two that may provide cardioprotection during I/RI. It will be important to examine this in post-ischemic samples and to look at activation of these proteins in future work in order to better elucidate the functional relevance of these patterns of expression.

7.4.5 Morphology of mitochondrial subpopulations is altered during postnatal development

7.4.5.1 All three mitochondrial subpopulations were smaller and less rounded in 14-day old hearts compared with adults

Previous work by Kalkhoran et al. (2017) showed that, in adult hearts, IF mitochondria are more elongated and less spherical than both PN and SSL, with SSL displaying a somewhat intermediate morphology between the other two subpopulations. While the authors found that SSL were similar in area to IF, but more akin to PN in terms of their sphericity, our work actually found that, in adults, only IF and SSL differed significantly in area, and that SSL – not PN – had the smallest area. Furthermore, our data showed that all three subpopulations differed significantly from one another in roundness, although only IF differed in AR from the two other subpopulations, with SSL showing the greatest degree of roundness as opposed to PN. Lower AR and greater roundness are suggested to result in mitochondria that are less branched, therefore interacting more with surrounding mitochondria as they do not extend into other regions, a phenotype attributed to PN (Kalkhoran et al. 2017). However, we found that, while PN did have the lowest AR, SSL had the greatest roundness in adults. This may relate to the theory that PN and SSL are more linked to cellular signalling due to their localisation at the cell membrane or around the nucleus, suggesting their

morphology allows for greater inter-mitochondrial signalling. In 14-day olds, the differences in morphology of the mitochondrial subpopulations more closely resembled those reported by Kalkhoran et al. (2017), with IF possessing a significantly greater area than both of the other subpopulations, PN and SSL displaying significantly higher roundness than IF, and PN showing an AR significantly lower than both IF and SSL.

Comparisons between the two age groups showed that, as expected, all subpopulations had a significantly greater area in adults compared with 14-day olds. However, adults also displayed a lower AR and greater roundness in all three subpopulations in comparison with 14-day olds. The significance of these differences is uncertain, but may imply a greater degree of local interaction between adult mitochondria, as opposed to communication and potentially signalling that extends to other regions of the cardiomyocyte. It will also be important to see how these morphological characteristics alter following ischemia and reperfusion.

7.4.5.2 Perinuclear mitochondria are present in higher numbers and density in 14-day compared to adult

Previous reports describe neonates as having more "homogenous networks" (Kuzmicic et al. 2011) of mitochondria distributed around the sarcolemmal membrane and nucleus, in contrast with the more distinct regions of mitochondria and greater density situated between the myofibrils seen in adults. In keeping with this, samples taken from 14-day old hearts displayed a much less organised distribution of mitochondria within cardiomyocytes, often presenting difficulty in finding clear areas of IF for measurements. The majority of mitochondria in 14-day olds – expressed as a percentage area of the cardiomyocyte covered by mitochondria – were PN (19% vs. 4% in adults), whereas the majority of adult

mitochondria were IF (33% vs. 8% in adults). Whilst the greater proportion of IF is to be expected in order to support contraction for the increased energy demands in adults, the significance of a higher proportion of PN in 14-day olds is uncertain, but may relate to their described role as providers of energy for gene transcription (Hwang and Kim 2013).

The importance of mitochondrial localisation to the nuclear region is supported by work reporting the effect of autologously derived mitochondria transplantation in the context of I/RI (Masuzawa et al. 2013). The authors reported that injection of these mitochondria into ischemic regions of the heart resulted in decreased CK release, troponin-I, apoptosis, and infarct size 4 weeks post-surgery, with the recovery of normal contraction within 10 minutes of reperfusion. Transplanted mitochondria were found to have been internalised within 2-8 hours, with an associated increase in cell viability, improved post-infarct cardiac function, and enhanced O_2 consumption. Further investigation of the localisation of these mitochondria showed that, in neonatal rat cardiomyocytes, mitochondria were internalised to the PN region following 24 hours of incubation (Masuzawa et al. 2013). These findings again suggest a potential link between the localisation of mitochondria to the nucleus and improved cardiac outcomes following I/RI, and may indicate that the greater proportion of mitochondria at this site in 14-day olds relates to their resistance to cardiac insult.

7.4.6 Summary & Conclusion

The abundance of both cardioprotective caveolae and MVBs was greater in 14-day old samples than adults, indicating a potential contribution to the greater resistance to I/RI seen in 14-day old hearts. Characterisation of both mitochondrial morphology and subpopulation distribution between the two age groups identified clear differences upon which further comparisons with post-ischemic samples can be built (**Chapter 8**).

Chapter 8: The effect of I/R on Cardiac Ultrastructure in adult and 14-day old hearts

8.1 Introduction

Having characterised differences between control 14-day old and adult hearts in the abundance and morphology of cardiac ultrastructures (**Chapter 7**), **Chapter 8** looks to address the sixth aim of this work; "To observe any changes that may occur in the cardiomyocyte structure and ultrastructure following ischemic insult and reperfusion." Data was collected from post-ischemic and post-I/RI samples from both age groups, and measurements taken for comparison both between age groups following cardiac injury, as well as to compare measurements with those obtained from control hearts within each age group.

8.2 Materials & Methods

8.2.1 Electron microscopy of post-ischemic hearts

The full methodology for preparation and analysis of electron micrographs has been described in **Section 2.7.2,** and the protocol of Langendorff perfusion for global ischemia in **Section 2.6.1**. To summarise, hearts were excised, cannulated onto Langendorff apparatus and perfused with Krebs-Henseleit solution for a period of stabilisation, prior to a 30 minute period of global ischemia. Hearts were then removed from the cannula, and small cubes of tissue taken from the left ventricular wall, left in the fridge overnight in fixative, and transferred into phosphate buffer to be sent for processing. Images were taken in several regions of each heart at a range of magnifications, from which measurements of mitochondrial area, length, width, as well as the area of cardiomyocyte covered, were taken for each of the three mitochondrial subpopulations. These images were also analysed for

the length of sarcomeres, abundance of caveolae, and abundance of putative exosome containing MVBs.

8.2.2 Electron microscopy of post-I/R hearts

Electron microscopy of hearts post-I/R was conducted for 14-day old (n = 3) and adult (n = 3) hearts as described in **Section 8.2.1**. For these hearts, however, an additional 60 minute period of reperfusion was performed following the 30 minutes of global ischemia. At the end of reperfusion, hearts were cut down and cubed sections of tissue taken for processing, as previously described.

8.3 Results

8.3.1 Effect of ischemia on sarcomere length

Average sarcomere length was statistically significantly lower in 14-day old than adult hearts in pre-ischemic samples, but significantly greater in post-ischemic samples. Comparison of pre- vs. post-ischemic samples within each age group showed that average sarcomere length decreased in both 14-day old ($p < 0.0001$) and adult ($p < 0.0001$) hearts, due to hypercontracture (rigor contracture) of the myocardium.

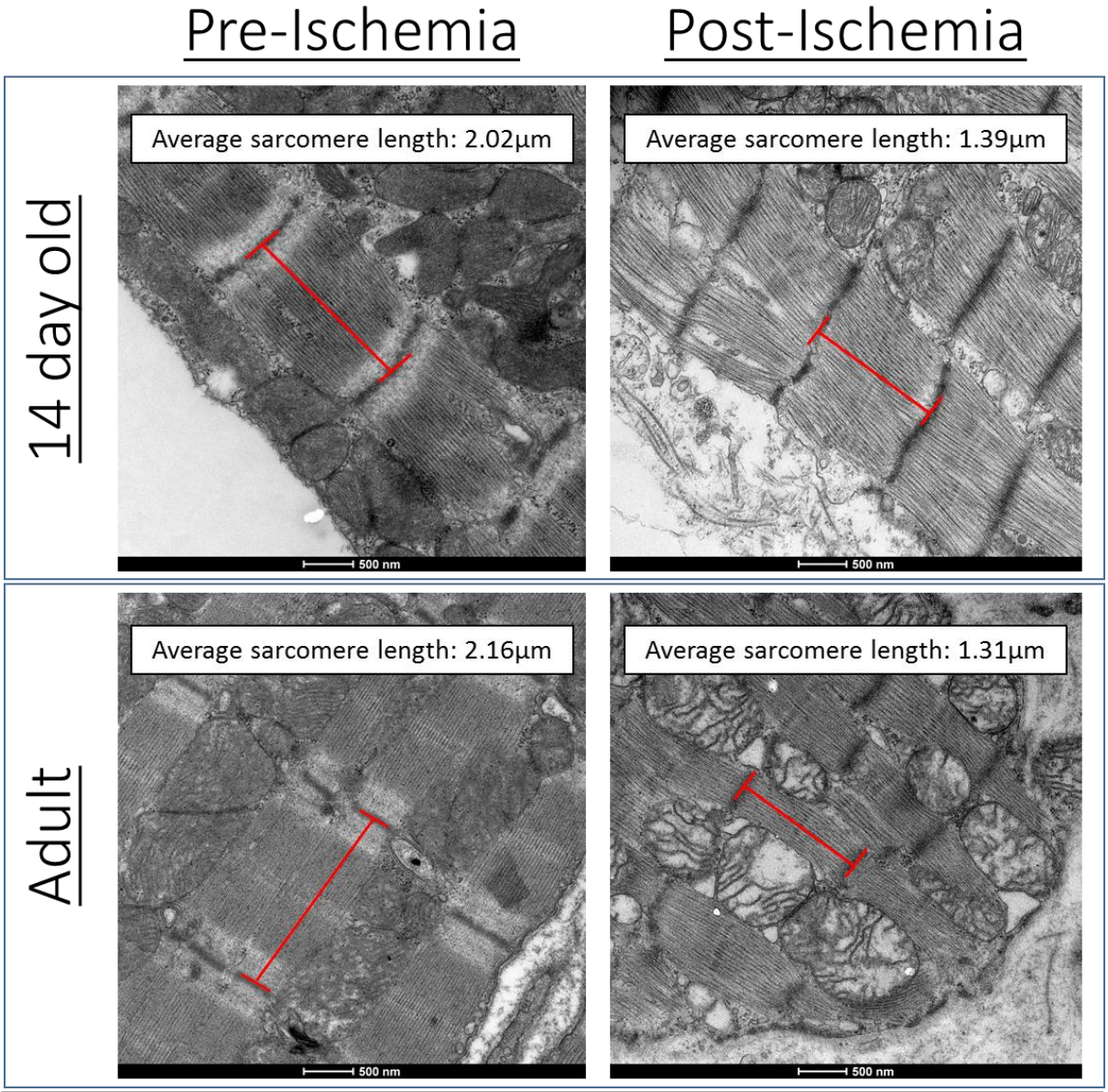

Figure 82. Representative images of sarcomere lengths in pre- vs. post-ischemic samples, at 14-days of age and in adult hearts. Red lines indicate the length of an individual sarcomere.

Reflective of the differences seen in sarcomere length between the two age groups described above, 14-day old samples appeared to show a slightly smaller decrease in average sarcomere length following ischemia than adult samples (31% vs. 38%), potentially indicating a relatively lower degree of hypercontracture in this age group and less severe response to ischemia.

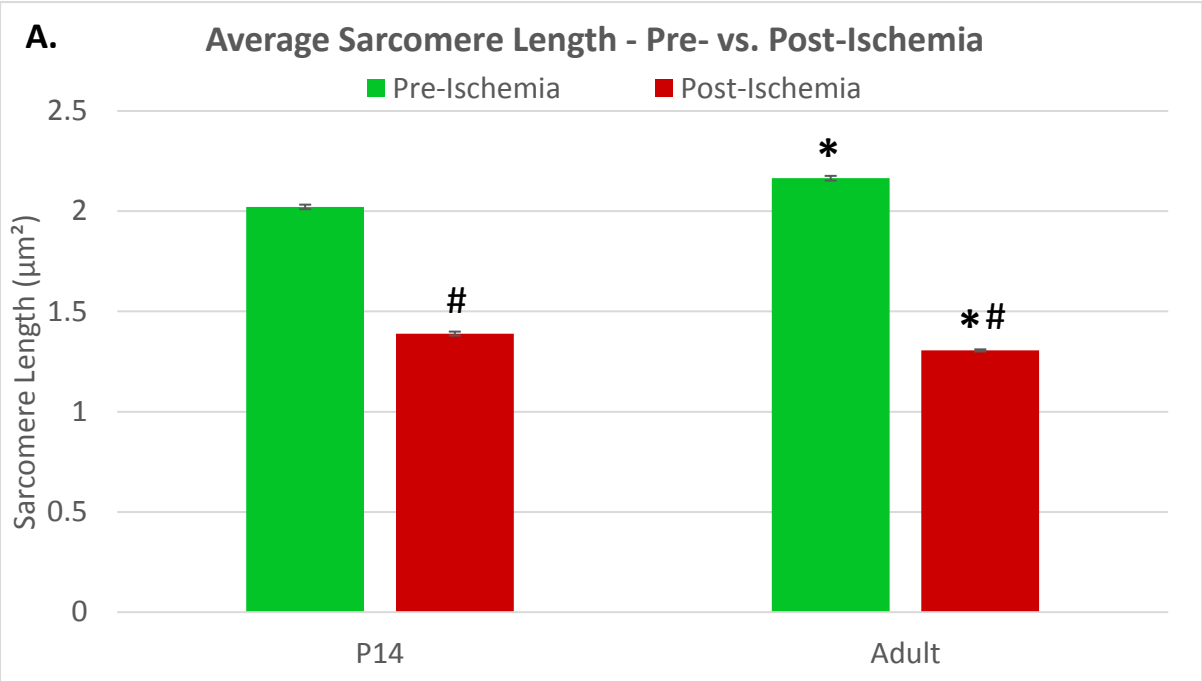

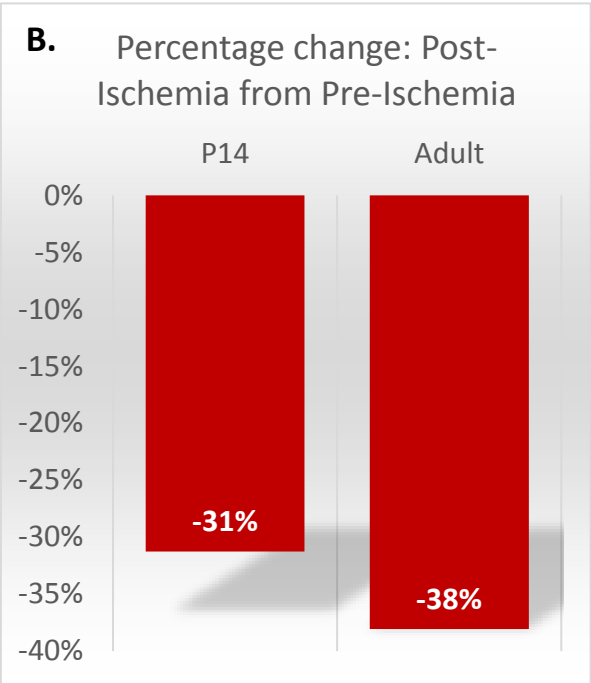

Figure 83. Average sarcomere lengths of pre- vs. post-ischemic hearts in 14-day old and adult samples. Data presented as mean ± SE. * = statistically significant difference compared to 14-day old samples ($p < 0.05$). # = statistically significant difference compared to pre-ischemic samples ($p < 0.05$). **(A)**. Percentage change in sarcomere length from pre- to post-ischemic samples in 14-day old vs. adult hearts **(B)**. (P14 n = 3 hearts, 1080 sarcomeres. Adult n = 3 hearts, 2352 sarcomeres).

8.3.2 The effect of ischemia on caveolae abundance in adult and 14-day old hearts

As mentioned in **Section 7.3.3.2**, the number of caveolae in control hearts is statistically significantly higher in 14-day old samples in comparison with adults ($p < 0.001$), in line with the higher levels of expression of Caveolin-1, -2 & -3 in 14-day old hearts detected by proteomic analysis. While this trend continues to be true post-ischemia, a statistically significant difference was not seen between the two age groups.

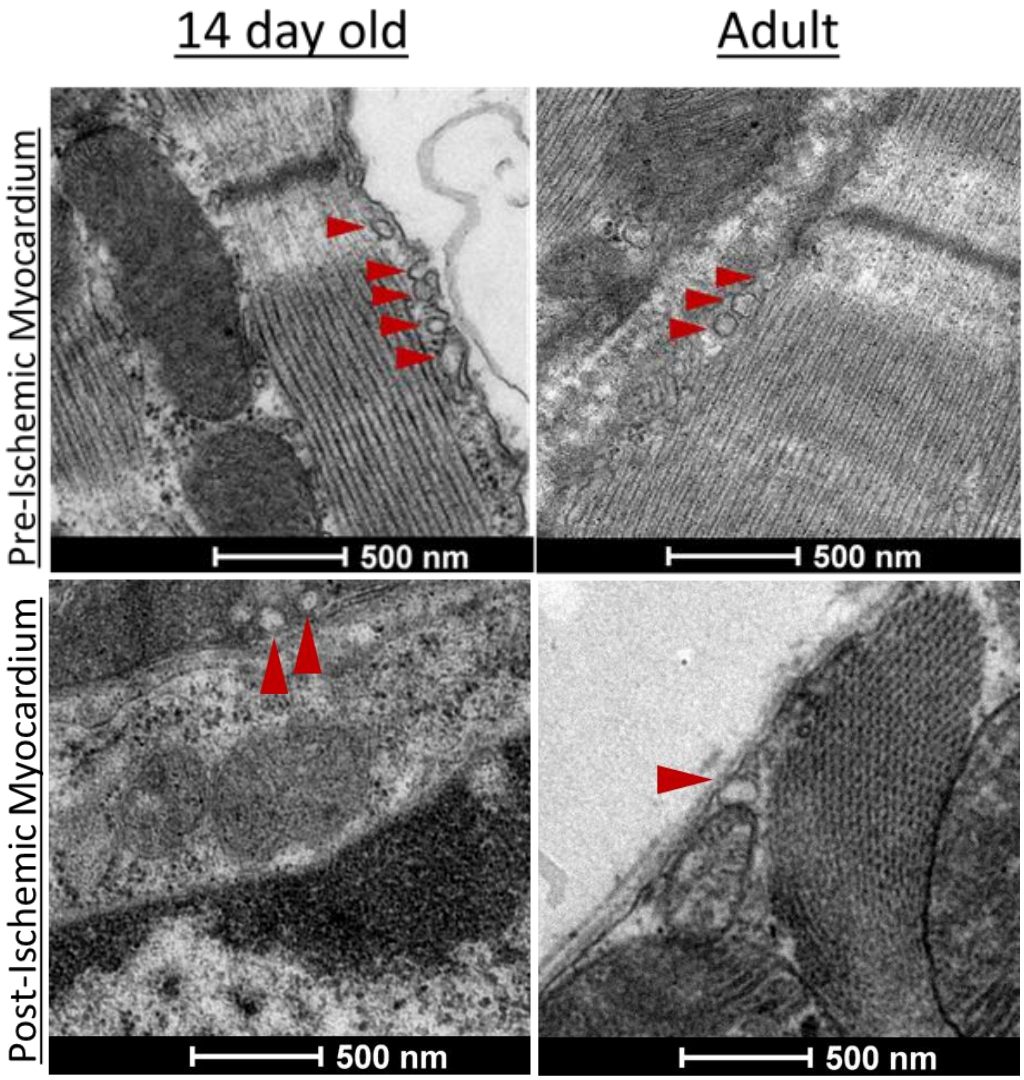

Figure 84. Electron micrograph examples showing the differences in average caveolae number between pre- & post-ischemic hearts, both in 14-day old and adult samples. Red arrows indicate caveolae.

Whilst the number of caveolae per µm decreased following ischemia in both 14-day old and adult samples, this reduction was only statistically significant in 14-day old samples ($p < 0.001$). However, the average number of caveolae in post-ischemic 14-day old samples remains higher than that seen in adults both pre- & post-ischemia (1.9 caveolae/µm vs. 1.5 caveolae/µm & 0.4 caveolae/µm, respectively).

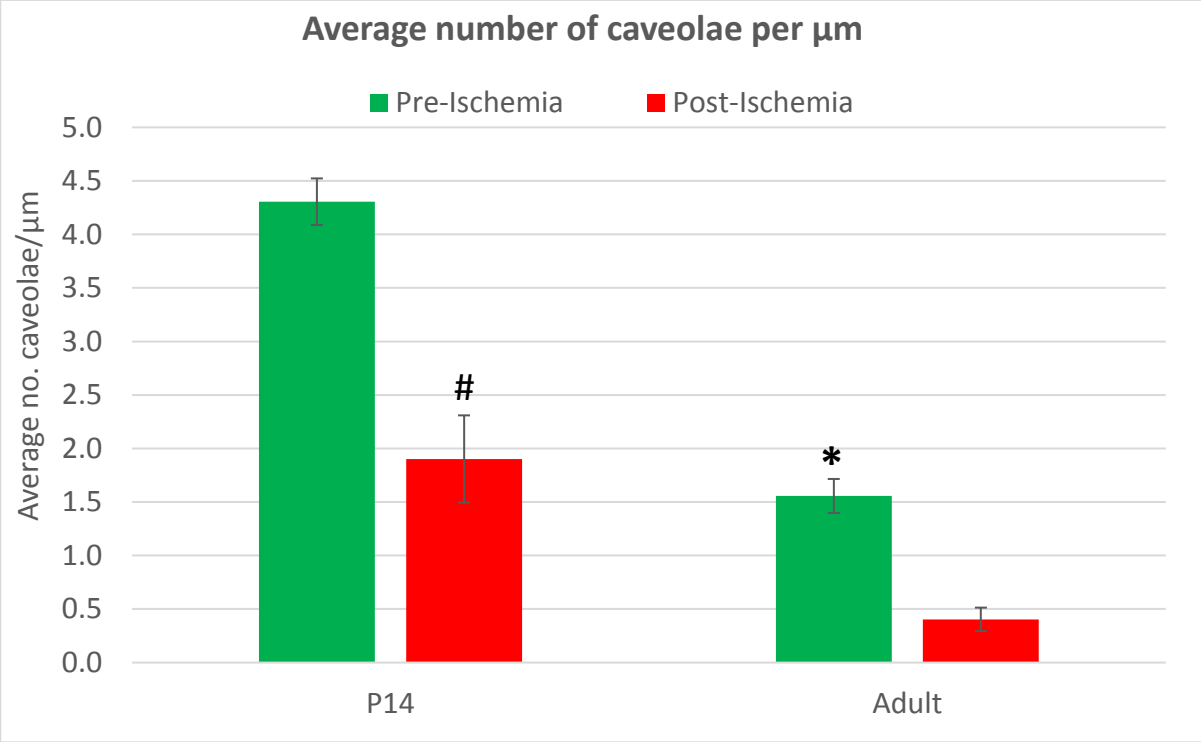

Figure 85. Graph showing the average number of caveolae per µm in pre-ischemic tissue in comparison with post-ischemic tissue, and between 14-day old and adult hearts. Data presented as Mean ± SE. * = statistically significant difference between P14 & adults ($p < 0.05$). # = statistically significant difference between pre- & post-ischemia ($p < 0.05$). (P14 n = 3 hearts, 13 fields. Adult n = 3 hearts, 5 fields.)

8.3.3 Effect of ischemia and reperfusion on MVB and exosome abundance in 14-day old and adult hearts

8.3.3.1 Effect of ischemia

Examination of Electron Micrographs taken from post-ischemic hearts found what appeared to be fewer clear MVBs, with large circular exosomes, in 14-day old post-ischemic hearts compared to control hearts. This could be due to many of those present in control hearts subsequently being exported from the myocardium during ischemia to trigger cardioprotective signalling. Indeed, the number of vesicles outside of the myocardium itself and between cardiomyocytes, as well as within the myofibres themselves as smaller structures reported to be free exosomes (Sahoo and Losordo 2014), seem to have increased following ischemia in 14-day olds. However, without exosome and MVB specific markers, it is difficult to determine precisely what these structures are and whether they are indeed excreted exosomes or MVBs previously seen in the myocardium possessing cardioprotective signalling properties.

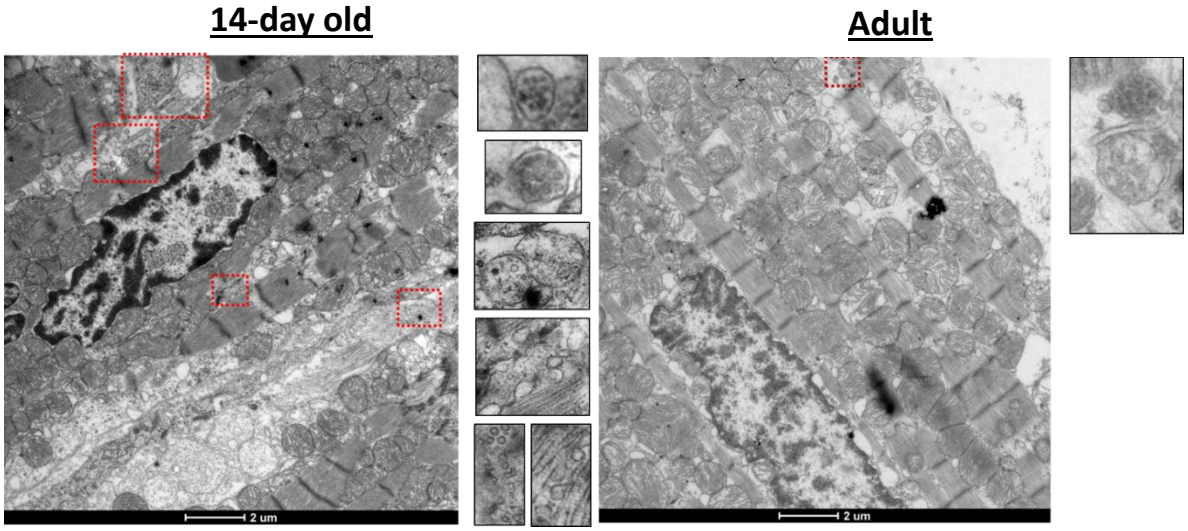

Figure 86. Representative images of putative MVBs containing exosomes in cardiac sections taken from post-ischemic tissue at (**Left**) 14-days of age and (**Right**) from adult rat hearts.

The number of putative MVBs and exosomes appears to remain low in adult samples following ischemia, and 14-day old samples continue to exhibit a greater number of these vesicles than adults. This supports the theory that these reportedly cardioprotective and survival signalling promoting vesicles are present in higher quantities in 14-day old than adult myocardium, and may therefore be related to the greater resistance to cardiac injury seen at this stage of postnatal development.

8.3.3.2 Effect of reperfusion following ischemia

Following reperfusion, the cardiomyocytes themselves appeared to have a much lower number of MVBs than seen in control hearts (**Section 7.3.3.3**), both in 14-day old and adult tissue. However, extracellularly there appeared to be large regions filled with vesicles and particulates, which may reflect released exosomes and related signalling particles resulting from the export of MVBs from the cardiomyocytes post-I/R. Consistent with this, a greater number of these MVBs were identified towards the cardiomyocyte membranes and extracellularly, suggesting efflux of these vesicles out of cardiomyocytes potentially to trigger survival signalling pathways. Moreover, a number of these putative MVBs were detected within or around other cells adjacent to the cardiomyocytes, which may suggest that, following their export out of cardiomyocytes, they are able to interact with and possibly recruit other cell types to areas of cardiac injury to promote healing, as will be discussed further in **Section 8.4**.

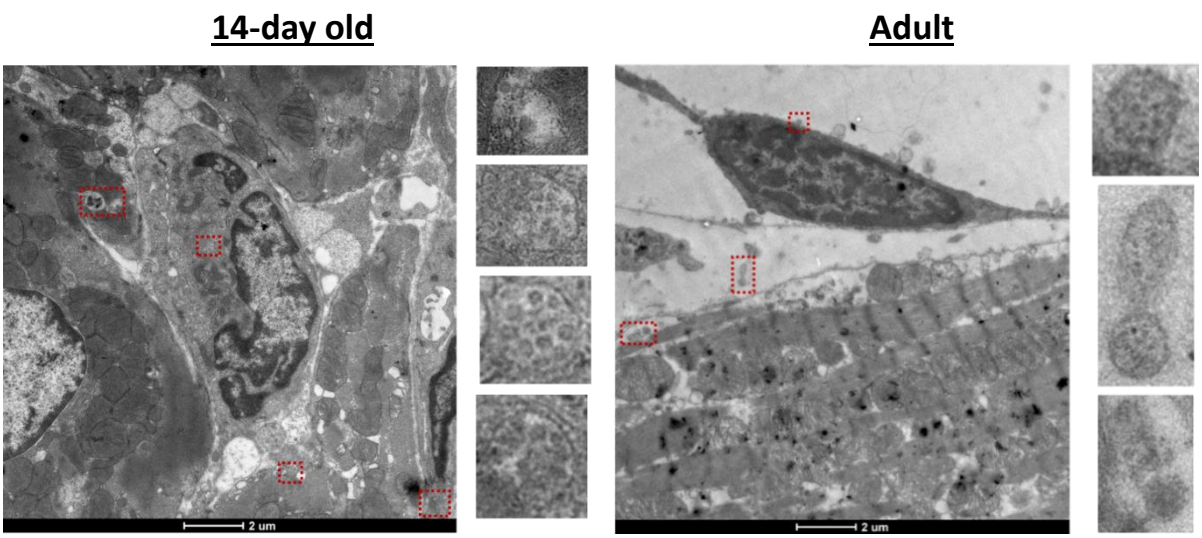

Figure 87. Representative images of putative MVBs containing exosomes in cardiac sections taken from post-I/R tissue at (**Top**) 14-days of age and (**Bottom**) from adult rat hearts.

Similarly to control and post-ischemic hearts, 14-day old samples appeared to have a greater number of these putative MVBs characterised with large, circular exosomes within each vesicle in comparison with adult samples. While adult samples did exhibit a number of vesicles containing smaller particulates, as seen in **Figure 87** above, they did not appear to contain the larger, circular components most commonly reported in existing literature as exosomes (**Section 7.1.2.2**).

8.3.4 The effect of ischemia on mitochondrial subpopulations in adult and 14-day old hearts

8.3.4.1 Changes in subpopulation distribution

In order to examine the relative numbers of each mitochondrial subpopulation present in the myocardium, and how this differs between the two age groups following ischemia, the area of cardiomyocyte, as well as the collective area of the cardiomyocyte covered by each subpopulation, were measured.

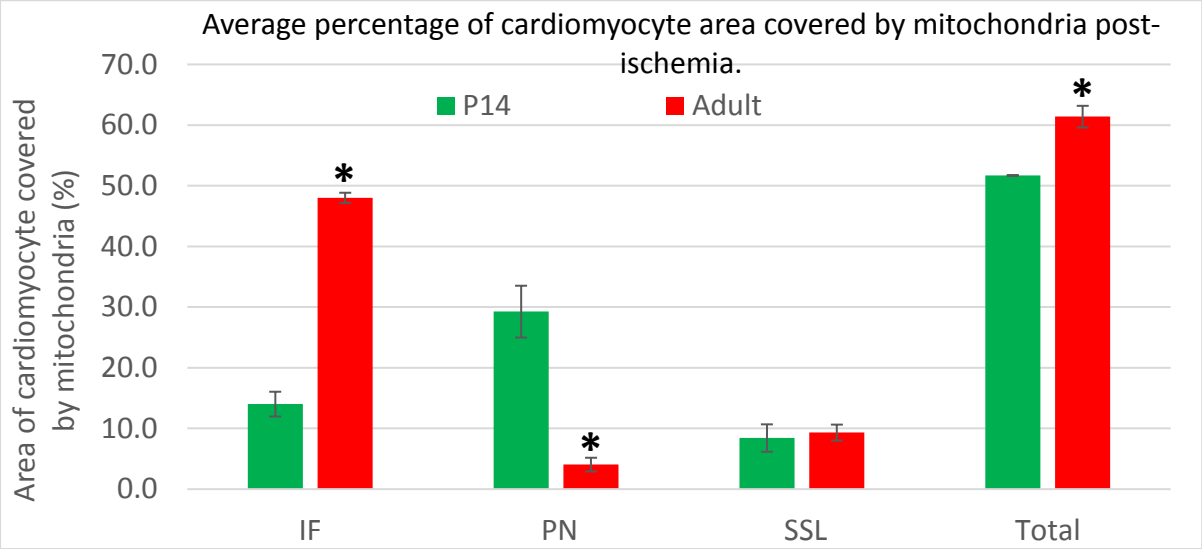

Figure 88. The average percentage of cardiomyocyte covered by mitochondria, by mitochondrial subpopulation. Data presented as Mean ± SE**. *** = statistically significant difference with P14 ($p < 0.05$). (P14 n = 3 hearts, 3 cardiomyocytes. Adult n = 3 hearts, 4 cardiomyocytes).

A greater proportion of the cardiomyocyte was covered by mitochondria in adults (61%) compared with 14-day old (52%). Of these areas, only 14% of the 14-day old cardiomyocyte was comprised of IF in comparison with 48% in adults. However, 14-day olds showed a greater percentage of PN in cardiomyocytes than adults (29% vs. 4%), but a similar proportion of SSL. These patterns of mitochondrial subpopulation abundance between the two age groups mimics that seen in control hearts (**Section 7.3.8**), although with increased percentages in the total area of the cardiomyocyte covered by mitochondria, likely resulting from swelling of the individual mitochondria during ischemia.

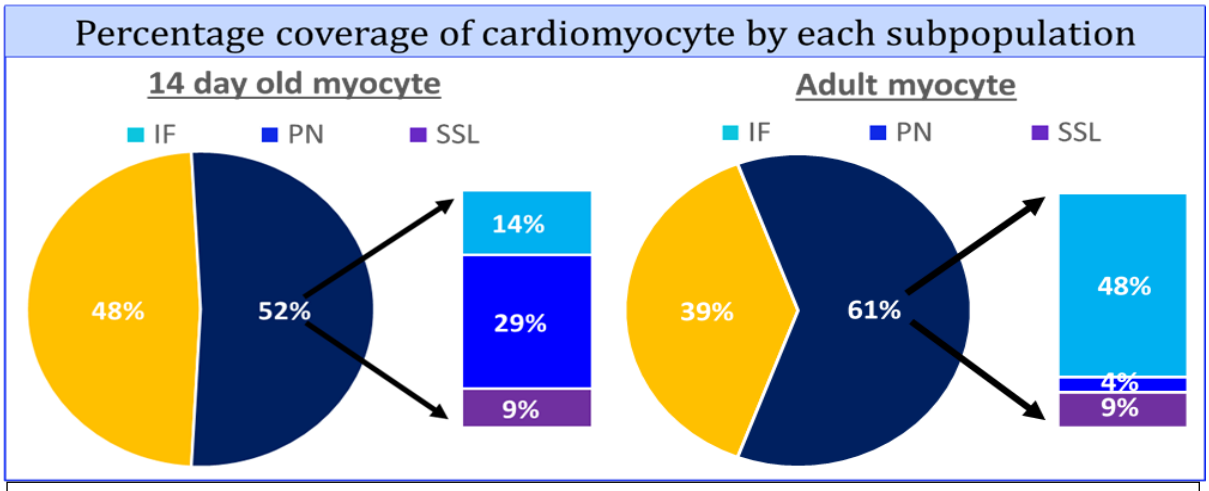

Figure 89. Charts comparing the relative percentages of each mitochondrial subpopulation covering a region of cardiac tissue between the two age groups. (P14 n = 3 hearts, 3 cardiomyocytes. Adult n = 3 hearts, 4 cardiomyocytes). Yellow segment indicates percentage of the cardiomyocyte cross-sectional area free of mitochondria.

Collected data for pre- vs. post-ischemic hearts in terms of the percentage of the cardiomyocyte area covered by each mitochondrial subpopulation was subsequently analysed for any changes in their relative abundance following ischemia (**Figure 90**).

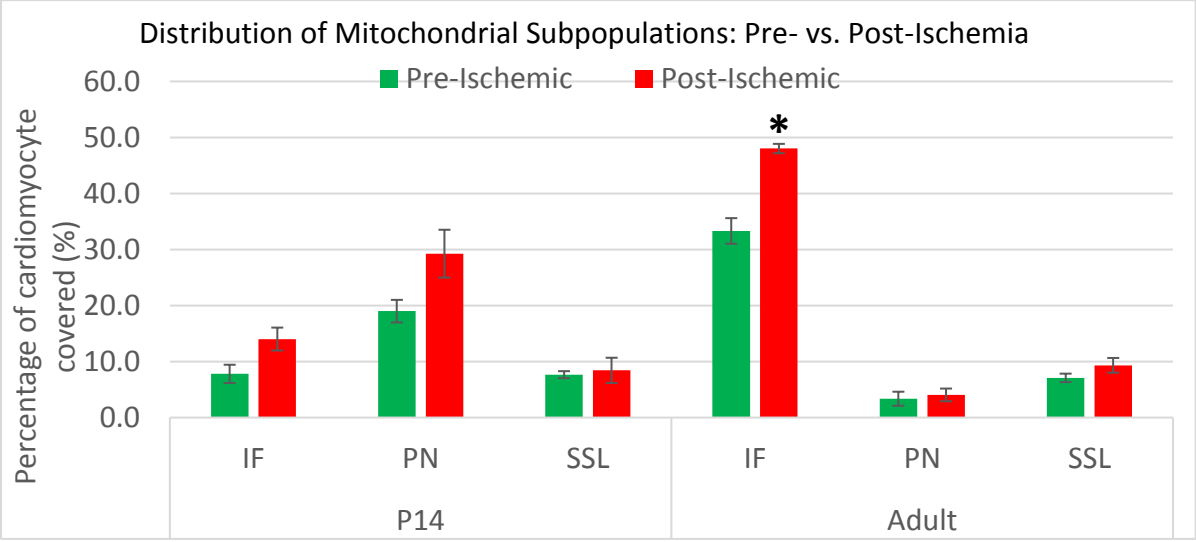

Figure 90. Comparison of the relative abundance of each of the three mitochondrial subpopulations in 14-day old and adult hearts, pre- vs. post-ischemia. Data is presented as mean ± SE. * = statistically significant difference in comparison with pre-ischemic hearts ($p < 0.05$). (n = 3 hearts/group. Pre-ischemic: P14 n = 7 cardiomyocytes, adult = 6 cardiomyocytes. Post-ischemic: P14 n = 3 cardiomyocytes, adult = 4 cardiomyocytes).

Statistically significant differences in the distribution of mitochondrial subpopulations following ischemia was seen only in adult hearts, with an increase in the percentage of

cardiomyocyte covered by IF mitochondria increasing from 33% in pre-ischemic to 48% in post-ischemic hearts ($p < 0.01$). However, it is possible that this change results from an increase in the size of individual mitochondria due to swelling as opposed to changes in the number of IF mitochondria, as the percentage of the other two subpopulations did not appear to change significantly, and it is unlikely that new mitochondria were generated post-ischemia. Similarly, 14-day old PN mitochondria – which are the most abundant subpopulation in this age group – showed a substantial increase in percentage post-ischemia, again likely owing to swelling of pre-existing mitochondria.

8.3.4.2 Changes in morphology

The morphological characteristics of each mitochondrial subpopulation were measured using ImageJ, with statistical analysis run for comparisons both within (**Figure 91 & 92**) and between (**Figure 93**) the two age groups.

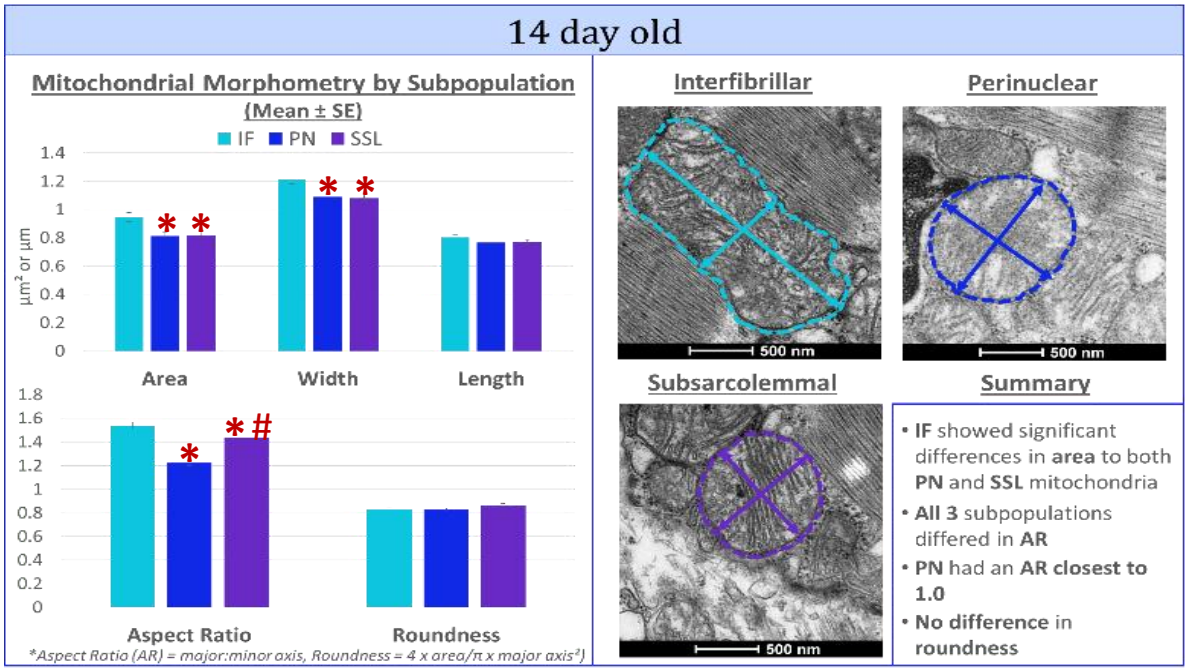

Figure 91. Mitochondrial morphometry in 14-day old hearts following 30 minutes ischemia by subpopulation. Data presented as Mean ± SE. * = statistically significant difference in comparison with IF mitochondria ($p < 0.05$). # = statistically significant difference in comparison with PN mitochondria ($p < 0.05$). Turquoise = Interfibrillar (IF), Blue = Perinuclear (PN), Purple = Subsarcolemmal (SSL). (n = 3 hearts, **IF** n = 342, **PN** = 515, **SSL** n = 326.)

Following ischemia, the area of IF mitochondria were significantly greater than both PN and SSL mitochondria in 14-day old hearts. While ischemia seemed to remove any of the previous differences in roundness seen between the three subpopulations, the AR of all three differed from one another, with PN possessing an AR closest to 1.0, and IF possessing an AR furthest from 1.0.

In adult hearts, all three subpopulations differed from one another in terms of area and AR, with PN possessing the smallest area and an AR closest to 1.0, while SSL had the greatest area and IF had an AR further from 1.0. IF also had the lowest measurement of roundness, whereas PN and SSL did not significantly differ from one another.

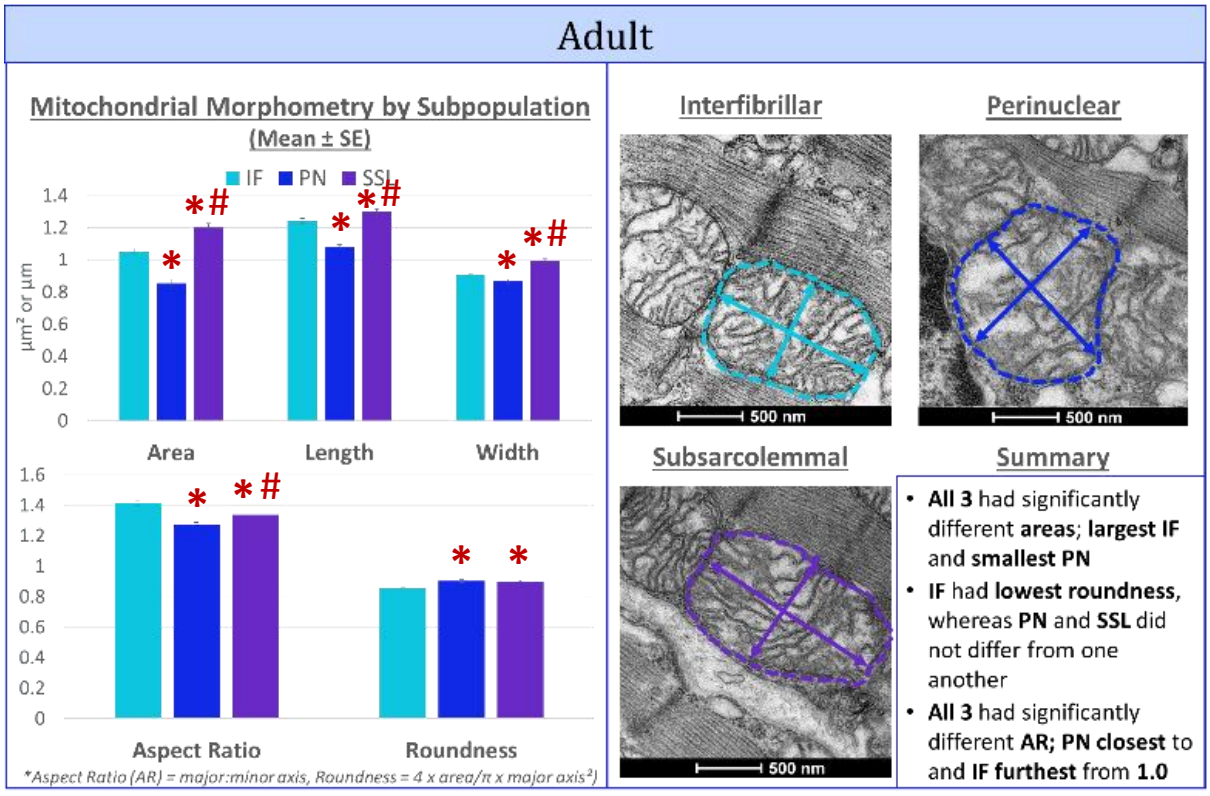

Figure 92. Mitochondrial morphometry in adult hearts following 30 minutes ischemia by subpopulation. Data presented as Mean ± SE. * = statistically significant difference in comparison with IF mitochondria ($p < 0.05$). # = statistically significant difference in comparison with PN mitochondria ($p < 0.05$). Turquoise = Interfibrillar (IF), Blue = Perinuclear (PN), Purple = Subsarcolemmal (SSL). (n = 3 hearts, **IF** n = 1054, **PN** = 381, **SSL** n = 514.)

Comparisons between the two age groups showed that, whilst IF had the greatest area, length and width in adults, as well as an AR furthest from 1.0, these mitochondria did not differ in roundness between the two age groups. In contrast, excluding the length of PN mitochondria, PN and SSL differed in each measurement between the two age groups, with smaller areas, AR closest to 1.0, and lower measurements of roundness in 14-day olds compared with adults. The greater roundness of adult PN and SSL mitochondria following ischemia may indicate a greater degree of mitochondrial fission in adults, with subsequent fragmented and rounded morphology (Ong and Hausenloy 2010).

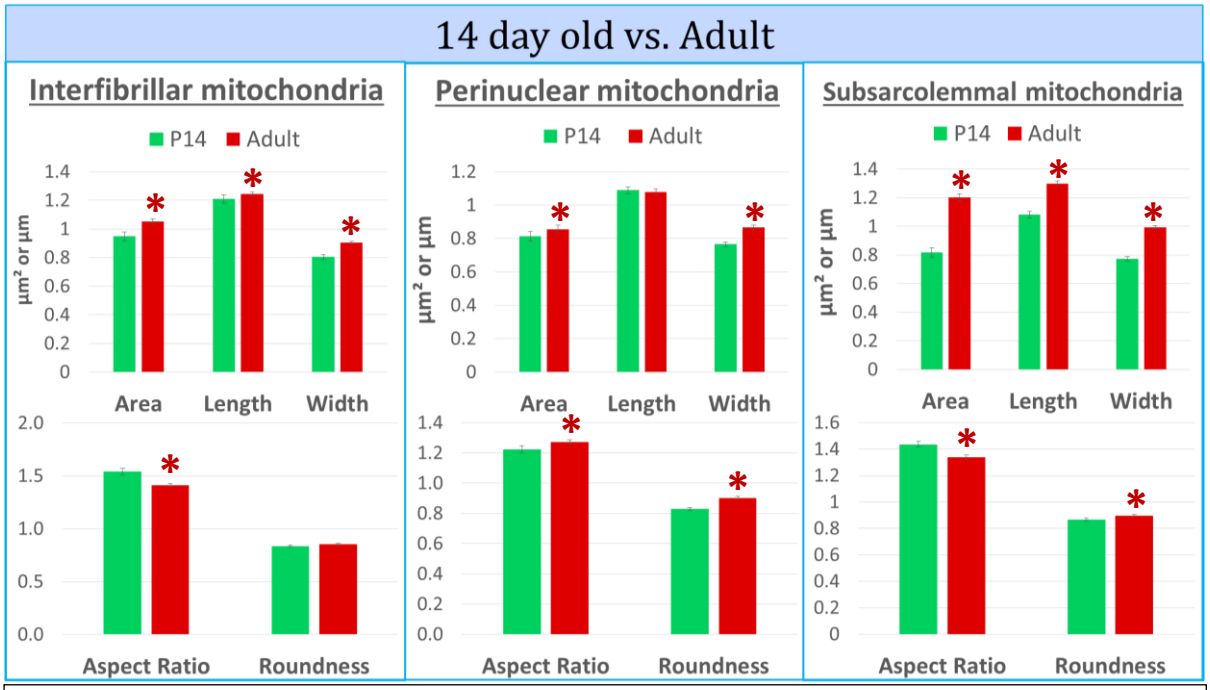

Figure 93. Mitochondrial morphological differences between P14 and Adult hearts, by mitochondrial subpopulation. Data presented as Mean ± SE. * = statistically significant difference in comparison with 14-day old hearts ($p < 0.05$). (n = 3 hearts/age group. P14: **IF** n = 342, **PN** = 515, **SSL** n = 326. Adult: **IF** n = 1054, **PN** = 381, **SSL** n = 514).

In order to assess the differences in changes to mitochondrial morphology following ischemia, analysis was performed to identify statistically significant differences between the three mitochondrial subpopulations within each age groups (**Figure 94**). In both age groups,

all three mitochondrial subpopulations showed significantly increased area, length, width, as well as ARs and roundness measurements closer to 1.0 following ischemia.

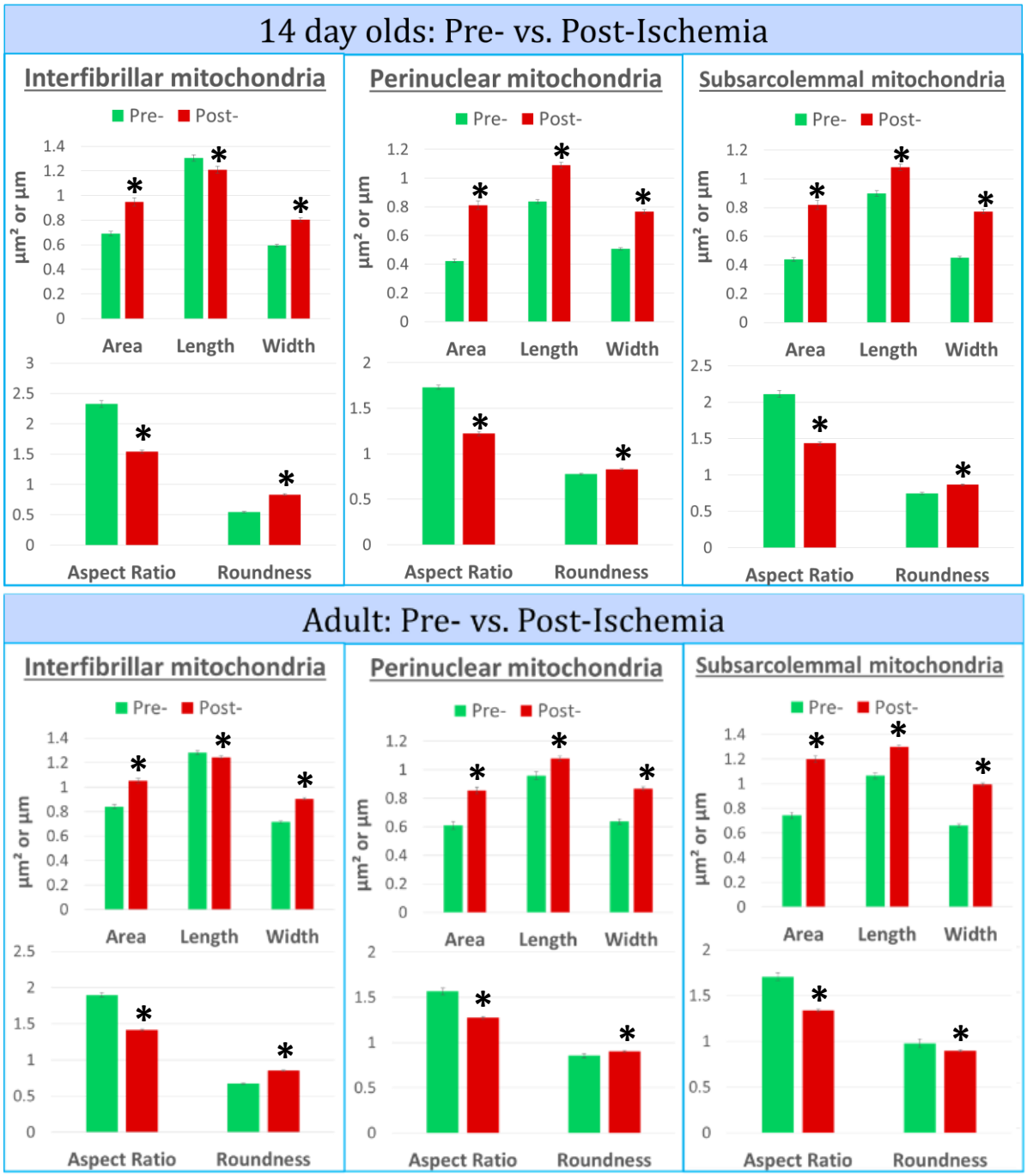

Figure 94. The average differences in mitochondrial morphometry following ischemia, by age group. Data presented as Mean ± SE. * = statistically significant difference with pre-ischemic hearts ($p < 0.05$). (n = 3 hearts/group.)

To compare post-ischemic morphological changes between the two age groups, the percentage change of each measurement from pre-ischemic to post-ischemic values was calculated. All three subpopulations showed a greater increase in area post-ischemia in 14-day old hearts, with the most dramatic change seen in PN (92% increase vs. 40% increase in area). In both age groups, however, the percentage change in PN roundness was similar (7% vs. 5%), becoming closer to 1.0 post-ischemia. In all three subpopulations, both age groups displayed a drop in AR towards 1.0, with an approximately 10% greater drop in 14-day olds than adults.

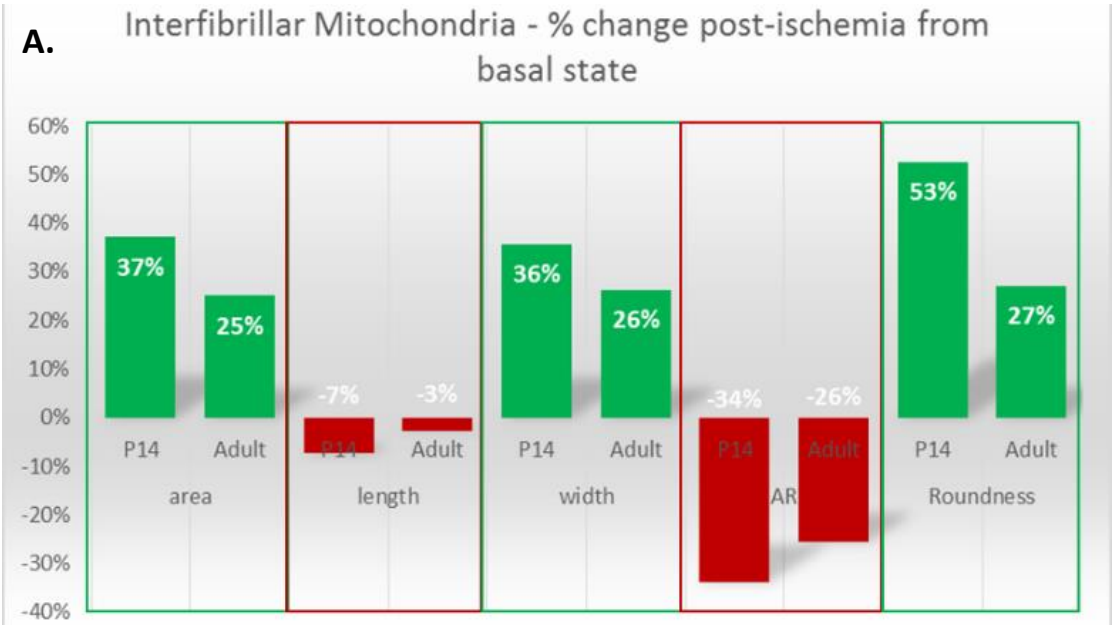

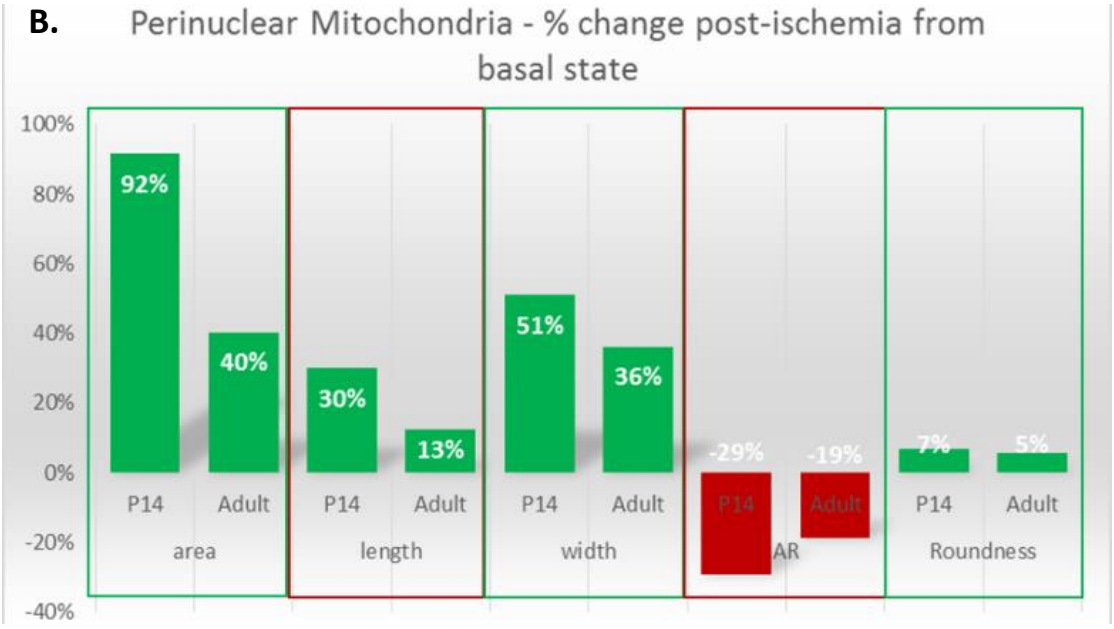

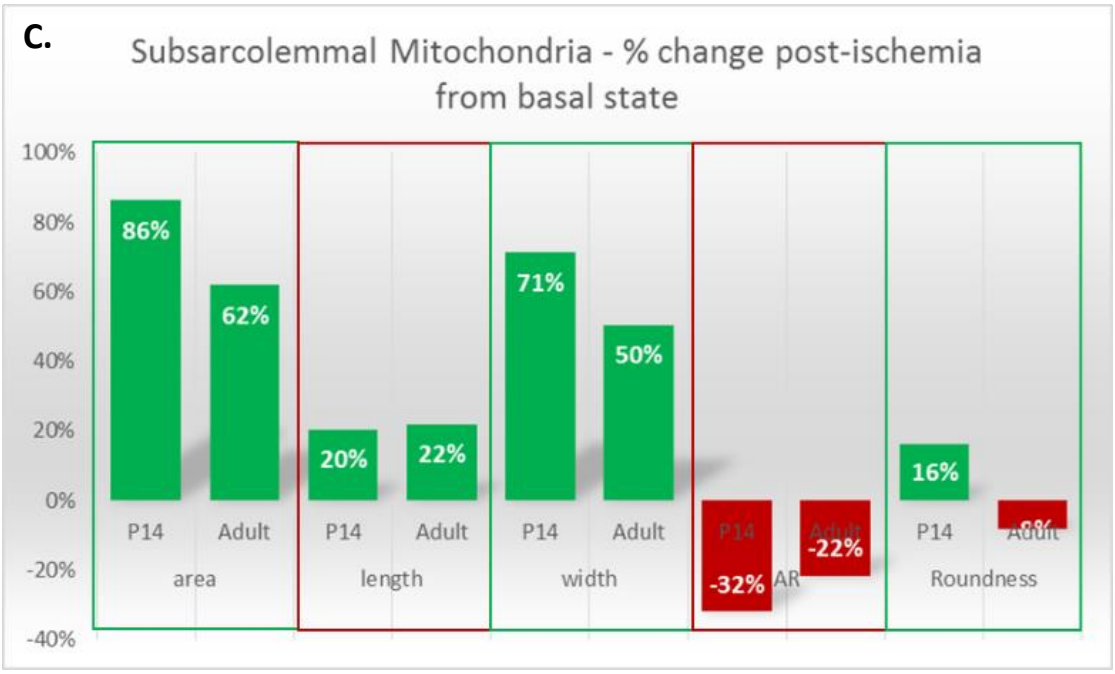

Figure 95. Comparison of percentage changes in mitochondrial morphology, calculated as the pre-ischemic to post-ischemic percentage change, between the two age groups for Interfibrillar (**A**), Perinuclear (**B**), and Subsarcolemmal (**C**) mitochondria.

Overall, post-ischemic changes in mitochondrial morphology, such as area, appeared to be more dramatic across all three subpopulations in 14-day old hearts than in adults.

8.3.4.3 Changes in intercristae space following ischemia

Following ischemic injury, mitochondrial swelling is known to occur as a result of factors such as an acidic cellular pH, breakdown of creatine phosphate and depletion of ATP levels, resulting in the disruption of the mitochondria and its functional abilities (Schmiedl et al. 1993). Indicators of swelling include an increase in the area of mitochondria, as well as disruption of the mitochondrial matrix and larger intercristae spaces. To assess the differences in this form of mitochondrial disruption, and the differences in the effect of ischemia on mitochondrial swelling between the two age groups, electron micrographs were analysed using ImageJ, highlighting regions within the mitochondria where the cristae were

no longer condensed, and intercristae spaces could be seen. **Figure 96** shows an example of post-ischemic IF in 14-day old and adult hearts.

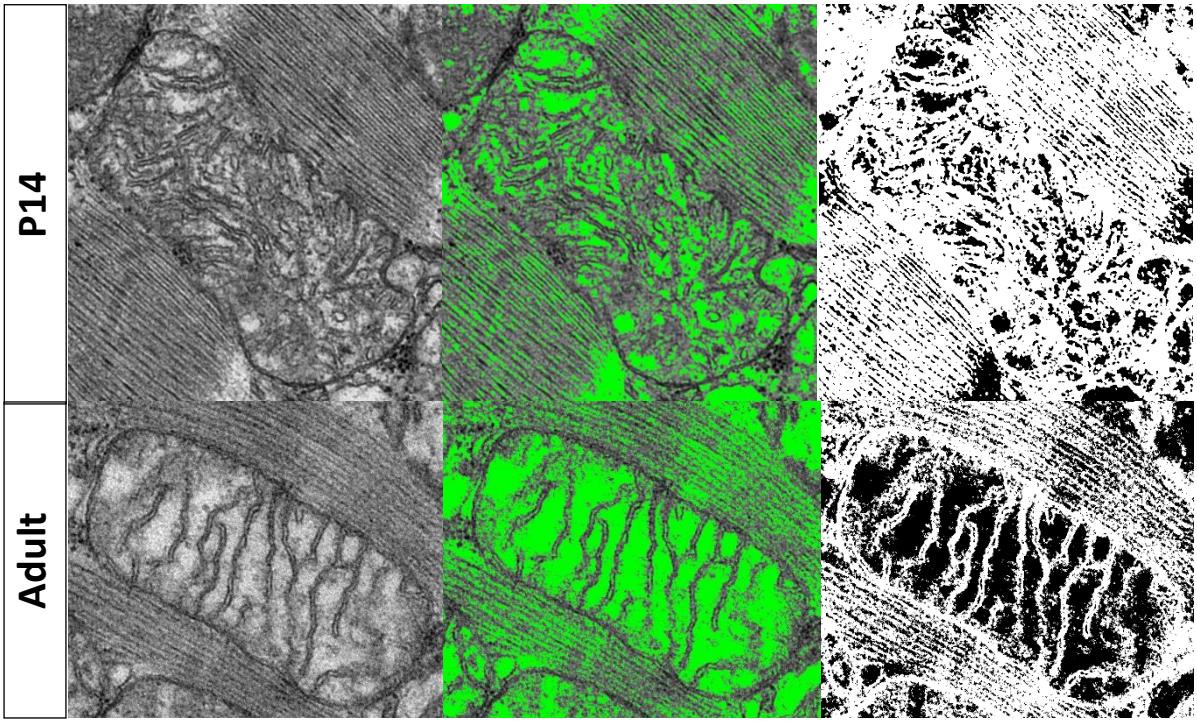

Figure 96. Examples of differences in mitochondrial swelling post-ischemia between the two age groups, as indicated by the size of intercristae spaces. Central (green) and right hand (negative) images taken during 'Threshold' selection for regions to be measured from ImageJ.

Intercristae spaces post-ischemia were greater in samples taken from adult hearts in comparison with 14-day old hearts, both in terms of the mean area of intercristae spaces (μm^2) ($p < 0.001$) and the percentage of the total mitochondrial area comprised of intercristae spaces ($p < 0.001$). This indicates a greater degree of mitochondrial disruption and swelling in adult mitochondria, and therefore more substantial cardiac injury in this age group than in 14-day olds.

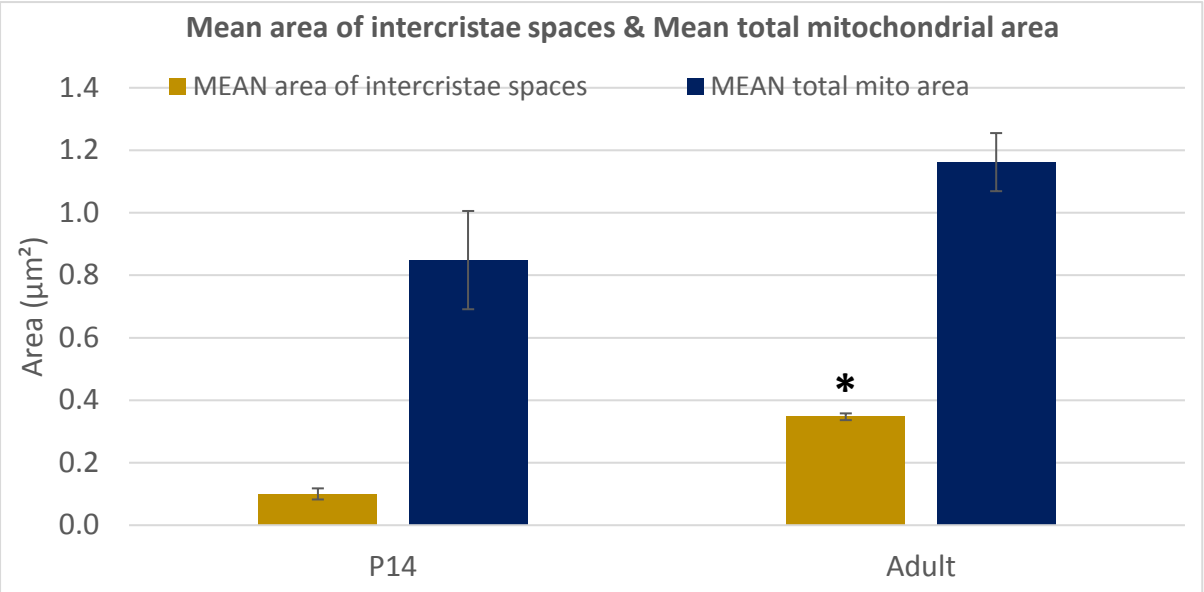

Figure 97. Changes in intercristae spaces compared with the total area of the mitochondria, by age group. Data presented as Mean ± SE. * = statistically significant difference compared to 14-day old hearts ($p < 0.05$). (n = 3 hearts/age group. P14 n = 8 fields, 36 mitochondria. Adult = 10 fields, 52 mitochondria).

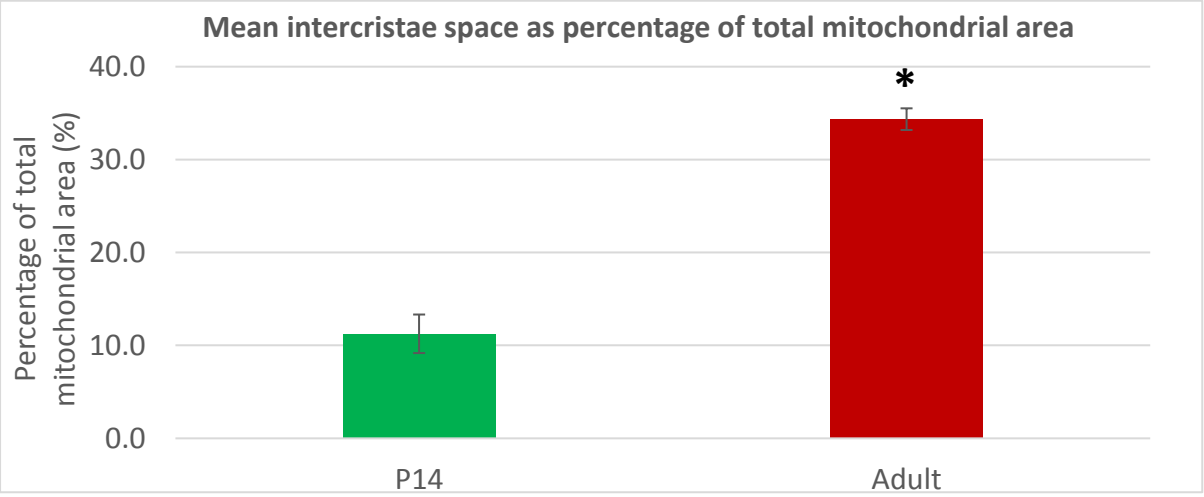

Figure 98. Intercristae spaces in interfibrillar mitochondrion comprised of, by age group. Data presented as Mean ± SE. * = statistically significant difference compared to 14-day old hearts ($p < 0.05$). (n = 3 hearts/age group. P14 n = 8 fields, 36 mitochondria. Adult = 10 fields, 52 mitochondria).

As no significant differences were seen in the sizes of intercristae spaces between the three different mitochondrial subpopulations, only data from IF mitochondria has been included to demonstrate the age-dependent differences following ischemia.

8.3.4.4 Changes in intercristae spaces following ischemia and reperfusion

As described in **Section 8.3.4.5**, mitochondria were assessed for the degree of mitochondrial disruption and swelling through measurement of the percentage of the mitochondrial area made up by intercristae spaces, in this case in samples taken from hearts following ischemia/reperfusion.

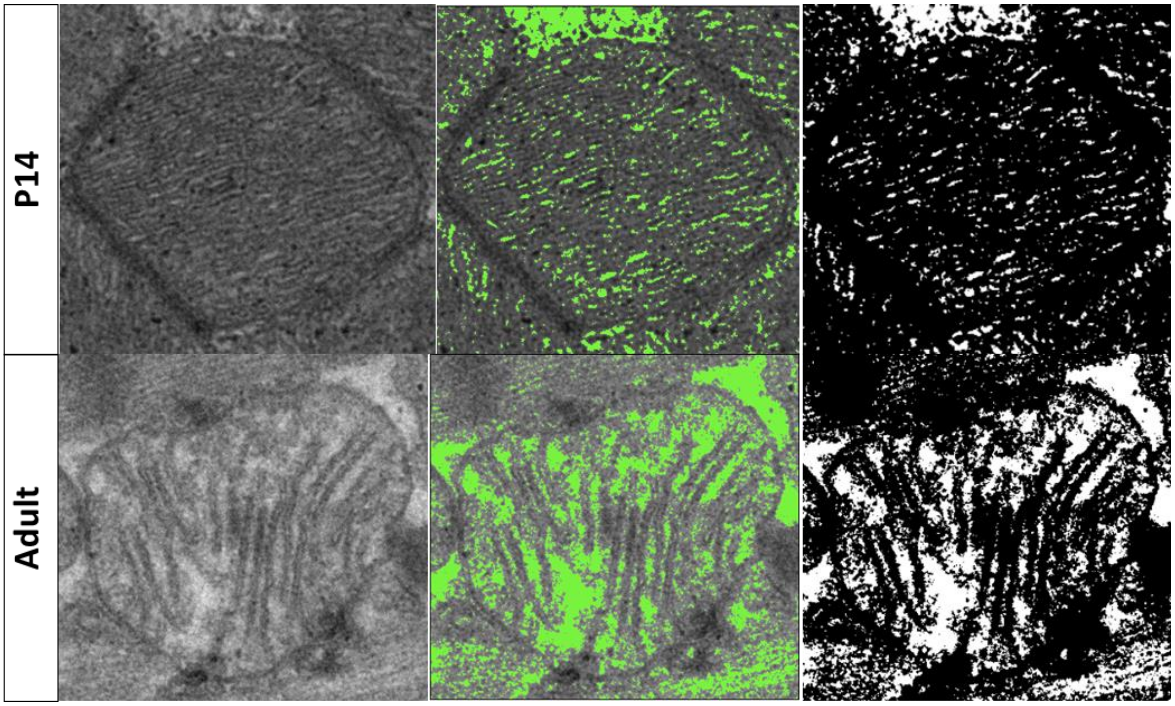

Figure 99. Examples of differences in mitochondrial swelling post-I/R between the two age groups, as indicated by the size of intercristae spaces. Central (green) and right hand (negative) images taken during 'Threshold' selection for regions to be measured from ImageJ.

Similarly to post-ischemic samples, intercristae spaces post-I/R were greater in samples taken from adult hearts in comparison with 14-day old hearts, both in terms of the mean area of intercristae spaces (μm^2) ($p < 0.001$) and the percentage of the total mitochondrial area comprised of intercristae spaces ($p < 0.05$). This indicates a greater degree of mitochondrial disruption and swelling in adult mitochondria, and therefore more substantial cardiac injury in this age group than in 14-day olds. No statistically significant differences were seen in intercristae spaces between post-ischemic and post-I/R mitochondria.

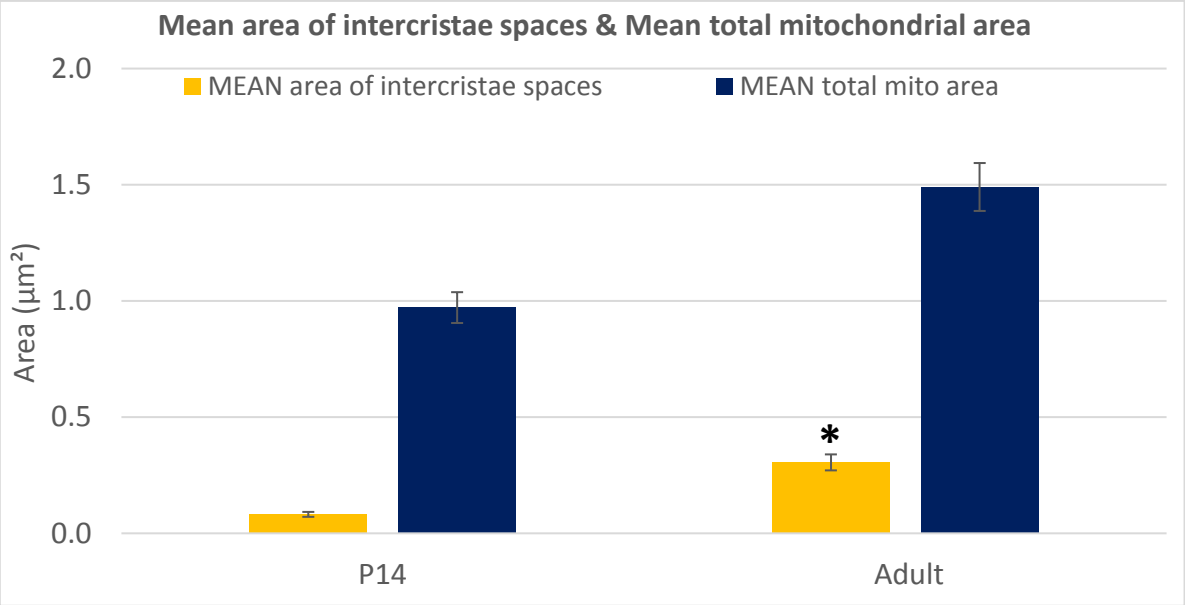

Figure 100. The mean area of intercristae spaces compared with the total area of the mitochondria, by age group. Data presented as Mean ± SE. * = statistically significant difference compared to 14-day old hearts ($p < 0.05$). (n = 3 hearts/age group. P14 n = 4 fields, 19 mitochondria. Adult n = 4 fields, 16 mitochondria).

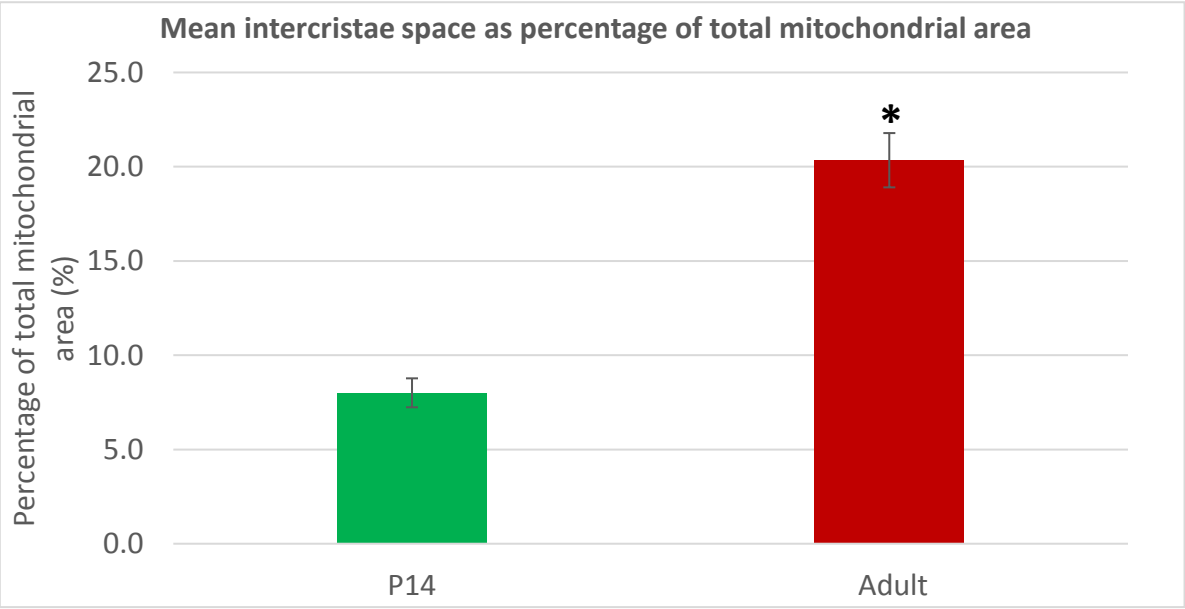

Figure 101. The mean percentage of each mitochondrion comprised of intercristae spaces, by age group. Data presented as Mean ± SE. * = statistically significant difference compared to 14-day old hearts ($p < 0.05$). (n = 3 hearts/age group. P14 n = 4 fields, 19 mitochondria. Adult n = 4 fields, 16 mitochondria).

8.4 Discussion

8.4.1 Changes in mitochondrial morphology and intercristae spaces during ischemia indicate less damage in 14-day olds compared to adults

Following ischemia, the pattern of differences in mitochondrial morphology between the two age groups remains similar, with adult mitochondria possessing a greater area and higher roundness than 14-day old mitochondria. However, calculation of the percentage changes in mitochondrial morphology showed that 14-day olds seemed to have the greatest increase in area, roundness, and decrease in AR across all three subpopulations in comparison with adults. Despite this, intercristae spaces were smaller in 14-day olds, indicating that although there appeared to be a greater degree of mitochondrial swelling in 14-day olds, there was less disruption to mitochondrial ultrastructure, indicating these mitochondria likely remain relatively healthy and functional in comparison with adults. Moreover, the smaller increase in mitochondrial area in adults may indicate a greater degree of fission than that seen in 14-day olds, and further work will be conducted to analyse indicators of mitochondrial fission. The incidence of mitochondrial fission will be important to identify in our two age groups, as mitochondrial fission is known to be harmful in the context of I/RI, with adult mitochondria exhibiting increased indicators of fission also showing an increased probability of mPTP opening (Kuzmicic et al. 2011). Furthermore, inhibition of mitochondrial fission has been shown to protect cardiomyocytes against I/RI (Ong et al. 2010), with specific inhibition of pro-fission protein, Drp-1, resulting in a greater number of mitochondria able to maintain their elongated morphology, inhibition of mPTP opening, and a resulting decrease in infarct size.

Whilst only focusing on IF and SSL, Kuzmicic et al. state that, in the context of diabetic cardiomyopathy, the majority of mitochondrial abnormalities tend to occur in IF, meaning

there is a drop in metabolic activity that causes mechanical deficiency in these hearts. In our adult samples, there is a greater degree of disruption in IF mitochondria – as illustrated by a larger percentage of the mitochondrial area being comprised of intercristae spaces – in comparison with 14-day olds. Combined with the fact that, as discussed in **Section 4.4.2**, adults have a much higher proportion of IF mitochondria in comparison with 14-day olds, this suggests it is possible that the greater vulnerability of this subpopulation, in addition to its dominance in the adult heart, may contribute to the reduced resistance of this age group to I/RI, and that the higher numbers of PN in 14-day olds confer some sort of cardioprotection in turn.

Kalkhoran et al. (2017) found that all three subpopulations exhibited increased sphericity following ischemia, as was the case for both age groups in our work. However, the authors state that an increase in area was seen only in PN, whereas all three subpopulations showed an increase in area in both our 14-day and adult samples. Nevertheless, other morphological features were shown to be altered post-ischemia, such as increased indicators of fragmentation in IF, a loss of elongated morphology in SSL, and decreased AR in PN (Kalkhoran et al. 2017). H_2O_2-mediated injury in neonatal cardiomyocytes results in increased roundness of the mitochondria as a result of disruptions to Ca^{2+}-handling and loss of the mitochondrial membrane potential (Akao et al. 2003), and while all three subpopulations did show increased roundness following ischemia, PN showed the smallest increase in both age groups. Whilst IF showed a 53% increase in roundness in 14-day olds compared with 27% in adults, and 16% compared with 8% in SSL mitochondria, PN only showed a 7% increase in 14-day olds and 5% in adults. Whether this is a result of a high starting roundness compared to other subpopulations even in control hearts, or whether this greater roundness is in some way protective to the heart, is uncertain. However, the

fact that this subpopulation appears to show the least drastic alterations in roundness following ischemia, and is also the most prevalent form in the 14-day old heart, may indicate that the predominance of this more resistant subpopulation in 14-day olds links to the reduced cardiac vulnerability in this age group. Interestingly, the greatest difference in percentage increase of area between the two age groups existed within PN, at more than double in 14-day olds (92% vs. 40%). Whilst SSM show a similar percentage increase in area (86%) to PN in 14-day olds, there is a much smaller difference in comparison with adults (62%). IF showed a lesser degree of swelling, with a 25% increased area in adults and 37% increase in 14-day olds, contrasting findings by Kalkhoran et al. which state that IF and SSL did not show any significant increase in area. However, it should be noted that this study used only a 20 minute period of ischemia, whereas hearts underwent 30 minutes ischemia in our work. Whether discrepancies between our findings and previous reports result from this difference in the ischemic period remains to be seen, but further work will need to be conducted, with an increase in n-numbers, to ensure that these trends hold true. Furthermore, it will be important to analyse mitochondrial morphology following reperfusion to see whether there are signs of recovery closer to control measurements, or further fragmentation and fission.

8.4.2 Mitochondrial disruption following I/R is greater in adult hearts

The data showing the change in mitochondria after I/R are similar to the changes seen after ischemia alone (as discussed in **Section 8.4.1**) where adult hearts showed larger intercristae spaces than those seen in 14-day old hearts. No significant differences were seen between post-ischemic and I/RI hearts within each age group, indicating the full extent of mitochondrial swelling does occur during ischemia. These data demonstrate that mitochondrial disruption is greater in adults than 14-day old hearts during both ischemia

and reperfusion, and that mitochondria in 14-day old hearts seem to maintain a more healthy and functional state following I/RI, potentially contributing to the greater resistance to cardiac injury seen in this age group.

8.4.3 Abundance of MVBs was higher in 14-day olds than adults with or without cardiac insult

As shown in **Section 7.3.3.3**, control 14-day old hearts had a greater number of MVBs present within cardiomyocytes themselves in comparison with adult samples. Whilst this difference in MVB abundance between 14-day old samples and adults appeared to remain following both ischemia and reperfusion, there appeared to be fewer within cardiomyocytes than that seen in control hearts. A potential explanation for this could be that many MVBs are present in control hearts, and that these are either exported from cardiomyocytes following ischemia and reperfusion to target and release transported exosomes directly into recipient cells, release free exosomes into the extracellular space to bind with receptors of target cells, or are released as free exosomes within the myofibres themselves to trigger cardioprotective signalling (Ailawadi, Wang et al. 2015). Although the nature of electron micrographs as a snapshot of molecular events is limiting, the drop in number of MVBs within cardiomyocytes themselves, particularly in 14-day old hearts, seemed to correspond to the presence of MVBs that appeared to be localised around other cell types, suggesting they may have been exported from the myocardium to target and recruit such cells. Previous studies have indeed suggested that exosomes may be able to signal to and mobilise stem and progenitor cells following I/RI in order to facilitate the repair and remodelling of damaged myocardium (Sahoo and Losordo 2014). Furthermore, exosomes have been demonstrated to be mediators of the cardioprotective effects of remote-iPC (RIPC), with depletion of exosomes or targeting and silencing of its components resulting in the loss of

the infarct size reducing effect of RIPC (Barile, Moccetti et al. 2017). As previously mentioned, iPreC has been shown to be ineffective in providing cardioprotection to the immature heart, which raises the possibility that these hearts already possess high levels of survival signalling pathway proteins ready for activation, in addition to a greater number of exosome containing MVBs in control hearts that can be released upon cardiac injury. In order to further investigate the potential role of MVBs and exosomes in the resistance of 14-day old hearts to I/RI, future work would require the use of exosome specific staining or quantitative methods with the inclusion of samples from 7-day old hearts.

8.4.4 The abundance of caveolae decreased post-ischemia only in 14-day old hearts

In-line with previous studies, the number of caveolae present in cardiomyocytes following ischemia decreased in comparison with control hearts in both age groups, although this difference was not statistically significant in adult samples. This may result from the difficulty in finding clear sections within samples from which these counts could be taken in adult samples, resulting in a relatively low number of fields of measurement. However, both pre- and post-ischemic samples from 14-day old hearts showed a greater number of caveolae than adults, which is consistent with previous reports that treatments preventing the loss of caveolae following I/R result in cardioprotection and decrease myocardial injury (Hu, Zhang et al. 2017).

8.4.5 Ischemia was associated with a decrease in sarcomere length

Sarcomere lengths were statistically significantly decreased following ischemia both in 14-day old and adult samples, in-line with the hypercontracture of cardiomyocytes that occurs. However, adult cardiomyocytes displayed significantly shorter sarcomere lengths in

comparison to 14-day old cardiomyocytes, despite being higher in pre-ischemic samples, indicating a greater degree of hypercontracture in adult hearts post-ischemia. As hypercontracture occurs as a result of ATP-depletion and Ca^{2+}-overload following cardiac insult, with greater degrees of hypercontracture shown to be associated with larger regions of necrotic contraction bands in infarcted tissue (Ruiz-Meana and Garcia-Dorado 2009), these findings indicate greater damage in adult hearts following ischemia, and that 14-day old hearts require longer than the implemented 30 minute period of ischemia in order to sustain equivalent degrees of myocardial injury.

8.4.6 Summary & Conclusion

The presence of cardioprotective structures such as MVBs and caveolae was found to be greater in 14-day old samples than adults following ischemia and reperfusion in a similar manner to control hearts, correlating with the greater resistance to cardiac injury seen in 14-day olds. Similarly, analysis of mitochondrial morphology and disruption found that adult samples displayed a greater degree of injury and mitochondrial dysfunction than 14-day old samples. These findings therefore indicate a greater resistance of mitochondria to cardiac injury, as well as a potential mechanism of cardioprotection through the greater abundance of MVBs and caveolae in 14-day olds. Future work will need to replicate these measurements in 7-day old samples in order to confirm that these differences also follow the biphasic profile seen in cardiac vulnerability over the course of postnatal development.

Chapter 9: Summary, Limitations & Future Work

9.1 Summary of work

The key findings of this work revolve around the identification of a number of central survival signalling-related proteins that demonstrated a biphasic profile of expression over the

course of postnatal development, correlating with the cardiac vulnerability profile across these age groups. This included important RISK-SAFE signalling proteins, such as Akt and PKCε, that are commonly discussed in the context of I/RI in the heart and demonstrated an overall biphasic trend, as summarised in **Figure 102**. However, it is important to note that statistically significant differences in expression between 7-day old and 14-day olds was not seen in Akt, PKCε, and a number of other RISK-SAFE related proteins – labelled 'trend' in blue (**Figure 102**) – with the lack of significance in comparison with 7-day olds likely resulting from the small sample number (n = 4) for this age group. It will therefore be important in future work to increase the sample size for these 7-day old hearts, in order to further investigate whether or not a true biphasic profile exists for these proteins, thus implicating them as causative in the vulnerability profile to I/RI seen across these four age groups.

In contrast, AMPK, which is linked to cell survival and interacts with a number of RISK-SAFE signalling proteins, was found to demonstrate a biphasic profile of expression with statistical significance between 14-day old hearts in comparison with 7-day old, 28-day old and adult hearts. Due to its known cardioprotective effects in the context of I/RI, through the upregulation of autophagy during ischemia as well as through its reported ability to inhibit mPTP opening during reperfusion, AMPK became the focus of experiments investigating the effect of its inhibition on both cardiomyocyte viability and infarct size in Langendorff perfused hearts in 14-day old and adult hearts.

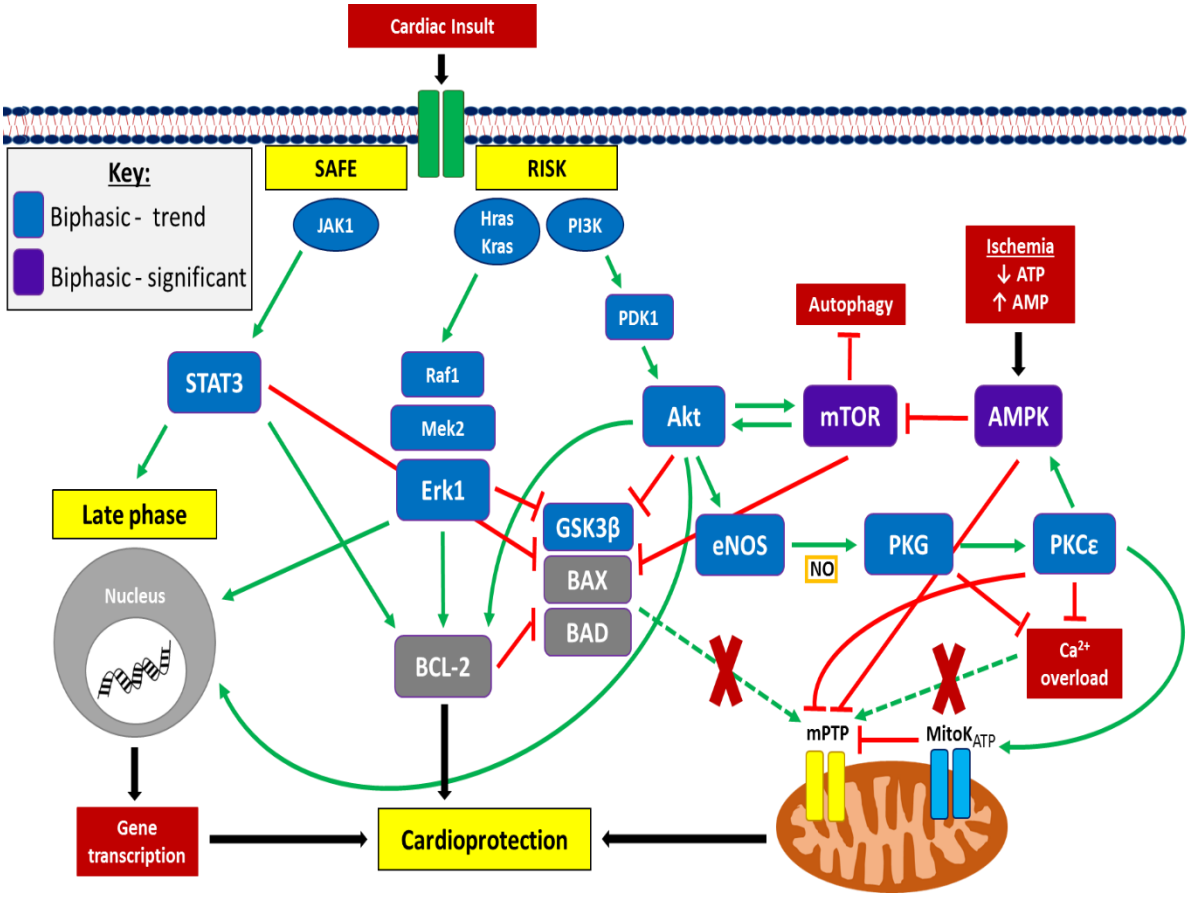

Figure 102. An overview of the RISK-SAFE survival signalling pathways, with proteins identified to be biphasically expressed during postnatal development in the proteomic output highlighted (**Key**: 'Trend' = proteins with overall biphasic profile of expression, but the difference did not reach statistical significance between 7-day and 14-day old. 'Significant' = proteins with statistically significant differences between 14-day old samples and all three age groups (7-day old, 28-day old, and adult).

In both isolated cardiomyocytes and whole heart perfusion, AMPK inhibition resulted in a significant decrease in cardiomyocyte viability and increase in infarct size in 14-day olds, but not adults. This supports the hypothesis that its peak in expression in 14-day old hearts relates to a potential role in the mechanism underlying the greater resistance of 14-day old hearts to I/RI in comparison to adult hearts. Whilst western blot analysis of cardiac samples obtained from these samples did not identify statistically significant changes in the expression of key AMPK signalling and survival signalling proteins, it is likely that this results from previously discussed issues with the experimental protocol. Indeed, bands visually

showed clear differences between the experimental groups that appeared consistent with the expected roles of each protein tested in cell survival and AMPK signalling (**Section 6.4**). This work has therefore identified AMPK as a target for future work into its role in the biphasic cardiac vulnerability profile, as well as a potential therapeutic target in the treatment of myocardial infarction.

In addition to these protein-based findings, important age-related differences in cardiac ultrastructure – both in control hearts and hearts that have undergone ischemia and reperfusion – were identified. Consistent with their importance to cellular survival, as well as being key end targets for survival signalling pathways, analysis of mitochondrial morphology demonstrated that those from 14-day old samples displayed characteristics both pre- and post-ischemia that indicated a lesser degree of injury and dysfunction, such as less rounded morphologies – an indicator of mitochondrial fission and fragmentation – and smaller intercristae spaces – indicating mitochondrial disruption – than adults. Additionally, significant differences in the distribution of mitochondrial subpopulations was identified between the two age groups, with 14-day old hearts displaying a greater number of perinuclear mitochondria, in comparison with the high number of interfibrillar mitochondria seen in adults. While the significance of this difference is currently uncertain, the fact that these two subtypes have distinct functional roles highlights this as an important avenue of future research. In addition to these mitochondrial findings, MVBs and exosomes were identified as an interesting target for future investigation, due to their apparent abundance in 14-day old hearts in comparison with adults, as well as their reported cardioprotective roles in the context of cardiac injury.

9.2 Limitations

9.2.1 Proteomics and phosphoproteomics

In our first run of proteomic analysis (**Chapter 3**), it was found that some phosphoproteins had a phosphosite present in both runs covering all three age groups, showing a concordant pattern of change with postnatal development as that seen in the total phosphoprotein, but that were labelled as being at sites two or so residues apart. This calls into question the accuracy of detection of the individual phosphosites when in close physical proximity to one another, as well as the comparability of these sites between the two runs of phosphoproteomic analysis in some cases.

A predominant limitation identified when conducting analysis of the second run of proteomic output (**Chapter 4**) was the fact that only four 7-day old samples were included, resulting in a large scatter for some proteins, and making the identification of outliers difficult in some cases. This may also have contributed to false negatives for proteins with statistically significant biphasic patterns of expression.

9.2.2 Cardiomyocyte isolation

Initial cardiomyocyte isolation experiments encountered issues in assessing the effect of simulated I/RI on viability (**Section 5.3.1**) as cell counts were initially performed manually using a cell counter and microscope. Due to the fact that this was undertaken during the experiment itself, and that a large number of cells from multiple fields were required in order to improve the reliability of these counts, the level of accuracy of these initial counts is uncertain. Furthermore, the time taken to perform these counts meant that there was a 20 minute delay between the measurements taken from the experimental cell group to the control cell group, during which time the number of viable cells is likely to have decreased

with uncertain significance, making direct comparison between the two groups difficult. The implementation of a protocol adjustment, instead taking photographs of the cells through the microscope and performing these counts using the ImageJ count tool after the experiment itself, improved the accuracy of these cell viability measurements, but may affect direct comparability with the initial manually counted data.

As mentioned in **Section 5.3.2**, analysis of protein expression in cells that had undergone simulated I/RI – with or without drug treatment – was difficult particularly for 14-day olds, as the number of cardiomyocytes that can be isolated from hearts of this age group are relatively low, therefore often producing samples with insufficient protein content to successfully run western blot analysis. Furthermore, protein was extracted from the cell pellets themselves, discarding the supernatant. However, other studies have shown that it may in fact be this supernatant that holds the relevant proteins released upon cell death, due to the necrosis-inducing action of H_2O_2 at the concentration used in this work (Marshall, Edwards et al. 2014). As a result, the lack of significant change in protein expression between the control and experimental groups in our isolated cardiomyocytes may not be representative of the true changes in protein expression following I/RI and the use of inhibitors.

Another issue encountered during this work was the lack of inhibitors or activators for some proteins found to have strong, statistically significant biphasic trends in expression, such as Caveolin-1, -2 and -3. As a result, testing the differential effects of inhibition or activation of these proteins between 14-day old and adult hearts would require overexpression or knockout models. For those proteins that we were able to inhibit in cardiomyocyte viability studies, one issue was that, in the case of PKCε, no inhibitor specific for this isoform of the

protein was available, and thus experiments used a pan PKC inhibitor - chelerythrine. As a result, it cannot be concluded definitively that any resulting effects of inhibition on cardiomyocyte viability were solely due to PKCε alone. Future work may therefore benefit from utilising methods such as PKCε-specific knockdown in order to establish that any effects do relate to its activity, and not any other PKC isoforms. Another issue was that addition of these drugs resulted in chronic inhibition, as they were left to incubate within the cell suspension for the full 2 hour experimental period. However, replication of this experiment in the case of AMPK inhibition was performed in whole hearts using Langendorff perfusion in order to address this issue. In addition to this, in many cases the inhibitors used are not isoform specific, or have been demonstrated to also affect other kinases that would likely have an effect on cell survival in these experiments. For example, chelerythrine was used to investigate the effects of PKCε inhibition, due to the lack of a specific inhibitor. This may account for the lack of a statistically significant change in pPKCε/PKCε expression in these isolated cardiomyocyte experiments (**Section 5.3.2.1.1.3**).

9.2.3 Western blotting

One of the most prominent limitations encountered during this work was the apparent variance in GAPDH expression between the different age groups, with the lowest levels seen in 14-day old protein samples. Repetition of protein quantification and sample preparation for western blotting produced these same differences in GAPDH expression, and was similarly seen in samples extracted from isolated cardiomyocytes. Similar age or nutrition-related differences in GAPDH have previously been reported in the literature, a difference that may result from the role of GAPDH in glycolysis and the metabolic differences that exist at different stages of postnatal development within the heart (Lowe, Degens et al. 2000, Mozdziak, Dibner et al. 2003, Uddin, Cinar et al. 2011). This variance in the expression of

supposed housekeeping proteins during western blotting means that differences in protein expression between the three age groups tested may have been exaggerated, with 14-3-3η, for example, showing statistically significant difference between 14-day old and 28-day old hearts in the western blotting data that was not seen in the proteomic output. However, switching to the use of Ponceau S staining appeared to solve this issue, as shown in the **Appendix** (**Figure 108**).

Another limiting factor was the fact that the electrophoresis gels used has a maximum number of 15 wells for sample loading, meaning samples had to be split onto two separate gels in order to be able to compare all experimental and age groups. While a pooled sample run on all gels was used in order to try and account for differences between the gels, this did not appear to be sufficient and the resulting data produced had large scatters and standard errors. This scatter is likely to account for the lack of statistically significant differences in protein expression seen, despite the clear differences visible when assessing the blots themselves.

9.2.4 Langendorff perfusion and analysis of cardiac injury

Analysis of cardiac injury in later experiments was limited by the fact that the original type of creatine kinase reagent used in initial experiments (**Section 6.3.1**) was subsequently discontinued, resulting in a switch to a supposedly equivalent product of smaller size. This meant that fresh bottles of reagent had to be made up often within individual runs – i.e. samples taken at 1-60 minutes of reperfusion for a single heart – as well as between control and inhibitor-treated hearts. This methodology appeared to produce a much larger variation in values and standard error in experiments described in **Section 6.3.2** in comparison with the initial experiments in **Section 6.3.1**, and may have played a part in the lack of statistical

significance seen in creatine kinase measurements between control and dorsomorphin dihydrochloride treated hearts, despite the significant differences seen in infarct size between the two groups.

Finally, measurement of infarct sizes themselves between the two age groups was difficult due to the greater resistance of 14-day old hearts to I/RI, and the subsequent smaller infarct sizes seen with the same 30 minute period of ischemia. 14-day old hearts therefore tended to only have regions of ischemia that were stained a light pink as opposed to the white regions seen in adult hearts. As a result, infarct sizes were measured as any regions not stained brick red in order to allow for direct comparison between the two age groups, which may therefore overlook differences in severe regions of infarction in adult hearts. Indeed, adult hearts treated with dorsomorphin dihydrochloride often appeared to have larger areas of tissue stained white than control hearts run simultaneously, which fits with previous reports of dorsomorphin dihydrochloride treatment increasing infarct size in adult rat hearts.

9.2.5 Analysis of electron micrographs

One of the main limitations encountered during analysis of electron micrograph data was the quality of sections, and the abundance of intact, correctly orientated sections of tissue to be able to accurately distinguish mitochondrial subtypes by location. This was particularly difficult in 14-day old samples, likely owing to the smaller cardiomyocyte size in this age group. Further disarray of tissue following reperfusion meant that it was not possible to find such sections in these samples, and thus mitochondrial morphology and subpopulation density measurements could not be collected. This also applied to finding intact sections of the membrane for caveolae quantification, with identification of caveolae in post-ischemic

samples becoming more difficult as a result of these distorted membranes and the presence of many vesicles around the membranes that arise following insult. In addition to this, quantitative measurements were not taken for MVB and exosome abundance due to similar issues in the identification and distinguishing of these structures from other vesicles in the myocardium. Many studies investigating MVBs and exosomes utilise, for example, immunogold staining of electron micrographs in order to correctly identify exosome carrying MVBs, as opposed to relying solely on visual identification.

9.3 Future Work

Having identified a number of potential candidates for the greater resistance of 14-day old hearts to I/RI, future work would benefit from further investigation of these proteins and their signalling partners, as well as confirmation of our current findings with greater sample sizes. This will be of particular importance to proteins that exhibited an overall biphasic trend in expression, but lacked statistical significance between 7-day old and 14-day old samples as a result of the scatter of proteomic data. Due to difficulties in analysing protein expression between multiple experimental and age groups using western blotting, alternatives such as proteomic and phosphoproteomic analysis of samples from all four age groups post-I/RI could eliminate these issues and provide a better understanding of potential changes in survival signalling proteins following cardiac injury between these age groups. It would also be important to include experiments supporting these inhibitor experiments, through use of specific activators of our proteins of interest to establish that these age-related differences are consistent both with inhibition and activation of such proteins. Moreover, replication of the dorsomorphin dihydrochloride experiments, but with the continued inhibition of AMPK throughout reperfusion as well as ischemia, may be of interest in order to identify any

potential resulting differences in cardiac injury between age groups, and in comparison to experiments with inhibition during ischemia alone. As current data mainly focus on 14-day old and adult hearts and samples, the inclusion of 7-day olds will be important to establish that these changes – for example, in the effect of AMPK inhibition or in the abundance of MVBs – also follow the biphasic trend of cardiac vulnerability seen during postnatal development. Clear differences between the 14-day old and adult samples in terms of mitochondrial morphology and their response to I/R were identified, in addition to expression of proteins linked to mitochondrial fission and fusion. As monitoring of these dynamic processes is limited using electron micrographs alone, future work would benefit from the inclusion of experiments, for example, using Mito Tracker in order to establish any differences between the age groups, and the subsequent effect this has on cardiac vulnerability. Finally, as localisation of signalling proteins and structures such as MVBs following I/RI is critical to their function and the conference of cardioprotection, future work using IHC would be necessary to assess differences between these age groups following injury.

10. References

Abdul-Ghani, S., K. J. Heesom, G. D. Angelini and M. S. Suleiman (2014). "Cardiac phosphoproteomics during remote ischemic preconditioning: a role for the sarcomeric Z-disk proteins." Biomed Res Int **2014**: 767812.

Achterberg, P. W., A. S. Nieukoop, B. Schoutsen and J. W. de Jong (1988). "Different ATP-catabolism in reperfused adult and newborn rat hearts." Am J Physiol **254**(6 Pt 2): H1091-1098.

Adler-Wailes, D. C., E. L. Guiney, J. Koo and J. A. Yanovski (2008). "Brief Genetic Analysis: Effects of Ritonavir on Adipocyte Gene Expression: Evidence for a Stress-Related Response." Obesity (Silver Spring, Md.) **16**(10): 2379-2387.

Adolph, E. (1967). "Ranges of heart rates and their regulations at various ages (rat)." American Journal of Physiology-Legacy Content **212**(3): 595-602.

Ailawadi, S., X. Wang, H. Gu and G. C. Fan (2015). "Pathologic function and therapeutic potential of exosomes in cardiovascular disease." Biochim Biophys Acta **1852**(1): 1-11.

Balaguru, D., P. S. Haddock, J. L. Puglisi, D. M. Bers, W. A. Coetzee and M. Artman (1997). "Role of the Sarcoplasmic Reticulum in Contraction and Relaxation of Immature Rabbit Ventricular Myocytes." Journal of Molecular and Cellular Cardiology **29**(10): 2747-2757.

Barile, L., T. Moccetti, E. Marban and G. Vassalli (2017). "Roles of exosomes in cardioprotection." Eur Heart J **38**(18): 1372-1379.

Barman, P., S. C. M. Choisy, J. C. Hancox and A. F. James (2011). "β-Adrenoceptor/PKA-stimulation, Na(+)-Ca(2+) exchange and PKA-activated Cl(-) currents in rabbit cardiomyocytes: a conundrum." Cell calcium **49**(4): 233-239.

Bassani, R. A., M. M. Fagian, J. W. M. Bassani and A. E. Vercesi (1998). "Changes in Calcium Uptake Rate by Rat Cardiac Mitochondria during Postnatal Development." Journal of Molecular and Cellular Cardiology **30**(10): 2013-2023.

Basso, F., F. Rocchetti, S. Rodriguez, M. Nesterova, F. Cormier, C. A. Stratakis, B. Ragazzon, J. Bertherat and M. Rizk-Rabin (2014). "Comparison of the effects of PRKAR1A and PRKAR2B depletion on signaling pathways, cell growth, and cell cycle control of adrenocortical cells." Hormone and metabolic research = Hormon- und Stoffwechselforschung = Hormones et metabolisme **46**(12): 883-888.

Berk, J. M., K. E. Tifft and K. L. Wilson (2013). "The nuclear envelope LEM-domain protein emerin." Nucleus **4**(4): 298-314.

Bers, D. M. (2002). "Cardiac excitation-contraction coupling." Nature **415**: 198-205.

Bicknell, Katrina A., Carmen H. Coxon and G. Brooks (2004). "Forced expression of the cyclin B1–CDC2 complex induces proliferation in adult rat cardiomyocytes." Biochemical Journal **382**(Pt 2): 411-416.

Boengler, K., R. Schulz and G. Heusch (2009). "Loss of cardioprotection with ageing." Cardiovasc Res **83**(2): 247-261.

Boerth, S. R., D. B. Zimmer and M. Artman (1994). "Steady-state mRNA levels of the sarcolemmal Na(+)-Ca2+ exchanger peak near birth in developing rabbit and rat hearts." Circ Res **74**(2): 354-359.

Calderon, J. C., Bolanos, P., Caputo, C. (2014). "The excitation-contraction coupling mechanism in skeletal muscle." Biphys. Rev **6**(1): 133-160.

Calvert, J. W., S. Jha, S. Gundewar, J. W. Elrod, A. Ramachandran, C. B. Pattillo, C. G. Kevil and D. J. Lefer (2009). "Hydrogen sulfide mediates cardioprotection through Nrf2 signaling." Circ Res **105**(4): 365-374.

Chang, Y. C., H. H. Lee, Y. J. Chen, G. M. Bokoch and Z. F. Chang (2006). "Contribution of guanine exchange factor H1 in phorbol ester-induced apoptosis." Cell Death Differ **13**(12): 2023-2032.

Chang, Z. F. and H. H. Lee (2006). "RhoA signaling in phorbol ester-induced apoptosis." J Biomed Sci **13**(2): 173-180.

Chaube, B. and M. K. Bhat (2016). "AMPK, a key regulator of metabolic/energy homeostasis and mitochondrial biogenesis in cancer cells." Cell Death and Disease **7**(1): e2044.

Chen, B., Ma, Y., Meng, R., Xiong, Z., Wang, H., Zeng, J., Liu, C., Dong, Y. (2010). "Activation of AMPK inhibits cardiomyocyte hypertrophy by modulating of the FOXO/MuRF1 signaling pathway in vitro." Acta Pharmacol Sin. **31**(7): 798-804.

Chen, H. W., S. L. Yu, W. J. Chen, P. C. Yang, C. T. Chien, H. Y. Chou, H. N. Li, K. Peck, C. H. Huang, F. Y. Lin, J. J. W. Chen and Y. T. Lee (2004). "Dynamic changes of gene expression profiles during postnatal development of the heart in mice." Heart **90**(8): 927-934.

Chen, H., Liu, S., Liu, X., Yang, J., Wang, F., Cong, X., Chen, X. (2017). "Lysophosphatidic acid pretreatment attenuates myocardial ischemia/reperfusion injury in the immature hearts of rats." Front Physiol. **8**: 153

Cohen, M. V. and J. M. Downey (2015). "Signalling pathways and mechanisms of protection in pre- and postconditioning: historical perspective and lessons for the future." Br J Pharmacol **172**(8): 1913-1932.

Couet, J., M. M. Belanger, E. Roussel and M. C. Drolet (2001). "Cell biology of caveolae and caveolin." Adv Drug Deliv Rev **49**(3): 223-235.

Dan, H. C., A. Ebbs, M. Pasparakis, T. Van Dyke, D. S. Basseres and A. S. Baldwin (2014). "Akt-dependent activation of mTORC1 complex involves phosphorylation of mTOR (mammalian target of rapamycin) by IκB kinase α (IKKα)." The Journal of biological chemistry **289**(36): 25227-25240.

Das, M., S. Das and D. K. Das (2007). "Caveolin and MAP kinase interaction in angiotensin II preconditioning of the myocardium." J Cell Mol Med **11**(4): 788-797.

Das, M., Gherghiceanu, M., Lekli, I., Mukherjee, S., Popescu, L. M., Das, D. K. (2008). "Essential role of lipid raft in ischemic preconditioning." Cell Physiol Biochem **21**(4): 325-334.

Davidson, S. M., D. Hausenloy, M. R. Duchen and D. M. Yellon (2006). "Signalling via the reperfusion injury signalling kinase (RISK) pathway links closure of the mitochondrial permeability transition pore to cardioprotection." Int J Biochem Cell Biol **38**(3): 414-419.

Di Maira, G., M. Salvi, G. Arrigoni, O. Marin, S. Sarno, F. Brustolon, L. A. Pinna and M. Ruzzene (2005). "Protein kinase CK2 phosphorylates and upregulates Akt//PKB." Cell Death Differ **12**(6): 668-677.

Dibrova, D. V., D. A. Cherepanov, M. Y. Galperin, V. P. Skulachev and A. Y. Mulkidjanian (2013). "Evolution of cytochrome bc complexes: from membrane-anchored dehydrogenases

of ancient bacteria to triggers of apoptosis in vertebrates." Biochimica et biophysica acta **1827**(0): 10.1016/j.bbabio.2013.1007.1006.

Doul, J., Z. Charvatova, I. Ostadalova, M. Kohutiar, H. Maxova and B. Ostadal (2015). "Neonatal rat hearts cannot be protected by ischemic postconditioning." Physiol Res.

Edwards, H. V., J. D. Scott and G. S. Baillie (2012). "The A-kinase-anchoring protein AKAP-Lbc facilitates cardioprotective PKA phosphorylation of Hsp20 on Ser(16)." Biochem J **446**(3): 437-443.

Eisner, D. A., Caldwell, J. L., Kistamas, K., Trafford, A. W. (2017). "Calcium and excitation-contraction coupling in the heart." Circulation Research **121**(2): 181-195.

Eun, S. Y., I. S. Woo, H.-S. Jang, H. Jin, M. Y. Kim, H. J. Kim, J. H. Lee, K. C. Chang, J.-H. Kim and H. G. Seo (2008). "Identification of cytochrome c oxidase subunit 6A1 as a suppressor of Bax-induced cell death by yeast-based functional screening." Biochemical and Biophysical Research Communications **373**(1): 58-63.

Fabiato, A. and F. Fabiato (1978). "CALCIUM-INDUCED RELEASE OF CALCIUM FROM THE SARCOPLASMIC RETICULUM OF SKINNED CELLS FROM ADULT HUMAN, DOG, CAT, RABBIT, RAT, AND FROG HEARTS AND FROM FETAL AND NEW-BORN RAT VENTRICLES*." Annals of the New York Academy of Sciences **307**(1): 491-522.

FAN, G., G. CHU and E. KRANIAS (2005). "Hsp20 and Its Cardioprotection." Trends in Cardiovascular Medicine **15**(4): 138-141.

Gangoda, L., M. Doerflinger, R. Srivastava, N. Narayan, L. E. Edgington, J. Orian, C. Hawkins, L. A. O'Reilly, H. Gu, M. Bogyo, P. Ekert, A. Strasser and H. Puthalakath (2014). "Loss of Prkar1a leads to Bcl-2 family protein induction and cachexia in mice." Cell death and differentiation **21**(11): 1815-1824.

Goetzman, E. S. (2011). "Animal models of human disease." Progress in Molecular Biology and Translational Science **100**: 389-417.

Gomez, L., M. l. Paillard, H. l. n. Thibault, G. v. Derumeaux and M. Ovize (2008). "Inhibition of GSK3β by Postconditioning Is Required to Prevent Opening of the Mitochondrial Permeability Transition Pore During Reperfusion." Circulation **117**(21): 2761-2768.

Granger, D. N. and P. R. Kvietys (2015). "Reperfusion injury and reactive oxygen species: The evolution of a concept." Redox Biol **6**: 524-551.

Gurusamy, N., K. Watanabe, M. Ma, P. Prakash, K. Hirabayashi, S. Zhang, A. J. Muslin, M. Kodama and Y. Aizawa (2006). "Glycogen synthase kinase 3beta together with 14-3-3 protein regulates diabetic cardiomyopathy: effect of losartan and tempol." FEBS Lett **580**(8): 1932-1940.

Gusev, N. B., O. V. Bukach and S. B. Marston (2005). "Structure, properties, and probable physiological role of small heat shock protein with molecular mass 20 kD (Hsp20, HspB6)." Biochemistry. Biokhimiia **70**(6): 629-637.

Gwinn, D. M. and R. J. Shaw (2010). AMPK Control of mTOR Signaling and Growth**:** 49-75.

Hahn-Windgassen, A., V. Nogueira, C.-C. Chen, J. E. Skeen, N. Sonenberg and N. Hay (2005). "Akt Activates the Mammalian Target of Rapamycin by Regulating Cellular ATP Level and AMPK Activity." Journal of Biological Chemistry **280**(37): 32081-32089.

Halestrap, A. P., S. J. Clarke and I. Khaliulin (2007). "The role of mitochondria in protection of the heart by preconditioning." Biochim Biophys Acta **1767**(8): 1007-1031.

Haraguchi, T., J. M. Holaska, M. Yamane, T. Koujin, N. Hashiguchi, C. Mori, K. L. Wilson and Y. Hiraoka (2004). "Emerin binding to Btf, a death-promoting transcriptional repressor, is disrupted by a missense mutation that causes Emery-Dreifuss muscular dystrophy." Eur J Biochem **271**(5): 1035-1045.

Hausenloy, D. J., S. Lecour and D. M. Yellon (2011). "Reperfusion injury salvage kinase and survivor activating factor enhancement prosurvival signaling pathways in ischemic postconditioning: two sides of the same coin." Antioxid Redox Signal **14**(5): 893-907.

Hausenloy, D. J., S. B. Ong and D. M. Yellon (2009). "The mitochondrial permeability transition pore as a target for preconditioning and postconditioning." Basic Res Cardiol **104**(2): 189-202.

Hausenloy, D. J., H. J. Whittington, A. M. Wynne, S. S. Begum, L. Theodorou, N. Riksen, M. M. Mocanu and D. M. Yellon (2013). "Dipeptidyl peptidase-4 inhibitors and GLP-1 reduce myocardial infarct size in a glucose-dependent manner." Cardiovasc Diabetol **12**: 154.

Hausenloy, D. J. and D. M. Yellon (2007). "Reperfusion injury salvage kinase signalling: taking a RISK for cardioprotection." Heart Fail Rev **12**(3-4): 217-234.

Hausenloy, D. J. and D. M. Yellon (2013). "Myocardial ischemia-reperfusion injury: a neglected therapeutic target." J Clin Invest **123**(1): 92-100.

Hernandez, V. J., J. Weng, P. Ly, S. Pompey, H. Dong, L. Mishra, M. Schwarz, R. G. Anderson and P. Michaely (2013). "Cavin-3 dictates the balance between ERK and Akt signaling." Elife **2**: e00905.

Heusch, G. (2015). "Molecular basis of cardioprotection: signal transduction in ischemic pre-, post-, and remote conditioning." Circ Res **116**(4): 674-699.

Hollander, J. M., D. Thapa and D. L. Shepherd (2014). "Physiological and structural differences in spatially distinct subpopulations of cardiac mitochondria: influence of cardiac pathologies." Am J Physiol Heart Circ Physiol **307**(1): H1-14.

Hong, T. and R. M. Shaw (2017). "Cardiac T-Tubule Microanatomy and Function." Physiol Rev **97**(1): 227-252.

Horikawa, Y. T., M. Panneerselvam, Y. Kawaraguchi, Y. M. Tsutsumi, S. S. Ali, R. C. Balijepalli, F. Murray, B. P. Head, I. R. Niesman, T. Rieg, V. Vallon, P. A. Insel, H. H. Patel and D. M. Roth (2011). "Cardiac-specific overexpression of caveolin-3 attenuates cardiac hypertrophy and increases natriuretic peptide expression and signaling." J Am Coll Cardiol **57**(22): 2273-2283.

Hu, Y., M. Zhang, X. Shen, G. Dai, D. Ren, L. Que, T. Ha, C. Li, Y. Xu, W. Ju and Y. Li (2017). "TIR/BB-loop mimetic AS-1 attenuates cardiac ischemia/reperfusion injury via a caveolae and caveolin-3-dependent mechanism." Sci Rep **7**: 44638.

Huang, C., W. Liu, C. N. Perry, S. Yitzhaki, Y. Lee, H. Yuan, Y. T. Tsukada, A. Hamacher-Brady, R. M. Mentzer, R. A. Gottlieb and R. A. Gottlieb (2010). "Autophagy and protein kinase C are required for cardioprotection by sulfaphenazole." American journal of physiology. Heart and circulatory physiology **298**(2): H570-579.

Huang, Y., J.-b. Chen, B. Yang, H. Shen, J.-J. Liang and Q. Luo (2014). "RhoA/ROCK pathway regulates hypoxia-induced myocardial cell apoptosis." Asian Pacific Journal of Tropical Medicine **7**(11): 884-888.

Hudlicka, O. and M. D. Brown (1996). "Postnatal growth of the heart and its blood vessels." J Vasc Res **33**(4): 266-287.

Hung, C.-W. and A. Tholey (2012). "Tandem Mass Tag Protein Labeling for Top-Down Identification and Quantification." Analytical Chemistry **84**(1): 161-170.

Hunter, J. C., Kostyak, J. C., Novotny, J. L., Simpson, A. M., Korzick, D. H. (2007). "Estrogen deficiency decreases ischemic tolerance in the aged rat heart: roles of PKCδ, PKCε, Akt, and GSK3β." Am J Physiol Regul Integr Comp Physiol **292**(2): R800-9.

Hutchins, E. J., J. L. Belrose and B. G. Szaro (2015). "Phosphorylation of heterogeneous nuclear ribonucleoprotein K at an extracellular signal-regulated kinase phosphorylation site promotes neurofilament-medium protein expression and axon outgrowth in Xenopus." Neuroscience Letters **607**: 59-65.

Hüttemann, M., S. Helling, T. H. Sanderson, C. Sinkler, L. Samavati, G. Mahapatra, A. Varughese, G. Lu, J. Liu, R. Ramzan, S. Vogt, L. I. Grossman, J. W. Doan, K. Marcus and I. Lee (2012). "Regulation of mitochondrial respiration and apoptosis through cell signaling: cytochrome c oxidase and cytochrome c in ischemia/reperfusion injury and inflammation." Biochimica et Biophysica Acta **1817**(4): 598-609.

Hwang, S. J. and W. Kim (2013). "Mitochondrial dynamics in the heart as a novel therapeutic target for cardioprotection." Chonnam Med J **49**(3): 101-107.

Iacovides, D. C., A. B. Johnson, N. Wang, S. Boddapati, J. Korkola and J. W. Gray (2013). "Identification and quantification of AKT isoforms and phosphoforms in breast cancer using a novel nanofluidic immunoassay." Molecular & cellular proteomics : MCP **12**(11): 3210-3220.

Ise, R., D. Han, Y. Takahashi, S. Terasaka, A. Inoue, M. Tanji and R. Kiyama (2005). "Expression profiling of the estrogen responsive genes in response to phytoestrogens using a customized DNA microarray." FEBS Letters **579**(7): 1732-1740.

Iseli, T. J., M. Walter, B. J. W. van Denderen, F. Katsis, L. A. Witters, B. E. Kemp, B. J. Michell and D. Stapleton (2005). "AMP-activated protein kinase beta subunit tethers alpha and gamma subunits via its C-terminal sequence (186-270)." The Journal of biological chemistry **280**(14): 13395-13400.

Jackson, C., I. Escobar, J. Xu and M. Perez-Pinzon (2018). "Effects of ischemic preconditioning on mitochondrial and metabolic neruoprotection: 5' adenosine monophosphate-activated protein kinase and sirtuins." Brain Circulation **4**(2): 54.

Janowski, E., L. Cleemann, P. Sasse and M. Morad (2006). "Diversity of Ca2+ signaling in developing cardiac cells." Ann N Y Acad Sci **1080**: 154-164.

Jiang, H., J. Xiao, B. Kang, X. Zhu, N. Xin and Z. Wang (2016). "PI3K/SGK1/GSK3β signaling pathway is involved in inhibition of autophagy in neonatal rat cardiomyocytes exposed to hypoxia/reoxygenation by hydrogen sulfide." Experimental Cell Research **345**(2): 134-140.

Johnson, W. T. and H. M. Brown-Borg (2006). "Cardiac cytochrome-c oxidase deficiency occurs during late postnatal development in progeny of copper-deficient rats." Exp Biol Med (Maywood) **231**(2): 172-180.

Jones, B. O., S. Pepe, F. L. Sheeran, S. Donath, P. Hardy, L. Shekerdemian, D. J. Penny, I. McKenzie, S. Horton, C. P. Brizard, Y. d'Udekem, I. E. Konstantinov and M. M. Cheung (2013). "Remote ischemic preconditioning in cyanosed neonates undergoing cardiopulmonary bypass: a randomized controlled trial." J Thorac Cardiovasc Surg **146**(6): 1334-1340.

Juhaszova, M., D. B. Zorov, S. H. Kim, S. Pepe, Q. Fu, K. W. Fishbein, B. D. Ziman, S. Wang, K. Ytrehus, C. L. Antos, E. N. Olson and S. J. Sollott (2004). "Glycogen synthase kinase-3beta

mediates convergence of protection signaling to inhibit the mitochondrial permeability transition pore." J Clin Invest **113**(11): 1535-1549.

Kasof, G. M., L. Goyal and E. White (1999). "Btf, a novel death-promoting transcriptional repressor that interacts with Bcl-2-related proteins." Mol Cell Biol **19**(6): 4390-4404.

Kassan, A., Pham, U., Nguyen, Q., Reichelt, M. E., Cho, E., Patel, P. M., Roth, D. M., Head, B. P., Patel, H. H. (2016). "Caveolin-3 plays a critical role in autophagy after ischemia-reperfusion." Am J Physiol Cell Physiol **311**(6): C854-C865.

Kim, S.-E., R. Mori, T. Komatsu, T. Chiba, H. Hayashi, S. Park, M. D. Sugawa, N. A. Dencher and I. Shimokawa (2015). "Upregulation of cytochrome c oxidase subunit 6b1 (Cox6b1) and formation of mitochondrial supercomplexes: implication of Cox6b1 in the effect of calorie restriction." Age **37**(3): 45.

Kong, Q., L. Dai, Y. Wang, X. Zhang, C. Li, S. Jiang, Y. Li, Z. Ding and L. Liu (2016). "HSPA12B Attenuated Acute Myocardial Ischemia/reperfusion Injury via Maintaining Endothelial Integrity in a PI3K/Akt/mTOR-dependent Mechanism." Scientific Reports **6**: 33636.

Konishi, M., G. Haraguchi, H. Ohigashi, T. Ishihara, K. Saito, Y. Nakano and M. Isobe (2011). "Adiponectin protects against doxorubicin-induced cardiomyopathy by anti-apoptotic effects through AMPK up-regulation." Cardiovascular Research **89**(2): 309-319.

Kosuru, R., Y. Cai, V. Kandula, D. Yan, C. Wang, H. Zheng, Y. Li, Michael G. Irwin, S. Singh and Z. Xia (2018). "AMPK Contributes to Cardioprotective Effects of Pterostilbene Against Myocardial Ischemia- Reperfusion Injury in Diabetic Rats by Suppressing Cardiac Oxidative Stress and Apoptosis." Cellular Physiology and Biochemistry **46**(4): 1381-1397.

Lacerda, L., S. Somers, L. H. Opie and S. Lecour (2009). "Ischaemic postconditioning protects against reperfusion injury via the SAFE pathway." Cardiovascular Research.

Lal, H., F. Ahmad, J. Woodgett and T. Force (2015). "The GSK-3 Family as Therapeutic Target for Myocardial Diseases." Circulation Research **116**(1): 138-149.

Larsson, H. P. (2010). "How is the heart rate regulated in the sinoatrial node? Another piece to the puzzle." The Journal of general physiology **136**(3): 237-241.

Lecour, S. (2009). "Activation of the protective Survivor Activating Factor Enhancement (SAFE) pathway against reperfusion injury: Does it go beyond the RISK pathway?" J Mol Cell Cardiol **47**(1): 32-40.

Lee, J. H., D. S. Byun, M. G. Lee, B. K. Ryu, M. J. Kang, K. S. Chae, K. Y. Lee, H. J. Kim, H. Park and S. G. Chi (2008). "Frequent epigenetic inactivation of hSRBC in gastric cancer and its implication in attenuated p53 response to stresses." Int J Cancer **122**(7): 1573-1584.

Lee, S.-Y., H.-C. Ku, Y.-H. Kuo, H.-L. Chiu and M.-J. Su (2015). "Pyrrolidinyl caffeamide against ischemia/reperfusion injury in cardiomyocytes through AMPK/AKT pathways." Journal of Biomedical Science **22**(1): 18.

Li, H. Y., L. Yang, W. Liu and J. Zuo (2011). "[GRP75 overexpression inhibits apoptosis induced by glucose deprivation via Raf/Mek/Erk1/2 signaling pathway]." Sheng Li Xue Bao **63**(1): 69-74.

Li, X., R. Luo, R. Jiang, X. Meng, X. Wu, S. Zhang and W. Hua (2013). "The role of the Hsp90/Akt pathway in myocardial calpain-induced caspase-3 activation and apoptosis during sepsis." BMC Cardiovasc Disord **13**: 8.

Liang, X.-Q., E.-H. Cao, Y. Zhang and J.-F. Qin (2004). "A P53 target gene, PIG11, contributes to chemosensitivity of cells to arsenic trioxide." FEBS Letters **569**(1-3): 94-98.

Liao, Y. and M.-C. Hung (2010). "Physiological regulation of Akt activity and stability." American journal of translational research **2**(1): 19-42.

Liaw, N. Y., L. S. Hoe, F. L. Sheeran, J. N. Peart, J. P. Headrick, M. M. Cheung and S. Pepe (2013). "Postnatal shifts in ischemic tolerance and cell survival signaling in murine myocardium." Am J Physiol Regul Integr Comp Physiol **305**(10): R1171-1181.

Lin, Z., P. Zhou, A. von Gise, F. Gu, Q. Ma, J. Chen, H. Guo, P. R. van Gorp, D. Z. Wang and W. T. Pu (2015). "Pi3kcb links Hippo-YAP and PI3K-AKT signaling pathways to promote cardiomyocyte proliferation and survival." Circ Res **116**(1): 35-45.

Lisanti, M. P., P. E. Scherer, Z. Tang and M. Sargiacomo (1994). "Caveolae, caveolin and caveolin-rich membrane domains: a signalling hypothesis." Trends Cell Biol **4**(7): 231-235.

Littlejohns, B., K. Heesom, G. D. Angelini and M. S. Suleiman (2014). "The effect of disease on human cardiac protein expression profiles in paired samples from right and left ventricles." Clinical Proteomics **11**(1): 34-34.

Liu, D. (2018). "Effects of procyanidin on cardiomyocyte apoptosis after myocardial ischemia reperfusion in rats." BMC cardiovascular disorders **18**(1): 35.

Liu, L., X. J. Zhang, S. R. Jiang, Z. N. Ding, G. X. Ding, J. Huang and Y. L. Cheng (2007). "Heat shock protein 27 regulates oxidative stress-induced apoptosis in cardiomyocytes: mechanisms via reactive oxygen species generation and Akt activation." Chin Med J (Engl) **120**(24): 2271-2277.

Liu, X., R. R. Chhipa, I. Nakano and B. Dasgupta (2014). "The AMPK inhibitor compound C is a potent AMPK-independent antiglioma agent." Molecular cancer therapeutics **13**(3): 596-605.

Liu, Y. (2006). "Fatty acid oxidation is a dominant bioenergetic pathway in prostate cancer." Prostate Cancer and Prostatic Diseases **9**: 230-234.

Lopaschuk, G. D. and J. S. Jaswal (2010). "Energy metabolic phenotype of the cardiomyocyte during development, differentiation, and postnatal maturation." J Cardiovasc Pharmacol **56**(2): 130-140.

Lowe, D. A., H. Degens, K. D. Chen and S. E. Alway (2000). "Glyceraldehyde-3-Phosphate Dehydrogenase Varies With Age in Glycolytic Muscles of Rats." The Journals of Gerontology Series A: Biological Sciences and Medical Sciences **55**(3): B160-B164.

Ma, S., Y. Wang, Y. Chen and F. Cao (2015). "The role of the autophagy in myocardial ischemia/reperfusion injury." Biochimica et Biophysica Acta (BBA) - Molecular Basis of Disease **1852**(2): 271-276.

Ma, Y., C. Lu, C. Li, R. Li, Y. Zhang, H. Ma, X. Zhang, Z. Ding and L. Liu (2013). "Overexpression of HSPA12B protects against cerebral ischemia/reperfusion injury via a PI3K/Akt-dependent mechanism." Biochimica et Biophysica Acta (BBA) - Molecular Basis of Disease **1832**(1): 57-66.

Maneechote, C., S. Palee, S. C. Chattipakorn and N. Chattipakorn (2017). "Roles of mitochondrial dynamics modulators in cardiac ischaemia/reperfusion injury." J Cell Mol Med **21**(11): 2643-2653.

Marshall, K. D., M. A. Edwards, M. Krenz, J. W. Davis and C. P. Baines (2014). "Proteomic mapping of proteins released during necrosis and apoptosis from cultured neonatal cardiac myocytes." American Journal of Physiology - Cell Physiology **306**(7): C639-C647.

Martin, K. R., Y. Xu, B. D. Looyenga, R. J. Davis, C. L. Wu, M. L. Tremblay, H. E. Xu and J. P. MacKeigan (2011). "Identification of PTPsigma as an autophagic phosphatase." J Cell Sci **124**(Pt 5): 812-819.

Matsui, Y., H. Takagi, X. Qu, M. Abdellatif, H. Sakoda, T. Asano, B. Levine and J. Sadoshima (2007). "Distinct Roles of Autophagy in the Heart During Ischemia and Reperfusion." Circulation Research **100**(6): 914-922.

Meiri, D., C. B. Marshall, D. Mokady, J. LaRose, M. Mullin, A. C. Gingras, M. Ikura and R. Rottapel (2014). "Mechanistic insight into GPCR-mediated activation of the microtubule-associated RhoA exchange factor GEF-H1." Nat Commun **5**: 4857.

Meng, Z., T. Moroishi, V. Mottier-Pavie, S. W. Plouffe, C. G. Hansen, A. W. Hong, H. W. Park, J. S. Mo, W. Lu, S. Lu, F. Flores, F. X. Yu, G. Halder and K. L. Guan (2015). "MAP4K family kinases act in parallel to MST1/2 to activate LATS1/2 in the Hippo pathway." Nat Commun **6**: 8357.

Milerova, M., Z. Charvatova, L. Skarka, I. Ostadalova, Z. Drahota, M. Fialova and B. Ostadal (2010). "Neonatal cardiac mitochondria and ischemia/reperfusion injury." Mol Cell Biochem **335**(1-2): 147-153.

Mitchelhill, K. I., B. J. Michell, C. M. House, D. Stapleton, J. Dyck, J. Gamble, C. Ullrich, L. A. Witters and B. E. Kemp (1997). "Posttranslational modifications of the 5'-AMP-activated protein kinase beta1 subunit." The Journal of biological chemistry **272**(39): 24475-24479.

Modi, P. and M.-S. Suleiman (2004). "Myocardial taurine, development and vulnerability to ischemia." Amino Acids **26**(1): 65-70.

Moussa, A. and J. Li (2012). "AMPK in myocardial infarction and diabetes: the yin/yang effect." Acta Pharmaceutica Sinica B **2**(4): 368-378.

Mozdziak, P. E., J. J. Dibner and D. W. McCoy (2003). "Glyceraldehyde-3-Phosphate Dehydrogenase Expression Varies With Age and Nutrition Status." Nutrition **19**(5): 438-440.

Murphy, E. and C. Steenbergen (2008). "Ion transport and energetics during cell death and protection." Physiology (Bethesda) **23**: 115-123.

Murphy, E. and C. Steenbergen (2008). "Mechanisms underlying acute protection from cardiac ischemia-reperfusion injury." Physiol Rev **88**(2): 581-609.

Na, Y., S. C. Kaul, J. Ryu, J. S. Lee, H. M. Ahn, Z. Kaul, R. S. Kalra, L. Li, N. Widodo, C. O. Yun and R. Wadhwa (2016). "Stress chaperone mortalin contributes to epithelial-mesenchymal transition and cancer metastasis." Cancer Res.

Narravula, S. and S. P. Colgan (2001). "Hypoxia-Inducible Factor 1-Mediated Inhibition of Peroxisome Proliferator-Activated Receptor α Expression During Hypoxia." The Journal of Immunology **166**(12): 7543-7548.

NCBI (2016). DCAF8L1 DDB1 and CUL4 associated factor 8 like 1 [Homo sapiens (human)].

Neary, M. T., K.-E. Ng, M. H. R. Ludtmann, A. R. Hall, I. Piotrowska, S.-B. Ong, D. J. Hausenloy, T. J. Mohun, A. Y. Abramov and R. A. Breckenridge (2014). "Hypoxia signaling controls postnatal changes in cardiac mitochondrial morphology and function." Journal of Molecular and Cellular Cardiology **74**(100): 340-352.

Nicolaou, P., R. Knöll, K. Haghighi, G.-C. Fan, G. W. Dorn, G. Hasenfuß and E. G. Kranias (2008). "Human Mutation in the Anti-apoptotic Heat Shock Protein 20 Abrogates Its Cardioprotective Effects." Journal of Biological Chemistry **283**(48): 33465-33471.

Nunez, R., Javadov, S., Escobales, N. (2017). "Angiotensin II-preconditioning is associated with increased PKCε/PKCδ ratio and prosurvival kinases in mitochondria." Clinical and Experimental Pharmacology and Physiology **44**(12): 1201-1212.

Oberhansli, I., G. Brandon and B. Friedli (1981). "Echocardiographic growth patterns of intracardiac dimensions and determination of function indices during the first year of life." Helv Paediatr Acta **36**(4): 325-340.

Okazaki, M., Y. Ishibashi, S. Asoh and S. Ohta (1998). "Overexpressed mitochondrial hinge protein, a cytochrome c-binding protein, accelerates apoptosis by enhancing the release of cytochrome c from mitochondria." Biochem Biophys Res Commun **243**(1): 131-136.

Olivetti, G., P. Anversa and A. V. Loud (1980). "Morphometric study of early postnatal development in the left and right ventricular myocardium of the rat. II. Tissue composition, capillary growth, and sarcoplasmic alterations." Circulation Research **46**(4): 503-512.

Ong, S. B. and D. J. Hausenloy (2010). "Mitochondrial morphology and cardiovascular disease." Cardiovasc Res **88**(1): 16-29.

Ong, S. B., S. B. Kalkhoran, H. A. Cabrera-Fuentes and D. J. Hausenloy (2015). "Mitochondrial fusion and fission proteins as novel therapeutic targets for treating cardiovascular disease." Eur J Pharmacol **763**(Pt A): 104-114.

Ong, S. B., S. Subrayan, S. Y. Lim, D. M. Yellon, S. M. Davidson and D. J. Hausenloy (2010). "Inhibiting mitochondrial fission protects the heart against ischemia/reperfusion injury." Circulation **121**(18): 2012-2022.

Ost'adalova, I. and A. Babicky (2012). "Periodization of the early postnatal development in the rat with particular attention to the weaning period." Physiol Res **61 Suppl 1**: S1-7.

Ostadal, B., I. Netuka, J. Maly, J. Besik and I. Ostadalova (2009). "Gender differences in cardiac ischemic injury and protection--experimental aspects." Exp Biol Med (Maywood) **234**(9): 1011-1019.

Ostadal, B. and P. Ostadal (2014). "Sex-based differences in cardiac ischaemic injury and protection: therapeutic implications." Br J Pharmacol **171**(3): 541-554.

Ostadal, B., I. Ostadalova and N. S. Dhalla (1999). "Development of Cardiac Sensitivity to Oxygen Deficiency: Comparative and Ontogenetic Aspects." Physiological Reviews **79**(3): 635-659.

Ostadal, B., I. Ostadalova, F. Kolar, Z. Charvatova and I. Netuka (2009). "Ontogenetic development of cardiac tolerance to oxygen deprivation - possible mechanisms." Physiol Res **58 Suppl 2**: S1-12.

Ostadal, B., I. Ostadalova, F. Kolar and D. Sedmera (2014). "Developmental determinants of cardiac sensitivity to hypoxia." Can J Physiol Pharmacol **92**(7): 566-574.

Ošťádalová, I., F. Kolář, B. Ošťádal, V. Rohlíček, J. Rohlíček and J. Procházka (1993). "Early Postnatal Development of Contractile Performance and Responsiveness to Ca2+, Verapamil and Ryanodine in the Isolated Rat Heart." Journal of Molecular and Cellular Cardiology **25**(6): 733-740.

Ostadalova, I., B. Ostadal, F. Kolar, J. R. Parratt and S. Wilson (1998). "Tolerance to ischaemia and ischaemic preconditioning in neonatal rat heart." J Mol Cell Cardiol **30**(4): 857-865.

Paiva, M. A., Z. Rutter-Locher, L. M. Gonçalves, L. A. Providência, S. M. Davidson, D. M. Yellon and M. M. Mocanu (2011). "Enhancing AMPK activation during ischemia protects the diabetic heart against reperfusion injury." American Journal of Physiology-Heart and Circulatory Physiology **300**(6): H2123-H2134.

Panisello-Roselló, A., A. Lopez, E. Folch-Puy, T. Carbonell, A. Rolo, C. Palmeira, R. Adam, M. Net and J. Roselló-Catafau (2018). "Role of aldehyde dehydrogenase 2 in ischemia reperfusion injury: An update." World Journal of Gastroenterology **24**(27): 2984-2994.

Polekhina, G., A. Gupta, B. J. Michell, B. van Denderen, S. Murthy, S. C. Feil, I. G. Jennings, D. J. Campbell, L. A. Witters, M. W. Parker, B. E. Kemp and D. Stapleton (2003). "AMPK β Subunit Targets Metabolic Stress Sensing to Glycogen." Current Biology **13**(10): 867-871.

Qi, D. and L. H. Young (2015). "AMPK: energy sensor and survival mechanism in the ischemic heart." Trends in endocrinology and metabolism: TEM **26**(8): 422-429.

Qian, J., X. Ren, X. Wang, P. Zhang, W. K. Jones, J. D. Molkentin, G.-C. Fan and E. G. Kranias (2009). "Blockade of Hsp20 Phosphorylation Exacerbates Cardiac Ischemia/Reperfusion Injury by Suppressed Autophagy and Increased Cell Death." Circulation Research **105**(12): 1223-1231.

Qu, Y., A. Ghatpande, N. el-Sherif and M. Boutjdir (2000). "Gene expression of Na+/Ca2+ exchanger during development in human heart." Cardiovasc Res **45**(4): 866-873.

Riva, E. and D. J. Hearse (1991). "Calcium and cardioplegia in neonates: dose-response and time-response studies in rats." American Journal of Physiology - Heart and Circulatory Physiology **261**(5): H1609-H1616.

Romero-Calvo, I., B. Ocon, P. Martinez-Moya, M. D. Suarez, A. Zarzuelo, O. Martinez-Augustin and F. S. de Medina (2010). "Reversible Ponceau staining as a loading control alternative to actin in Western blots." Analytical Biochemistry **401**(2): 318-320.

Ruiz-Meana, M. and D. Garcia-Dorado (2009). "Translational cardiovascular medicine (II). Pathophysiology of ischemia-reperfusion injury: new therapeutic options for acute myocardial infarction." Rev Esp Cardiol **62**(2): 199-209.

Sahoo, S., E. Klychko, T. Thorne, S. Misener, K. M. Schultz, M. Millay, A. Ito, T. Liu, C. Kamide, H. Agrawal, H. Perlman, G. Qin, R. Kishore and D. W. Losordo (2011). "Exosomes from human CD34(+) stem cells mediate their proangiogenic paracrine activity." Circ Res **109**(7): 724-728.

Sahoo, S. and D. W. Losordo (2014). "Exosomes and cardiac repair after myocardial infarction." Circ Res **114**(2): 333-344.

Sanz, P., T. Rubio and M. A. Garcia-Gimeno (2013). "AMPKbeta subunits: more than just a scaffold in the formation of AMPK complex." FEBS Journal **280**(16): 3723-3733.

Sarras, H., S. Alizadeh Azami and J. P. McPherson (2010). "In search of a function for BCLAF1." ScientificWorldJournal **10**: 1450-1461.

Schmidt, M. R., N. B. Stottrup, H. Contractor, J. A. Hyldebrandt, M. Johannsen, C. M. Pedersen, R. Birkler, H. Ashrafian, K. E. Sorensen, R. K. Kharbanda, A. N. Redington and H. E. Botker (2014). "Remote ischemic preconditioning with--but not without--metabolic support protects the neonatal porcine heart against ischemia-reperfusion injury." Int J Cardiol **170**(3): 388-393.

Schmidt, M. R., N. B. Stottrup, M. M. Michelsen, H. Contractor, K. E. Sorensen, R. K. Kharbanda, A. N. Redington and H. E. Botker (2014). "Remote ischemic preconditioning impairs ventricular function and increases infarct size after prolonged ischemia in the isolated neonatal rabbit heart." J Thorac Cardiovasc Surg **147**(3): 1049-1055.

Schmiedl, A., Schnabel, P. A., Richter, J., Bretschneider, H. J. (1993). "Close correlations between mitochondrial swelling and ATP-content in the ischemic canine myocardium: a combined morphometric and biochemical study." Pathol Res Pract. **189**(3): 342-351.

Schroder, E. A., Y. Wei and J. Satin (2006). "The developing cardiac myocyte: maturation of excitability and excitation-contraction coupling." Ann N Y Acad Sci **1080**: 63-75.

Schull, S., S. D. Gunther, S. Brodesser, J. M. Seeger, B. Tosetti, K. Wiegmann, C. Pongratz, F. Diaz, A. Witt, M. Andree, K. Brinkmann, M. Kronke, R. J. Wiesner and H. Kashkar (2015). "Cytochrome c oxidase deficiency accelerates mitochondrial apoptosis by activating ceramide synthase 6." Cell Death Dis **6**: e1691.

Sciarretta, S., M. Volpe and J. Sadoshima (2014). "Mammalian Target of Rapamycin Signaling in Cardiac Physiology and Disease." Circulation Research **114**(3): 549-564.

Seki, S., M. Nagashima, Y. Yamada, M. Tsutsuura, T. Kobayashi, A. Namiki and N. Tohse (2003). " Fetal and postnatal development of Ca²⁺ transients and Ca²⁺ sparks in rat cardiomyocytes ." Cardiovascular Research **58**(3): 535-548.

Sharma, V., Sharma, A., Saran, V., Bernatchez, P. N., Allard, M. F., McNeill, J. H. (2011). "β-receptor antagonist treatment prevents activation of cell death signaling in the diabetic heart independent of its metabolic actions." Eur J Pharmacol. **657**(1-3): 117-125

Sharp, W. W., Y. H. Fang, M. Han, H. J. Zhang, Z. Hong, A. Banathy, E. Morrow, J. J. Ryan and S. L. Archer (2014). "Dynamin-related protein 1 (Drp1)-mediated diastolic dysfunction in myocardial ischemia-reperfusion injury: therapeutic benefits of Drp1 inhibition to reduce mitochondrial fission." FASEB J **28**(1): 316-326.

Shaw, R. J. (2009). "LKB1 and AMP-activated protein kinase control of mTOR signalling and growth." Acta physiologica (Oxford, England) **196**(1): 65-80.

Shen, S., J. Zhou, S. Meng, J. Wu, J. Ma, C. Zhu, G. Deng and D. Liu (2017). "The protective effects of ischemic preconditioning on rats with renal ischemia-reperfusion injury and the effects on the expression of Bcl-2 and Bax." Experimental and therapeutic medicine **14**(5): 4077-4082.

Shintani-Ishida, K., M. Inui and K. Yoshida (2012). "Ischemia-reperfusion induces myocardial infarction through mitochondrial Ca(2)(+) overload." J Mol Cell Cardiol **53**(2): 233-239.

Shishido, T., C. H. Woo, B. Ding, C. McClain, C. A. Molina, C. Yan, J. Yang and J. Abe (2008). "Effects of MEK5/ERK5 association on small ubiquitin-related modification of ERK5: implications for diabetic ventricular dysfunction after myocardial infarction." Circ Res **102**(11): 1416-1425.

Skarka, L., Bardova, K., Brauner, P., Flachs, P., Jarkovska, D., Kopecky, J., Ostadal, B. (2003). "Expression of mitochondrial uncoupling protein 3 and adenine nucleotide translocase 1 genes in developing rat heart: putative involvement in control of mitochondrial membrane potential." Journal of Molecular and Cellular Cardiology **35**(3): 321-330.

Solari, F. A., Dell'Aica, M., Sickmann, A., Zahedi, R. P. (2015). "Why phosphorproteomics is still a challenge." Mol. BioSyst. **11**: 1487-1493.

Tamareille, S., V. Mateus, N. Ghaboura, J. Jeanneteau, A. Croue, D. Henrion, A. Furber and F. Prunier (2011). "RISK and SAFE signaling pathway interactions in remote limb ischemic perconditioning in combination with local ischemic postconditioning." Basic Res Cardiol **106**(6): 1329-1339.

Tao, J., H.-y. Wang and C. C. Malbon (2010). "AKAR2-AKAP12 fusion protein "biosenses" dynamic phosphorylation and localization of a GPCR-based scaffold." Journal of Molecular Signaling **5**(1): 1-10.

Tondera, D., S. Grandemange, A. Jourdain, M. Karbowski, Y. Mattenberger, S. Herzig, S. Da Cruz, P. Clerc, I. Raschke, C. Merkwirth, S. Ehses, F. Krause, D. C. Chan, C. Alexander, C. Bauer, R. Youle, T. Langer and J. C. Martinou (2009). "SLP-2 is required for stress-induced mitochondrial hyperfusion." EMBO J **28**(11): 1589-1600.

Tripathy, M. K. and D. Mitra (2010). "Differential modulation of mitochondrial OXPHOS system during HIV-1 induced T-cell apoptosis: up regulation of Complex-IV subunit COX-II and its possible implications." Apoptosis **15**(1): 28-40.

Tsang, A., D. J. Hausenloy, M. M. Mocanu and D. M. Yellon (2004). "Postconditioning: a form of "modified reperfusion" protects the myocardium by activating the phosphatidylinositol 3-kinase-Akt pathway." Circ Res **95**(3): 230-232.

Tsunekawa, K., F. Kondo, T. Okada, G.-G. Feng, L. Huang, N. Ishikawa and S. Okada (2013). "Enhanced expression of WD repeat-containing protein 35 (WDR35) stimulated by domoic acid in rat hippocampus: involvement of reactive oxygen species generation and p38 mitogen-activated protein kinase activation." BMC Neuroscience **14**(1): 1-11.

Tsutsumi, Y. M., Y. T. Horikawa, M. M. Jennings, M. W. Kidd, I. R. Niesman, U. Yokoyama, B. P. Head, Y. Hagiwara, Y. Ishikawa, A. Miyanohara, P. M. Patel, P. A. Insel, H. H. Patel and D. M. Roth (2008). "Cardiac-specific overexpression of caveolin-3 induces endogenous cardiac protection by mimicking ischemic preconditioning." Circulation **118**(19): 1979-1988.

Uddin, M. J., M. U. Cinar, D. Tesfaye, C. Looft, E. Tholen and K. Schellander (2011). "Age-related changes in relative expression stability of commonly used housekeeping genes in selected porcine tissues." BMC Research Notes **4**: 441-441.

Vicencio, J. M., D. M. Yellon, V. Sivaraman, D. Das, C. Boi-Doku, S. Arjun, Y. Zheng, J. A. Riquelme, J. Kearney, V. Sharma, G. Multhoff, A. R. Hall and S. M. Davidson (2015). "Plasma Exosomes Protect the Myocardium From Ischemia-Reperfusion Injury." Journal of the American College of Cardiology **65**(15): 1525-1536.

Voigt, N., Pearman, C. M., Dobrev, D., Dibb, K. M. (2015). "Methods for isolating atrial cells from large mammals and humans." J Mol Cell Cardiol **86**: 187-198.

VORNANEN, M. (1992). "Force-frequency relationship, contraction duration and recirculating fraction of calcium in postnatally developing rat heart ventricles: correlation with heart rate." Acta Physiologica Scandinavica **145**(4): 311-321.

Vornanen, M. (1996). "Excitation-contraction coupling of the developing rat heart." Mol Cell Biochem **163-164**: 5-11.

Vucicevic, L., M. Misirkic, K. Janjetovic, U. Vilimanovich, E. Sudar, E. Isenovic, M. Prica, L. Harhaji-Trajkovic, T. Kravic-Stevovic, V. Bumbasirevic and V. Trajkovic (2011). "Compound C induces protective autophagy in cancer cells through AMPK inhibition-independent blockade of Akt/mTOR pathway." Autophagy **7**(1): 40-50.

Waldenstrom, A., N. Genneback, U. Hellman and G. Ronquist (2012). "Cardiomyocyte microvesicles contain DNA/RNA and convey biological messages to target cells." PLoS One **7**(4): e34653.

Waldenstrom, A. and G. Ronquist (2014). "Role of exosomes in myocardial remodeling." Circ Res **114**(2): 315-324.

Wang, W., Y. Peng, Y. Wang, X. Zhao and Z. Yuan (2009). "Anti-apoptotic effect of heat shock protein 90 on hypoxia-mediated cardiomyocyte damage is mediated via the phosphatidylinositol 3-kinase/AKT pathway." Clin Exp Pharmacol Physiol **36**(9): 899-903.

Wang, X., A. J. Merritt, J. Seyfried, C. Guo, E. S. Papadakis, K. G. Finegan, M. Kayahara, J. Dixon, R. P. Boot-Handford, E. J. Cartwright, U. Mayer and C. Tournier (2005). "Targeted deletion of mek5 causes early embryonic death and defects in the extracellular signal-regulated kinase 5/myocyte enhancer factor 2 cell survival pathway." Mol Cell Biol **25**(1): 336-345.

Warden, S. M., C. Richardson, J. O'Donnell, D. Stapleton, B. E. Kemp, L. A. Witters and L. A. Witters (2001). "Post-translational modifications of the beta-1 subunit of AMP-activated protein kinase affect enzyme activity and cellular localization." The Biochemical journal **354**(Pt 2): 275-283.

Wekstein, D. R. (1965). "Heart rate of the preweanling rat and its autonomic control." American Journal of Physiology-Legacy Content **208**(6): 1259-1262.

Wessely, R., S. Seidl and A. Schömig (2005). "Cardiac involvement in Emery–Dreifuss muscular dystrophy." Clinical Genetics **67**(3): 220-223.

Williams, H., King, N., Griffiths, E. J., Suleiman, M. S. (2001). "Glutamate-loading Stimulates Metabolic Flux and Improves Cell Recovery Following Chemical Hypoxia in Isolated Cardiomyocyte." J Mol Cell Cardiol **33**(12): 2109-2119.

Wong, R., A. M. Aponte, C. Steenbergen and E. Murphy (2010). "Cardioprotection leads to novel changes in the mitochondrial proteome." Am J Physiol Heart Circ Physiol **298**(1): H75-91.

Wu, Y. and E. X. Wu (2009). "MR study of postnatal development of myocardial structure and left ventricular function." Journal of Magnetic Resonance Imaging **30**(1): 47-53.

Xie, M., D. Zhang, S. C. Wang, M. Sano, X. Wang, J. S. Pocius, G. E. Taffet, L. H. Michael, M. L. Entman, D. L. Mann, T.-H. Tan and M. D. Schneider (2007). "Abstract 1949: The Protein Kinase MAP4K4 Is Activated in Failing Human Hearts and Mediates Cardiomyocyte Apoptosis in Experimental Models, in vitro and in vivo." Circulation **116**(Suppl 16): II_420-II_420.

Xing, H., S. Zhang, C. Weinheimer, A. Kovacs and A. J. Muslin (2000). "14-3-3 proteins block apoptosis and differentially regulate MAPK cascades." EMBO J **19**(3): 349-358.

Yaniv, Y., M. Juhaszova, A. E. Lyashkov, H. A. Spurgeon, S. J. Sollott and E. G. Lakatta (2011). "Ca2+-regulated-cAMP/PKA signaling in cardiac pacemaker cells links ATP supply to demand." Journal of molecular and cellular cardiology **51**(5): 740-748.

Yin, Z., G. N. Jones, W. H. Towns, X. Zhang, E. D. Abel, P. F. Binkley, D. Jarjoura and L. S. Kirschner (2008). "Heart-Specific Ablation of Prkar1a Causes Failure of Heart Development and Myxomagenesis." Circulation **117**(11): 1414-1422.

Yin, Z., D. R. Pringle, G. N. Jones, K. M. Kelly and L. S. Kirschner (2011). "Differential role of PKA catalytic subunits in mediating phenotypes caused by knockout of the Carney complex gene Prkar1a." Mol Endocrinol **25**(10): 1786-1793.

Zaha, V. G., Qi, D., Su, K. N., Palmeri, M., Lee, H.-Y., Hu, X., … Young, L. H. (2016). AMPK Is Critical for Mitochondrial Function during Reperfusion after Myocardial Ischemia. *Journal of Molecular and Cellular Cardiology*, *91*, 104–113.

Zeng, Q., H. He, X.-B. Wang, Y.-Q. Zhou, H.-X. Lin, Z.-P. Tan, S.-F. He and G.-Z. Huang (2018). "Electroacupuncture Preconditioning Improves Myocardial Infarction Injury via Enhancing AMPK-Dependent Autophagy in Rats." BioMed research international **2018**: 1238175.

Zhai, P., S. Sciarretta, J. Galeotti, M. Volpe and J. Sadoshima (2011). "Differential Roles of GSK-3β During Myocardial Ischemia and Ischemia/Reperfusion." Circulation Research **109**(5): 502-511.

Zhang, H., M. Bosch-Marce, L. A. Shimoda, Y. S. Tan, J. H. Baek, J. B. Wesley, F. J. Gonzalez and G. L. Semenza (2008). "Mitochondrial Autophagy Is an HIF-1-dependent Adaptive Metabolic Response to Hypoxia." Journal of Biological Chemistry **283**(16): 10892-10903.

Zhang, J-Y., Chen, Z-W., Yao, H. (2012). “Protective effect of urantide against ischemia-reperfusion injury via protein kinase C and phosphatidylinositol 3’-kinase-Akt pathway.” Canadian Journal of Physiology and Pharmacology, **90**: 637-645

Zhang, S., Y. Zhou, L. Zhao, X. Tian, M. Jia, X. Gu, N. Feng, R. An, L. Yang, G. Zheng, J. Li, H. Guo, R. Fan and J. Pei (2018). "κ-opioid receptor activation protects against myocardial ischemia-reperfusion injury via AMPK/Akt/eNOS signaling activation." European Journal of Pharmacology **833**: 100-108.

Zhang, Y., Chen, Z-W., Irwin, M. G., Wong, T-M. (2005). “Remifentanil mimics cardioprotective effect of ischemic preconditioning via protein kinase C activation in open chest of rats.” Acta Pharmacologica Sinica, **26**: 546-550.

Zhou, H., J. Qian, C. Li, J. Li, X. Zhang, Z. Ding, X. Gao, Z. Han, Y. Cheng and L. Liu (2011). "Attenuation of cardiac dysfunction by HSPA12B in endotoxin-induced sepsis in mice through a PI3K-dependent mechanism." Cardiovascular Research **89**(1): 109-118.

Zhou, J., Huang, W., Tao, R., Ibaragi, S., Lan, F., Ido, Y., Wu, X., Alekseyev, Y. O., Lendburg, M. E., Hu, G., Luo, Z. (2009). "Inactivation of AMPK alters gene expression and promotes growth of prostate cancer cells." Oncogene **28**(18): 1993-2002.

Zhou, T. Y., E. R. Prather, D. E. Garrison and L. Zuo (2018). "Interplay between ROS and Antioxidants during Ischemia-Reperfusion Injuries in Cardiac and Skeletal Muscle." International Journal of Molecular Sciences **19**(2).

Zuurbier, C. J., Eerbeek, O., Goedhart, P. T., Struys, E. A., Verhoeven, N. M., Jakobs, C., Ince, C. (2004). "Inhibition of the pentose phosphate pathway decreases ischemia-reperfusion-induced creatine kinase release in the heart." Cardiovascular Research **62**(1): 145-153.

11. Appendix: Effect of age on housekeeping proteins expression

Figure 103. Comparison of western blot analysis for GAPDH expression by age in two different sample preparations.

Samples of cardiac tissue prepared using the Lowry method of quantification ('First Preparation') found a statistically significant difference in GAPDH expression between 14-day old, 28-day old and Adult samples. 14-day old samples showed significantly lower levels of GAPDH than both 28-day old ($p < 0.05$) and adult samples ($p < 0.05$). To ensure that these differences were not caused by an error in protein quantification, samples from the same source underwent repeat quantification, this time using the Bradford method ('Second Preparation') and western blot analysis of GAPDH expression was repeated. 14-day old samples again showed a statistically significantly lower expression of GAPDH than both 28-day old ($p < 0.0001$) and adult ($p < 0.0001$) samples.

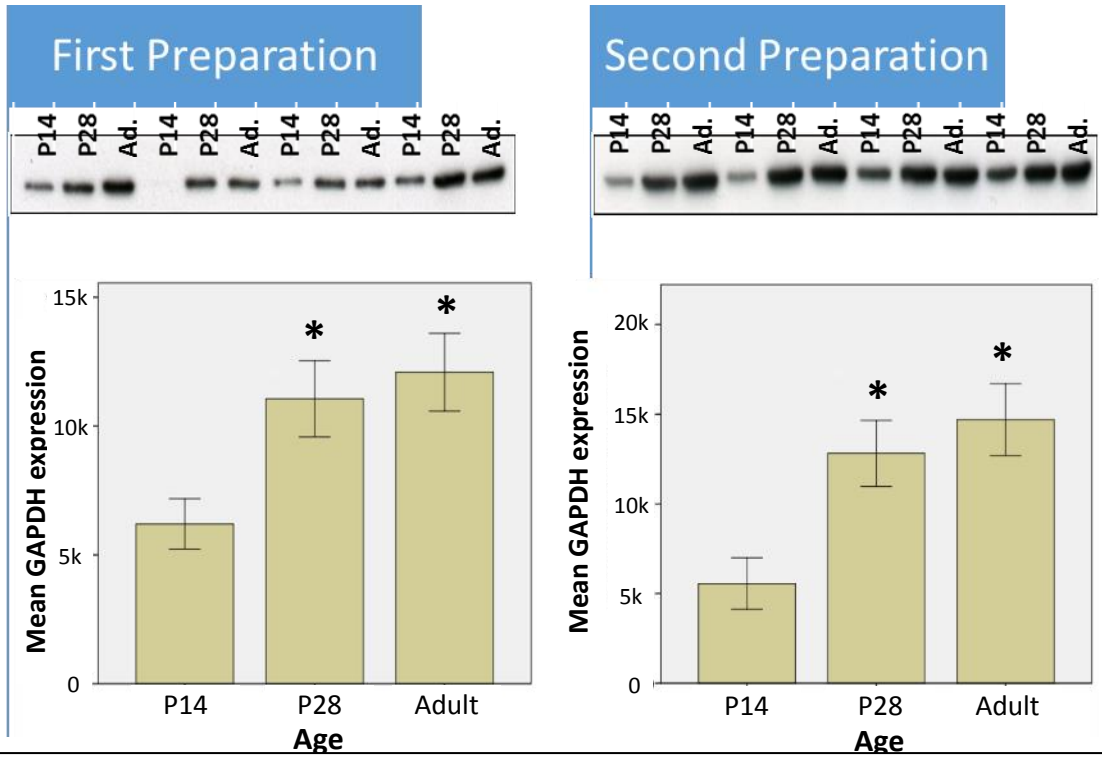

Figure 103. Graphs to show mean expression of GAPDH from western blot analysis across three age groups 14-day old (n = 20), 28-day old (n = 20) and Adult (Ad.) (n = 20) samples. Data presented as Mean ± SE. * = statistically significant difference in comparison with 14-day old samples.

Figure 104. Comparison of changes in GAPDH expression in 14-day old and adult samples following ischemia, I/R and drug treatment

Western blotting was performed on Langendorff perfused samples – discussed in **Chapter 6** – and showed differences in GAPDH expression between 14-day old hearts and adult hearts both in control hearts and hearts treated with dorsomorphin dihydrochloride ($p < 0.05$).

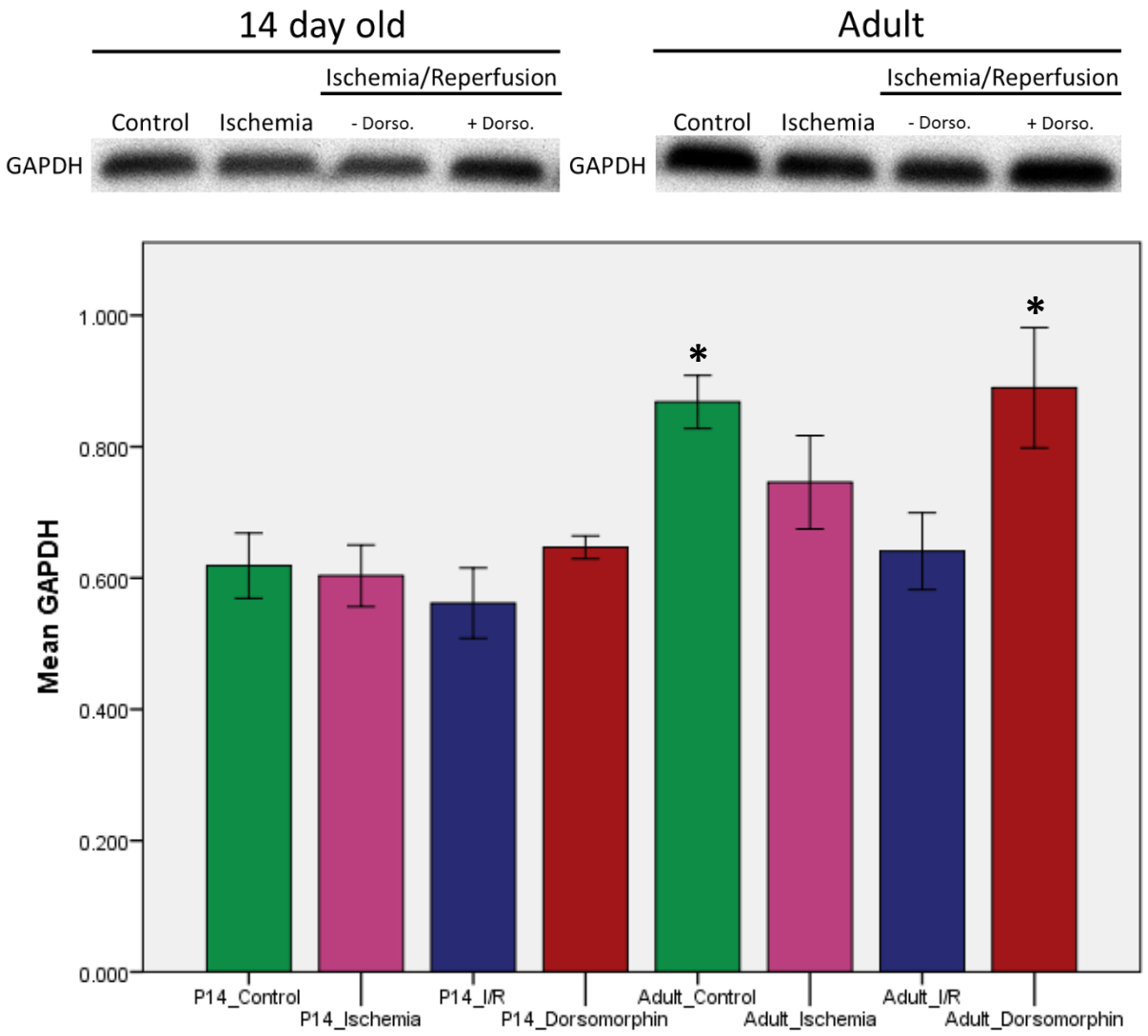

Figure 104. Graph to show the expression of GAPDH in cardiac samples taken from 14-day old and adult rats either pre-ischemia (control), post-ischemia (ischemia), post-ischemia/reperfusion (I/R) or post-ischemia/reperfusion + dorsomorphin dihydrochloride (dorsomorphin). Data presented as mean ± SE. * = Statistically significant difference in comparison with 14-day old samples. (n = 6/group)

Figure 105. Comparison of GAPDH expression between age groups in the proteomic output

GAPDH expression was found to change in the proteomic output, with significantly greater expression in 28-day old and adult samples in comparison to both 7-day old and 14-day old samples ($p < 0.05$).

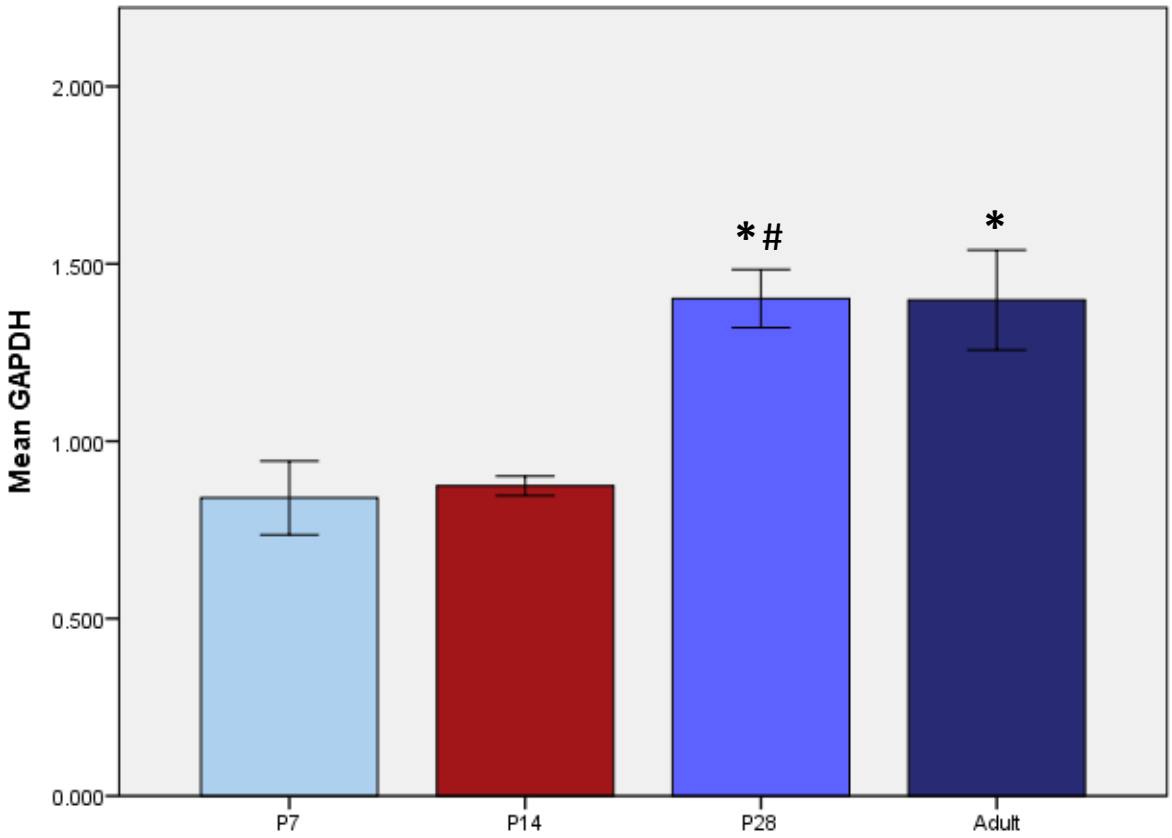

Figure 105. The trend in expression of GAPDH as detected by proteomic analysis across the 4 age groups (7-day (n = 4), 14-day (n = 8), 28-day (n = 8) and adult (n = 7)). Data presented as Mean ± SE. * = Statistically significant difference in comparison with 7-day old samples. # = Statistically significant difference in comparison with 14-day old samples.

*Figure 106. Comparison of changes in **β**-actin expression in 14-day old and adult samples following ischemia, I/R and drug treatment*

Whilst statistically, no significant differences were detected in β-actin expression between 14-day old and adult samples, blots showed clearly that strong bands could be detected in 14-day olds, whereas no bands were detected in adult samples.

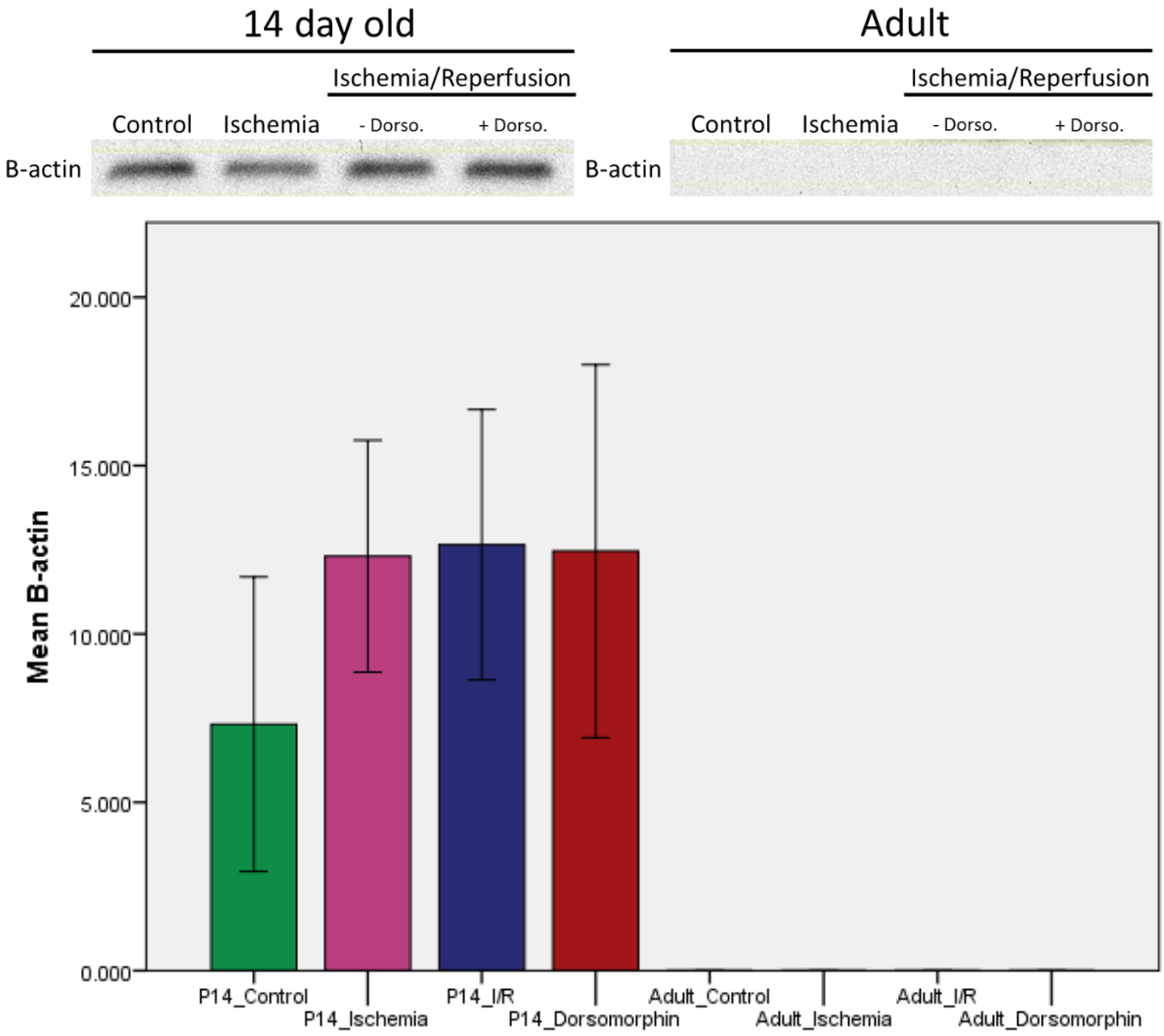

Figure 106. Graph to show the expression of B-actin in cardiac samples taken from 14-day old and adult rats either pre-ischemia (control), post-ischemia (ischemia), post-ischemia/reperfusion (I/R) or post-ischemia/reperfusion + perfusion with dorsomorphin dihydrochloride (dorsomorphin). Data presented as mean ± SE. (n = 3/group)

Figure 107. Comparison of β-actin expression between age groups in the proteomic output

Proteomic analysis showed statistically higher expression of β-actin in both 7-day old and 14-day old samples in comparison with adult samples ($p < 0.01$).

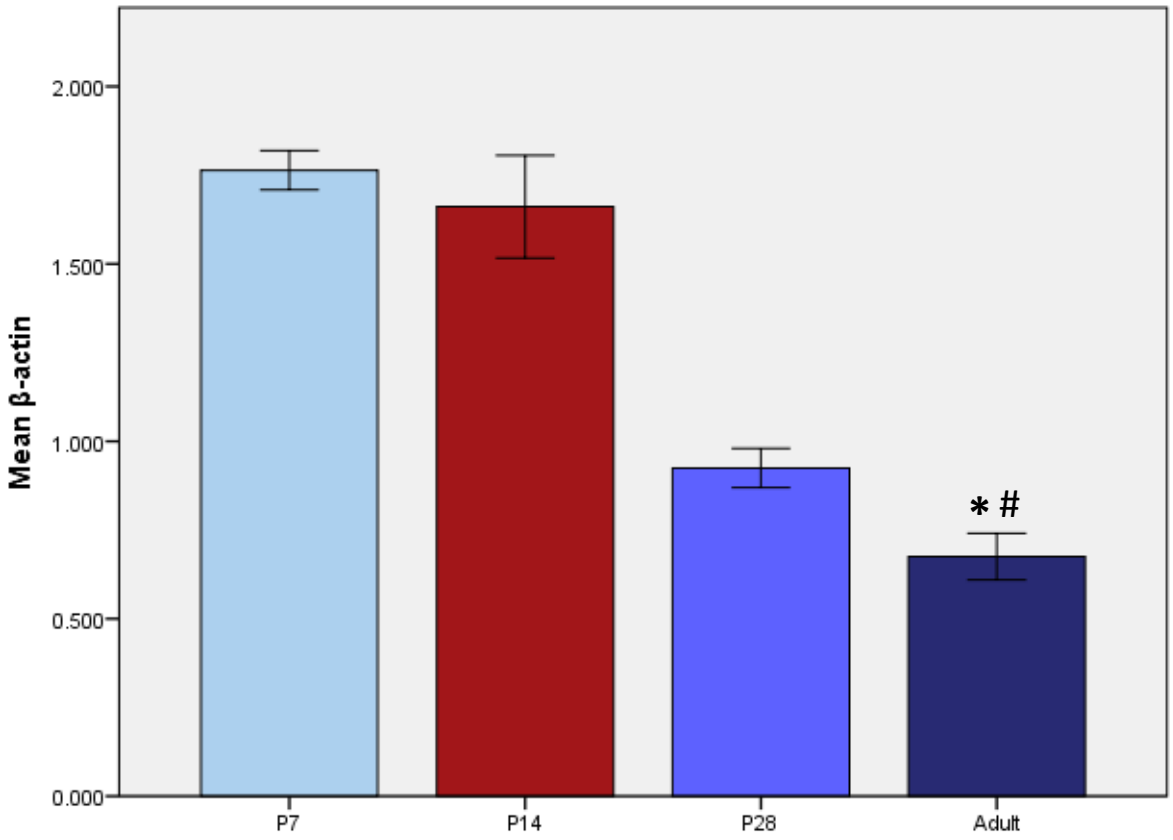

Figure 107. The trend in expression of B-actin as detected by proteomic analysis across the 4 age groups (7-day (n = 4), 14-day (n = 8), 28-day (n = 8) and adult (n = 7)). Data presented as Mean ± SE. * = Statistically significant difference in comparison with 7-day old samples. # = Statistically significant difference in comparison with 14-day old samples.

Figure 108. Comparison of whole lane protein staining using Ponceau S

Other studies have demonstrated that the use of Ponceau S staining is an effective alternative to traditionally used housekeeping proteins to normalise protein bands (Romero-Calvo, Ocon et al. 2010). In order to confirm Ponceau S staining as a viable alternative to traditional housekeeping proteins as a loading control, membranes were reversibly stained,

and whole lane band intensities were measured using ImageJ. No statistically significant differences in the mean intensities were found between the three age groups.

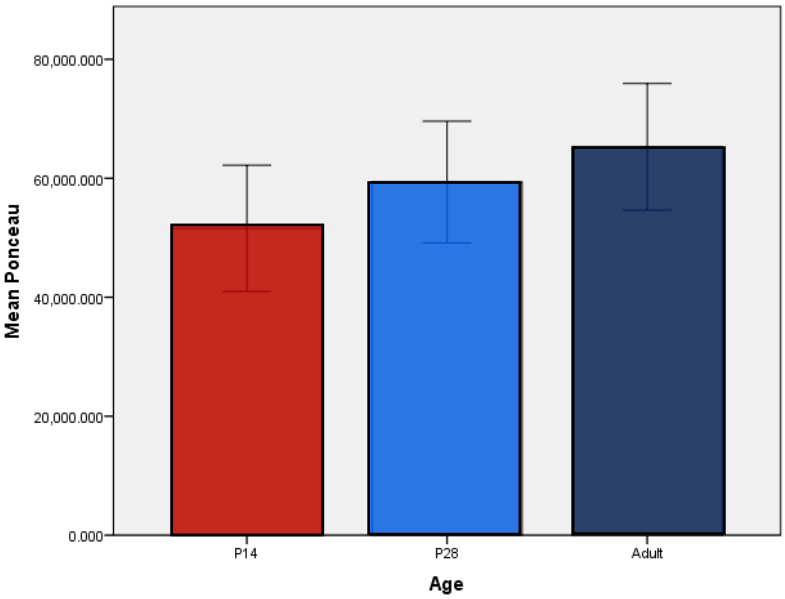

Figure 108. Graph to show mean Ponceau S lane intensity across three age groups 14-day old (n = 20), 28-day old (n = 20) and Adult (n = 20) samples. Data presented as Mean ± SE.